Improvement in the Design and Operation of Bio-reactors and Bio-separators Based on SMB Technology

Zhang Yan

NATIONAL UNIVERSITY OF SINGAPORE

2006

Improvement in the Design and Operation of Bio-reactors and Bio-separators Based on SMB Technology

Zhang Yan
(M. Eng., Tianjin University, P. R. C)

A THESIS SUBMITTED

FOR THE DEGREE OF DOCTOR OF PHILOSOPHY

DEPARTMENT OF CHEMICAL & BIOMOLECULAR ENGINEERING

NATIONAL UNIVERSITY OF SINGAPORE

2006

Acknowledgements

I would like to express my sincere appreciation to my supervisors, *Prof. Ajay Kumar Ray* and *Prof. Kus Hidajat*, for their encouragement, insight, support and incessant guidance throughout the course of this research project. I am extremely grateful to them for spending so much time on explaining my questions on the research work and sharing their broad and profound knowledge with me.

I am also thankful to *Prof. Chee-Hua Wang* and *Prof. Samavededham Lakshminarayanan* for rendering me suggestions and guidance. My gratitude also goes to *Mdm. Chiang*, *Mdm. Koh*, *Mdm. Jamie Siew*, *Mr. Boey*, *Mr. Mao Ning*, *Ms. Tay Choon Yen* and *Dr. Rajarathnam* for their help. I am very thankful to the SVU team for their excellent support in my computational work. The research scholarship from the *National University of Singapore* is also gratefully acknowledged.

I thank all my lab-mates, especially my seniors *Dr. Weifang Yu*, *Dr. Anjushri S. Kurup* and *Mr. Faldy Wongso* for their cooperative assistance and numerous discussions on research work. I also thank all my friends both in Singapore and abroad, who have enriched my life personally and professionally.

I owe a special debt to my husband, *Penghui and* my son*, Yangyang*. Without their understanding and support, it is impossible for me to pursue my Ph. D study in NUS, let alone complete this thesis. I have no words to express my gratitude to them for their love, support and dedication.

Finally, to my parents goes my eternal gratitude for their love, encouragement and support.

Table of Contents

Summary

Simulated moving bed (SMB) technology is probably one of the most remarkable achievements in the development of preparative chromatography. Due to its high separation power, SMB technology has received great interests in isolation and purification of pharmaceuticals and bio-molecules in pharmaceutical, biochemical and fine-chemical industries. In addition, the separation potential of SMB has also been exploited to improve the conversion of reactants and enhance product purity of some reversible reactions. However, the complexity with respect to the layout and operation of the SMB process makes the selection of operating parameters a highly complicated issue. The nonlinear adsorption features of the bio-molecules and the presence of mass transfer effects, in particular, present great challenges for this process. Research is needed to develop an efficient design and optimization strategy for such an intricate problem.

This dissertation presents a comprehensive study on the optimal design and operation of bio-reactors and bio-separators using SMB technology. The purpose of this work is twofold. Firstly, this study aims to develop and optimize a modified SMBR system for isomerization of glucose, an important industrial process to produce high fructose syrup (HFS) to compete with the Hashimoto's famous hybrid SMBR system; secondly, it aims to implement a complete separation of racemic pindolol on a laboratory established SMB set-up based on a short-cut design strategy. A robust, state-of-the-art non-traditional optimization technique known as non-dominated sorting genetic algorithm with jumping genes (NSGA-II-JG) is applied to solve all the multi-objective optimization problems considered in this study.

It has been found that 4-section modified SMBR with one or two reactors could

achieve the same or even better performance than that obtained by Hashimoto's system with 7 reactors due to the sufficient separation of glucose and fructose at the inlet of each reactor. Besides, distribution of the adsorption column in each section also has an important influence on the performance of the modified system.

Theoretical and experimental investigations of SMB and Varicol process for enantioseparation of racemic pindolol on Chiral-AGP stationary phase are considered in this work for a more efficient design and optimization strategy, which could guide the selection of the proper operating parameters of SMB and Varicol process for nonlinear systems in the presence of mass transfer effects. After biLangmuir isotherm parameters are obtained from the least-square fitting of the proposed model to the experimental elution curves of racemic pindolol, a short-cut design strategy based on triangle theory is presented to find the suitable operating parameters of SMB and Varicol. Good agreement between the experimental data and simulation results are obtained for 4 SMB runs and one Varicol operation. It has been found that regeneration of the solids is critical for achieving the desired separation due to the intense adsorption of both components on the chiral stationary phase. SMB with configuration of 1/2/1/1 and Varicol with 1.5/1.5/1/1 are the best choice for this system.

Results from the systematic multi-objective optimization study of the above system indicate that higher feed concentration and higher recycling flow rate are desirable for improving both recovery and purity of the two enantiomers. The observation that optimal flow rate ratios obtained from rigorous optimization fall completely into the separation region acquired from the short-cut design strategy manifests the robustness and reliability of the short-cut design strategy.

Nomenclature

a_v	specific surface area, cm^2/cm^3
b	equilibrium constant for Langmuir isotherm, l/g
b_{ns}	equilibrium constant for non-selective site, l/g
b_s	equilibrium constant for selective site, l/g
c	concentration in the mobile phase, mol/l or g/l
D_a	apparent dispersion coefficient, cm^2/min
F	error function
H	Henry's constant
I	modified objective function
J	objective function
K	distribution coefficient
K_e	equilibrium constant for reaction
k_f	lumped mass transfer coefficient, cm/min
L	column length, cm
m	net mass flow ratio
N	number of columns
N_p	effective plate number
Pr	productivity, g/h
Pur	purity
q	concentration in the solid phase, mol/l or g/l
Q	volumetric flow rate, ml/min
q_{ns}	saturation capacity of the non-selective site, g/l
q_s	saturation capacity of the selective site, g/l

r	concentration ratio of fructose to glucose at inlets of reactors
R	rate of the isomerization, mol/l/min
Rec	recovery
t	time, min
t_S	switching time, min
T	temperature, K
u	superficial liquid velocity, cm/min
V	geometric volume of the column, cm^3
X	conversion
z	axial distance, cm

Greek Symbols

γ	flow rate ratio
ε	external porosity
ε_t	total column porosity
ζ	dimensionless distance
τ	dimensionless time
φ	phase ratio, $\varphi=(1-\varepsilon_t)/\varepsilon_t$
χ	column configuration, $N_1/N_2/N_3/N_4$

Subscript and superscript

0	initial
1,2,3,4	section 1, 2, 3, 4
A	strongly adsorbed component
b	bed

B	weakly adsorbed component
cal	calculated
D	desorbent; dead volume
Ex	extract
exp	experimental
f	feed
F	fructose
G	glucose
i	component i
j	column j
N	N^{th} switching period
p	particle
P	product
R	reactor; retention
R2	second reactor in the modified SMBR system
Ra	raffinate
s	solid
S	separator
T	total
Φ	section index, 1-4

List of Figures

List of Tables

Chapter 1 Introduction

Preparative liquid chromatography is a widely adopted separation technique for the isolation and purification of pharmaceuticals, bio-molecules and other value added products. Traditional batch mode operation of liquid chromatography (LC) shows the disadvantages of low loading capacity, high eluent consumption and low adsorbent utilization. Continuous chromatographic processes are desirable to overcome these disadvantages. The simulated moving bed (SMB) process (Broughton and Gerhold, 1961), patented 4 decades ago by Universal Oil Product, is a practical implementation of the continuous countercurrent chromatographic process. Unlike elution chromatography in which feed and solvent have to be injected successively, solvent and the compounds to be separated in the SMB process are injected into and withdrawn from a ring of chromatographic columns at rotating points between the columns simultaneously. This technique simulates the countercurrent movement of the chromatographic bed, against the solvent stream and allows for continuous recovery of the desired compound. Thus, it provides all the advantages while avoiding the technical problems of a true moving bed (TMB).

Recently, further improved processes, e.g., Varicol (Adam et al., 1998, Ludemann-Hombourger et al., 2000) and variable flow rate SMB (Kloppenburg and Gilles, 1999; Zhang et al., 2003), have been developed based on the standard SMB process to either improve the productivity/ purity with a fixed amount of adsorbent or reduce the costs of stationary phase and solvent consumption for a fixed throughput. These modified systems offer additional degrees of freedom in the selection of column configuration or flow rates during the operation, which lead to a higher efficiency in

terms of separated product per amount of solid-phase compared to a SMB process (Toumi et al., 2003).

SMB systems can also be integrated to include reactions, which provide economic benefits for equilibrium limited reversible reaction, such as hydrogenation (Ray *et al*., 1994), isomerization (Hashimoto *et al.*, 1983a; Silva et al., 2006), etherification (Zhang *et al*., 2001), esterification (Yu *et al*., 2003a) and acetalization (Silva and Rodrigues, 2005) reactions. In-situ separation of the products facilitates the reversible reaction to completion beyond thermodynamic equilibrium and at the same time helps to obtain products of high purity. A better use of adsorbent/catalyst and a reduction in solvent requirement can also be achieved by coupling reaction and separation in a simulated moving bed reactor (SMBR).

Due to its high separation power, SMB technology has been widely used in the separation and purification of chemicals which are difficult to be separated by other methods. In recent years, a surge of interest in SMB for enantioseparation has been instigated by the rapid development in life science and the increasingly stringent restrictions on pharmaceuticals. Applications of SMB in bio-separations and bio-reactions are also widely studied. The use of SMB in amino acid separation (Wu et al., 1998; Xie et al., 2003), insulin and antibody purification (Xie, et al., 2002; Imamoglu, 2002; Mun et al., 2003) has also been reported. In addition, integrated simulated moving bed reactors (SMBR) have been designed for various enzymatic catalysis reactions, e.g., isomerization of glucose (Hashimoto et al., 1983a, b; Silva et al., 2006), sucrose inversion to glucose and fructose (Akintoye et al., 1990, 1991; Azevedo and Rodrigues, 2001; Kurup et al., 2005a), biosynthesis of dextran (Barker et al., 1992) and enzyme catalyzed production of lactosucrose (Kawase et al., 2001; Pilgrim et al., 2006).

Nevertheless, the advantages of SMB/SMBR processes are achieved by a higher complexity with respect to layout and operation, which makes an empirical design quite difficult (Schulte et al., 2005). Modeling and simulation of an SMB unit prior to plant operation is an unavoidable and complicated task. Although many authors have proposed theoretical models to describe the performance and internal profiles of SMB units (Ruthven and Ching, 1989; Storti et al., 1989; Zhong and Guiochon, 1996; Strube et al., 1997; Pais et al., 1997, Ma and Wang, 1997), most of these theories are based on the TMB model and have proved efficient in the design and optimization of SMB for linear system under ideal conditions only. However, the complex sorption mechanism of bio-molecules tends to render the system work under nonlinear conditions and with the presence of mass transfer effects. Design and optimization of such complicated systems is still a challenge. Numerical design and optimization method seems to be the only possible choice.

The necessity of optimizing SMB processes for bio-separations and bio-reactions results from the high separation costs and numerous parameters involved. Normally, product purity and recovery, eluent consumption and productivity are exploited to characterize the SMB and Varicol performance. Systematic optimization aimed to find the optimal design and operating parameters to achieve one or more than one of the above mentioned objectives is necessary. Although several studies have been reported in published literature on the optimization of SMB systems (Storti et al., 1988, 1995; Proll and Kusters, 1998; Dünnebier and Klatt, 1999; Strube et al., 1999, Dünnebier et al., 2000), most of these studies involve the optimization of only a single (scalar) objective function, which may taken as a weighted-average of several conflicting objective functions. This parametric approach has the drawback that certain optimal solutions may be lost since they may never be explored, particularly when

non-convexity of objective function gives rise to a duality gap (Goicoechea et al., 1982). The use of multi-objective optimization helps to obtain a set of equally good (non-dominated) solutions corresponding to all objectives considered and allows for more feasible decisions on the optimal operating point.

Non-dominated sorting genetic algorithm (NSGA) is one of the several methods available to solve multi-objective optimization problems. NSGA is a nontraditional search and optimization method (Srinivas and Deb, 1995) that has become quite popular in engineering optimization (Bhaskar et al., 2000a, b, 2001; Rajesh et al., 2001). The search for global optima is conducted by means of operations such as reproduction, crossover and mutation which are motivated by the principles of natural genetics and natural selection. A ranking selection method and a niche method were used to emphasize better non-dominated sets and to create diversity among the solutions respectively. Good traits of fitter individuals are passed on to the next generation as evolution progresses. Its population-based nature has lessened the possibility of being trapped in problems where multi-modality exists (Bhaskar et al., 2000a; Wongso et al., 2005).

Several research studies have adopted NSGA for multi-objective optimizations of SMB processes. Optimization of SMB as well as its modification, Varicol and distributed feed systems, for enantioseparation of 1,2,3,4-tetrahydro-1- naphthol was investigated by Zhang et al. (2002a, 2003). Wongso et al. (2004, 2005) carried out the multi-objective optimization of SMB and Varicol processes for enantioseparation of SB-553261 and 1,1′-bi-2-naphtol. Multi-objective optimization for reactive SMB and Varicol was also studied for sucrose inversion (Kurup et al., 2005a). Pareto solutions, a set of equally good solutions with respect to all objectives for operating parameters as well as design parameters were obtained in these studies. Significant improvement in

terms of increasing productivity/purity using less desorbent has been achieved by applying multi-objective optimization.

Although systematic multi-objective optimization studies of SMB technology have been carried out for several biochemical applications, the aforementioned studies are all confined to modeling work; few experimental studies have been performed to verify the optimization results. Therefore, both theoretical and experimental investigations of a SMB unit for enantioseparation of racemic pindolol are carried out in this work. Separation of racemic pindolol is of great commercial value due to the extremely high price of S-pindolol. In addition, pindolol shows nonlinear characteristic even under very low concentrations. Comprehensive study of the design and operation of SMB and Varicol for such a nonlinear system in the presence of mass transfer resistance and dispersion effect is therefore of great technical significance. The purpose of this study is to achieve the complete separation of racemic pindolol using the laboratory SMB unit and to demonstrate that NSGA is a robust and efficient approach in the design and optimization of the SMB unit for nonlinear system under non-ideal conditions.

Multi-objective optimization of hybrid SMBR systems for isomerization of glucose will also be presented in this dissertation. Glucose isomerization is an important industrial process to produce high fructose syrup (HFS). The bottleneck for production of HFS is the consumption of solvent. Hybrid simulated moving bed reactor (SMBR) systems are optimized to minimize the solvent consumption without a considerable sacrifice of productivity. By performing multi-objective optimization, we intend to deepen the understanding of SMBR and its modification processes and provide a wider range of useful operating conditions for decision makers.

This dissertation is organized into eight chapters. Following this brief introduction,

development and recent applications of SMB technology are reviewed. This is followed by a brief introduction of several commonly used design and optimization strategies of SMB process.

Chapter 3 focuses on the multi-objective optimization of Hashimoto's 3-zone SMBR system for glucose isomerization (Hashimoto et al., 1983a). Some double-objective optimization problems are solved to determine the optimum design and operating parameters for Hashimoto's system. Effects of reaction temperature and the feed compositions on the Pareto solutions are also discussed.

Chapter 4 presents modifications to Hashimoto's hybrid SMBR system. Two different configurations of a 4-zone SMBR system are developed to overcome the disadvantage of Hashimoto's system, i.e., low utility of reactors with feed being a 50/50 blend of glucose and fructose. By applying multi-objective optimization, optimal operating parameters for the modified systems are obtained. Optimization results for the modified systems indicate that equivalent or even better performance than that of Hashimoto's system can be achieved by modified systems with much fewer reactors.

Chapters 5 to 7 present the enantioseparation of racemic pindolol using SMB technology.

BiLangmuir isotherm and equilibrium-dispersive model are adopted to describe the dynamic behavior of the single column. NSGA is employed to derive the isotherm parameters by least-square fitting of the model predictions to the recorded experimental elution curves of racemic pindolol in Chapter 5. Validity of the isotherm parameters is tested by comparing the experimental and simulated band profiles at various operating conditions. In addition, effects of column degradation on the isotherm parameters are also briefly discussed.

Following Chapter 5, enantioseparation of racemic pindolol using SMB and Varicol processes are presented in Chapter 6. A shortcut design strategy for choosing the operation conditions is first developed based on the mathematical model and experimentally determined adsorption isotherm. Several SMB and Varicol experiments are then carried out to validate the model predictions under a relatively wide range of operating parameters. Influences of the column configuration and isotherm parameters on the SMB performance are finally investigated.

Chapter 7 describes the optimization of the performance of SMB and Varicol processes based on the experimentally verified mathematical model for the separation of racemic pindolol presented in Chapter 6. Multi-objective optimization is first performed for the existing laboratory set-up and some of the optimum results are verified experimentally. Thereafter, optimization at the design stage is carried out to further improve the recovery of the desired component using the minimum desorbent consumption.

Finally, this thesis ends with Chapter 8 which summarizes all the inferences and conclusions drawn from this research. A section on recommendations for future work is also included in this chapter.

Chapter 2 Literature Review

2.1 Development of SMB technology

Chromatographic separation was biased towards the batch mode during its earlier applications. Modes for continuous operation are more attractive due to their inherent advantages in acquiring higher productivity and lower solvent consumption with a more flexible and unattended operation (Ray, 1992). Among the various continuous operation approaches, countercurrent mode is considered to be more efficient due to its high separation driving force. Therefore, countercurrent chromatography has been developed extensively in the last few decades and realized by simulated moving bed (SMB) approach. This section is dedicated to a brief review of the development of the countercurrent chromatography.

2.1.1 True moving bed chromatography

The ideal countercurrent system, which involves the actual circulation of solids with a constant flow rate, is known as the true moving bed (TMB) process. A typical TMB system is illustrated in Figure 2.1 for binary separation of components A and B, with component A being the more retained species. Four external streams, including two inlet streams (feed and desorbent) and two outlet streams (extract and raffinate) divide the column into four sections with different flow rates of the mobile phase. Each of the four sections in TMB system plays a specific role in the process. Section 1 is to desorb the more retained component and regenerate the solid phase. Section 2 is used to desorb the less retained component. The more retained component is adsorbed in section 3 and carried towards the extract port through the movement of the solid. Whereas the role of section 4 is to adsorb the less retained component and regenerate the desorbent.

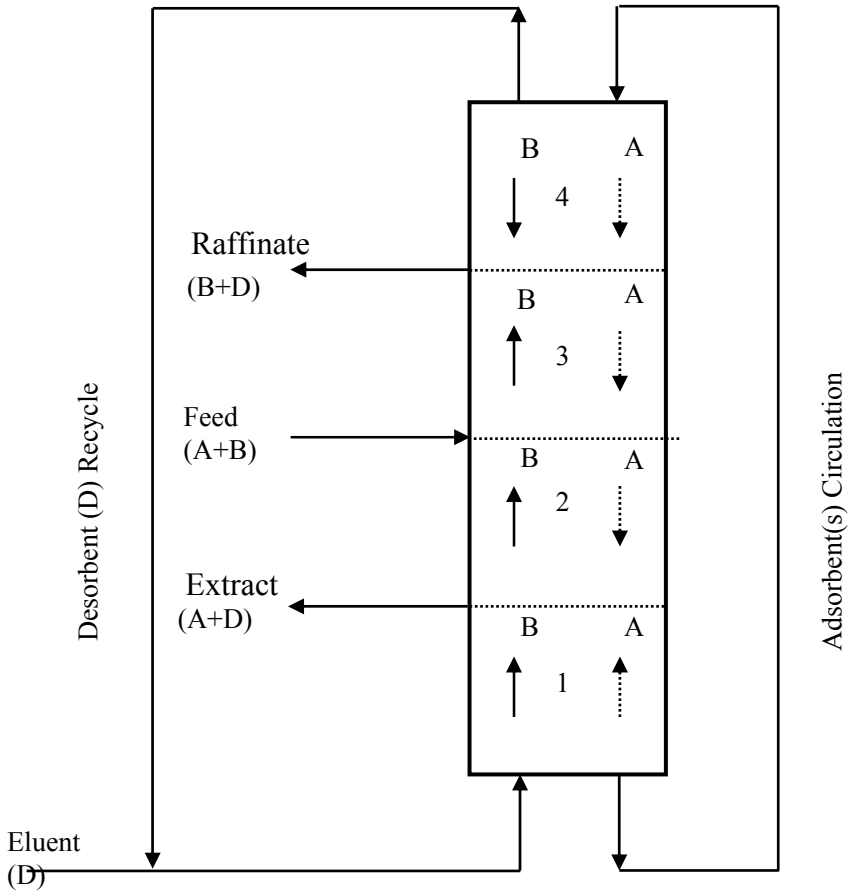

Figure 2.1 Typical configuration of a TMB chromatography

The key to this process is the proper choice of the internal flow rates in all the sections and the solid phase velocity to ensure that each section performs its specific separation task. The desired migration direction for components A and B to facilitate separation in the four sections is shown in Figure 2.1. The net flow of the strongly adsorbed species A should be downwards with the solid in the sections 2 to 4, while upwards with fluid in section 1, enabling the recovery of A at the extract port. On the contrary, B, the weakly adsorbed species should travel upward with fluid in sections 1 to 3 and downwards with solid in section 4, making it easier for its collection at the raffinate port. As a result, feed F (mixture of A and B) is split up into two streams

namely, the extract containing A and D (the desorbent) with little B and the raffinate containing B and D with very little of A. A difficult separation of A and B is transformed into two easier separations (A-D and B-D).

Unfortunately, movement of the stationary phase, which in most cases consists of porous particles in the micrometer range, is technically impossible. Therefore, other technical solutions had to be developed. The breakthrough was achieved with SMB process, which will be presented in the next section.

2.1.2 Simulated moving bed chromatography

SMB technology was first patented by Universal Oil Product (UOP) for the purification and recovery of bulk chemicals in the 1960s (Broughton and Gerhold, 1961). SMB unit consists of a number of fixed bed columns which are connected each other as illustrated in Figure 2.2. Countercurrent movement of the two phases is achieved by periodically and simultaneously switching the inlet and outlet ports in the direction of the fluid flow with the aid of multi-position valves connected to each column. Therefore, most benefits of continuous countercurrent operation can be achieved in SMB system without the problems associated with moving the solids. Due to the port switching, SMB exhibits a cyclic steady state behavior, in which the unit shows the same time dependent behavior during each time period between two successive switches of the inlet and outlet ports.

Another characteristic of the SMB setup is the implementation of a so-called recycle pump to ensure the fluid flow in one direction. Generally, four cases can be distinguished (Schulte at al., 2005). In the first case, the recycle pump is at a fixed position between two columns and the flow rate of this pump need to be adjusted depending on the section it is located since all columns are moving during the

operation. A rigorous control system is required in this case for the control of recycle flow rate. The second approach is characterized by a moving recycle pump that is always located near the desorbent line by using an additional multi-position valve. Though one more valve is required, this operation mode has the advantage in that the flow rate to be pumped is constant and the recycle pump never comes into contact with the feed line of sample. The first and second approaches belong to the closed-loop SMB. Besides the closed-loop operation, two open-loop operation modes are also widely adopted where no additional recycle pump is required. In the third case, outlet of section 4 is not directly recycled to section 1 but introduced to the desorbent tank instead. While, in the last case, no recycling of the solvent takes place, this method is only applied when the regeneration of the desorbent turns out to be very difficult and the fresh solvent is not too expensive.

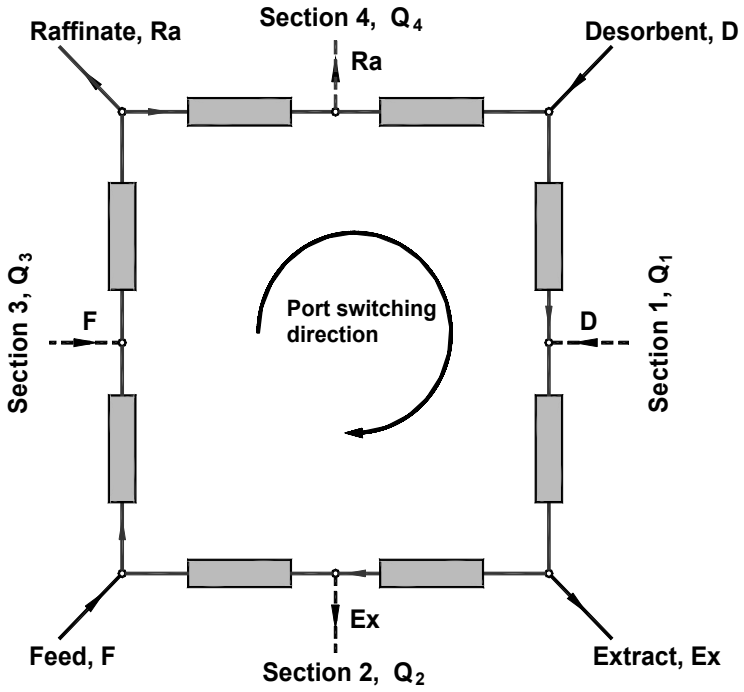

Figure 2.2 Schematic diagram of a four-zone SMB chromatography

Major applications of SMB technology were found in petrochemical industry and sugar industry during the earlier stage. Since 1990, SMB has been successfully down-scaled for preparation of enantiopure chemicals. Details of the recent applications of SMB technology will be presented in section 2.2.

2.1.3 SMB chromatography with variable conditions

Recently, more improved continuous countercurrent chromatographic processes have been developed and reported in the open literature. They are all based on the standard SMB technology but operated under variable process conditions to either improve the productivity or reduce the consumption of desorbent with the same column hardware and stationary phase.

2.1.3.1 Varicol

Varicol is a novel multi-column continuous chromatographic system first reported by Ludemann-Hombourger et al. (2000). It shows a notable improvement over the SMB due to the more flexibility in column configurations arising from the asynchronous shift of the injection and withdrawal ports within a switching period. The principle of Varicol operation during one switching period (t_s) is explained in this section and illustrated in Figure 2.3 together with an equivalent SMB operation for comparison.

Figure 2.3(a) depicts a conventional 4-zone SMB set-up with 6 columns distributed as 1/2/2/1, which means 1, 2, 2 and 1 column(s) in sections 1 to 4 respectively. During one switching period from 0 to t_s in Figure 2.3(b) there is only one column configuration in the SMB process, because all the input/output ports stand still before there is a simultaneous and equal shift of all the columns by one column. However, in Varicol operation, input/output ports may shift non-simultaneously and unequally as

shown in Figure 2.3(c) for a four-subinterval Varicol process. The column configuration in such case changes from 1/2/2/1 (0~t_s/4) to 2/1/2/1 (t_s/4~t_s/2) by shifting the extract port one column forward, then to 2/2/1/1 (t_s/2~3/4t_s) by shifting the

(a) 6-column SMB/Varicol set-up

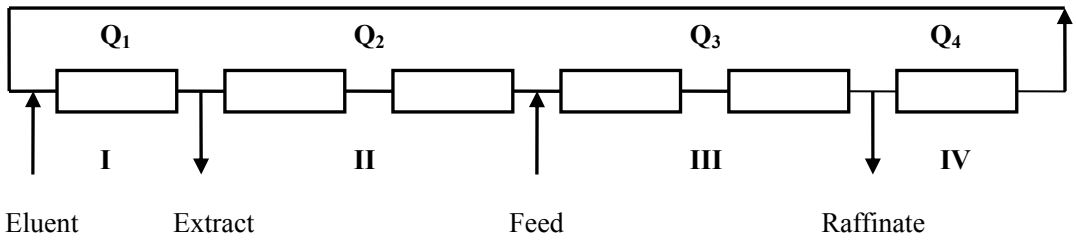

(b) SMB

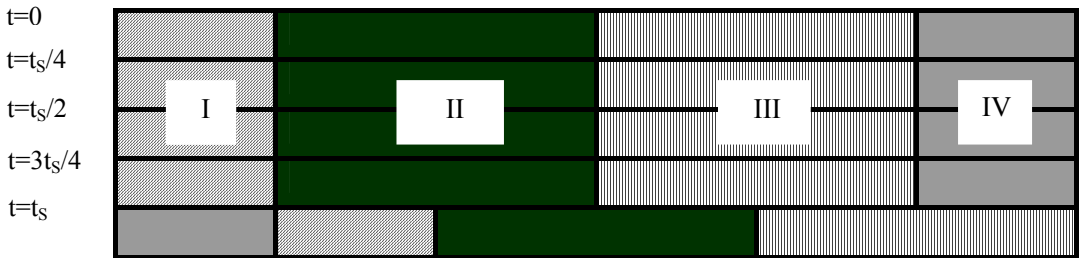

(c) Varicol

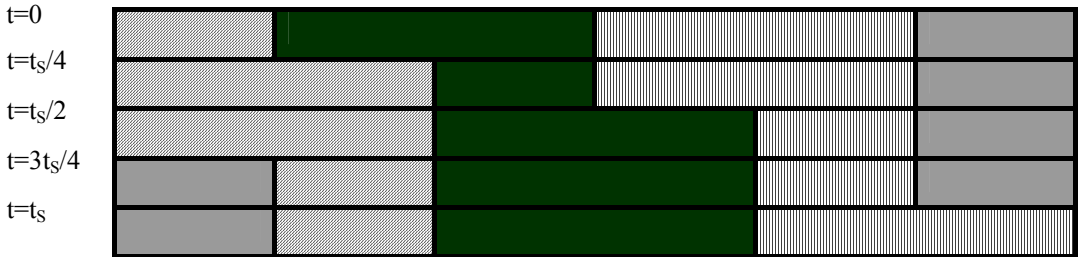

Figure 2.3 Example of SMB (b) and 4-subinterval Varicol (c) port switching schedule on a 6-column set-up (a)

feed port one column forward, and then to 1/2/1/2 ($3/4t_s$~t_s) by shifting the desorbent port one column forward. Therefore, there can be four different column configurations for the four time intervals during one global switching period of the Varicol system. After the 4^{th} sub-interval, the column configuration returns back to 1/2/2/1 by shifting the raffinate port one column forward, and once again another global switching begins and the four sub-switching schedules repeat.

Thus, input/output ports in Varicol, quite different from SMB, are shifted neither simultaneously nor equally. Furthermore, each port may shift more than once during one switching period, either forward or backward. Thus, Varicol process offers high flexibility, especially for the systems with a low number of columns.

In the open literature, only a couple of studies have been reported on the implementation of Varicol process for the enantioseparation of 1,2,3,4-tetrahydrol-1-naphthol (Ludemann- Hombourger et al., 2000) and for the enantioseparation of SB-553261 (Ludemann- Hombourger et al., 2002). In both cases Chiralpak AD 20μm (Chiral Technologies Europe, France) was used as the chiral stationary phase (CSP). Their simulation and experimental results indicates that Varicol is indeed superior to SMB in terms of product purity and productivity. For example, they showed an 18.5% improvement in productivity using Varicol, with the same product purity at the same desorbent consumption and on the same 5-column set-up (Ludemann-Hombourger et al., 2000). In their most recent article, results demonstrated that 4-column Varicol set-up was able to perform on par with a 6-column SMB for a given separation task at the cost of slightly higher desorbent consumption rate (Ludemann- Hombourger et al., 2002). It is worth noting that Varicol improves the system performance without introducing any additional cost.

Few works on the optimization of Varicol processes were also reported in the open literature. Toumi et al. (2002) have discussed the strategy for obtaining the optimal operating conditions of Varicol on two systems, separation of amino acids, trytophan and phenylamine, and separation of fructose and glucose. Zhang et al. (2002a), Subramani et al. (2003) and Wongso et al. (2004) have presented the multi-objective optimization of Varicol process using genetic algorithm for various separation systems. In addition, Yu et al. (2003b) and Subramani et al. (2003) have also reported the multi-objective optimization of reactive Varicol for the synthesis of methyl acetate and synthesis of methyl tertiary butyl ether respectively.

2.1.3.2 SMB with variable flow rates

Recently, Kloppenburg and Gilles (1999) proposed another process to improve the SMB performance, by varying the fluid flow-rates in the switching interval. In contrast to the asynchronous switching of the external ports in the Varicol process, this new process permits the external flow rates (Q_F, Q_D, Q_{Ex} and Q_{Ra}) to vary with time within one switching interval. Consequently, the internal flow rates also change within a switching period. The purpose of varying the flow rates is to obtain a better distribution of the solutes in the fluid and solid phase and hence increase the utility of the adsorbent. As reported by Zhang et al. (2003) the performance of this new process is similar to Varicol with respect to product purities, productivity and eluent consumption and thus better than the conventional SMB process. However, this improved performance is achieved with increased complexity of operation and design.

2.1.3.3 Gradient SMB chromatography

In usual, SMB processes are operated under isocratic conditions. It is observed that isocratic conditions often lead to a severe tailing of the disperse front of the less retained component due to insufficient desorption. Similar to batch chromatography, a

gradient can improve the SMB separation if the selectivity of the components is very large or a separation under isocratic conditions is impossible. This can be achieved by tuning the retention behavior of the solutes to be separated along the unit, namely by enforcing weak adsorption conditions in sections 1 and 2 and strong adsorption conditions in sections 3 and 4. By far, three operation modes, i.e., temperature gradient, pressure gradient and solvent gradient SMB processes have been realized in SMB separation.

- **Solvent-gradient SMB chromatography**

Solvent-gradient SMB chromatography is usually achieved by desorbent entering the plant with high elution strength while the feed stream is introduced with a lower solvent strength. This procedure leads to the formation of a step gradient with a regime of high desorption power in sections 1 and 2 and a region of improved adsorption in sections 3 and 4. Therefore, separation performance in terms of productivity, product concentration and solvent consumption can be significantly improved.

Abel et al. (2002, 2004) have investigated the application of solvent gradient SMB for the separation of α-ionone racemate with both linear and Langmuir isotherms. In their studies design criteria to achieve complete separation were developed in the frame of equilibrium theory. Experimental investigations were also carried out to verify their designs. Experimental results proved that solvent gradient operation really helped to achieve the complete separation which is not achievable under the isocratic condition. However, precise process optimization and control are indispensable for such a complex operation. And such optimization requires rather detailed information on retentions and solubility at different mobile phase compositions, which goes beyond what is normally required for isocratic SMB design.

- **Supercritical fluid SMB chromatography**

Supercritical fluid chromatographic (SFC) systems are operated above critical pressure and temperature of the mobile phase. In most cases the main component of the mobile phase is carbon dioxide (CO_2) which offers several advantages, i.e. cheap, non-toxic and non-flammable. In the supercritical region density and the solvating power of the fluid is highly dependent on the pressure and temperature, and so is the affinity of a given solute. With a higher operating pressure, the density increases, the elution strength is improved and smaller retention time can be realized.

The coupling of SFC with SMB was initiated by Clavier et al. (1996) for the separation of fatty acids. The most impressing benefit of supercritical fluid SMB (SFC-SMB) is given by the fact that under supercritical conditions it is possible to apply a pressure gradient along the four sections of a SMB to decrease elution strength (Schulte and Strube, 2001). With the highest pressure in section 1 (maximum desorbent strength needed to elute the more retained component from the adsorbent) and the lowest in section 4 much steeper fronts of the internal concentration profile can be obtained. The varied adsorption strength of the mobile phase enables higher feed load therefore increasing productivity.

Design strategy for the SFC-SMB processes was developed under linear (Mazzotti et al., 1997) and non-linear systems (Di Giovanni et al., 2001). For linear system, it was found that the complete separation regime is no longer of triangular shape but either a truncated or full rectangle. Moreover, the size of the regime has been shown to increase, which indicates that pressure gradient mode is in favor of separation compared to isocratic mode. For non-linear system, different desorption isotherm must be used in different sections. Linear isotherm was used for fluid phase with low concentration while competitive Langmuir isotherm was used for the more

concentrated fluid. In the frame of equilibrium theory, the complete separation regime for non-linear condition follows the triangular shape of an isocratic operation, especially at higher feed concentration, while the pure regime for linear condition still has the shape of rectangle.

The limitation of the SFC-SMB is the limited solvating power for the elution of polar and large molecules (Schulte and Strube, 2001). The introduction of modifier, in most cases an alcohol or ether, can help to solve part of the problem since the presence of the modifier may increase the solvating power of the supercritical fluid while at the same time it also causes deactivation of the most active sites of the adsorbent.

- **Temperature-gradient SMB chromatography**

The basic advantage of gradient SMB system is the enhanced desorption, especially of the extract component in section 1. Adsorption strength modulated by variation of solvent composition or column pressure has already been discussed; mode by varying temperature within a SMB chromatography will be presented subsequently.

The reason for applying a temperature gradient is obvious. As the adsorption equilibrium constant is a function of heat of adsorption and temperature. Increasing temperature will lead to an increased desorption. Therefore, the improvement of separation performance is also obtainable if a temperature increase in the desorption sections of a SMB unit is applied. One drawback of such a process is the heat capacity of the system and the slow change of temperature. This has to be considered especially when a column shifts to another section and its temperature has to be changed.

Ching and Ruthven (1986) first applied this non-isothermal operation in a 3-zone SMB unit for the separation of glucose and fructose. Recently, a temperature increase in section 1 has been investigated by Migliorini et al. (2001). Their results indicated

that a temperature increase in section 1 leads to a decrease of the desorbent consumption and a larger enrichment of component A. However, adoption of such a complex system should be with great care as its operation is still associated with a lot of uncertainties and its overall economic advantage needs to be assessed based on a detailed evaluation of the entire system.

2.1.4 Simulated moving bed chromatographic reactor

Combination of chemical reaction and separation into a single unit can significantly improve the course of reaction and separation efficiency (Fricke et al., 1999a, b). Apart from the financial benefits achieved through process intensification, the integrated reaction-separation also enhances conversions of reversible reactions beyond equilibrium limit by removing one or more of the product from the reaction section and thus shifting the equilibrium. The concept of integrated chromatographic separator and reactor was initiated almost simultaneously in the USSR by Roginskii et al. (1961) and in the United States by Magee (1963). With the advent of the more powerful SMB chromatographic process, research on the simulated moving bed reactors (SMBR) has also become popular in the last few decades.

Like SMB process, SMBR also consists of a series of packed columns where chemical reaction and separation take place simultaneously. The counter-current movement between the solid and fluid phase is simulated by periodically switching the input and output ports along the columns in the same direction of the fluid flow. Proper catalyst and adsorbent, towards which products and reactants have different adsorption affinities, are packed in the columns as the stationary phase. Catalyst and adsorbent can be packed either in a single column or in separate columns according to the requirements of different reaction systems. Normally, when high temperature is needed for catalytic reaction or products rather than reactants are the strongly retained species,

multiple beds with separate catalyst and adsorbent should be employed (Tonkovich et al., 1993).

SMBR has been successfully applied in various types of reactions, such as esterification (Mazzotti et al., 1996; Kawase et al., 1996; Migliorini et al., 1999b; Dünnebier et al., 2000; Lode et al., 2001; Yu et al., 2003a,b), etherification (Zhang et al., 2001), acetalization (Silva and Rodrigues, 2005), hydrogenation (Ray, 1992; Ray et al., 1994; Ray and Carr, 1995a, b) and isomerization (Hashimoto et al., 1983a, b; Toumi and Engell, 2004, Silva et al., 2006). These works show that substantial improvements in terms of product purities and conversions can be achieved in SMBR compared to fixed bed operation.

2.2 Recent applications of SMB technology

In the last few decades, SMB has been used for large-scale separations, notably the Parex process by UOP for extraction of p-xylene from c_8 aromatic mixture. Before 1990s, major applications were in petrochemical industry (Broughton and Gerhold, 1961; Broughton, 1968; Broughton et al., 1970; Rosset et al., 1976; Seko et al., 1982; Broughton, 1984), the corn wet milling industry (Lefevre, 1962; Hongisto, 1977a, b) and sugar industry (Buckley and Norton, 1991). A review of SMB in various industrial systems can be found in Ruthven and Ching (1989). However, after 1990, SMB has found its new life in pharmaceutical and fine-chemical industry due to the increasing stringent restrictions on pharmaceuticals and fine chemicals. The demand for preparation of the low cost optical pure chemicals largely stimulates the application of SMB technology in this field. Therefore, this section will focus on the developments and applications of SMB in chiral separations. In addition, recent applications of SMB technology on ternary-system separations and biochemical reactions are also reviewed.

2.2.1 Preparation of enantiopure chemicals

Preparation of the pure enantiomers of chiral drugs is essential in the pharmaceutical industry. To achieve this with maximum economy is difficult and needs careful evaluation of all possible techniques (asymmetric synthesis, biocatalysis, kinetic resolution, chiral chromatography). Among these techniques chiral preparative chromatography offers two advantages: it is a quick method in small scale (up to several kg) and it can be scaled up reliably with the use of different modeling approaches. Simulated moving bed (SMB) chromatography, which provides significant benefits in terms of productivity and solvent consumption due to the increased exchange capabilities between the two phases, has gained a wide acceptance for chiral separations in the pharmaceutical and fine chemical industry (Strube et al., 1999; Chankvetadze, 2001).

The first successful chromatographic enantioseparation by SMB was published by Negawa and Shoji (1992) who separated 1-phenylethanol on chiralcel OD. This pioneering work showed the superiority of SMB chromatography over batch chromatography with regard to increased productivity and decreased eluent consumption (1:87, SMB: batch). Afterwards, many applications have been developed and reported in the past ten years. Table 2.1 gives a comprehensive summary of various enantiosepartions by SMB technology so far reported in the open literature.

SMB process has shown to be reliable, economical and scaleable on laboratory- and pilot-scale for enantioseparations. The first industrial scale SMB system was installed by UCB-Pharma in Belgium for multi-ton production of a pharmaceutical compound. Several other pharmaceutical and fine-chemical companies, such as Bayer (Leverkusen, Germany), Universal Pharma Technologies (Lexington, MA, USA), Daicel (Himeji, Japan) and Aeroject Fine Chemicals (Rancho Cordova, CA, USA)

Table 2.1 Detailed descriptions of various investigations of enantioseparations using SMB technology

Substance	CSP& MP	System	Description of the work	Conclusions/contributions	References
1-phenylethanol	CSP: Chiralcel OD MP: n-hexane/isopropanol (90:10)	Laboratory set-up with 8-column(15cm×2.0cm ID) χ=1/4/2/1 A controller system Model 802-SC (Jasco) was used to control the recycle pump and the rotary valves.	Both batch mode and SMB experiments were carried out and compared. Loading: Q_f=0.5 ml/min c_f=39.1 g/l SMB purity: Ra: 98.0% Ex: 92.0%	SMB was superior to batch mode in achieving: (1) increased productivity (2) lower solvent consumption (3) higher raffinate concentration	Negawa & Shoji (1992)
pranziquantel	CSP: microcrystalline cellulose triacetate (MCTA) 25-40μm MP: n-hexane/2-propanol (80:20)	Laboratory set-up with 4-column (44.5cm×1.25 cm ID), χ=1/1/1/1; 2 pumps were used to control the feed and eluent flow rate; 2 flow meters to monitor the raffinate and extract flow rates with one needle valve to adjust the extract flow rate.	Experimental investigation was carried out. Loading: Q_f=0.3 ml/min c_f=50 g/l Purity: Ra: 90.09% Ex: 93.68%	Enantioseparation of racemic pranziquantel was achieved by the laboratory 4-zone SMB unit.	Ching et al. (1993)
1a,2,7,7a-tetrahydro-3-methoxynaphth-[2,3b] oxirene	CSP: cellulose triacetate (CTA) 25-40μm MP: methanol	Licosep 12-26 system from Novasep (France) with 12 columns (11cm ×2.6cm ID) , χ=3/3/3/3	Both simulation and experimental studies were carried out. A modified Langmuir isotherm obtained by single column experiments was used in the simulation. Effect of the recycle flow rate on the product purity was studied.	For a fixed switching time there existed an optimal recycle flow rate. Specific productivity could be improved either by using fewer columns or increasing the recycle flow rate. Higher recycle flow rate could help to increase the throughput. But product purity decreased when fewer columns were used.	Nicoud et al. (1993)

	CSP: ChiralCel OD 20μm MP: n-hexane/isopropanol (90:10)	Laboratory made set-up with 12 columns (10cm × 1.6cm ID), χ=3/3/3/3 A controller system Model 802-SC (Jasco) was used to control the recycle pump and the rotary valves.	Enantioseparation of a racemic epoxide was demonstrated on a semi-preparative SMB unit. Operating conditions were selected with the help of a single chart which depicted visually the relationship between the system flow rates and design criteria.	This empirically designed SMB unit performed better than the batch mode LC system in term of a lower consumption of the eluent.	Küsters et al. (1995)
	CSP: Microcrystalline cellulose triacetate (MCTA) 45μm MP: methanol	Licosep 12-26 system from Novasep (France) with 8 columns (9.9cm ×2.6cm ID) , χ=2/2/2/2	A transient TMB model combined with a competitive biLangnuir isotherm was used to simulate the system. The model predictions were in good agreement with the experimental results.	A simple optimization procedure was developed to obtain the complete separation area.	Pais et al. (1998a, b)
			A steady state TMB model was developed to describe the system performance with mass transfer resistance. The influence of mass transfer resistance on the complete separation region was analyzed and verified with experiments.	The complete separation was numerically predicted since biLangmuir isotherm was involved. Mass transfer resistance affected the separation region considerably when high purity requirement was desired.	Pais et al. (2000)
			The influence of mass transfer resistance on the selection of the SMB operating conditions and on	The presence of mass transfer resistance can significantly affect the performance of SMB, reducing the size of complete separation	Rodrigues & Pais (2004)

			the constraints of flow rate ratio in each section for nonlinear separation of enantiomers were presented in this work. The concept of separation volume was used to illustrate how the constraints of flow rate ratios have to be modified.	region. Besides, more restrictive constraints of flow rate ratios in sections 1 & 4 should be applied in the presence of mass transfer resistance. And a three –dimensional separation volume instead of a two-dimensional separation area was required to determine the operating conditions under non-ideal conditions.	
EMD 53986	CSP: cellusphere 20-45μm MP: methanol	Licosep 12-26 system with 12 columns (χ=3/3/3/3) was applied. Column length with 8.5 cm and 8 column with configuration of χ=2/2/2/2 were observed to give extremely good separation.	Design of a SMB unit for the enantioseparation of EMD 53986 was accomplished in this work. The effects of the column efficiency and particle size on the selection of column length were studied. Feed concentration was also optimized in this work.	The optimal design of a SMB process for the enantioseparation was first investigated. Equilibrium stage model and modified Langmuir isotherm were applied to the modeling of the system. Good agreement of the experimental data and simulations results were achieved.	Charton & Nicoud (1995)
	CSP: (1)cellulose-(p-methyl) tribenzoate beads 20–30 μm; (2) poly(N-acryloyl-amino acid ester) silica 20μm; (3) ChiralCel OJ 20μm; (4) ChiralPak AD 20μm MP: methanol / ethanol / ethyl acetate	Licosep 12-26 system with 8 columns	Enantioseparation of EMD 53986 was performed using Licosep 12-26 system on four different CSPs to find the most suitable CSP which gave the maximum specific productivity.	All the 4 CSPs are suitable to produce the desired enantiomer with a purity of 99%. ChiralCel OJ consumed the lowest amount of eluent while ChiralPak AD gave the highest specific productivity.	Schulte et al. (1997)

Tramadol	CSP: ChiralPak AD 20μm MP: 2-propanoal/benzine/ Diethylamine (5:95:0.1)	Laboratory set-up with 12 columns (10.0cm×2.12 cm ID), χ=3/4/3/2; 2 pumps were used for control the feed and eluent flow rate; 2 mass-flow meters and 2 control valves were used to control the raffinate and extract flow rates. A laboratory developed software was used to control the system	Very good separation of the enantiomers was achieved by the laboratory SMB set-up. Loading: Q_f=10 ml/min c_f=20 g/l Purity: Ra>99.9% Ex>99.5%	Both high productivity and low solvent consumption were obtained in SMB process compared with batch mode separation.	Cavoy et al. (1997)
Guaifenesin	CSP: ChiralCel OD 20μm MP: n-heptane/ethanol (65:35)	Sorbex Prep system (UOP, USA) equipped with 16 columns (6 cm ×2.1 cm ID)	Enantioseparation of three different racemates were accomplished on two kinds of CSPs. Good separation results were obtained for all the three chiral drugs. Effect of feed concentration and extract flow rate on the productivity and purity were also discussed.	More than 80% of the mobile phase could be saved by SMB. There is an optimal extract flow rates yielding both enantiomers with high purity.	Francotte & Richert (1997)
Formoterol Aminoglutethi-mide	CSP: ChiralCel OJ 20μm MP: n-heptane/ethanol (65:35)	Sorbex Prep system (UOP, USA) equipped with 16 columns (6cm×1.6 cm ID)			
SB202026	CSP: ChiralPak AD 20μm MP:n-hexane/2-propamol/ Diethylamine (95:5:0.1)	Licosep 12-26 system with 8 columns (10.5 cm ×2.6 cm ID), χ=2/2/2/2.	Both batch mode and SMB were operated. Loading: Q_f=2.6/4.3 ml/min c_f=20 g/l Purity: Ra=99.5%; Ex=97.8%	The Licosep 12-26 demonstrated its ability to produce over 60 g/day of each enantiomer with purities greater than 97.5% and a recovery exceeding 98%.	Guest (1997)

1,1'-bi-2-naphthol	CSP: 3,5-dinitrobenzoyl phenyl-glycine 25-40μm MP: heptane / isopropanol (72:28)	Licosep 12-26 system with 8 columns (10.5 cm ×2.6cm ID) , χ=2/2/2/2	A transient TMB model and biLangmuir isotherm model were adopted to simulate the system. Two SMB runs were performed to verify the simulation results. Loading: Q_f=3.64 ml/min c_f=2.9 g/l; Purity: Ra≥96.2%; Ex≥93.0% Recovery Ra≥91.6%; Ex≥97.3%	Process simulation could give a good prediction for the experimental operation, leading to high extract and raffinate purities as well as high recoveries acquired.	Pais et al. (1997)
			A steady state TMB model was developed to describe the system performance with mass transfer resistance. The influence of mass transfer resistance on the complete separation region was analyzed and verified with experiments.	The complete separation was numerically predicted since BiLangmuir isotherm was involved. Mass transfer resistance affected the separation region considerably when high purity requirement was desired.	Pais et al. (2000)
guaifenesin	CSP: ChiralCel OD 20μm MP: heptane/ethanol (65:35)	Sorbex Prep (UOP) system Equipped with 16 columns (6cm×2.1cmID), χ=5/5/5/1. As Q_4=0, actually this is a 3-zone SMB system	Triangle theory was applied to find the optimal operating conditions for the nonlinear system with ideal equilibrium model. 19 experimental runs were conducted to verify the design strategy.	Triangle theory provides a useful tool for the design of SMB process. It also concluded that within the complete separation region, increasing feed flow rate yielded an improvement of the productivities of both enantiomers.	Francotte et al. (1998)

Tröger's base	CSP: microcrystalline cellulose triacetate (MCTA) 15-25μm MP: ethanol	Laboratory made set-up with 8 columns (25cm×0.46 cm ID), χ=2/2/2/2 An open-loop mode was adopted which generated a total of five flow rates. 4 flow rates are controlled by 4 HPLC pumps.	Both theoretical and experimental investigations of the SMB process were performed in this work. Experimental results indicated that triangle theory provides a useful tool for selection of the operating parameters.	Triangle theory in qualitative terms was applied to provide guidelines for selecting the operating parameters. The role of extra-column dead volume in determining SMB performance has been analyzed and properly accounted for through the introduction of the generalized flow rate ratio parameter.	Pedeferri et al. (1999)
			SMB equipped with online monitoring system consisting of a UV detector and a polarimeter in series was developed in this work. The accuracy of the method was accessed by comparison with the off-line HPLC analyses.	The online monitoring system developed in this work has been proved effective for monitoring the absolute enantiomer concentrations in the product streams. The delay of the measurement caused by the back mixing in the line between the SMB loop and detector was solved by applying an appropriate control algorithm.	Zenoni et al. (2000)
			An experimental technique to design nonlinear SMB separations was presented. The predictions of the method were compared with experimental results. The effect of mass transfer and extra-column broadening were elucidated.	This method allowed rigorous solution of the equilibrium theory model to be approximated without knowing the exact adsorption equilibria. Therefore, it is extremely useful in developing a new separation system.	Migliorini et al. (2002)

	CSP: ChiralPak AD 20μm MP: 2-propanol	ICLC 16-10 (Novasep, France) with 8 columns (10cm×0.46cm ID), χ=2/2/2/2 Online monitoring system consisting of a UV-detector and a polarimeter afforded the possibility to obtain the internal concentration profiles of each enantiomer.	An unusual multilayer adsorption isotherm model adopted in this work made the numerical simulation the only way to define the separation area. SMB experiments for several selected operating points were also conducted to verify the calculation results. The influence of the heterogeneity of the column on the performance of SMB was also studied.	This work demonstrated that SMB process could be numerically designed for complex isotherms with an inflection point. The heterogeneity of the column, extra column volume and the behavior of the impurities in the feed could generate performance fluctuations during a whole switching cycle.	Mihlbachler et al. (2004)
DOLE	CSP: ChiralCel OF 20μm MP: n-hexane/2-propanol (50:50)	Licosep 12-100 system with 8 columns (10 cm ×10 cm ID), χ=2/2/2/2 Laboratory unit by UOP with 16 columns (15 cm ×3 cm ID) χ=6/6/3/1	Experiments using two different SMB set-ups were carried out based on the systematic simulations.	It was confirmed that higher flow-rate, shorter step time, can bring about larger productivity within the limitation of mechanical durability of equipment. ChiralCel OF has never indicated the limit of loadability for racemic DOLE in the range of operating conditions they have taken.	Nagamatsu et al. (1999)
two unknown racemates	not specified	A SMB system with 12 columns (11.6cm ×4.8 cm ID) An online analytical system was developed to get the cyclic steady state concentration profiles.	Both theoretical and experimental investigations were carried out in this work. The effect of the feed concentrations and the column configurations were discussed.	The online analytical system was first reported in obtaining the separation results.	Lehoucq et al. (2000)

1,2,3,4-tetrahydro-1-naphthol	CSP: ChiralPak AD 20μm MP: n-heptane/2-propamol/ trifluoroacetic acid (95:5:0.2)	μ-lab, a unit scaled down form Novasep pilot, with 8 columns (10cm × 1 cm ID)	The basic principle of Varicol process was first reported. Numerical examples compared the performances of Varicol with SMB and verified with several experiments.	Varicol performed better than SMB due to its high flexibility in the column configurations. The results in this work showed that an improvement of 18.5% in productivity could be achieved due to the introduction of Varicol operation mode for a 5-column system.	Ludemann-Hombourger et al. (2000)
			Systematic study on multi-objective optimization of both SMB and Varicol processes were first presented by using non-dominated sorting genetic algorithm (NSGA). Formulations for different combinations of objectives were developed. Optimal separation performances of SMB and varicol processes were compared.	NSGA is quite robust in providing a set of equally good solutions (Pareto solutions) for both SMB and Varicol processes. Performance of Varicol process is superior to that of a SMB in terms of either treating more feed using less eluent or producing better product purity for fixed productivity and solvent consumption.	Zhang et al. (2002a)
	CSP: ChiralCel OD MP: supercritical CO_2/ ethanol	Novasep unit with 8 columns (20cm×3.3cm ID) χ=2/2/2/2	The application of SFC- SMB was first reported for enantioseparation in this work. Experiments for both the pressure gradient mode and isocratic mode were performed.	Triangle theory has been extended to allow for different pressure values in different sections of the unit. Results demonstrated that almost 3-fold increase in productivity could be achieved in the pressure gradient rather than isocratic mode.	Denet et al. (2001)

mandelic acid	CSP1: teicoplanin 5µm MP1: ethanol/water (50:50), unbuffered MP2: ethanol/water (50:50) pH6.56 MP3:methanol/acetonitrile /triethylammonium-acetate/ acetic acid (54.5:45:0.25:0.25) pH6.5 MP4: methanol/water (20:80) pH4.02	Column dimension (15 cm ×0.46 cm ID)	The influence of different sets of adsorption isotherms on the achievable productivities in the enantiomers by SMB technology was studied. Langmuir isotherm parameters on two different CSPs using 5 different mobile phases were measured. Several SMB experiments were also carried out to study the impact of isotherm parameters.	Parametric studies revealed the selectivity factor has a large impact on the process productivity. For preparation applications the column saturation capacity and solubility limits of the solutes have important impact on system performance.	Kaspereit et al. (2002)
	CSP2: nucleodex 5µm MP5: water/acetic acid/ Acetonitrile (86.4:9.1:4.5) pH3.0	Column dimension (20 cm×0.4 cm ID)			
ibuprofen	CSP: Kromasil CHI-TBB 10µm MP: CO_2/isopropanol	Laboratory unit with 8 columns (9.7 cm×3 cm ID)	SFC-SMB separation of ibuprofen was studied in the linear range with a dilute feed. Several experiments were carried out to verify the simulation results.	A good agreement between model predictions and experimental results was obtained. By changing the column configuration from 2/2/2/2 to 2/2/3/1, an improvement of productivity was also achieved.	Peper et al. (2002)
SB-553162	CSP: ChiralPak AD 20µm MP: acetonitrile/methanol (80:20)	Column dimension (8.1 cm ×1 cm ID)	Vaicol process was used to perform the separation of optical isomers of SB-553261	Varicol performs better than SMB with respect to both increased specific productivity and reduced eluent consumption.	Ludemann-Hombourger et al. (2002)

			The performances of SMB and Varicol were optimized with NSGA for the enantioseparation of SB-553261. A few single and two-objective optimization problems were presented.	Significant improvement could be made for both SMB and Varicol by the systematic optimization. Performance of Varicol is superior to that of a SMB in terms of increasing productivity and achieving better product quality.	Wongso et al. (2005)
Unknown racemate	CSP: ChiralPak AD 20μm MP: methanol	(1) Laboratory Licosep 12-16 unit with 8 columns (9.5cm×3cm ID) (2) Pilot SMB unit with 8 columns (8.8cm×20cm ID)	Batch and SMB were utilized for the chromatographic resolution of more than 1 ton of racemate.	High productivities and lower solvent usage were observed with SMB relative to batch chromatography. Impurities in the feed or solvent resulted in a decrease of productivity with time in the pilot SMB unit.	Miller et al. (2003)
α-ionone	CSP: Nucleodex-β-PM 10μm MP: methanol	Laboratory made set-up with 8 columns (25cm×0.46 cm ID), χ=1/1/2/4 An open-loop mode was adopted which generated a total of five flow rates. 4 flow rates re controlled by 4 HPLC pumps.	Both SMB and PowerFeed experiments were conducted based on the rigorous simulation and optimization study.	PowerFeed can outperform SMB with the same desorbent consumption and throughput provided the proper switching time is selected. Both raffinate and extract purities in PowerFeed are better than the corresponding values in the SMB process. Good agreement between the simulation and experimental results revealed that PowerFeed is one of the feasible implementations for multicolumn continuous chromatography.	Zhang et al. (2004)

Nadolol	CSP: perpheyl carbamoylated β-cyclodextrin MP: water/methanol (80:20) pH5.5	Laboratory made 5 section SMB unit with 10 columns (25×1cm ID), χ=2/2/2/2/2	Continuous separation of a ternary mixture of nadolol in either 2-raffinate or 2-extract SMB system with 5 sections was studied in this work. Design strategy based on the triangle theory was developed to both 2-raffinate and 2-extract configurations. Experiments were also performed to verify the design.	Desired enantiomer of Nadolol can be produced with a high purity and yield in the 2-raffinate configuration while a high purity but considerably decreased yield of this component was obtained in 2-extract configuration. Experimental results indicated that SMB process has the ability for difficult chiral separations, especially for that of 2-chiral center drugs, which could be difficult to fulfill in the batch mode, provided the same efficiency of column was employed.	Wang & Ching (2005)

possess SMB units of various capacities. In spite of the success of the aforementioned attempts, further research is still needed to reduce the production costs. Besides, robust and efficient on-line detection and control systems are also need to be developed to guarantee that SMB performs as desired.

2.2.2 Ternary separations

The major limitation of a 4-zone SMB chromatographic system is that it can only perform a binary separation, which means feed containing two or more components can be split only in two fractions. However, there can be a situation where the separation of three or more components is necessary. In such a case, performing multi-component separation becomes essential. Attempts to overcome the limitation of classical SMB for ternary separation have been reported sporadically and a total of four types of modifications can be found. The first is done by alternating two different adsorbents in the four section configuration (Hashimoto et al., 1993) for the separation of starch-glucose-NaCl mixture. The second type of modification is to separate the ternary mixture using two different desorbents in a six zone SMB system (Hotier et al., 1990).

Modification by adding a fifth section (Navarro et al., 1997) or combining two conventional units into a single device, the third type, has been investigated extensively. In case a separation of a ternary mixture with components A, B and C, in which C is the most weakly adsorbed component, A the most strongly adsorbed while B is the intermediate of the two in terms of adsorption affinity, 5-zone SMB actually can be regarded as a modification of classical 4-zone SMB with a side stream introduced at the point of highest concentration of component B. The introduction of the side-stream in section 2 would result in the division of that section. The separator would then have five sections in total and two extract streams, with the feed located

(a)

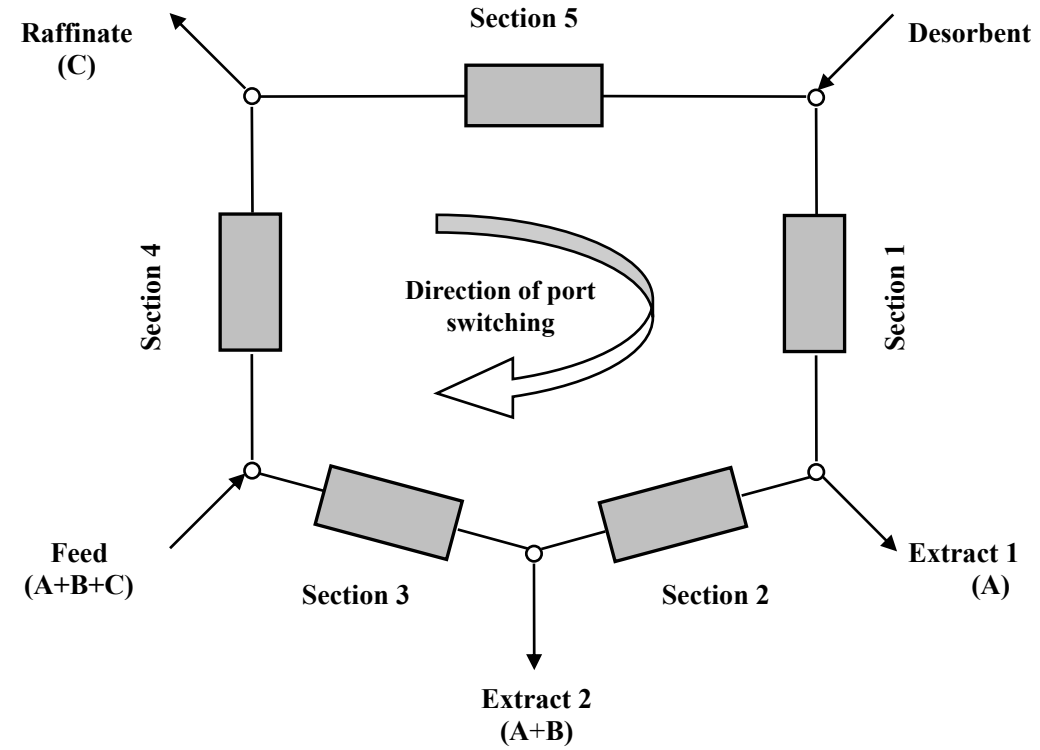

(b)

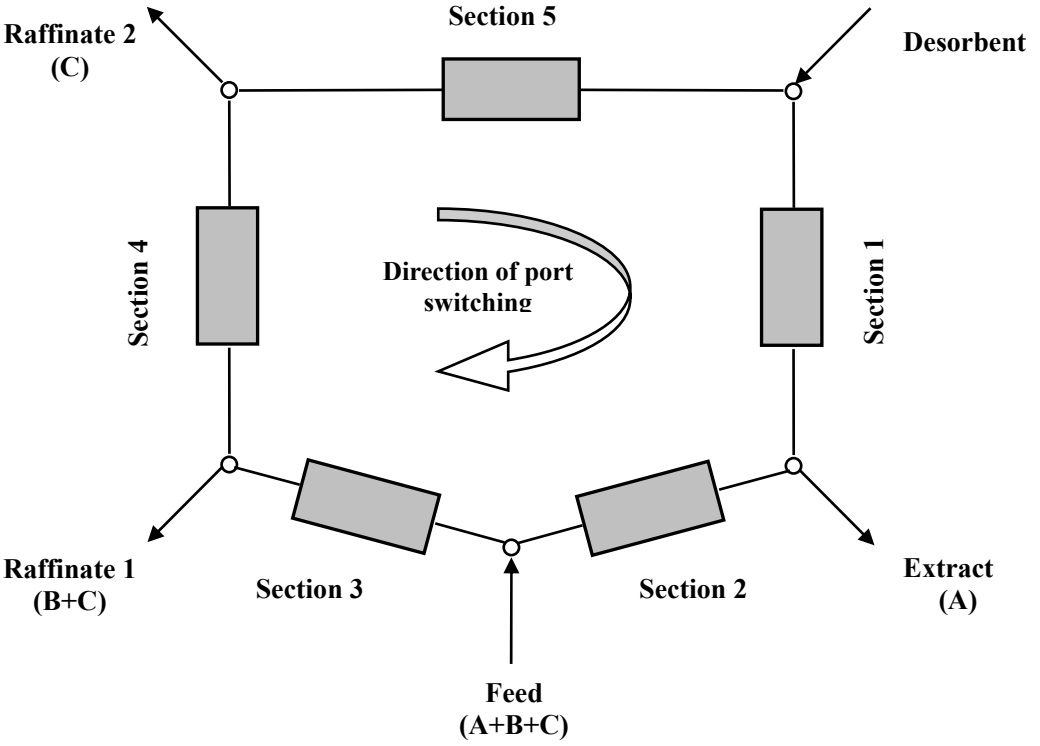

Figure 2.4 Five-zone SMB for ternary separation, (a) five-zone SMB with two extract streams, (b) five-zone SMB with two raffinate streams

between sections 3 and 4 (Figure 2.4a). Similarly, positioning the side-stream in the raffinate region would create the separator with two raffinate streams and a feed located between sections 2 and 3 (Figure 2.4b). For both configurations, desired separation is achieved if each component migrates to its corresponding product outlet as described in Figures 2.4a & b. However, it should be noted that in both cases only pure A and C can be obtained, component B has to be collected either with A in the 2-extract configuration or with C in the 2-raffinate configuration. If three components are equally valuable and have to be obtained at high purity and yield, two binary SMBs or eight/nine zone SMB would be necessary.

Figures 2.5a & b illustrate an 8-zone system coupling of two 4-zone SMBs and a 9-zone system combined a 5- and 4-zone SMB respectively. Three inlet streams (feed and two desorbent inlets), three product outlet streams and the bypass stream withdrawn from one point to another point split the system into eight sections. In case of 9-zone system an additional product outlet is available. 8-zone SMB has been reported in Chiang (1998) and Nicolaos et al. (2001a and b). 9-zone SMB was first applied by Wooley et al. (1998) to recover two sugars, glucose and xylose from a biomass hydrolyzate. It was shown that 9-zone SMB is more favorable for obtaining complete separation of a ternary system and that the most difficult separation has to be performed by the second SMB.

Another type of modification is the pseudo-SMB process. Pseudo-SMB process is patented as JO SMB process by the Japan Organo Company (Ando et al., 1990). It is initially applied in sugar industry when Sayama et al. (1992) recovered raffinose from beet molasses. The application was extended to multi component mixtures containing raffinose, sucrose, glucose and betaine (Masuda et al., 1993). This process is divided into two steps as described in Figure 2.6 based on a 4-zone SMB. In the first step, feed

(a)

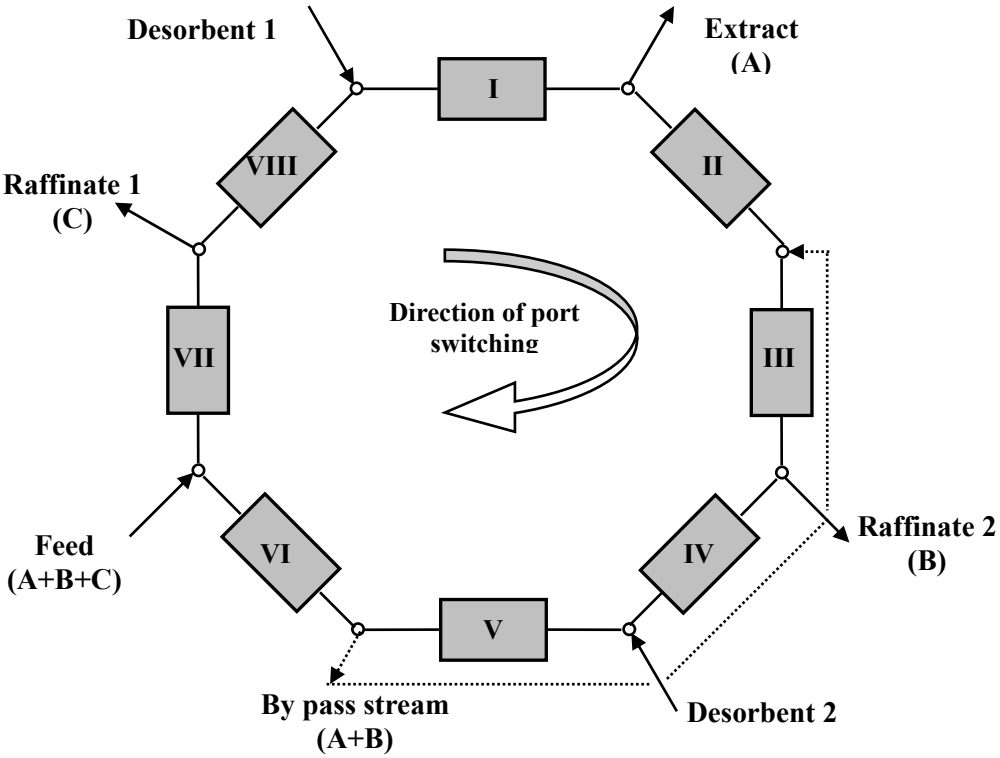

(b)

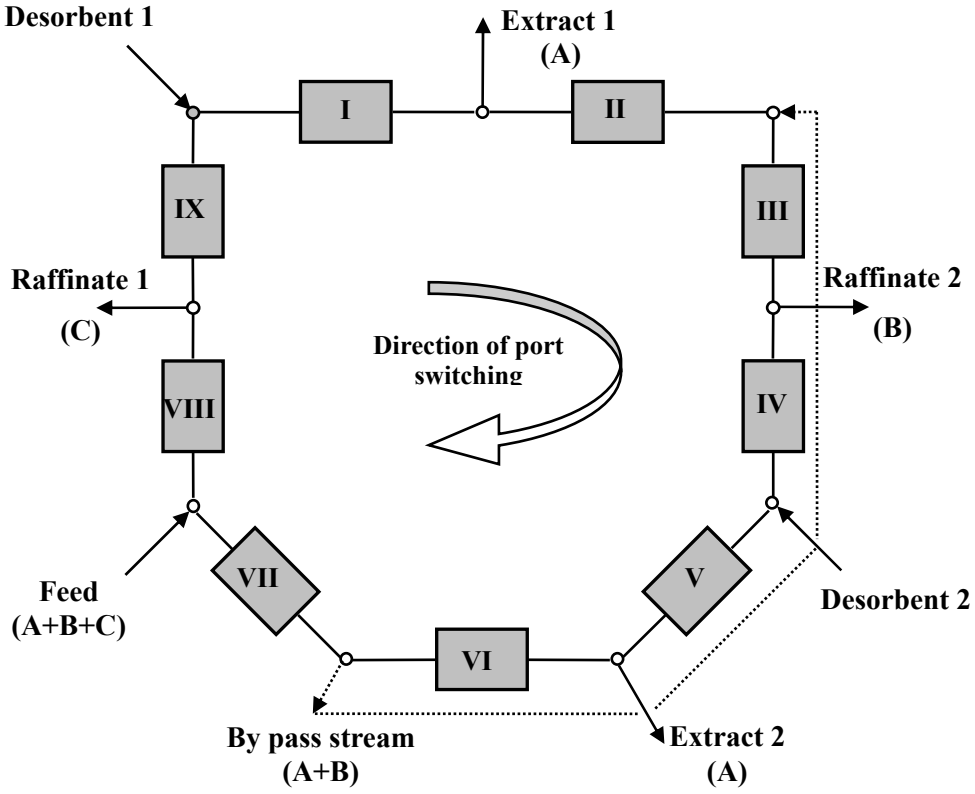

Figure 2.5 Eight-zone SMB (a) and nine-zone SMB(b) systems for ternary separation

and desorbent streams are introduced into the system, which works as a series of chromatographic columns without any port switching, an intermediate stream containing component B comes out from the end of section 2. In the second step, the system operates in the same way as it does in the SMB mode except for the absence of feed, and the most retained component A is collected in the extract while the least retained component C is collected in the raffinate.

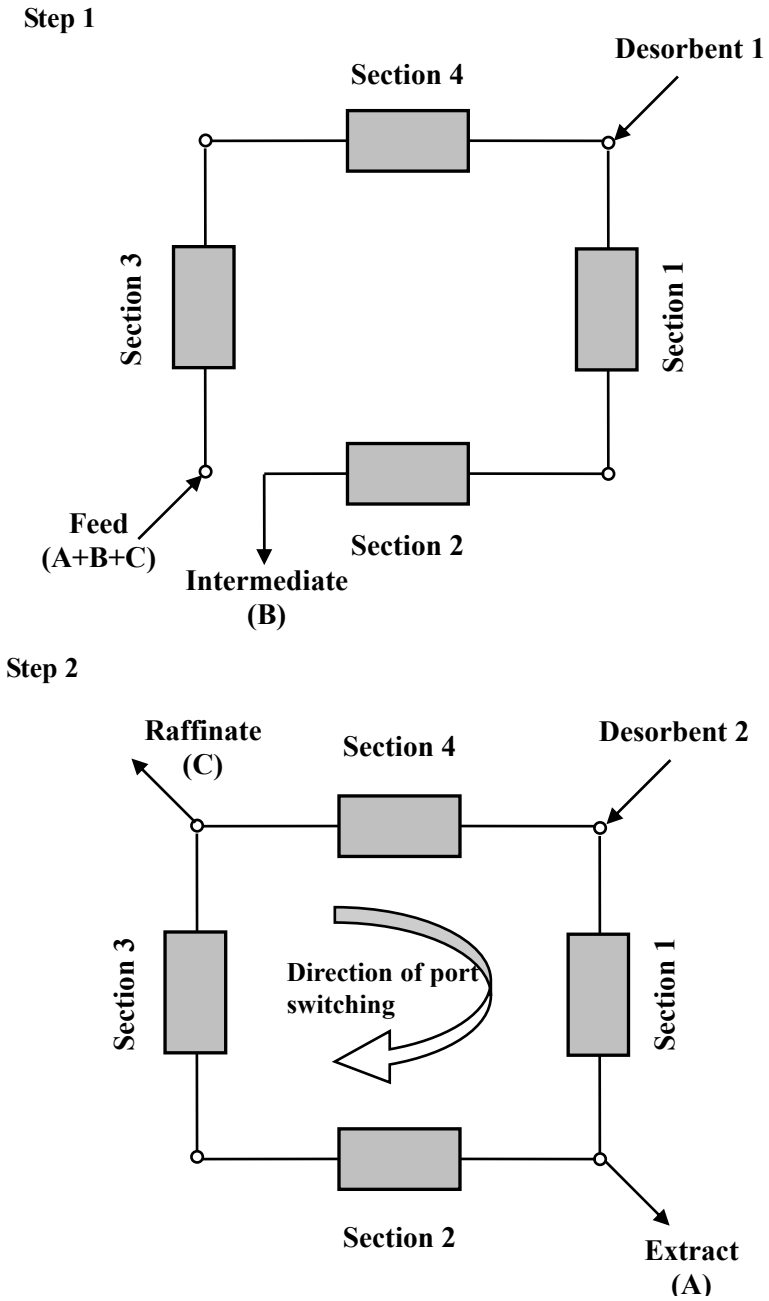

Figure 2.6 Pseudo-SMB system for ternary separation

Selection of the relative migration velocities of the three components is of great importance in the application of this pseudo SMB process. Only with the suitable migration velocities, three components can be well distributed in the two phases and the complete separation of them becomes possible. Normally, it is required that towards the end of step 2 component A should stay with the solid in section 1 and comes out in the extract stream, and component B is well separated with component A and completely inside section 2 while component C migrates with the fluid and comes out in the raffinate. Then, during the first step of the next cycle, component B accumulated in the solids of section 2 can be collected in the intermediate stream thus enabling the continuous separation of a ternary system. Theoretical study for the pseudo-SMB system can be found in Mata and Rodrigues (2001) and Kurup et al. (2006).

2.2.3 Biochemical reactions

Applications of simulated moving bed chromatographic reactors in the biochemical field have also attracted a lot of interest. Hashimoto et al. (1983a) first developed a hybrid SMB bioreactor system for the production of high-fructose syrup by enzymatic isomerization of glucose. A 3-zone SMBR system without raffinate was used. Reactors and adsorption columns were arranged alternatively in section 3, while only adsorption columns were used in the two desorption sections. By applying this system, high fructose syrup containing more than 55% of fructose could be produced using less amount of desorbent compared with the conventional process.

Barker and colleagues investigated the enzymatic conversion of sugars using the calcium form of an ion-exchange resin as the adsorbent (Barker et al., 1987; Barker and Ganetsos, 1988; Akintoye et al., 1990, 1991; Barker et al., 1992). A preparative

scale unit consisted of 12 columns was used in their studies. Three kinds of reactions including sucrose inversion to glucose and fructose, biosynthesis of dextran and saccharification of a modified starch were studied and the calcium form of either a purolite ion-exchange resin or a Korela resin was used as adsorbents. Since the enzymatic reactions occur in the aqueous phase, enzymes, at low concentrations were added to the system with the water eluent.

Akintoye et al. (1990, 1991) found that in-situ separation of glucose and fructose helped to minimize the substrate-inhibition problem which is apparent in the presence of products. Sucrose inversion was readily carried out to completion at 25°C in their system even for concentrated solutions. Enzyme usage was only 20% of that consumed in the stirred batch reactor without removal of glucose and fructose.

The results of biosynthesis of dextran from sucrose using enzyme dextransucrase were a little complicated (Barker et al., 1992). Initially, complete conversion of sucrose was obtained at a relatively lower throughput and a dextran-rich product free of fructose was recovered due to the simultaneous removal of the byproduct fructose. However, the separation of dextran and fructose deteriorated after 50 h of operation and glucose was found to be present as the experiment progressed. The gradual build up of the glucose-forming side reaction was caused by the displacement of Ca^{2+} from the resin by some amount of K^{+} and Na^{+} in the enzyme. Although on-line regeneration of resin with calcium nitrate relieved such a problem, undesired glucose byproduct still could not be eliminated due to the formation of leven.

For the production of maltose and dextrin from modified starch, starch conversion of 60% was achieved with maltose purity of 96%. Enzyme consumption was substantially reduced compared with a conventional batch bioreactor (Shieh and Barker, 1995). The effect of the eluent flow rate, switching time, feed concentration

and enzyme activity on the maltose yield, starch conversion and product purity were investigated. Conflict interactions among these variables were observed, e.g. increased switching time improved the purity of maltose, however, decreased the starch conversion.

Unlike Barker's study of the irreversible reactions, Kawase and co-workers (Kawase et al., 2001, Pilgrim et al., 2006) took up the application of SMBR to a reversible multi-reaction system, i.e. the enzyme catalyzed production of lactosucrose. In this process, lactosucrose was produced by an enzymatic transfer reaction from sucrose and lactose using β-fructofuranosidase accompanied by hydrolysis of sucrose to glucose and fructose and hydrolysis of lactosucrose to fructose and lactose. The primary reaction is reversible while the other two are irreversible. A 4-zone SMBR system consisted of 12 columns was developed to carry out the experimental investigation. A linear driving force model was adopted to calculate the saccharides concentrations. Mathematical model and system parameters were verified with experimental data. The effect of various operating parameters was investigated. By optimizing the flow rates, substrate and enzyme concentration and the reaction temperature, a maximum predicted yield of lactosucrose could reach 69% at 65°C, which represented an increase of 36% relative to the equilibrium yield.

Studies on the optimization of the various SMBR systems for the sucrose inversion have also been reported (Meurer et al., 1996; Azevedo and Rodrigues, 2001; Dünnebier et al., 2000; Kurup et al., 2005a).

2.3 Design and optimization strategies for SMB process

Many design and optimization strategies have been developed for the SMB process over the past few decades. Triangle Theory, Standing Wave concept and Separation

Volume are probably the most important design methods widely used. This section is dedicated to a brief introduction of the methods for the design and optimization of SMB process.

2.3.1 Triangle theory

Similarity between true moving bed (TMB) and simulated moving bed (SMB) processes makes the TMB approach applicable to estimate the operating parameters of SMB unit. Operating parameters for TMB process are the liquid flow rates in the four sections (Q_{ϕ}^{TMB}), and the volumetric flow rate of the adsorbent (Q_s). These TMB parameters can be transferred into SMB operating parameters (Q_{ϕ}^{SMB}, t_s) following the relationship as below.

$$\frac{V}{t_s} = \frac{Q_s}{1-\varepsilon_b} \tag{2.1}$$

$$Q_{\phi}^{SMB} = Q_{\phi}^{TMB} + \frac{Q_s \varepsilon_b}{1-\varepsilon_b} \tag{2.2}$$

An ideal TMB process model, which neglects axial dispersion and mass transfer resistances, is considered for the separation of a binary system consisting of components A and B (with A being the more strongly adsorbed component).

$$\frac{\partial}{\partial \tau}[\varepsilon_t c_i + (1-\varepsilon_t) q_i] + (1-\varepsilon_b)\frac{\partial}{\partial \xi}[m_{\phi} c_i - q_i] = 0 \tag{2.3}$$

where τ and ξ are the dimensionless time and space coordinates; ε_t is the overall void fraction of the column, ε_b is the intraparticle porosity; m_{ϕ} is the ratio between the net fluid and the solid flow in each section.

Triangle theory, proposed by Storti et al. (1993) and Mazzotti et al. (1997) was one of the approaches based on the analytical solutions of the above described TMB model. In this method, a triangular region, which denotes the complete separation area, is

formed by a (m_2, m_3) plane for the linear or non-linear isotherm with or without mass transfer resistance. Criteria for the selection of the dimensionless flow rate ratio (m_ϕ) was developed for the design of a TMB or SMB unit. In terms of the operating parameters of an equivalent SMB unit, m_ϕ is defined as:

$$m_\phi = \frac{Q_\phi^{SMB} t_s - V\varepsilon_t}{V(1-\varepsilon_t)} \tag{2.4}$$

Constraints of m_ϕ values, which lead to the complete separation of a binary mixture with linear isotherm, are listed below.

Section 1: $H_A < m_1 < \infty$ (2.5a)

Section 2: $H_B < m_2 < H_A$ (2.5b)

Section 3: $H_B < m_3 < H_A$ (2.5c)

Section 4: $m_4 < H_B$ (2.5d)

An additional constraint, $m_2 < m_3$, required by positive feed flow rate, combines constraints on m_2 (Eq. 2.5b) and m_3 (Eq. 2.5c) into one,

$$H_B < m_2 < m_3 < H_A \tag{2.5e}$$

This inequality defines the projection of the four-dimensional region of complete separation region to the (m_2, m_3) plane shown in Figure 2.7a. If the constraints on m_1 and m_4 are fulfilled, the whole region of the (m_2, m_3) plane is divided into four parts. The triangular-shaped region in the middle of the diagram indicates the complete separate region, where 100% pure products can be collected both in the extract and raffinate. However, in the pure extract region, the third constraint is not fulfilled, consequently, the strong adsorbed component A is carried upwards from section 3 into section 4 thus polluting the raffinate stream, whereas extract is still 100% pure. Similarly, in the pure raffinate region, where m_2<H_B, only 100% pure raffinate can be

obtained. The region in the top-left corner where both $m_3 > H_A$ and $m_2 < H_B$ corresponds to operating conditions under which none of the 100% pure product can be collected either in extract or in raffinate.

Triangle theory was further applied to nonlinear systems, where adsorption equilibrium properties are described by means of competitive Langmuir isotherm:

$$q_i = \frac{H_i c_i}{1 + \Sigma b_i c_i} \qquad \text{(i=A, B)} \tag{2.6}$$

The same equilibrium model was employed to determine the design conditions on flow rate ratios for nonlinear system, and the following conditions were obtained for complete separation (Mazzotti et al., 1994; Mazzotti at al., 1996a):

$$H_A = m_{1,\min} < m_1 < \infty \tag{2.7a}$$

$$m_{2,\min}(m_2, m_3) < m_2 < m_3 < m_{3,\max}(m_2, m_3) \tag{2.7b}$$

$$\frac{-\varepsilon_p}{1-\varepsilon_p} < m_4 < m_{4,\max}(m_2, m_3) = \frac{1}{2}\left\{H_B + m_3 + b_B c_{B,f}(m_3 - m_2)\right\} - \sqrt{[H_B + m_3 + b_B c_{B,f}(m_3 - m_2)]^2 - 4H_B m_3} \tag{2.7c}$$

The lower bound on m_1 and upper bound on m_4 are explicit, whereas the latter one is dependant on the flow rate ratios m_2 and m_3. However, the implicit constraints of m_2 and m_3, independent of m_1 and m_4, define the complete separation region, which is also a triangle-shaped region illustrated in Figure 2.7b. It was found that in case of nonlinear systems, the shape of the complete separation region depends on the feed concentration. The effect of the overall feed concentration on the region of complete separation in the (m_2, m_3) plane is shown in Figure 2.7c. The area of complete separation region decreases with the increase of feed concentration.

The procedure described so far requires a detailed knowledge of the adsorption equilibrium. However, experimental determination of the isotherm parameters might

consume a lot of time and substance. Recently, a simplified short-cut approach was reported to determine the constraints of m_ϕ values without knowing the exact adsorption equilibria for the Langmuir –type isotherms (Pais, et al., 1998a; Susanto et al., 2005).

It is known that retention times for desorption and adsorption fronts can be calculated by the derivative of the isotherm and the secant of the isotherm respectively, according to the following equations:

$$t_{R,i}^{des}(c^+) = t_0\left(1+\frac{1-\varepsilon_t}{\varepsilon_t}\cdot\left.\frac{\partial q_i}{\partial c_i}\right|_{c^+\to 0}\right) \tag{2.8}$$

$$t_{R,i}^{ads}(c^+) = t_0\left(1+\frac{1-\varepsilon_t}{\varepsilon_t}\cdot\left.\frac{q_i}{c_i}\right|_{c^+=c_f}\right) \tag{2.9}$$

These equations can be transferred to continuous SMB or TMB chromatography where dispersive desorption as well as adsorption shock fronts are present. Flow rate ratio m_ϕ can be described as the function of either the initial slope or the secant of the isotherm. Criteria for the constraints of m_ϕ values listed in the followings are recommended based on the analysis of the situation in each section of a SMB unit.

Section 1: $$m_{1,\min} = \left.\frac{\partial q_A}{\partial c_A}\right|_{c_A\to 0;c_B=0} \tag{2.10a}$$

(more retained component A to be desorbed while no B being present)

Section 2: $$m_{2,\min} = \left.\frac{\partial q_B}{\partial c_B}\right|_{c_A=0;c_B\to 0} \tag{2.10b}$$

(less retained component B to be desorbed here)

Section 3: $$m_{3,\max} = \left.\frac{q_A}{c_A}\right|_{c_A=c_f;c_B=c_f} \tag{2.10c}$$

(component A to be adsorbed in this section; the highest possible velocity to occur

when both components being at their highest possible concentrations.)

Section 4: $$m_{4,\max} = \left.\frac{q_B}{c_B}\right|_{c_A=0;c_B=c_f} \tag{2.10d}$$

(component B to be adsorbed and no A being present)

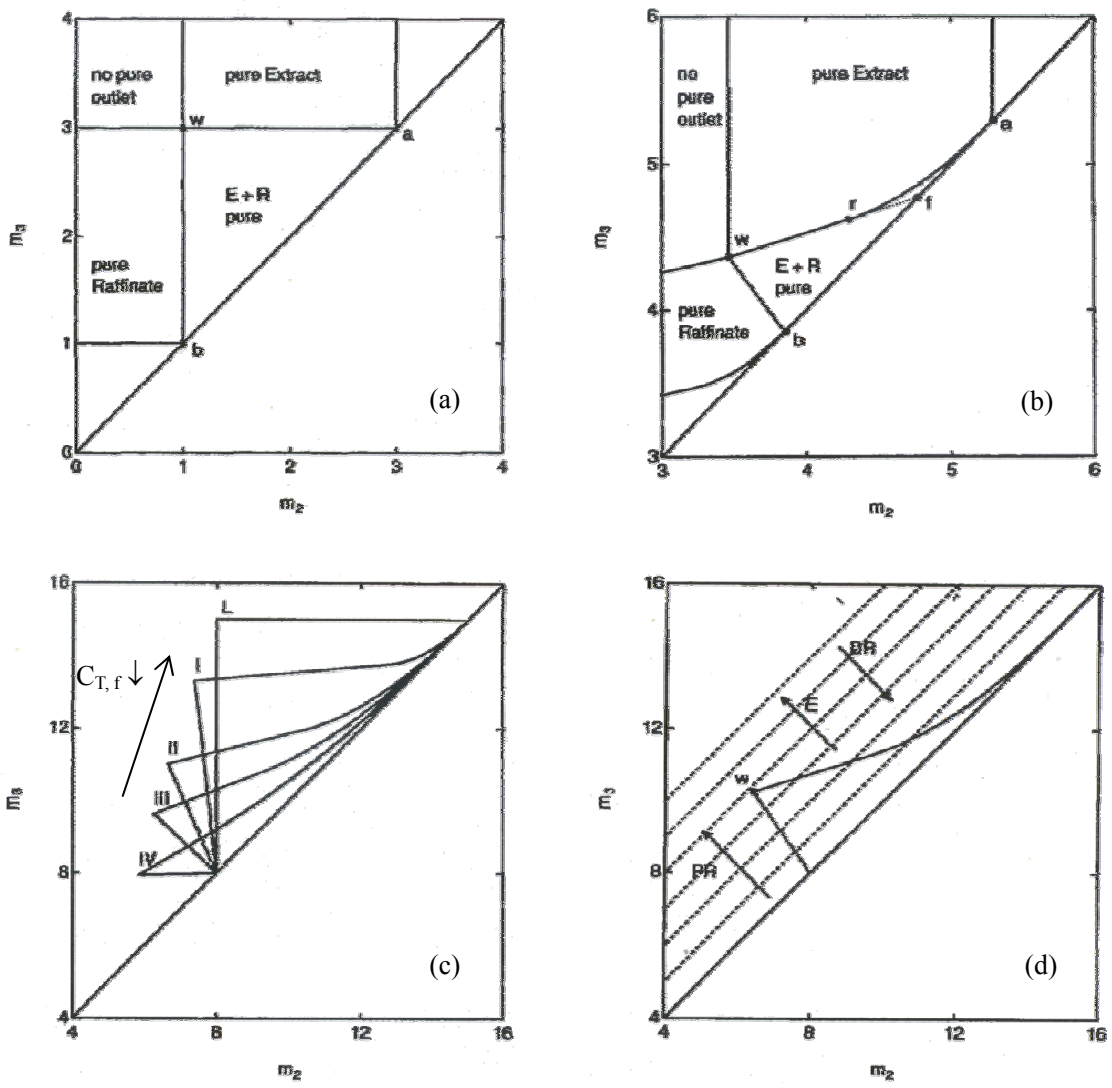

Figure 2.7 Triangle theory: Regions of the (m_2, m_3) plane with different separation regimes in terms of purity of the outlet streams

(Storti et al., 1993; Mazzotti et al., 1996a, 1997)

(a) System described by a Linear Adsorption isotherm
(b) System described by a Langmuir adsorption isotherm
(c) Effect of the overall concentration of the feed mixture on the region of complete separation in the (m_2, m_3) plane
(d) Application of Triangle theory to the design of optimal operating conditions

Comparison of the results obtained from this short-cut method with those from constraints in Eq. 2.7a to Eq. 2.7c shows that this short-cut method gives a rather accurate guess of the operating parameters within the complete separation area (Pais et al., 1998a).

Application of the method described so far neglects the effects of axial dispersion and other mass transfer resistances within the SMB system. Design strategy of the SMB or TMB process in the presence of axial dispersion and mass transfer resistance was also reported (Migliorini et al., 1999a; Biressi et al., 2000). However, in this case the method becomes more complicated and a trial and error method has to be employed.

2.3.2 Separation volume analysis

Explicit criteria for the choice of SMB operating conditions are obtainable from the equilibrium model if axial mixing and mass transfer resistance are negligible. In case of the columns with low efficiency, effects of axial dispersion and mass transfer resistance are the main source of deviation from the results of equilibrium theory, and the regions of the separation will virtually reduce in comparison with the ideal region. If the constraint on the purity is too strict, the separation region may eventually not exist. In such a case, constraints of the flow rate ratios derived from the equilibrium model in triangle theory need to be modified. The methodology, called "separation volume analysis" provided the ways to solve the problem (Azevedo and Rodrigues, 1999; Rodrigues and Pais, 2004).

Unlike triangle theory, in which the complete separation is defined by a two dimensional (m_2, m_3) plane provided that the constraints of m_1 and m_4 are satisfied, in separation volume analysis, a three-dimensional plot ($\gamma_1 \times \gamma_2 \times \gamma_3$) is employed to

visualize the volume region where separation can be achieved within the purity constraints fixed by the operator. Here, γ_ϕ is also a flow rate ratio and is related to m_ϕ used in triangle theory by $\gamma_\phi = (1-\varepsilon_b)m_\phi / \varepsilon_b$. Results from the SMB separations of both linear and nonlinear systems indicated that mass transfer resistances could affect the constraints of γ_1 and γ_4 significantly. Critical value of γ_1 higher than that stated by the equilibrium theory is required in the presence of mass transfer resistances and the lower the mass transfer coefficient, the higher the critical value for γ_1. In addition, complete separation regions have the varying size for various values of γ_1. Only when γ_1 is greater than a certain value, the separation region reaches a constant size. However, the effect of the mass transfer resistance on the critical value for γ_4 is not as obvious as it is for γ_1.

It must be emphasized that under non-ideal conditions, numerical simulation is necessary to find the three-dimensional separation volume instead of the two-dimensional separation area. Separation volume analysis has been successfully applied to the design and optimization of SMB processes for the glucose and fructose separation (Azevedo and Rodrigues, 2001) and p-xylene separation (Minceva and Rodrigues, 2002, 2005).

2.3.3 Standing wave concept

A research group in Purdue University, US, has proposed another novel method, the standing wave concept, to derive the design equations of the SMB process. A series of explicit algebraic equations are derived from the analysis to link product purity and recovery to section lengths, fluid velocities in the four sections, solid movement velocity, column capacity factors and mass-transfer coefficients. Optimal interstitial and bed velocities can be found from these equations. Efficiency for the search of the

design and operating parameters that guarantee desired separation has been improved significantly by avoiding the trial and error process in this method. Standing wave concept has been applied to analyze the separation of raffinose and fructose (Ma and Wang, 1997), separation of fructose and glucose (Mallmann et al., 1998), amino acid separation (Wu et al., 1998), paclitaxel separation (Wu et al., 1999), and insulin purification (Xie et al., 2002; Mun et al., 2003).

Based on the idea that each section should perform its own specific separation role to ensure product purities, standing wave concept analyzes the concentration waves of the two solutes in each section of a TMB. By proper choice of the four flow rates and the solid movement velocity in a TMB (or equivalent port switching time in SMB), the advancing front of the less retained component B can be made standing in section 4 and its desorption front standing in section 2. While, the adsorption front of the more retained component A is made standing in section 3 and its desorption front standing in section 1, as shown in Figure 2.8 for linear system with mass transfer resistance (Wu et al., 1999).

Similar to triangle theory, an equivalent true moving bed (TMB) model was also used to derive the standing wave equations. For example, in section 1, the transport equations for a component in the mobile phase and in the pore phase are:

$$\frac{\partial c_{bi}}{\partial t} = Da_i^1 \frac{\partial c_{bi}}{\partial z^2} - u_1^{TMB} \frac{\partial c_{bi}}{\partial z} - Pk_{fi}^1 (c_{bi} - c_{pi}) \tag{2.11}$$

$$\varepsilon_p \frac{\partial c_{pi}}{\partial t} + (1-\varepsilon_p)\frac{\partial q_i}{\partial t} = k_{fi}^1 (c_{bi} - c_{pi}) + u_s \varepsilon_p \frac{\partial c_{pi}}{\partial z} + (1-\varepsilon_p) u_s \frac{\partial q_i}{\partial z} \tag{2.12}$$

where P is the phase ratio related to the bed viodage ε by P=(1-ε)/ ε; ε_p is intraparticle voidage; Da_i^1 and k_{fi}^1 are axial dispersion coefficient and lumped mass-transfer coefficient in section 1 respectively. The equivalent SMB interstitial

velocities are related to TMB interstitial velocities by:

$$u_i^{SMB} = u_i^{TMB} + u_s \tag{2.13}$$

For a linear system with negligible axial dispersion and mass transfer resistance, the following equation was derived form Eqs 2.11 and 2.12 (Ma and Wang, 1997):

$$(1+P\delta_i)\frac{\partial c_{bi}}{\partial t} + [u_1^{SMB} - u_s(1+P\delta_i)\frac{\partial c_{bi}}{\partial z} = 0 \tag{2.14}$$

where $\delta_i = \varepsilon_p + (1-\varepsilon_p)H_i$; H_i is the linear equilibrium constant of component i.

From Eq. 2.14, the linear velocity of the concentration wave of component i (u_{wi}) relative to the feed point is:

$$u_{wi} = -\frac{dz}{dt} = \frac{u_1^{SMB}}{1+P\delta_i} - u_s = u_{sol,i} - u_s \tag{2.15}$$

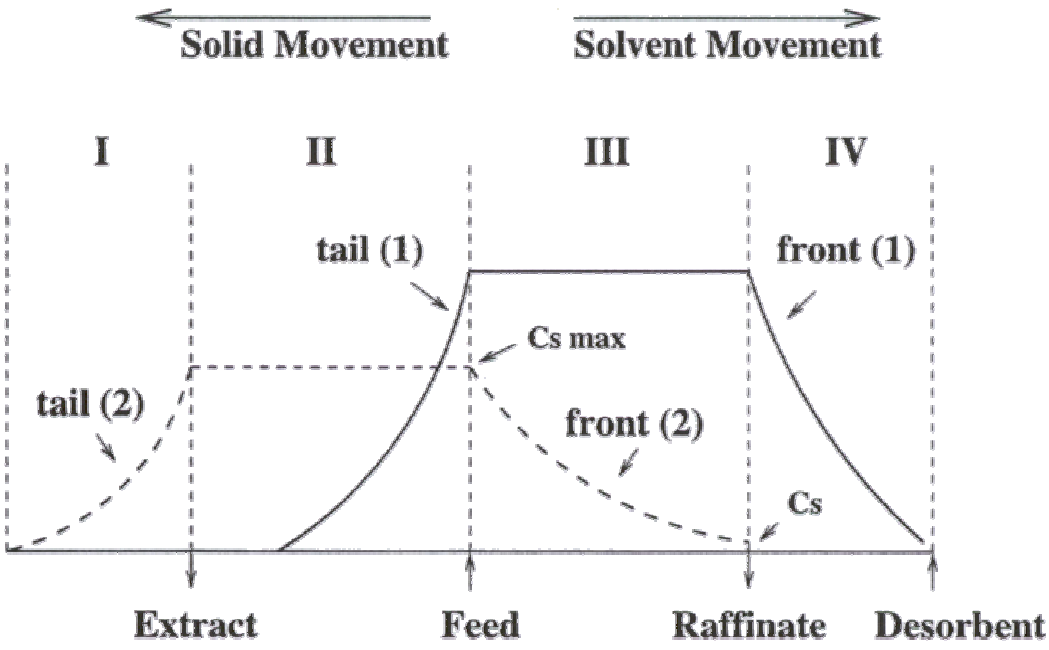

Figure 2.8 Standing Wave in a linear TMB system (Wu et al., 1999)

Therefore, u_{wi} is determined by two independent linear velocities, i.e. the solid movement velocity (u_s) and the solute migration velocity ($u_{sol,i}$). In order to have separation, the migration velocity wave of the more retained component (A) should be less than u_s in section 3 and that of the less retained component (B) should be less than u_s in section 4; the desorption wave of solute A should be greater than u_s in section 1 and that of solute B should be greater than u_s in section 2. In summary, the following conditions for the velocities in each section were proposed to be satisfied for a complete separation.

Section 1: $u_{sol,A} - u_s > 0$ (2.16a)

Section 2: $u_{sol,B} - u_s > 0$ (2.16b)

Section 3: $u_{sol,A} - u_s < 0$ (2.16c)

Section 4: $u_{sol,B} - u_s < 0$ (2.16d)

To achieve the four standing waves, fluid velocity in each section which results in highest feed flow rate and lowest solvent flow rate should be selected according to the following relationships corresponding to the boundary values defined in Eqs. 2.16a-d.

$$u_1^{SMB} = (1 + P\delta_A)u_s \quad (2.17a)$$

$$u_2^{SMB} = (1 + P\delta_B)u_s \quad (2.17b)$$

$$u_3^{SMB} = (1 + P\delta_A)u_s \quad (2.17c)$$

$$u_4^{SMB} = (1 + P\delta_B)u_s \quad (2.17d)$$

Any other values that satisfy Eqs. 2.16a-d result in higher u_1^{SMB} and u_2^{SMB} and lower u_3^{SMB} and u_4^{SMB}, and in turn result in a lower feed flow rate and a higher eluent flow rate for a fixed solid velocity. If one more condition, either the feed flow

rate Q_f or desorbent flow rate Q_D is given, all the fluid and solid phase movement velocities can be calculated from Eqs, 2.16a-d and one of the following mass balance equations.

$$\frac{Q_f}{\varepsilon A} = u_3^{SMB} - u_2^{SMB} \tag{2.18a}$$

$$\frac{Q_D}{\varepsilon A} = u_1^{SMB} - u_4^{SMB} \tag{2.18b}$$

When mass transfer effects were taken into account, steady –state model was used to derive the analytical solutions, which means the time derivative item in mass balance equations 2.11 and 2.12 was omitted. The complete solutions of the linear fluid velocities for the four sections can be found from the following four equations (Eqs 2.19a-d) and one of the mass balance equations in Eq. 2.18a or b.

$$u_1^{SMB} = (1 + P\delta_A)u_s - \beta_A^I\left(\frac{Da_A^I}{L^I} + \frac{Pu_s^2\delta_A^2}{k_{f,A}^I L^I}\right) \tag{2.19a}$$

$$u_2^{SMB} = (1 + P\delta_B)u_s - \beta_B^{II}\left(\frac{Da_B^{II}}{L^{II}} + \frac{Pu_s^2\delta_B^2}{k_{f,B}^{II} L^{II}}\right) \tag{2.19b}$$

$$u_3^{SMB} = (1 + P\delta_A)u_s + \beta_A^{III}\left(\frac{Da_A^3}{L^{III}} + \frac{Pu_s^2\delta_A^2}{k_{f,A}^{III} L^{III}}\right) \tag{2.19c}$$

$$u_4^{SMB} = (1 + P\delta_B)u_s + \beta_B^{IV}\left(\frac{Da_B^{IV}}{L^{IV}} + \frac{Pu_s^2\delta_B^2}{k_{f,B}^{IV} L^{IV}}\right) \tag{2.19d}$$

where superscripts I to IV represent the sections 1 to 4 in a SMB system; β_i is the purity requirement of component i, defined as the ratio of the highest to the lowest concentration of the standing wave in one section, e.g., $\beta_B^{III} = \ln\left(\frac{c_B|_{z=0}}{c_B|_{z=L^{III}}}\right)$.

The standing wave concept was further developed to nonlinear systems, but without mass transfer effects (Mallmann et al., 1998).

The advantages of all the approaches based on the stationary TMB process are simple models and, in some cases, the possibility of direct analytical solutions. Although deviations of the results obtained from these approaches may happen due to the simplified assumptions, these methods still provide the basis for a more or less proper guess of the operating parameters. By combining with a more detailed SMB model and applying a robust optimization algorithm, these approaches can become very useful tools for us to obtain the optimal operating parameters for the real SMB processes.

2.3.4 Numerical optimization methods

Numerical optimization is very useful in obtaining the optimal operating parameters of a SMB unit. Especially for nonlinear system with mass transfer resistance, numerical optimization seems to be the only possible choice. Quite a few studies have been reported in the open literature on numerical optimization of SMB processes (Storti et al., 1988; Proll and Kusters, 1998; Karlsson et al., 1999; Dünnebier et al., 2000; Toumi et al., 2002, 2003; Zhang et al., 2002a, b; Subramani et al., 2003; Yu et al., 2003b; Wongso et al., 2004). All these studies fall into two categories. One is the single-objective optimization with any of the separation cost, purity of the desired product or productivity of the product as the objective. Decision variables that are related to system flow rates were optimized while the certain requirements on the product purities and maximum flow rate acted as constraints. The other is the multi-objective optimization where two or three objectives could be optimized at the same time. The reason for applying multi-objective optimization is due to the fact that in case of SMB separation conflict objectives, such as maximizing productivity of the desired product while minimizing solvent consumption, exist.

Multi-objective optimization problems are conceptually different with those of

single-objective. In multi-objective optimization, there may not be a best solution with respect to all objectives. Instead, there could be an entire set of optimal solutions that are equally good. These solutions are known as Pareto-optimal (non-inferior) solutions. A Pareto set is defined such that when we move from any one point to another, at least one objective function improves and at least one other worsens. Thus, one cannot say that any one of these points is superior (or dominant) to any other, and therefore, any one of the non-inferior solutions in the Pareto set is an acceptable solution. The choice of one solution over other solutions requires additional knowledge of the problem, and often this knowledge is intuitive and non-quantifiable. The Pareto set narrows down the choices and helps to guide a decision-maker in selecting a desired operating point from the restricted set of Pareto-optimal points rather than from a much larger number of possibilities (Bhaskar et al., 2000a).

A research group in National University of Singapore has attempted the multi-objective optimization study of SMB processes. A novel state-of-the-art optimization technique, the Genetic Algorithm (Holland, 1975) was adopted to find the Pareto solutions for the multi-objective optimization problems. Genetic algorithm mimics the process of natural selection and natural genetics. Darwinian's principle of 'survival of the fittest" is used to generate improved solutions (Deb, 2001). The Elitist Non-dominated Sorting genetic Algorithm, NSGA-II (Deb et al., 2002) has proved to give better convergence criteria as it maintains the concept of elitism in which the good population is preserved by introducing dummy fitness value and later characterized in several fronts. The recent adaptation with jumping genes (Kasat et al., 2002) has improved the diversity of hypothetic mating pool leading to a much better spreading of solutions at increased convergence speed. The jumping gene operations adapt a modified mutation operator, borrowing from the concept of jumping genes in

natural genetics.

Several research papers have been published to present their optimization studies of SMB processes using NSGA-II and NSGA-II-JG. Zhang et al. (2002a) reported the application of NSGA in the optimization of a SMB unit for the enantioseparation of 1,2,3,4-tetrahydrol-1-naphthol and also exemplified the merits of using a Varicol for this separation. Another article by Zhang et al. (2002b) presented the multi-objective optimization of a reactive SMB process in which methyl tertiary butyl ether (MTBE) was directly synthesized from tertiary butyl alcohol (TMA) and methanol. In both studies, quite a few double objective optimization problems were formulated and solved to obtain Pareto-optimal solutions. Yu et al. (2003b) reported multi-objective optimization studies on reactive SMB and Varicol for the synthesis of methyl acetate using NSGA-II. Considerable improvements in terms of purity and yield of methyl acetate were obtained for the existing experimental set-up by applying multi-objective optimization. Wongso et al. (2004) carried out the multi-objective optimization of SMB process for enantioseparation of SB-553261 racemate. Results showed that significant improvement of process performance could be made by applying the multi-objective optimization study. Also recently, multi-objective optimization of an industrial–scale SMB process for recovery of p-xylene has been accomplished by Kurup et al. (2005b). Significant improvement could be obtained for SMB performance by optimizing the column length and its distribution in various sections.

Very recently, a method called standing wave annealing technique (SWAT) was introduced to solve either single- or multi-objective optimization problems of SMB (Cauley et al., 2004). A stochastic optimization algorithm, simulated annealing was used to solve the nonlinear mathematical models based on Standing Wave Concept for two SMB systems, the separation of glucose from sulfuric acid and the separation of

insulin from an impurity. The simulated annealing algorithm provides a powerful tool for overcoming the computational challenges resulting from the nonconvexity in the model. However, this method still can not be applied to nonlinear separation systems with mass transfer resistance due to the difficulty in obtaining the explicit algebraic standing wave equations.

Chapter 3 Optimal Design and Operation of Hashimoto's Hybrid SMB Bioreactors

3.1 Introduction

The commercial applications of immobilized enzymes are of increasing interest, both in the food industry and in the synthesis of numerous compounds (Vos et al., 1990). The inversion of corn syrup to enhance fructose content, catalyzed by glucose isomerase, is a paradigm of success of the industrial application of enzymatic technology (Giordano, et al., 2000). High fructose syrup (HFS) is a sweetener used in numerous foods and beverages (starting from bread to pasta sauces to bacon to beer) as sugar substitute because of its high quality characteristics, stability, high osmotic pressure, and crystallization control. HFS is extremely soluble, retains moisture, resists drying out, prevents microbiological growth and blends easily with many foods and flavorings. As such, HFS is extremely similar to regular table sugar (sucrose), which is a 50/50 blend of fructose and glucose, but fructose is about 75% sweeter than sucrose. Three standard grades of HFS, namely, HFS42, HFS55 and HFS90 are produced containing 42%, 55% and 90% fructose respectively, with the remaining being mainly glucose and some higher saccharides. HFS42 is popular in canned fruits, condiments and other processed foods, which need mild sweetness. Sweeter HFS55 is commonly used in soft drinks, ice cream and frozen desserts, while, HFS90 is used in low calorie foods.

In producing these sweetener products, starch, a polymer of glucose, is heated and processed with enzymes that hydrolyze the starch into 98-100% glucose syrup. In order to produce fructose syrups, glucose is further processed in the presence of an isomerase enzyme, which converts glucose into its isomer, fructose. The conversion is

equilibrium limited and with the current enzymatic isomerization technology, the conversion of glucose to fructose is economically limited to 42% fructose. Since soft drink industries require HFS55 product, simulated moving bed (SMB) chromatographic separation is used to concentrate the fructose to 90%, which is then blended with HFS42 to produce HFS55. However, in order to obtain HFS90, a relatively large amount of desorbent (water) and energy are consumed, thus it is not a particularly economic method for producing HFS55 in industry.

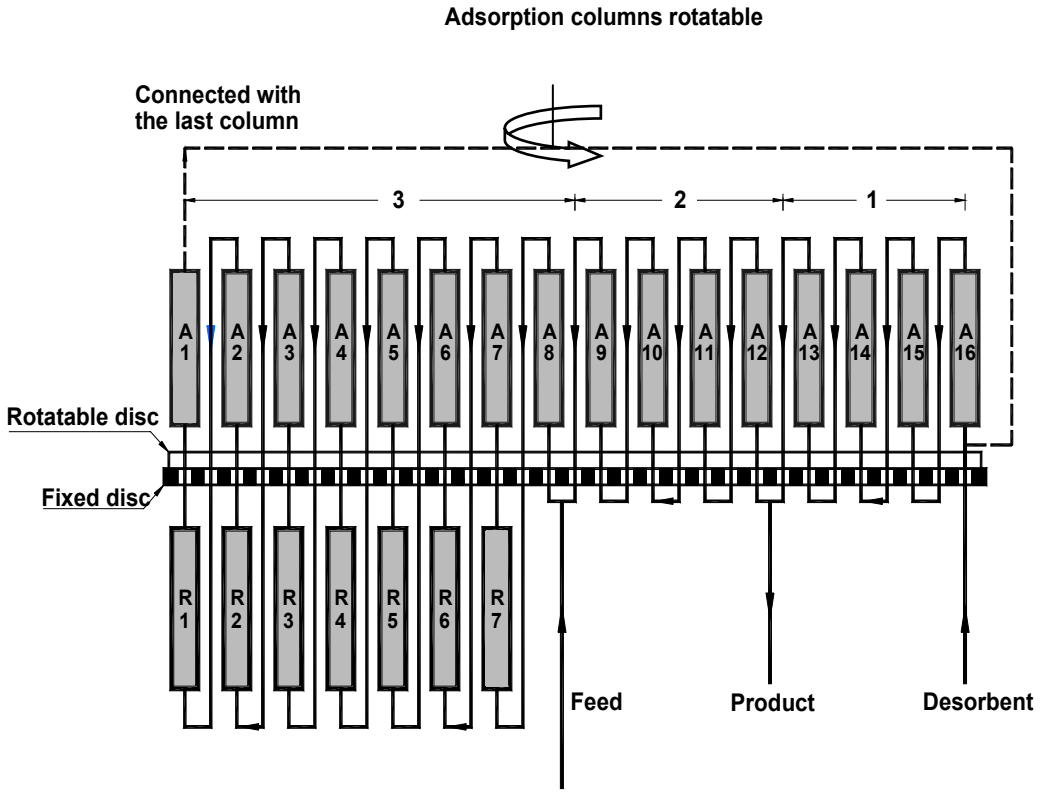

Figure 3.1 Schematic diagram of Hashimoto's SMBR unit for isomerization of glucose to fructose

The thermodynamics of the isomerization reaction favors fructose production at higher temperatures and HFS55 could be produced directly if the enzyme reactors were operated at around 370 K, which is still a challenge to enzyme technology. Hashimoto et al. (1983a, b) developed a hybrid SMB system to produce HFS by combining immobilized enzyme catalyzed isomerization reaction with adsorptive separation of glucose and fructose. Figure 3.1 shows schematically the system consisting of 16 adsorption columns and 7 enzymatic reactors. The introduction of feed, desorbent and withdrawal of product streams divided the system into three zones. The reactors and adsorption columns were arranged alternately in zone 3 while zones 1 and 2 consisted of only adsorption columns. The continuous countercurrent movement of the liquid streams and solid adsorbent were simulated by advancing the adsorption columns against the fixed inlets and outlets of liquid streams, while the enzyme reactors remained stationary. Synchronous switching of the three ports in the direction of the fluid flow mimicked the movement of solid phase countercurrently. Feed stream flows into the adsorption column A8 where fructose is primarily adsorbed and glucose rich stream leaving column A8 enters reactor R7. In the reactor, glucose is converted to fructose almost to the equilibrium level. By introducing the mixture through the adsorption columns and reactors alternatively in zone 3, most of the glucose in the mixture is converted to fructose, which is preferentially adsorbed in the subsequent adsorption columns. Hence, the liquid stream emerging from zone 3 contains very little of either glucose or fructose, and are recycled as part of the desorbent. Fructose adsorbed in zone 3 is carried to zones 1 and 2 by port switching. Zone 2 functions to recycle glucose into zone 3 while most of the fructose adsorbed in zone 3 is desorbed in zone 1 and is recovered in the product stream. The adsorption columns in zone 1 are simultaneously regenerated. By proper adjustment of the switching time and fluid flow

rates in each zone, fructose of required purity could be collected at the product port. Hashimoto et al. (1983a) compared the desorbent consumptions between their new hybrid SMBR systems with that of the conventional SMB separation system. Results indicated that although conventional SMB separation can produce high fructose content, the new system can produce HFS55 with much less desorbent consumption.

Many factors influence the design and performance of such a complex process, which must be optimized systematically (Charton and Nicoud, 1995; Lode et al., 2001; Ray and Carr, 1995b). The relative large number of variables such as switching time, lengths and number of columns and flow rates in various zones, complicates the optimization problem. Clearly, the bottleneck for the production capacity of HFS55 is the consumption of solvent (water), and therefore, compromise has to be reached in order to optimize the economics of the process. Optimization study in this chapter aims at finding the optimum design and operating parameters for Hashimoto's hybrid SMBR system to obtain higher productivity of HFS55 using minimum desorbent. Because the two objectives, namely maximizing the net productivity of fructose and minimizing the desorbent consumption cannot be achieved simultaneously, multi-objective optimization is needed for the system. As both continuous and discrete decision variables needed to be optimized in this hybrid SMBR process, traditional optimization algorithms seem to be inapplicable. Non-dominated sorting genetic algorithm with jumping genes (NGSA-II-JG), which allows handling of these complex optimization problems, is utilized in this study.

3.2 Mathematical model

In order to optimize the hybrid SMBR system, an accurate mathematical model is absolutely necessary. Two different modeling approaches are generally used to describe the process behavior. The first is the SMBR model which takes into account

of the shifting of inlet and outlet streams of the process (Hashimoto et al., 1983a; Storti et al., 1988; Pais et al., 1998; Strube, 1999; Zhang et al., 2002b and Yu et al., 2003a). Mathematically, SMBR model is achieved by linking the models of individual columns with the mass balances for the external inlet and outlet streams. The change of the boundary conditions for every individual column due to the port switching is also taken into account in the SMBR model. The second approach is the TMBR model which neglects the discrete dynamics and assumes a true counter-current flow of the solid and the liquid phase due to the analogy between the two processes. TMBR model can be simply developed from the model for batch column by adding a convection item in the mass balance with the solid velocity u_S. The TMB modeling strategy requires much less computational effort to be solved and steady state can be calculated directly; while, SMB modeling strategy is more precise and allows the visualization of the axial movement of concentration profiles and variations in extract and raffinate concentration within a switching period (Ray and Carr, 1995a; Azevedo and Rodrigues, 2001).

In this work, the more accurate SMBR model (same as that reported by Hashimoto et al. (1983a)) was adopted based on linear adsorption isotherm and linear driving force approximation for the adsorption kinetics. The mass balance equations in the fluid and solid phase for component i (glucose or fructose) in the j^{th} adsorption column during the N^{th} switching period are given by

$$\frac{\partial c_{ij}^N}{\partial t} + \frac{u}{\varepsilon_S}\frac{\partial c_{ij}^N}{\partial z} + \frac{1-\varepsilon_S}{\varepsilon_S}\frac{\partial q_{ij}^N}{\partial t} = 0 \tag{3.1}$$

$$(1-\varepsilon_S)\frac{\partial q_{ij}^N}{\partial t} = k_f a_v (c_{ij}^N - c_{ij,e}^N) \tag{3.2}$$

The adsorption isotherm is given by

$$q_{ij}^{N} = K_i c_{ij,e}^{N} \tag{3.3}$$

The mass balance equations in the reactors are given by

$$\varepsilon_R \frac{\partial c_{G,j}}{\partial t} = -u \frac{\partial c_{G,j}}{\partial z} - (1-\varepsilon_R)R \tag{3.4}$$

$$\varepsilon_R \frac{\partial c_{F,j}}{\partial t} = -u \frac{\partial c_{F,j}}{\partial z} + (1-\varepsilon_R)R \tag{3.5}$$

The rate equation for the isomerization of glucose to fructose, is expressed by

$$R = \frac{R_m (c_G - c_F / K_e)}{K_m + c_G + c_F} \tag{3.6}$$

Initial conditions for the system are

When $N = 0$; $c_{ij}^{0} = 0$ (3.7)

When $N \geq 1$

$$c_{ij}^{N} = c_{i,j+1}^{N-1} \quad \text{for} \quad j = 1 \sim (N_{S1}+N_{S2})$$

$$c_{ij}^{N} = c_{i,j+2}^{N-1} \quad \text{for} \quad j = (N_{S1}+N_{S2}+1), (N_{S1}+N_{S2}+3) \sim (N_T-2)$$

$$c_{ij}^{N} = c_{i1}^{N-1} \quad \text{for} \quad j = N_T \tag{3.8}$$

Boundary conditions for the system are

Eluent inlet point:

$$c_{i,1}^{N}\,|_{z=0} = \frac{Q_3}{Q_1} c_{i,N_T}^{N-1}\Big|_{z=L_S} \tag{3.9}$$

Product withdrawal point:

$$c_{i,N_{S1}+1}^{N}\,|_{z=0} = c_{i,N_{S1}}^{N}\,|_{z=L_S} \tag{3.10}$$

Feed point:

$$c_{i,N_{S1}+N_{S2}+1}^{N}\,|_{z=0} = \frac{Q_2}{Q_3} c_{i,N_{S1}+N_{S2}}^{N}\Big|_{z=L_S} + \frac{Q_f}{Q_3} c_{i,f} \tag{3.11}$$

For reversible reaction, achieving high conversion of the reactant and high purity

of product are the major objectives in SMBR system. Net productivity of fructose (Pr_F), conversion of glucose (X_G) and purity of fructose in the product (Pur_F) are the three parameters used to evaluate the performance of the SMBR system. The three parameters are defined as

$$Pr_F = \frac{\int_0^{t_S} (Q_P c_{F,P} - Q_f c_{F,f}) dt}{t_S} \tag{3.12}$$

$$X_G = \frac{\int_0^{t_S} (Q_P c_{F,P} - Q_f c_{F,f}) dt}{Q_f c_{G,f} t_S} \tag{3.13}$$

$$Pur_F = \int_0^{t_S} \frac{c_{F,P}}{c_{F,P} + c_{G,P}} dt \tag{3.14}$$

Concentration profiles within the columns are obtained by solving equations 3.1-3.11 numerically. The PDEs were first discretized by finite difference method to convert into a set of ODE-IVPs and then the resultant first-order ODEs were solved using DIVPAG (based on Gear's algorithm) in IMSL library. In this study, 50 cycles which means 800 switches of the adsorption columns were applied in the simulation to assure that cyclic steady state has been reached. The operating parameters for two experimental runs of Hashimoto et al. (1983a) are listed in Table 3.1. Figure 3.2 compares the concentration profiles of our simulation results with that of the experimental as well as the simulation results reported by Hashimoto et al. (1983b). Figure 3.2 clearly shows that our simulation results can predict the experimental concentration profiles within the columns better than reported by them. The sums of square error (SSE) of C_G and C_F between our simulation results and the experimental data for Run 6 are 28.9% and 47.6% lower than those between their simulation results and experimental data.

Table 3.1 Operating conditions for isomerization of glucose

(Hashimoto et al., 1983a)

Run		R-6	R-7
$c_{G,f}$	mol/l	1.0	1.0
$c_{F,f}$	mol/l	1.0	1.0
Q_f	ml/min	0.144	0.144
Q_D	ml/min	0.438	0.378
Q_3	ml/min	3.948	4.0
t_s	min	3.0	3.0
K_m	mol/l	0.14	0.37
R_m	mol/l/min	0.1272	0.0528
K_e		1.0	1.0
$k_f a_v$	min^{-1}	0.041	0.041
T_R	K	323	323
χ		4/4/8/7	4/4/8/7
d	cm	1.38	1.38
L_S	cm	10.2	10.2
L_R	cm	18.0	18.0

Table 3.2 Kinetic parameters and system performance at different T_R

T_R K	$K_{m,}$ mol/l	R_m mol/l/min	K_e	Pr_F g/h	Pur_F	X_G
323	0.14#	0.1272#	1.0#	0.382	0.633	0.245
333	0.31*	0.567*	1.129*	0.457	0.658	0.295

Hashimoto et al. (1983a); * Camacho-Rubio et al. (1995)

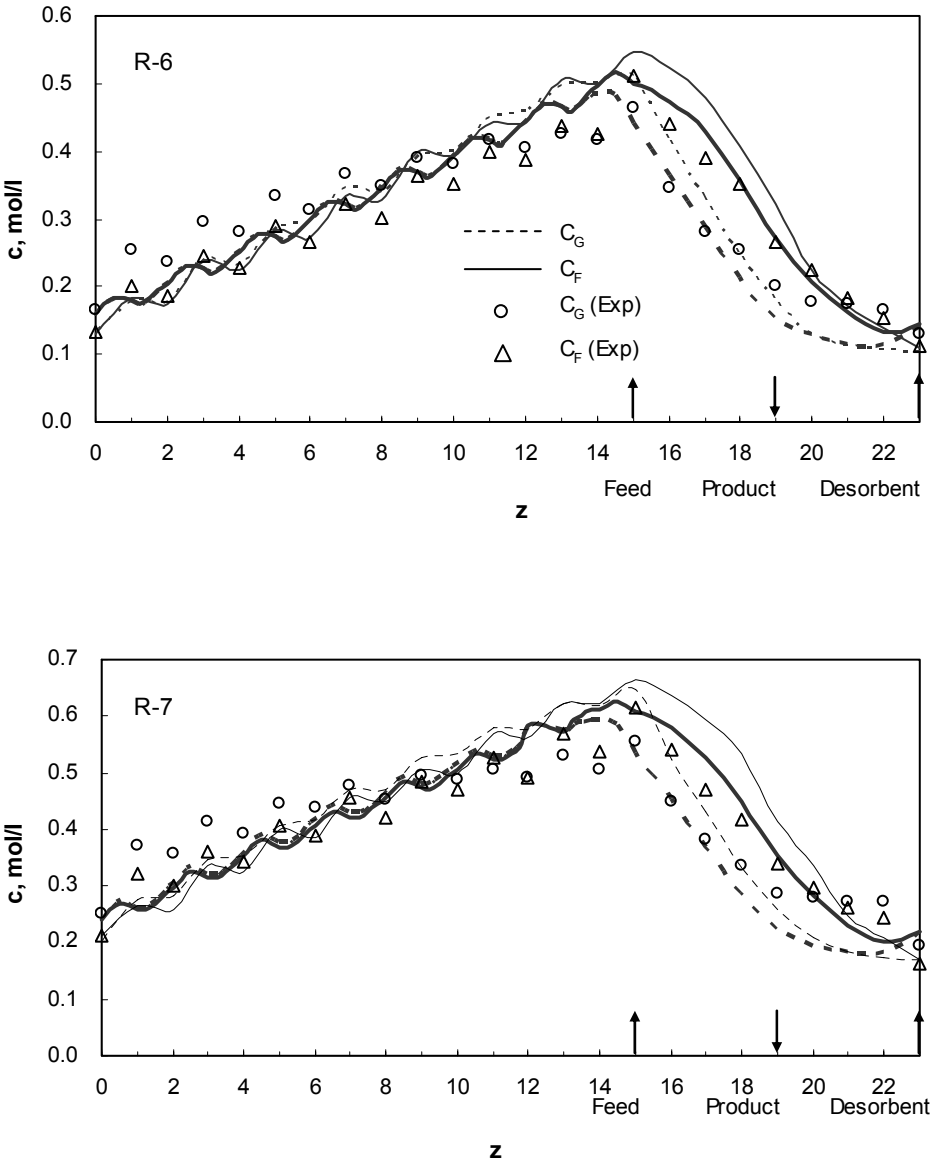

Figure 3.2 Concentration profiles of glucose and fructose after 800 switching periods.

R-6: *PrF* =0.382 g/h, Pur_F = 0.633, X_G = 0.245; R-7: Pr_F = 0.41 g/h, Pur_F = 0.612, X_G = 0.204. Symbols and thin lines are R-6 and R-7 reported in Hashimoto et al. 1983a; Thick lines: our prediction. Details of process parameters are given in Table 3.1.

Temperature is a very important operating parameter for this system since it affects both the adsorption isotherm and the reaction rate. In Hashimoto's study, the operating temperature was set as 323K. At this temperature, the equilibrium constant for the isomerization reaction is 1.0 and hence, the conversion for the glucose is only 24.5%. Camacho-Rubio et al. (1995) reported kinetic study of glucose-fructose isomerization at different temperature and reported equilibrium constant to be 1.129 at 333 K. Table 3.2 lists the reaction rate constants and simulation results at different reaction temperatures. The results indicate that both the productivity and the purity of fructose increase when the reaction temperature increases from 323K to 333K even when the other operating parameters are kept constant. In the following optimization study, 333K was chosen as the operating reactor temperature.

3.3 Multi-objective optimization for Hashimoto's hybrid SMBR system

A few double-objective optimization studies were conducted in this work to improve the productivity of HFS55 while keeping on reducing the desorbent consumption. In all the optimization runs presented in this chapter, 50 chromosomes (solutions) were considered and results were obtained after 50 generations. It should be noted that optimization problems involved both continuous variables such as column length, flow rates and switching time and discrete variables such as number of the columns in various sections. Table 3.3 describes the list of the optimization problems formulated and solved in this study.

3.3.1 Case I. Optimization of the existing set-up

Case I aims at optimizing the existing SMBR set-up in obtaining maximum productivity of fructose (Pr_F) of at least 60% purity using minimum desorbent (Q_D). The optimization problem is represented mathematically by:

Maximize $J_1 = Pr_F(Q_3, Q_D, t_s)$ (3.15a)

Minimize $J_2 = Q_D(Q_3, Q_D, t_s)$ (3.15b)

Subject to $Pur_F \geq 0.6$ (3.15c)

$X_G \geq 0.3$ (3.15d)

Three decision variables were selected as indicated in Eq.3.15a: the desorbent flow rate (Q_D), switching time (t_s), and internal flow rate in Zone 3 (Q_3), which controls the maximum pressure drop in the system. In addition to the requirement of $Pur_F \geq 0.6$, we imposed another constraint of $X_G \geq 0.3$ in order to achieve conversion greater than the experimental reported value. The bounds of the decision variables and fixed parameter values used are summarized in Table 3.3.

In solving constrained optimization using NSGA, penalty methods have been mostly used with large value of constant, w (in this case 1000 is used). The objective function (Eq. 3.15a & b) had to be modified in order to incorporate the two inequality constraints (Eq. 3.15c & d) by introducing suitable penalty functions (Zhang et al., 2002a, b). In addition, NSGA is designed only for maximization of objective functions; therefore, the modified objective functions in this case should be as following.

Maximize $I_1 = Pr_F + w[(Pur_F\text{-}0.6)\text{-}|Pur_F\text{-}0.6|]^2 + w[(X_G\text{-}0.3)\text{-}|X_G\text{-}0.3|]^2$ (3.16a)

Maximize $I_2 = \frac{1}{1+J_2} + w[(Pur_F\text{-}0.6)\text{-}|Pur_F\text{-}0.6|]^2 + w[(X_G\text{-}0.3)\text{-}|X_G\text{-}0.3|]^2$ (3.16b)

Optimization runs were performed with three different feed compositions of glucose and fructose to see its effect on system performance. For convenience of comparison, total feed concentration ($c_{T,f}$) was kept constant at 2.0 mol/l. Feed 1 contains equal moles of glucose and fructose ($r_f = 1$), each with concentration of 1.0 mol/l in the solution. Feed 2 contains more glucose than fructose ($r_f = 0.724$), with

1.16 mol/l glucose and 0.84 mol/l fructose in the feed stream while Feed 3 contains only glucose ($r_f = 0$) of concentration of 2.0 mol/l.

Table 3.3 Description of the optimization problems for Hashimoto's hybrid SMBR system

Case	Obj. Functions	Constraints	Decision variables	Fixed variables
I	Max Pr_F Min Q_D	$Pur_F \geq 0.6$ $X_G \geq 0.3$	$3.0 \leq t_s \leq 6.0$ min $1.0 \leq Q_3 \leq 5.0$ ml/min $0.144 \leq Q_D \leq 0.72$ ml/min	Q_f=0.144 ml/min $c_{T,f}$ =2.0 mol/l r_f = 0, 0.724, 1 T_R= 333K L_S = 10.2 cm L_R = 18.0 cm χ= 4/4/8/7, N_T = 23
II			$3.0 \leq t_s \leq 6.0$ min $1.0 \leq Q_3 \leq 5.0$ ml/min $0.144 \leq Q_D \leq 0.72$ ml/min $8.0 \leq L_S, L_R \leq 30.0$ cm $1 \leq N_{S2} \leq 8$, $2 \leq N_{S3} \leq 9$	Q_f=0.144 ml/min $c_{T,f}$ =2.0 mol/l r_f =0.724, T_R = 333 K $N_R = N_{S3}$-1 N_T =19, 21, 23
III			$3.0 \leq t_s \leq 6.0$ min $1.0 \leq Q_3 \leq 5.0$ ml/min $0.144 \leq Q_D \leq 0.72$ ml/min $0.1 \leq Q_{f1} \leq 0.27$ ml/min $0.0 \leq Q_{f2} \leq 0.2$ml/min $0.0 \leq Q_{f3} \leq 0.2$ ml/min $1 \leq N_{S2} \leq 8$; $2 \leq N_{S3} \leq 9$	$Q_{f,av}$ =0.144 ml/min $c_{T,f}$ =2.0 mol/l r_f =0.724, T_R = 333 K L_S = 15.08 cm L_R = 28.1 cm $N_R = N_{S3}$-1, N_T = 23
IV		$Pur_F \geq 0.6$ $X_G \geq 0.27$ *$r_{R1} \leq 0.97$ $r_{R2} \leq 0.97$	$3.0 \leq t_s \leq 8.0$ min $1.0 \leq Q_3 \leq 5.0$ ml/min $0.144 \leq Q_D \leq 0.72$ ml/min $8.0 \leq L_S, L_R \leq 40.0$ cm $2 \leq N_{S2} \leq 5$	Q_f=0.144 ml/min $c_{T,f}$ =2.0 mol/l r_f = 1, T_R = 323 K N_R = 2 N_{S3} = 3, N_T = 13

* r represents the concentration ratio of fructose to glucose at the inlet of the two reactors. Subscript R1 represents the first reactor while R2 the second reactor.

Figure 3.3 illustrates optimization results for the three different feed streams. Significant improvement in net productivity of fructose (Pr_F) compared to the experimental results was obtained through optimization. Notable increase in Pr_F was observed when the glucose content of the feed composition was increased even though purity of the product (Pur_F) decreased. Results indicate that reducing fructose content in the feed is beneficial for the forward reaction to proceed further thereby increasing the conversion of glucose (X_G). However, increasing glucose content of the feed deteriorates the performance of zone 2 in desorbing glucose and hence reduces the purity of fructose in the product stream.

It can be seen from Figure 3.3b & c, that for Feed 1 ($r_f = 1$) and Feed 3 ($r_f = 0$), the optimal switching time (t_s), and optimal internal flow rate (Q_3) converged to fixed values for the entire range of Q_D. However, for Feed 2 ($r_f = 0.724$) two sets of optimal t_s and Q_3 are obtained. When Q_D is lower, lower Q_3 and higher t_s are the optimal solutions whereas when Q_D is higher, higher Q_3 and relatively lower t_s are the optimal choice for the system. These results demonstrate that at lower desorbent flow rate, lower fluid flow rates and longer residence times are required for improved performance while at higher desorbent flow rate, the relatively higher fluid flow rate and shorter residence time is more suitable. The above results also indicate that if HFS55 is the desired product, feed containing higher glucose content would impart the highest net productivity of fructose for a given desorbent consumption. Besides, there is no need for another reactor to convert D-glucose to HFS42 in advance.

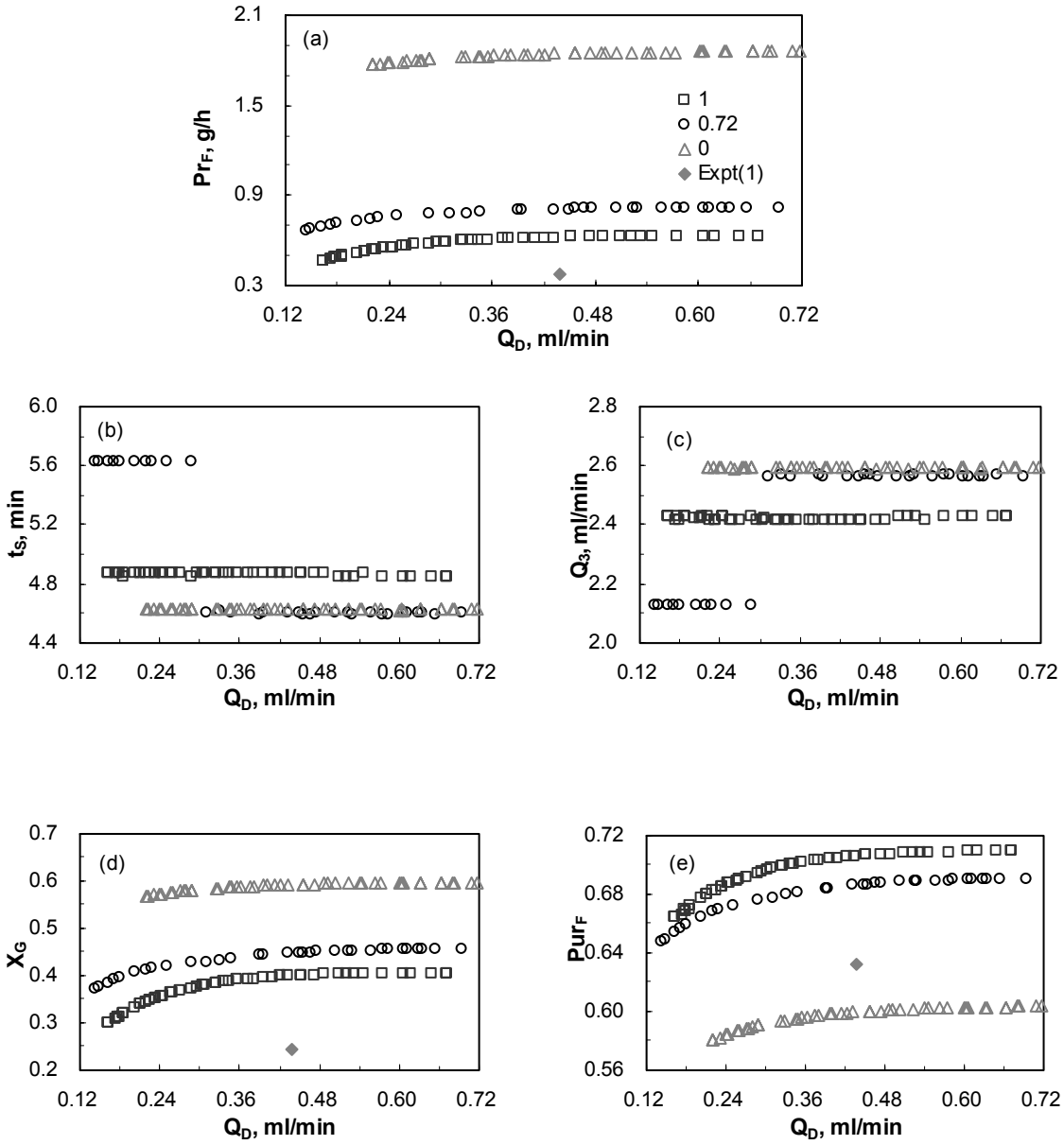

Figure 3.3 Comparison of Pareto optimal solutions and the corresponding decision variables, and calculated values of X_G and Pur_F for different feed compositions (r_f). Case I: T_R = 333 K, N_T = 23

3.3.2 Case II. Optimization at design stage

The optimization at the design stage allows more flexibility as one can determine optimal values of length, number and distribution of columns in different zones in addition to the three decision variables used in case I. Once again we solved three cases, N_T equal to 19, 21 and 23 (for $r_f = 0.724$) to see whether fewer columns can be used without a significant decrease in the system performance, maximum Pr_F using minimum Q_D. Additional decision variables, the length of each separator (L_S) and reactor (L_R) and the column configuration (χ), are included in the optimization formulation, which is summarized in Table 3.3.

Optimization results are shown in Figure 3.4. Results show that significant improvement is possible in Pr_F at any specific Q_D at the design stage compared to the existing stage (N_T= 23, symbol ○) and improvement is more pronounced at higher Q_D. When total number of columns are reduced the net productivity of fructose, the conversion of glucose and purity of fructose decrease slightly. For example, when Q_D is 0.39 ml/min, the conversion of the glucose and the purity of fructose are 47.2% and 69.7% for N_T = 19; 49.6% and 71.3% for N_T = 21; and 51.3% and 72.4% for N_T = 23.

The corresponding optimal column configurations χ for the three systems are given in Table 3.4. For example, χ= 3/7/5/4 means there are 3, 7 and 5 adsorption columns each of length L_S in zones 1, 2 and 3 respectively, and a total 4 reactors each of length L_R in zone 3. Table 3.4 indicates that the optimal column configuration for the three systems is different. Optimal values of χ not only relate to the total number of the columns but also depend on the desorbent flow rate. For N_T = 19 the optimal χ changes from 5/5/5/4 in section AB to 4/6/5/4 in section BC and 3/7/5/4 in section CD with the increase of Q_D as shown in Figure 3.4. Similar trend can also be observed when N_T = 21 except number of reactors required is 5 instead of 4. The result indicates

that more columns are needed in zone 1 for desorption of fructose when Q_D is low, while at higher desorbent flow rate desorption of glucose in zone 2 becomes crucial for the improvement system performance, and therefore more columns are needed in zone 2 as Q_D is increased. In case of N_T= 23, the optimal number of reactor columns required is 6 at very high Q_D. At high Q_D, optimal χ = 3/7/7/6 (line PQ) while at low Q_D, optimal χ = 6/6/6/5 (line MN) are required as shown in Figure 3.4 and Table 3.4. These results indicate that desorption of fructose and glucose is very important in achieving good system performance. If the adsorbent cannot be regenerated completely, higher productivity is difficult to be attained by just adding the number of the reactors. In comparison with the optimization results from case I, it is easily seen that the system performance can be improved by optimizing the column length and column configuration. However, the optimal lengths for the separators and reactors obtained in Case II are longer than those of the existing set-up. This implies that lower desorbent flow rate is required for longer columns in order to maintain the good system performance.

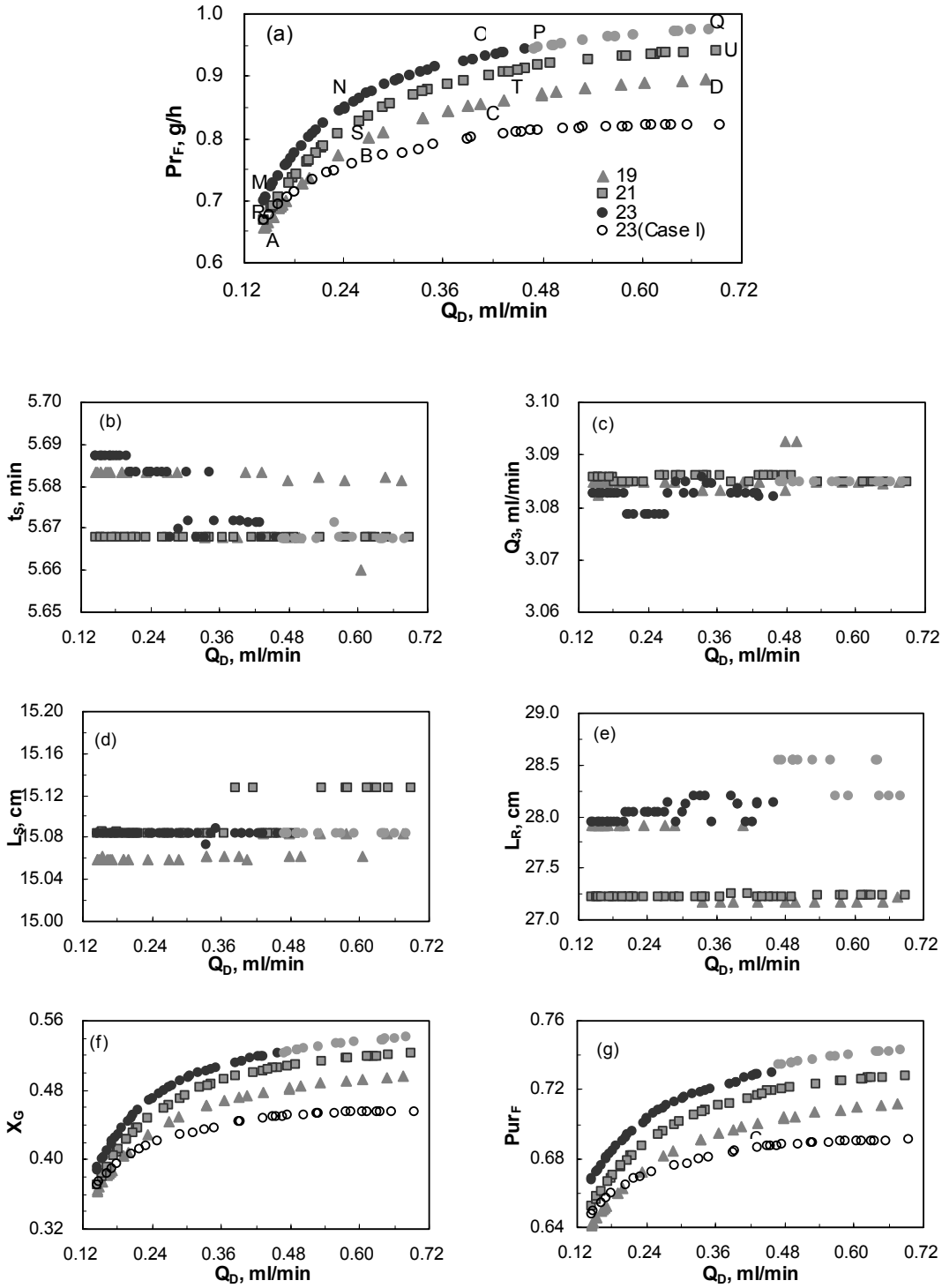

Figure 3.4 Comparison of Pareto optimal solutions and the corresponding decision variables, and calculated values of X_G and Pur_F for different N_T. Case II: T_R = 333 K, r_f = 0.724

3.3.3 Case III. Optimization with variable feed flow rate

The advantages of applying variable flow rates to SMB processes have been discussed earlier (Zang and Wankat, 2002a; Zhang et al., 2003; Yu et al., 2003b). It is worthwhile to see the applicability and advantages achieved when this concept is applied for Hashimoto's hybrid SMBR system. Without raffinate withdrawal in this system, product flow rate (Q_P) in the extract stream is directly related to the desorbent and feed flow rates. Any variations of the feed or desorbent flow rate within the switching time will result in the changes of the internal flow rates and therefore affects the system performance. Complex interplay of the process parameters and too many decision variables make the optimization of simultaneous variation of the desorbent and feed flow rates in this SMBR infeasible. Therefore, only feed flow rate is allowed to vary during the operation to evaluate the efficiency of the variable flow mode and to determine the extent to which the performance of SMBR could be improved.

Switching time in this case is divided into four subintervals and feed flow rate was not kept constant at Q_f =0.144 ml/min as in the previous cases for the entire switching period, instead was allowed to vary according to the following equations

$$0.1 \le Q_{f1} \le 0.27 \text{ ml/min}; \quad 0 \le Q_{f2}, Q_{f3} \le 0.2 \text{ml/min} \tag{3.17a}$$

$$Q_{f4} = 4Q_{f,av} - (Q_{f1} + Q_{f2} + Q_{f3}) \tag{3.17b}$$

where, Q_{f1}, Q_{f2}, Q_{f3} and Q_{f4} are the feed flow rates in the sub-interval 1, 2, 3 and 4 respectively. Eq. 3.17b is used to guarantee that total feed flow rate is the same as that of the constant feed flow rate in order to facilitate the comparison between the optimum results obtained. Decision variables in this case include Q_{f1}, Q_{f2}, Q_{f3}, Q_D, Q_3, t_S and χ, while L_S, L_R and Q_f are fixed at the optimal solutions obtained in Case II. Details of the optimization formulations can be found in Table 3.3. Comparison of the

optimal solutions for the variable feed flow rates and the equivalent SMBR systems are illustrated in Figure 3.5. The optimal column configurations for the variable flow rate mode are listed in Table 3.4.

Slightly improvement of both Pr_F and Pur_F for the system with variable feed flow rates can be observed from Figure 3.5. Optimal solutions for Q_3 and t_s are quite close to those obtained in Case II due to the same lengths of the columns adopted. Figure 3.5d shows the values for the decision variables Q_{f1}, Q_{f2}, Q_{f3}, the calculated value Q_{f4} as well as the constant feed flow rate $Q_{f,av}$ associated with the Pareto points in Figure 3.5a. It is obvious that Q_{f1} always takes the highest value followed by Q_{f2} and Q_{f3}, while Q_{f4} is always the lowest. Since Q_D keeps constant during the operation, extract flow rate follows the same variation within the switching time. And this variation of the extract flow rate leads to the improvement of both Pr_F and Pur_F in the hybrid SMBR system. The reason may be well comprehended by looking at the variation of adsorbate concentrations with time at the extract port. Extract purity and fructose concentration are higher at the beginning of the switching period and gradually decrease as time passes. The optimal solutions obtained in this case allow the system to operate such that higher quantity of fructose is collected in the early switching period when concentration of fructose is higher and less quantity is collected when concentration is lower, thus keeping the mean extract flow rate constant over the switching time. Therefore, both Pr_F and Pur_F increase.

However, slight improvement of Pr_F and Pur_F also indicate that manipulation based on changing the wave velocity does not yield much benefit in this SMBR system. Efforts should be made to increase conversion of glucose within reactors.

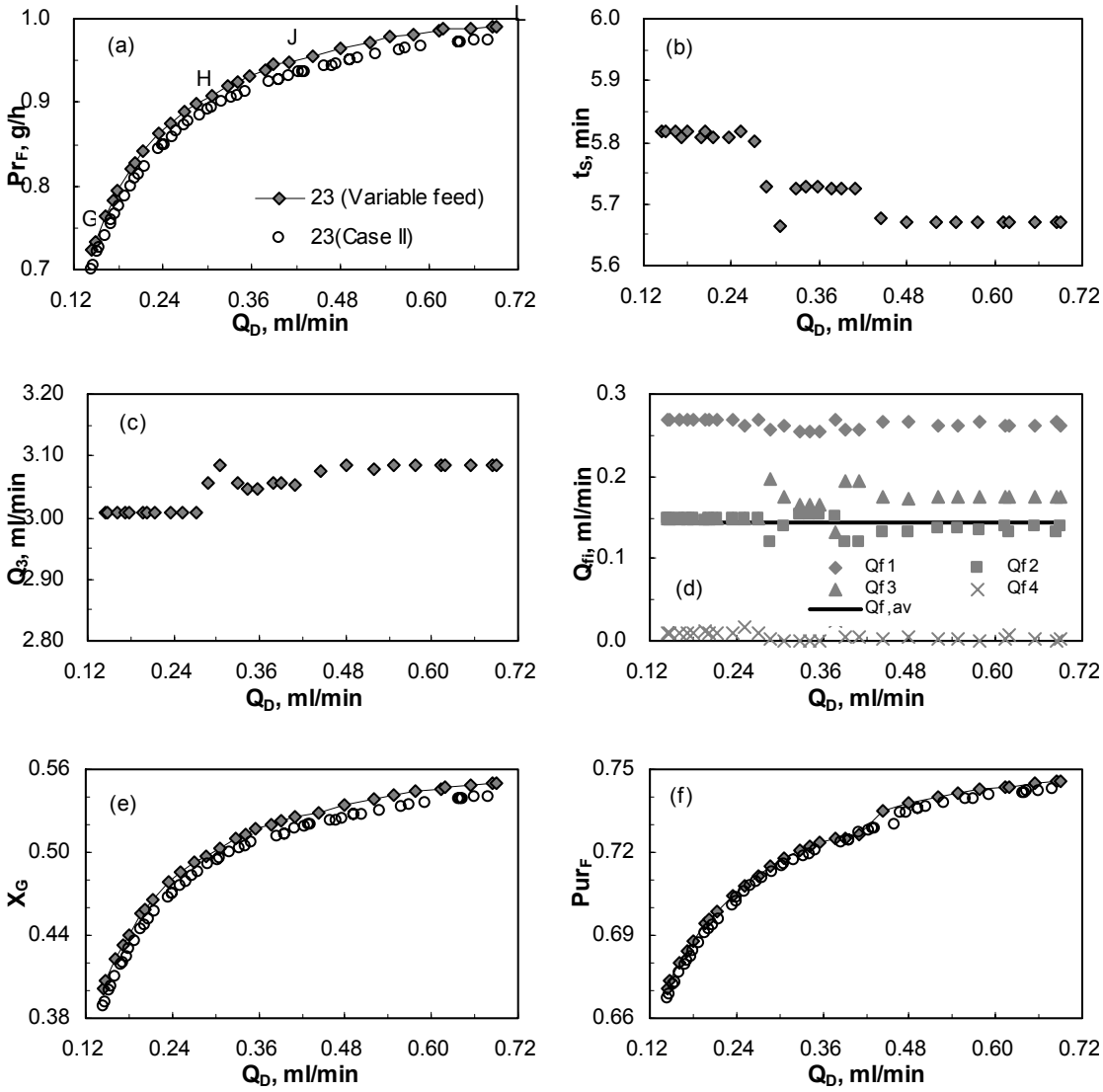

Figure 3.5 Pareto optimal solutions and the corresponding decision variables, and calculated values of X_G and Pur_F with variable feed flow rates. Case III: T_R = 333 K, r_f = 0.724

Table 3.4 Optimum column configurations (χ) for SMBR system in Cases II-IV

Case	Figure	N_T	Pareto Line	χ
II	3.4	19	AB	5/5/5/4
			BC	4/6/5/4
			CD	3/7/5/4
		21	RS	5/5/6/5
			ST	4/6/6/5
			TU	3/7/6/5
		23	MN	6/6/6/5
			NO	5/7/6/5
			OP	4/8/6/5
			PQ	3/7/7/6
III	3.5	23	GH	6/6/6/5
			HJ	5/7/6/5
			JL	3/7/7/6
IV	3.6	13	XY	4/4/3/2
			YZ	3/5/3/2

Table 3.5 Comparison of the system performance at various operating conditions (Case IV)

Point in Fig. 3.6		Q_D ml/min	Q_3 ml/min	t_s min	L_S cm	L_R m	χ	Pr_F g/h	Pur_F	X_G
A	N_T = 13	0.468	3.16	7.6	20.8	38.6	3/5/3/2	0.511	0.667	0.328
	N_T= 23						3/7/7/6	0.774	0.751	0.498
B	N_T = 13	0.468	2.86	7.67	19.0	34.5	3/5/3/2	0.493	0.661	0.318
	N_T = 23						3/7/7/6	0.747	0.744	0.48

3.3.4 Case IV. Optimization at design stage with additional constraints

The purpose of the optimization study for Case IV is to further improve the system performance particularly when the operating reactor temperature is 323 K, as at this temperature K_e is equal to 1 (see Table 3.2) and use of 7 reactors is rather meaningless since even though reactors and separators are arranged alternately, due to forward and reverse reaction rates being equal glucose will be reproduced from fructose. In order to see whether only two reactors would be sufficient, we perform an optimization study with a total of 13 columns including only two reactors, but with an additional constraint that the ratio of fructose to glucose concentration ($r = c_F / c_G$) at the inlet of the two reactors be at least less than 0.97. This ensures that feed to reactor contains more glucose than fructose thereby increasing effective conversion of glucose to fructose. This new constraint will either force the system to choose longer separator length, or to increase switching time (thereby increasing residence time) to increase separation between glucose and fructose. The case IV optimization problem is solved for T = 323K and r_f = 1 contrary to earlier three cases. The optimization formulation is given in Table 3.3.

Figure 3.6 compares the optimization results for Case IV with optimization results for N_T = 23 obtained without the constraint $r \leq 0.97$. The experimental value reported by Hashimoto *et al*. (1983a) for N_T = 23 (χ= 4/4/8/7) is also shown in the figure. The optimal column configurations for N_T=23 (T=323K) without the constraint $r \leq 0.97$, quite similar with the results in Case II, vary with Q_D and the optimal number of reactors are 5 and 6 at lower (Q_D<0.345 ml/min) and higher Q_D ($Q_D \geq$ 0.345 ml/min) respectively. Certainly, 23 columns (with optimum 5/6 reactors) outperforms 13 columns (with only 2 reactors) but if the efficiency, defined as net productivity per unit time per unit total volume of all columns (Pr_F*), is compared with the new

modification, 13-column system outperforms the 23-column system as shown in Figure 3.6f. Figure 3.6 also shows that the optimum solution is selecting longer reactor length as well as switching time to increase residence time to compensate for 3 or 4 fewer reactors used in this case. Moreover, optimum length of the separators selected was also slightly higher compare to the 23-column system. Table 3.4 lists the optimal column distribution. The steady-state concentration profiles of glucose and fructose corresponding to two optimal solutions represented by points A and B are shown in Figure 3.7. From Figure 3.7a, it is observed that fluid with higher concentration of glucose and fructose breaks through from zone 3 to zone 1 due to the reduction of both reactors and separators in zone 3. A breakthrough of glucose into zone 1 results in the decrease of Pur_F and lower conversion.

The enhancement in the reactor performance due to imposition of the additional constrains of $r \leq 0.97$ at the reactor inlet can be seen from the optimal and simulation values shown in Table 3.5. Point A (in Figure 3.6 and Table 3.5) corresponds to optimal solution for N_T = 13 with additional constraint (case IV) while point B corresponds to optimal solution for N_T = 23 without the additional constraint. When a simulation is performed with 23 columns (χ= 3/7/7/6) using the optimal conditions for Q_D, Q_3, t_s, L_R, L_S obtained for N_T = 13 (row 1 in the Table 3.5), the system performance criteria (Pr_F, Pur_F and X_G) obtained for 23-column system with the additional constraint (row 2 in Table 3.5) were better than the optimal solutions obtained for Point B without the additional constraint (row 4 in Table 3.5). Similar improvement was observed when simulation result without additional constraint for N_T = 13 were computed (shown in row 3 of Table 3.5) using optimal conditions for Q_D, Q_3, t_s, L_R, L_S for N_T = 23 and the results are compared with the optimal solutions for N_T = 13 with the additional constraint (row 1 of Table 3.5). The results in Table 3.5

clearly show that imposing an additional constraint on the fructose concentration at the reactor inlet improves the system performance.

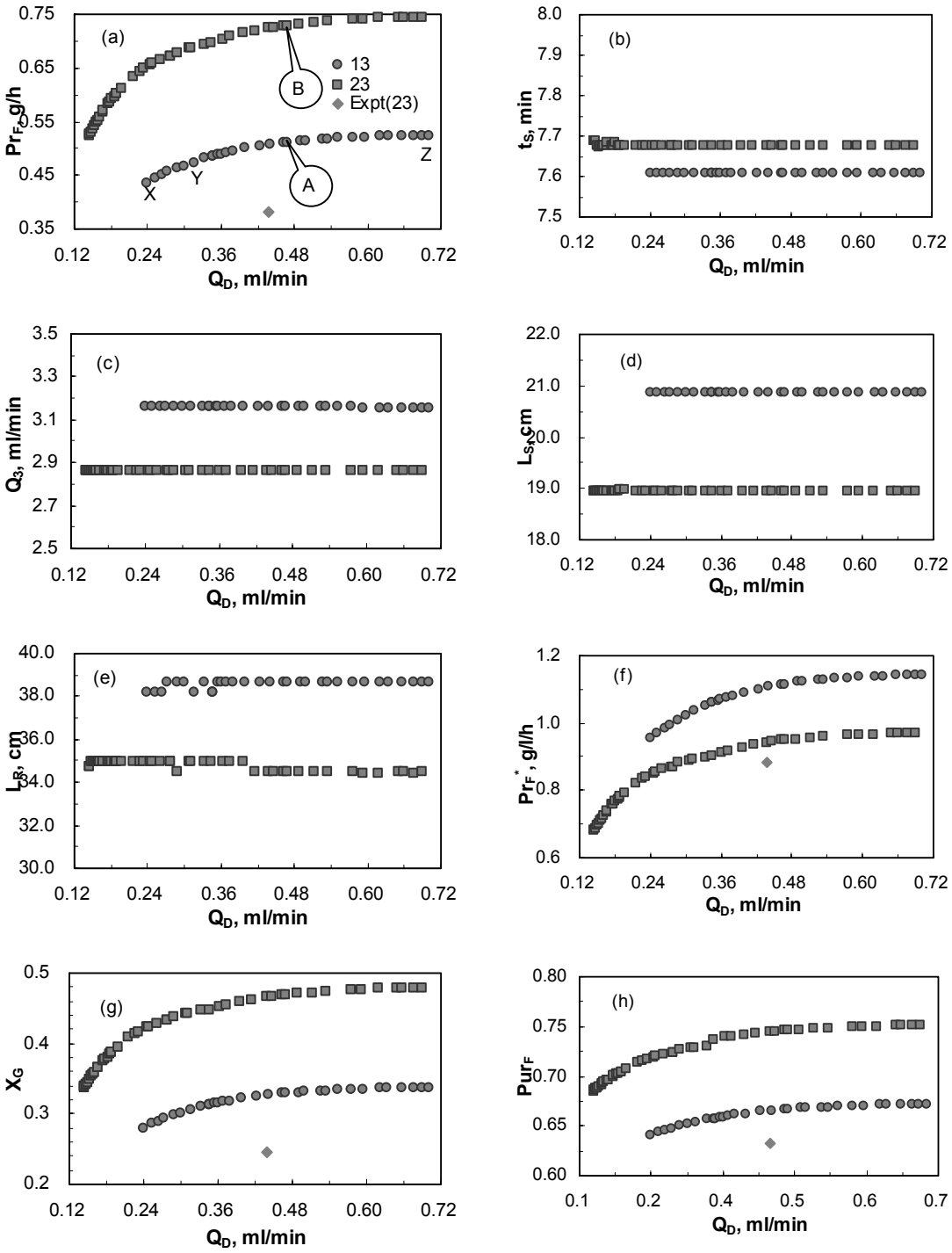

Figure 3.6 Effect of additional constraint on the Pareto optimal solution. Case IV: T_R = 323 K, r_f = 1

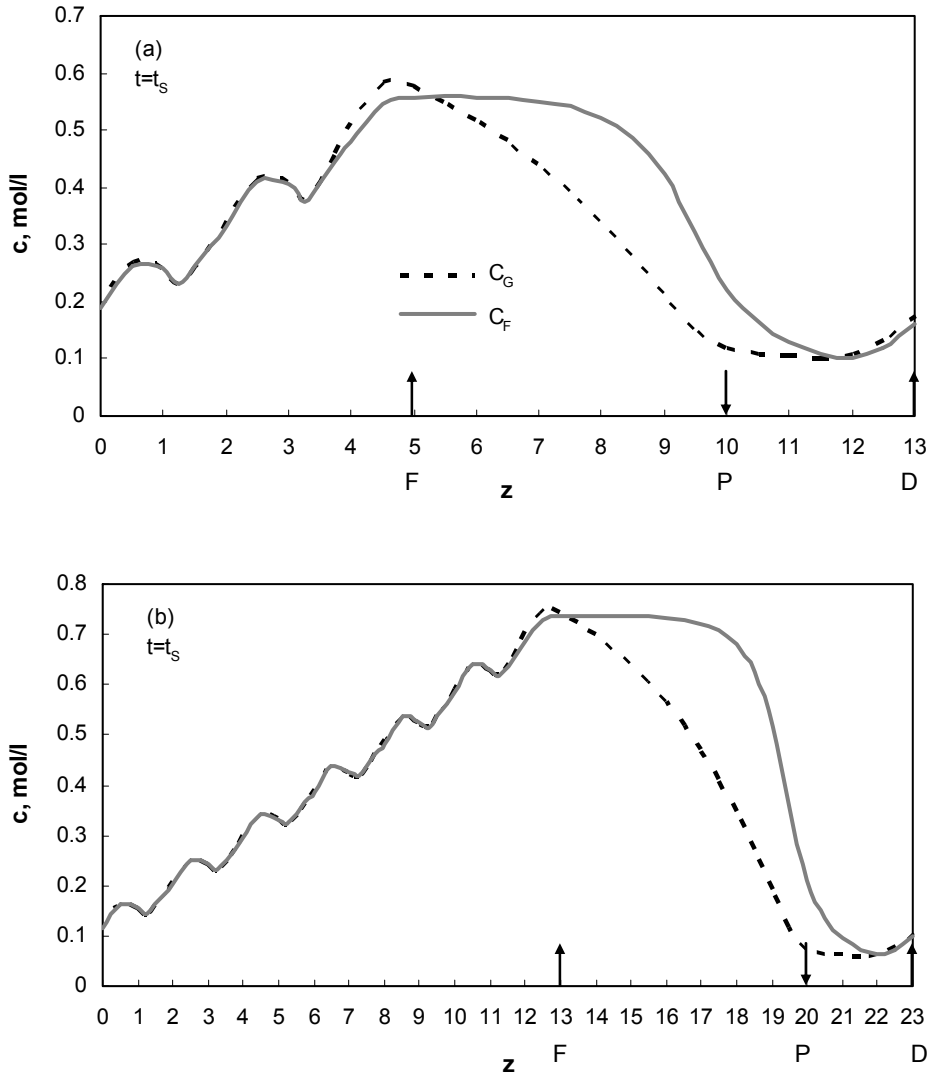

Figure 3.7 Steady state concentration profiles of glucose and fructose corresponding to the optimal solutions represented by points A and B in Figure 3.6 (a): Point A in Fig. 3.6 (N_T = 13), (b): Point B in Fig. 3.6 (N_T = 23)

3.4 Conclusions

The simulation and multi-objective optimization study for the isomerization of glucose to fructose in Hashimoto's hybrid simulated moving bed reactor (SMBR) has been performed to predict the optimal operating conditions for such an important industrial reaction and separation process. Numerical simulation based on dynamic SMBR model could predict the published experimental results quite well. Systematic optimization was then carried out to simultaneously maximize the net productivity of fructose and minimize the eluent flow rate at different operating conditions. An adaptation of the state-of-the-art AI-based robust optimization technique, non-dominated sorting genetic algorithm with jumping genes (NSGA-II-JG) was used to obtain the Pareto (non-dominated) solutions for both the existing as well as SMBR system at design stage.

By optimizing the system with different feed compositions, effect of feed composition on system performance was studied. Results indicated that higher net productivity of fructose can be achieved with feed containing less amount of fructose. Productivity of fructose could be further improved by incorporating column lengths and column configuration into decision variables. Column configuration is an important parameter for this SMBR system and optimal column configurations change with both eluent flow rate (Q_D) and total number of column (N_T). Results from the optimization with variable feed flow rates and with additional constraints demonstrated that manipulation based on changing the wave velocity does not yield much benefit for this SMBR system. Efforts should be made to increase conversion of glucose within reactors.

Chapter 4 Modified Reactive SMB for Production of High Fructose Syrup by Isomerization of Glucose to Fructose

4.1 Introduction

In the last chapter, Hashimoto's hybrid SMBR system consisting of 16 adsorption columns and 7 enzymatic reactors was optimized to obtain HFS55 using experimentally verified dynamic SMBR model. Systematic multi-objective optimization was performed to improve system performance in terms of maximization of fructose productivity and minimization of desorbent flow rate at different reaction temperature and feed compositions. Although significant improvement of system performance had been obtained through multi-objective optimization for the above system, it was observed that when feed is a 50/50 blend of glucose and fructose, as shown in Figure 4.1 the concentrations of fructose and glucose in the reactors were about the same since equilibrium constant for the isomerization reaction is 1.0. As a result, conversion of glucose in each reactor was quite low. Results from the chapter 3 also suggested that modification based on the manipulation of the wave velocity does not yield much benefit for the system. Efforts should be made to increase conversion of glucose within reactors. In addition, design of a 3-zone process without the raffinate withdrawal causes a breakthrough of glucose into section 1, which should also be avoided.

In this study, modified reactive SMB and Varicol systems are presented for production of HFS55 by isomerization of glucose. The purpose of the current study is to design modified SMBR system with fewer reactors. This study also aims at finding the optimal design and operating parameters for the modified reactive SMB and Varicol system to achieve simultaneously maximum productivity of fructose using

minimum desorbent consumption.

4.2 Modified SMBR systems

The essential concept in the design of modified SMBR systems is to achieve sufficient separation of glucose and fructose so that stream rich in glucose (high concentration) can be fed into the reactor. Therefore, a process design with four sections, including a rafinate port was chosen to increase the purity and concentration of the glucose at the inlet of the reactor and to prevent more glucose in breaking through to section 1. Two different configurations were envisioned to implement this strategy.

Modified Configuration 1 (MC1) is a 4-zone SMBR consisting of only one reactor and several adsorption columns as illustrated in Figure 4.2. Unlike the conventional 4-section SMB, where glucose and fructose are withdrawn from raffinate and extract ports respectively, raffinate stream in MC1 is fed to the reactor, where glucose is converted into fructose by enzyme isomerase and the outlet stream from the reactor is recycled back with the fresh feed. By operating the system in this way, continuous coupling of separation and reaction in one unit is feasible. By proper adjustment of the switching time and fluid flow rate in each section, fructose (the strongly adsorbed component) is retained while glucose (the weakly adsorbed component) is allowed to breakthrough from section 3 and directed to the reactor. Therefore, stream rich in glucose is fed into reactor and gets opportunity to be converted to fructose continuously. Subsequently, glucose emerging from section 3 is adsorbed in section 4 and fructose adsorbed in sections 3 and 4 is desorbed in section 1 by port switching. Fructose of required purity is as usual collected at the extract port located between sections 1 and 2.

Modified Configuration 2 (MC2) shown in Figure 4.3 is a modification of MC1 based on the observed concentration profiles of MC1. For any 4–section SMB/SMBR, the function of section 4 is to retain the weakly adsorbed species, which is glucose in this system. Due to the relatively slow adsorption rate of glucose, optimization studies reveal that more columns have to be used in section 4 to completely retain glucose. Hence, the outlet stream from the first adsorption column (A6 in Figure 4.3) in section 4 still contains high concentration of glucose, particularly during the initial part of the switching period. It is therefore appears that it will be an incentive to add one additional reactor between adsorption columns A6 and A4 in section 4 to increase conversion of glucose.

One distinguished feature in the design of MC2 is the use of an on-off valve in the pipeline connecting A6 to the second reactor (R2). The role of this on-off valve is to feed outlet stream from A6 partially to R2 at a high rate during the initial part of the switching period when concentration of glucose is high and stop the flow of this stream to R2 when concentration of fructose becomes higher. Hence, in the earlier part of the cycle, the outlet stream from R2 is recycled back to the inlet of A4, while in the latter part of the cycle MC2 works the same way as MC1 as if there is no reactor. By adding this additional reactor, more glucose is expected to be converted into fructose. The operation and analysis of MC2 is more complicated due to three additional operating parameters involved: the flow rate to R2 (Q_{R2}), feed time to R2 (t_{R2}) and length of R2 (L_{R2}). In this work, systematic simulation and optimization study of these two modified configurations of SMBR is considered for isomerization of glucose into fructose to produce high concentrated fructose syrup.

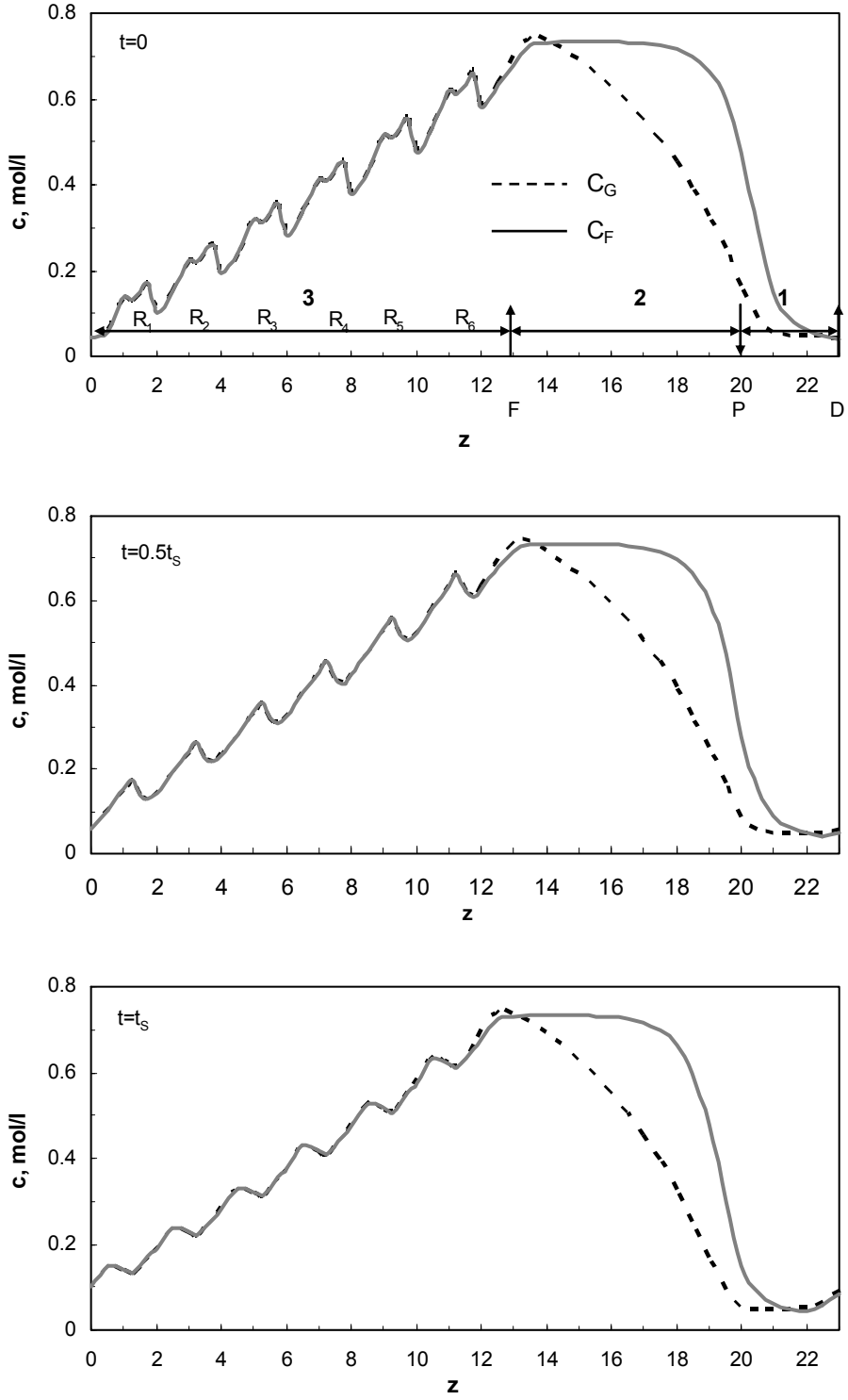

Figure 4.1 Comparison of the steady state concentration profiles of glucose and fructose for the two systems

(See Table 4.5 for operating conditions)

(a)

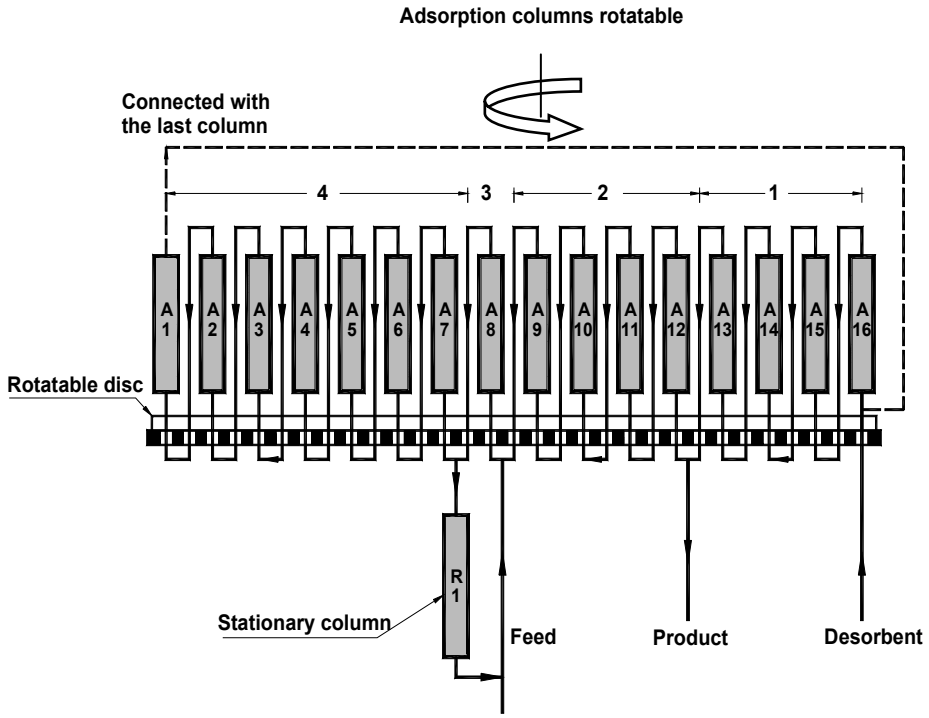

(b)

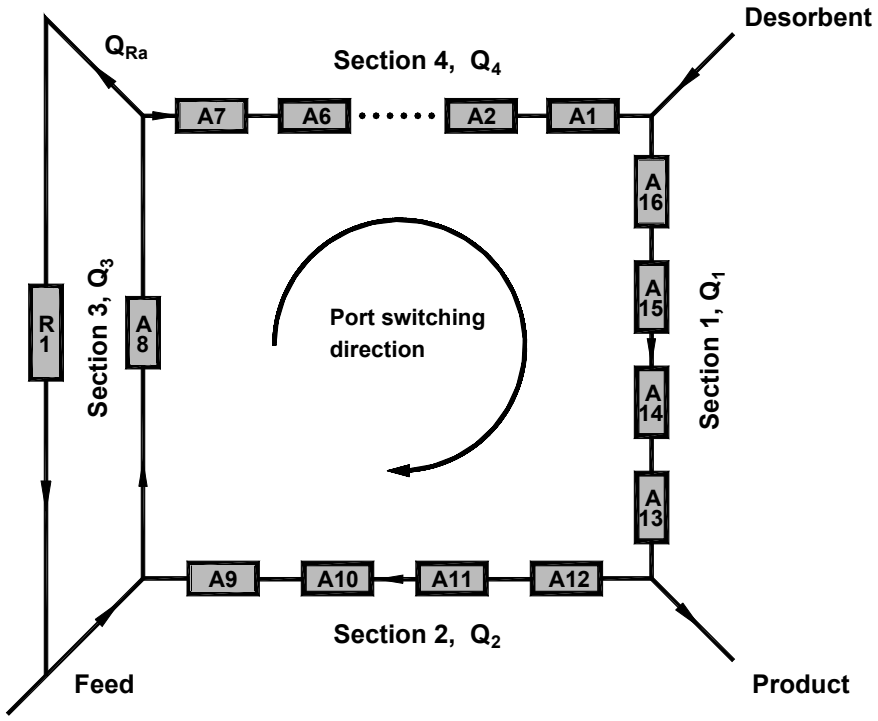

Figure 4.2 Schematic diagram of modified configuration 1 (MC1)

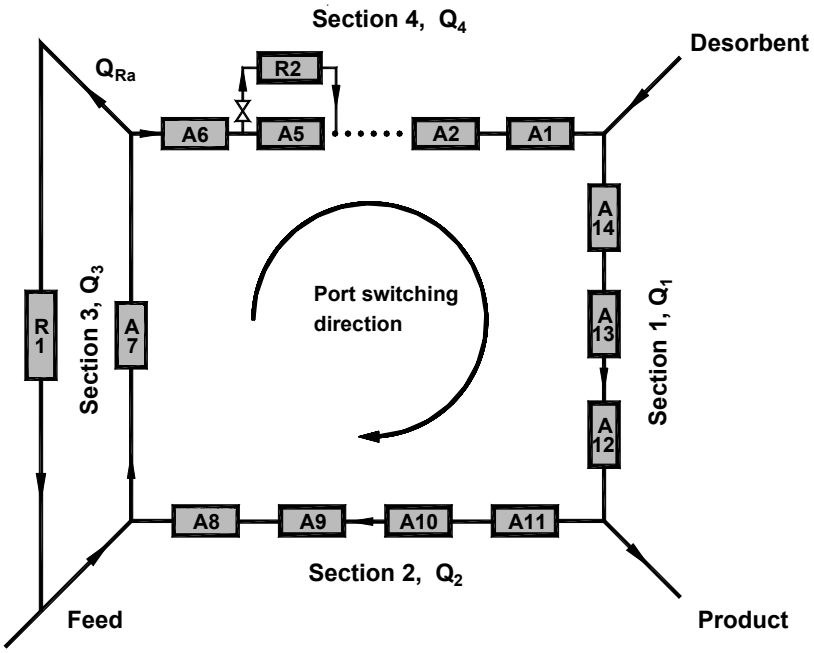

Figure 4.3 Schematic diagram of modified configuration 2 (MC2)

4.3 Mathematical model

For convenience of comparison, the same mathematical model as that described in the previous chapter was used in this study for the two modified SMBR configurations and is not repeated here for brevity. Nevertheless, the initial and boundary conditions for the two modified configurations are different, therefore, only initial and boundary conditions are given here.

The initial conditions for the systems

When $N = 0$; $\quad C_{ij}^{0} = 0$ (both MC1 and MC2) (4.1)

When $N \geq 1$

For MC1:

$$C_{ij}^{N} = C_{i,j+1}^{N-1} \qquad \text{for} \quad j = 1\sim(N_T\text{-}2)$$

$$C_{ij}^{N} = C_{i,1}^{N-1} \qquad \text{for} \quad j = N_T\text{-}1 \tag{4.2a}$$

For MC2:

$$C_{ij}^{N} = C_{i,j+1}^{N-1} \qquad \text{for} \quad \text{j = 1~(} N_{\text{T}}\text{-3)}$$

$$C_{ij}^{N} = C_{i,1}^{N-1} \qquad \text{for} \quad \text{j = } N_{\text{T}}\text{ -2} \tag{4.2b}$$

The boundary conditions for the system

Eluent inlet point:

For MC1:

$$C_{i,1}^{N}\,|_{z=0} = \frac{Q_4}{Q_1} C_{i,N_T-1}^{N-1}\Big|_{z=L_S} \tag{4.3a}$$

For MC2:

$$C_{i,1}^{N}\,|_{z=0} = \frac{Q_4}{Q_1} C_{i,N_T-2}^{N-1}\Big|_{z=L_S} \tag{4.3b}$$

Product withdrawal point:

$$C_{i,N_{S1}+1}^{N}\,|_{z=0} = C_{i,N_{S1}}^{N}\,|_{z=L_S} \qquad \text{(both MC1 and MC2)} \tag{4.4}$$

Feed point:

For MC1:

$$C_{i,N_{S1}+N_{S2}+1}^{N}\,|_{z=0} = \frac{Q_2}{Q_3} C_{i,N_{S1}+N_{S2}}^{N}\Big|_{z=L_S} + \frac{Q_f}{Q_3} C_{i,f} + \frac{Q_{Ra}}{Q_3} C_{i,N_T}^{N}\Big|_{z=L_S} \tag{4.5a}$$

For MC2:

$$C_{i,N_{S1}+N_{S2}+1}^{N}\,|_{z=0} = \frac{Q_2}{Q_3} C_{i,N_{S1}+N_{S2}}^{N}\Big|_{z=L_S} + \frac{Q_f}{Q_3} C_{i,f} + \frac{Q_{Ra}}{Q_3} C_{i,N_T-1}^{N}\Big|_{z=L_S} \tag{4.5b}$$

Inlet of R1:

For MC1:

$$C_{i,N_T}^{N}\,|_{z=0} = C_{i,N_{S1}+N_{S2}+N_{S3}}^{N}\,|_{z=L_S} \tag{4.6a}$$

For MC2:

$$C_{i,N_T-1}^{N}\,|_{z=0} = C_{i,N_{S1}+N_{S2}+N_{S3}}^{N}\,|_{z=L_S} \tag{4.6b}$$

Inlet of R2:

$$C_{i,N_T}^{N} \mid_{z=0} = C_{i,N_{S1}+N_{S2}+N_{S3}+1}^{N} \mid_{z=L_S} \tag{4.7}$$

Adsorption isotherm parameters, reaction rate constants as well as operating parameters for the modified systems are the same of those of previous work and are listed in Table 4.1. Different performance evaluation parameters used in this work are defined as follows

$$\text{Conversion of glucose, } X_G = \frac{\int_0^{t_s} (Q_P C_{F,P} - Q_f C_{F,f}) dt}{Q_f C_{G,f} t_s} \tag{4.8}$$

$$\text{Purity of fructose in the product stream, } Pur_F = \int_0^{t_S} \frac{C_{F,P}}{C_{F,P} + C_{G,P}} dt \tag{4.9}$$

$$\text{Net productivity of fructose, } Pr_F = \frac{\int_0^{t_s} (Q_P C_{F,P} - Q_f C_{F,f}) dt}{t_s} \tag{4.10}$$

Concentration profiles, productivity and purity of fructose and conversion of glucose were obtained by solving the above equations numerically using the same method presented in detail in the last chapter.

Table 4.1 Fixed Parameters used for the modified SMBR System
(Hashimoto et al., 1983a)

SMBR unit geometry	Operating parameters	Model parameters
d=1.38 cm	$c_{G,f}$=1.0 mol/l	K_F=0.686
	$c_{F,f}$=1.0 mol/l	K_G=0.586
	Q_f=0.144 ml/min	K_m=0.14 mol/l
	T_R=323 K	R_m=0.1272 mol/l/min
		K_e=1.0
		$k_f a_v$=0.41 min^{-1}

4.4 Optimization of the modified SMBR systems

From the previous discussions of modified system, it is apparent that more operating parameters than those of Hashimoto's are present in the four-zone SMBR. The complexity of the process behavior for the SMBR system makes the empirical optimization of this process impossible. Determination of the optimal operating conditions and the suitable design parameters must rely on systematic optimization study (Charton et al., 1995). The importance of application of the concept of multi-objective optimization for chemical and biochemical systems in general (Bhaskar et al., 2000a) and for SMB in particular (Zhang et al., 2002a; Subramani et al., 2003; Yu et al., 2003b; Zhang et al., 2004) have been reported. Objectives selected in this work are to maximize net productivity of fructose (Pr_F) and minimize desorbent consumption (Q_D). The conflicting effect of these two objective functions necessitates multi-objective optimization study of the modified SMBR systems. In this chapter, systematic multi-objective optimization study of the two modified SMBR systems is presented. Optimization was done using a state-of-the-art AI-based optimization technique, non-dominated sorting genetic algorithm with jumping genes (NSGA-II-JG). The details of the methodologies have been presented in Chapter 2, and will not be repeated here for brevity.

4.4.1 Case I. Multi-objective optimization of Modified Configuration 1 (MC1)

The MC1 system consists of only one reactor (instead of 7 reactors) but contains 16 adsorption columns (the same number of adsorption columns as in Hashimoto's system). The goal of this study is to see whether MC1 consisting of total 17 columns can achieve the same or even better performance than that of Hashimoto's 23-column SMBR system. Decision variables used for this case include switching time (t_s), desorbent flow rate (Q_D), flow rates in the section 4 (Q_4), flow rate of raffinate stream

(Q_{Ra}), lengths of reactor and separators (L_R and L_S), as well as adsorption column distribution in different zones (χ=$N_{S1}/N_{S2}/N_{S3}/N_{S4}$). In addition, we impose two inequality constraints, one to meet the requirement of purity of fructose, $Pur_F \geq 0.65$, the other to achieve conversion of glucose greater than the experimental reported value, $X_G \geq 0.3$. The optimization formulation along with the constraints, the bounds of the decision variables and fixed parameter values used are summarized in Table 4.2.

Table 4.2 Description of the optimization problems for modified SMBR system

<table>
<tr><th colspan="2">Case</th><th>Objective functions</th><th>Constraints</th><th>Decision variables</th><th>Fixed parameters</th></tr>
<tr><td colspan="2">I
17-column SMBR
(MC1)</td><td rowspan="4">Max Pr_F
Min Q_D</td><td rowspan="4">$Pur_F \geq 0.65$
$X_G \geq 0.3$</td><td>$2.0 \leq t_s \leq 14.0$ min
$1.0 \leq Q_4 \leq 5.0$ mol/l
$0.144 \leq Q_D \leq 0.72$ ml/min
$0.1 \leq Q_{Ra} \leq 3.0$ ml/min
$10.0 \leq L_S, L_R \leq 55.0$ cm
$2 \leq N_{S1} \leq 5$
$2 \leq N_{S2} \leq 5$
$1 \leq N_{S3} \leq 4$</td><td>Q_f=0.144 mol/l
$c_{T,f}$ =2.0 mol/l
$r_f = 1$
N_R=1
$N_T = 17$
$T_R = 323$ K</td></tr>
<tr><td rowspan="2">II
(MC1)</td><td>15-column SMBR</td><td>Same as Case I</td><td>Same as Case I except for $N_T = 15$</td></tr>
<tr><td>15-column Varicol</td><td>$2.0 \leq t_s \leq 14.0$ min
$1.0 \leq Q_4 \leq 5.0$ ml/min
$0.144 \leq Q_D \leq 0.72$ ml/min
$0.1 \leq Q_{Ra} \leq 3.0$ ml/min
$10.0 \leq L_S, L_R \leq 55.0$ cm
χ (see Table 4.4)</td><td>Same as 15-column SMBR</td></tr>
<tr><td colspan="2">III
(MC2)</td><td>$12.0 \leq t_s \leq 12.8$ min
$0.144 \leq Q_D \leq 0.72$ ml/min
$0.3Q_4 \leq Q_{R2} \leq 0.9Q_4$
$0.15t_s \leq t_{R2} \leq 0.35t_s$
$10.0 \leq L_{R2} \leq 20.0$ cm</td><td>Q_4=4.374 ml/min
Q_{Ra}=1.61 ml/min
L_S=48.2 cm
L_{R1}=27.6 cm
N_R=2
χ= 3/4/1/6
same as Case I</td></tr>
</table>

Figure 4.4 illustrates the Pareto optimal solutions for MC1 consisting 17 columns (1 reactor and 16 adsorption columns represented by ◆) and compares the performance with that of Hashimoto's configuration consisting of 23 total columns (shown by ○ obtained in Case IV of Chapter 3). Pareto optimal solutions reveal that Pr_F for the modified system containing only one reactor can rival the optimal values of Pr_F obtained by Hashimoto's system consisting of 7 reactors (experimental result reported by Hashimoto is shown by ■ was not optimized) when Q_D is greater than 0.468 ml/min. However, if Q_D is less than 0.468 ml/min, both Pr_F and Pur_F are lower than those of Hashimoto's 23-column system. Significant improvements are observed in both Pr_F and Pur_F at any Q_D for MC1 compared to Hashimoto's 13-column system with two reactors (represented by ∗ obtained in Case IV of Chapter 3) and improvement is more pronounced at higher Q_D. These results indicate that with the proper design of modified system, performance achieved previously with 23-column containing optimum 5 or 6 reactors can be obtained with 17 columns consisting of just one reactor.

Figure 4.4 also shows optimum values of the decision variables corresponding to the Pareto optimal solutions. It can be seen that the optimal solutions of Q_4, L_S and t_s for MC1 are considerably higher than the values of Q_3 (internal flow rate in zone 3 of Hashimoto's system), t_s and L_S obtained for Hashimoto's system. The underlying reason for the higher optimal values of Q_4, t_s and L_S in MC1 is related to the optimal column distribution of MC1. The optimal column distributions (χ) for the modified system are listed in Table 4.3. As there is only one adsorption column in section 3, a relatively longer adsorption column is required for sufficient separation of glucose and fructose. Higher fluid velocity and relatively longer switching time are, therefore, needed to match the separation requirement. In addition, longer L_R is also observed

from Figure 4.4f for MC1. However, as only one reactor is used in modified system, total length of the reactor is reduced remarkably and the efficiency of the reactor has been improved greatly.

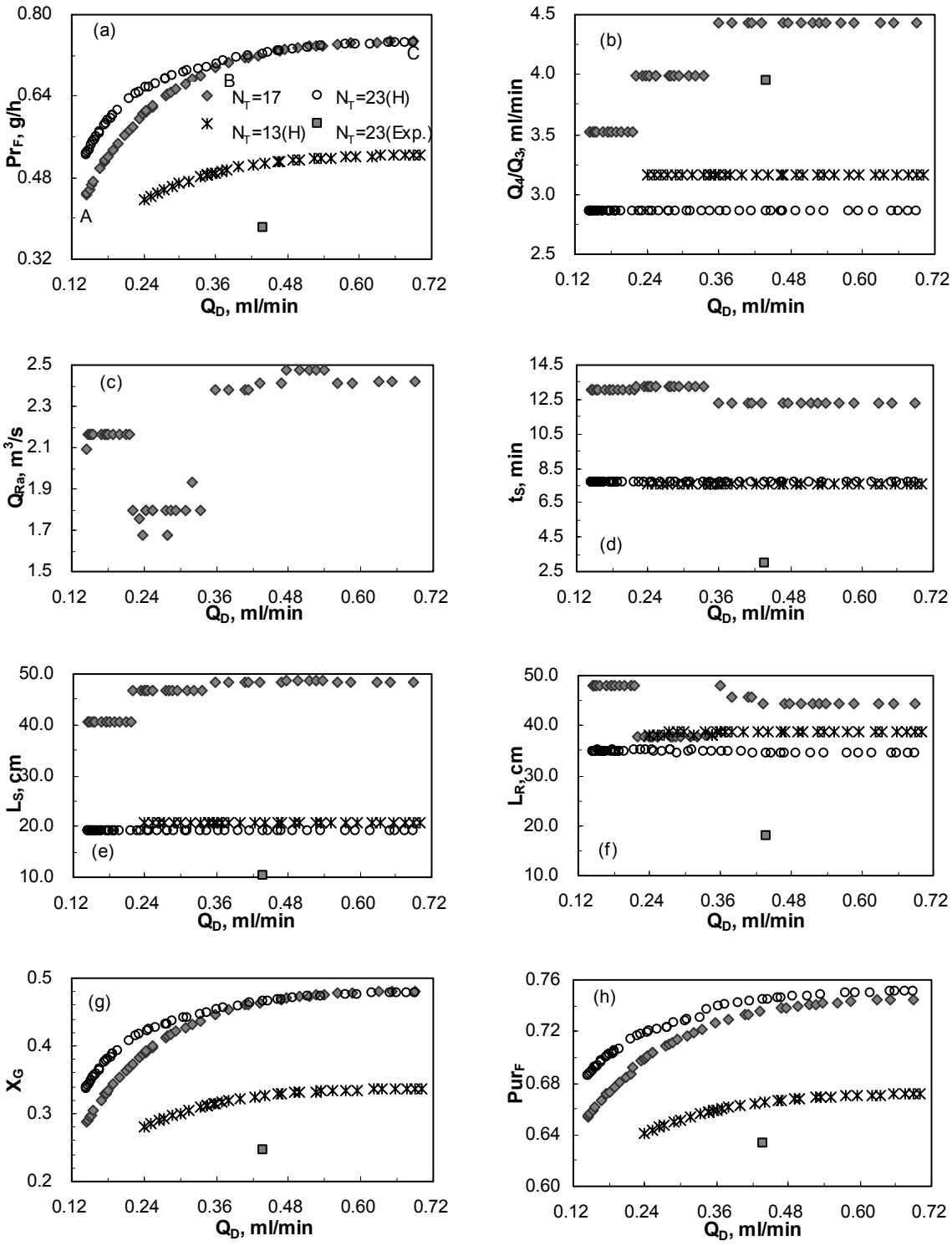

Figure 4.4 Comparison of Pareto optimal solutions for MC1 and Hashimoto system

Internal flow rates play a very important role in obtaining the desired performance for the SMBR system. With Q_4 and Q_{Ra} being used as the decision variables, other internal flow rates are fixed and can be determined by mass balance. Unlike the optimal values obtained for Hashimoto's 23- and 13-column systems, optimal solutions of Q_4 for MC1 converged to different values at different Q_D. Q_4 converged to a lower value when Q_D is lower, while when Q_D required is higher the optimal solutions for Q_4 obtained are also higher. This is expected since higher Q_D is required for the complete regeneration of adsorbent in sections 1 and 2 to adapt to the higher adsorption rate in sections 3 and 4 arising from the higher Q_4. Q_{Ra}, which is directly related to Pr_F or X_G is a unique decision variable used for the modified system. It is observed from Figure 4.4 that the optimal solution for Q_{Ra} depends on the values of L_R. Longer L_R requires higher Q_{Ra}. When other decision variables are fixed, results from Figure 4.4c implies that there exists an optimal value of Q_{Ra} with either higher or lower will deteriorate system performance.

Figure 4.4 and Table 4.3 demonstrate that optimal column distribution of MC1 varies with Q_D. When Q_D is lower (Pareto line AB), the optimal column distribution is χ= 4/5/1/6, while when Q_D is higher (Pareto line BC), χ changes into 3/5/1/7. The column distributions obtained here coincide with the optimal solutions of Q_4. It is seen that at lower internal flow rates (lower Q_4 and Q_D being used), more solutes are with the solid phase and desorption of the more retained component will become very important in achieving the high X_G and Pur_F. Therefore, one more column is required in section 1 (N_{S1}=4) compared with the case when higher Q_D and Q_4 are used. On the contrary, when internal flow rates are higher due to the higher Q_4 and Q_D, more columns are needed in section 4 (N_{S4}=7) to prevent the breakthrough of glucose into section 1 and ensure the high performance of modified system.

Table 4.3 Optimum column configurations (χ) for MC1

Case		Figure	Pareto line	*χ
I	17-column SMB	4.4	AB	4/5/1/6
			BC	3/5/1/7
II	15-column SMB	4.5	EF	A
			FG	B
	15-column Varicol		HJ	B-B-B-A
			JK	I-B-B-A
			KL	I-I-B-B

* Column distribution χ only defines the number of the adsorption columns in each section. For example, 4/5/1/6 represents there are 4, 5, 1 and 6 adsorption columns in sections 1 to 4 respectively.

Table 4.4 Possible column configurations (χ) for N_T=15

N_T=15 (including 1 reactor)			
*χ	Column configuration	χ	Column configuration
A	4/4/1/5	I	2/5/1/6
B	3/4/1/6	J	2/5/2/5
C	2/4/1/7	K	3/5/2/4
D	2/4/2/6	L	4/5/2/3
E	3/4/2/5	M	3/6/1/4
F	4/4/2/4	N	2/6/1/5
G	4/5/1/4	O	2/6/2/4
H	3/5/1/5	P	3/6/2/3

* Column distribution χ only defines the number of the adsorption columns in each section.

4.4.2 Case II. Optimization of performance of SMBR and Varicol for MC1

Ludemann-Hombourger et al. (2000) showed experimentally that Varicol system can perform better than its equivalent SMB system due to the flexibility in its operation. Later Zhang et al. (2002a) and Subramani et al. (2003) showed through systematic optimization studies that Varicol can outperform conventional SMB. Hence, optimization of reactive SMB and Varicol were carried out for MC1 with 14 adsorption columns instead of 16 to reduce the number of adsorption columns and to

explore how much improvement can be achieved when system shifts from reactive SMB to reactive Varicol. The optimization formulation of the 15-column reactive SMB and Varicol are given in Table 4.2.

Let us first look at the optimization results of 15-column SMBR. Figure 4.5 illustrates the Pareto-optimal solution of 15-column SMBR and corresponding decision variables. Results indicate that when total number of columns is reduced from 17 to 15, both Pr_F and Pur_F decrease slightly. Compared to 17-column SMBR, the optimal values of L_S, Q_4 change slightly, while the differences in the values of t_s, L_R and Q_{Ra} are more obvious. The corresponding optimal column configurations χ for 15-column SMBR changes from A (χ =4/4/1/5) in section EF to B (χ =3/4/1/6) in section FG, the similar trend as that in 17-column SMBR system.

Optimization for 4-subinterval 15-column reactive Varicol was carried out with χ as an additional variable. With 14 adsorption columns in this reactive Varicol system, there could be over 100 possible column configurations. In order to reduce the searching range of column configuration for the optimization of Varicol process, some simulations were performed to determine the possible configurations which may lead to better system performance. Based on the optimal column configurations obtained in 15-column SMBR and the results of simulations, 16 configurations listed in Table 4.4 were selected as the possible column configurations for 15-column reactive Varicol.

The Pareto solutions and corresponding optimal decision variables for 15-column reactive Varicol are presented in Figure 4.5a ~ h. Results reveal that the performance of 15-column Varicol is better than that of 15-column SMBR and on par with that of 17-column SMBR in Case I. Improvements in both Pr_F and Pur_F are achieved in the more flexible Varicol system compared to the rigid SMBR unit and the improvements are more pronounced at lower Q_D. The differences between optimal solutions of t_s and

L_S for SMBR and reactive Varicol are larger at lower Q_D; while the differences are much smaller at higher Q_D. Optimal column distributions for reactive Varicol obtained are B-B-B-A, I-B-B-A and I-I-B-B for Pareto lines HJ, JK and KL respectively. These optimal column distributions imply that adsorption of glucose to prevent its breakthrough into section 1 is of great importance in achieving high purity and productivity of fructose in MC1. The optimum results show that at least 5 columns should be used in section 4 ($N_{S4} \geq 5$).

It is worth noting that optimal column distributions of both optimization studies reported in Cases I and II indicate only 1 adsorption column in section 3. Normally, more adsorption columns in section 3 are beneficial to achieve high purity of glucose in the raffinate stream. However, the concentration of glucose in the raffinate flow will decrease if more adsorption columns are used in section 3. The conflicting effects of N_{S3} on the purity and concentration of glucose to the inlet of reactor result in the selection of lower number of column in section 3 but of longer length. In addition, the number of the adsorption columns in sections 1 and 2 changes during the global switching time. At the beginning of switching period, fewer columns in section 1 and more columns in section 2 are selected; while at the later part of the switching period, one additional column is selected by moving a column from section 2 to section 1.

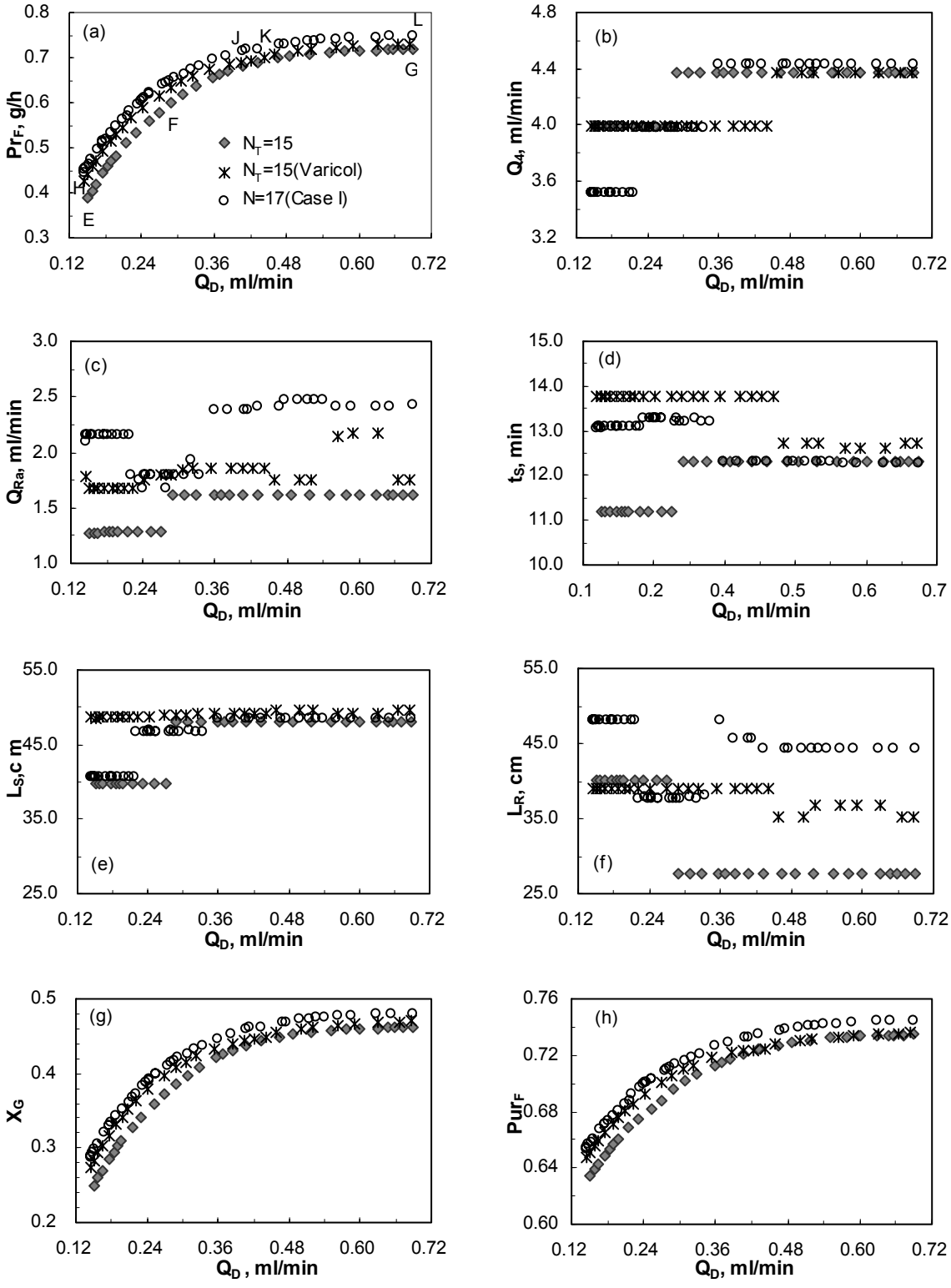

Figure 4.5 Comparison of Pareto optimal solutions for 15-column SMBR and Varicol for MC1

4.4.3 Case III. Multi-objective optimization of Modified Configuration 2 (MC2)

The importance of the flow rate (Q_{R2}) and feed time to R2 (t_{R2}) for MC2 configuration has been discussed in section 4.2. The purpose of the optimization study for MC2 is to find out the optimal values of Q_{R2}, t_{R2} and L_{R2} (the length of the second reactor) in order to further maximize Pr_F and minimize Q_D simultaneously. Five parameters, i.e., Q_D, t_s, Q_{R2}, t_{R2} and L_{R2} were used as decision variables, while other operating parameters such as Q_4, Q_{Ra}, L_S, L_{R1} and χ were fixed at the optimal values obtained in Case II. Mathematical description of this optimization problem is also given in Table 4.2.

Figure 4.6 demonstrates the Pareto solutions of Case III (2 reactors, 14 adsorption columns) together with the optimal results obtained for Case II (1 reactor, 14 adsorption columns) and Hashimoto's configuration with 23 columns. Results in Figure 4.6a indicate that MC2 outperforms both MC1 and Hashimoto's system particularly at higher Q_D. Although Pr_F for MC2 is lower than that of Hashimoto's when Q_D is less than 0.246 ml/min, significant improvements in Pr_F and Pur_F for MC2 is observed when Q_D is greater than 0.324 ml/min. This result once again confirms the importance of the desorbtion of fructose for system performance. Results from Figure 4.6 c & d indicate that optimal values for Q_{R2} is between 83.5% and 85.0% of Q_4 and t_{R2} is between 20% and 22% of the global switching time (t_s). These results suggest that higher Q_{R2} and relatively lower t_{R2} are favorable in achieving better system performance, which is consistent with our previous analysis for MC2. Except for section 1, all the internal flow rates are fixed for MC2 in Case III, the optimal solutions for t_s indicate the narrow range selected for the switching time is suitable.

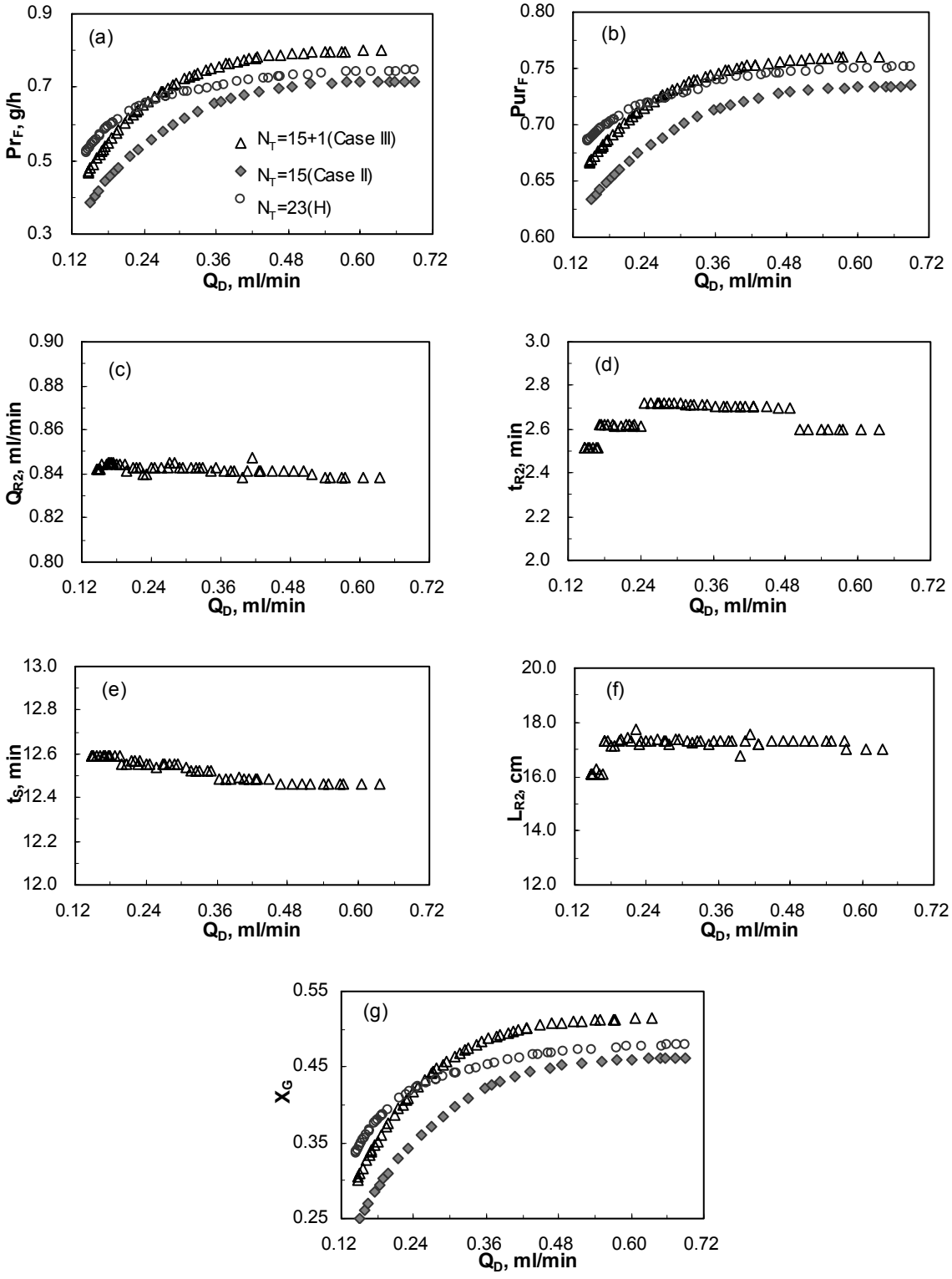

Figure 4.6 Comparison of Pareto optimal solutions between MC1, MC2 and Hashimoto's system

4.5 Performance comparison at optimal operating conditions

Table 4.5 compares the performances of the two modified configurations with that of Hashimoto's configuration at the same desorbent flow rate. We will first look at the results of MC1 and Hashimoto's configuration. Even though X_G and Pur_F obtained in MC1 with just one reactor and 14 adsortption columns are lower than those obtained in Hashimoto's 23-column system with 6 reactors and 17 adsorption columns, the calculated X_G and Pur_F for MC1 in this reference case are 46.0% and 73.34% respectively, which are very close to the upper limits of this isomerization reaction. As equilibrium constant for the reaction is 1.0 at the temperature of 323K and only one reactor is used in the system, the maximum theoretical X_G and the highest Pur_F that can be obtained are 50% and 75% respectively when feed containing 50% glucose and 50% fructose. Compared with the 13-column Hashimoto system with 2 reactors, X_G and Pur_F obtained for MC1 have increased by 12.46% and 6.34% respectively. A realization of such good system performance is due to the significant separation of glucose and fructose in section 3 of the new configuration. Figure 4.7 shows the steady state concentration profiles of glucose and fructose for MC1 at the same eluent flow rates (Q_D) as that of Hashimoto's system shown in Figure 4.1. It can be seen that much higher concentration difference between glucose and fructose is achieved in the separator of section 3 for MC1. The relatively high purity and high concentration of glucose in the raffinate stream lead to the high conversion of glucose and high purity of fructose in the product stream. The effectiveness of the reactor is therefore improved significantly. Besides, from Figure 4.7 it is also observed that concentration of glucose at the outlet of the first adsorption column (A6) in Section 4 of MC1 is much higher than that of fructose, which in fact triggered the idea for modified system MC2.

Results from Table 4.5 indicate that both Pr_F and Pur_F have been increased considerably by adding one additional reactor in MC2. Compared with MC1, Pr_F and Pur_F have increased 11.7% and 2.66% respectively at the same Q_D. A more compelling outcome is that Pr_F and Pur_F obtained in MC2 have already exceeded the corresponding values of Hashimoto's system consisting of 23 columns.

The reason in achieving such a good performance in MC2 is ascribed to the unique design of MC2 which makes R2 effective in converting residual glucose from the first reactor into fructose. It must be emphasized that the feed time to R2 (t_{R2}) plays a very important role in achieving the good performance. From the sensitivity analysis of this parameter, we noticed that t_{R2} should not exceed 40% of the global switching time. If this feed time is longer, glucose will be re-produced in R2 and improvement of X_G and Pur_F cannot realized in such a case.

The increase X_G and Pur_F can be further proved by comparison of the concentration profiles of the two configurations presented in Figure 4.7. It is observed that c_G of MC2 decreases drastically and c_F increases considerably in section 4 compared with those of MC1, which indicates more glucose has been converted into fructose in MC2. Moreover, both fructose and fructose are adsorbed by the solids in section 4. However, when this section shifts to section 1 due to switching, fructose with higher concentration is desorbed at extract port in MC2 while concentration of glucose in MC2 at the extract port is relatively lower than that of MC1, which lead to an increase of productivity and purity of fructose.

It should be mentioned that the number of the adsorption columns in the modified system can be reduced if more efficient adsorbent such as DOWEX MONOSPHERE 99 Ca separation resin is used. Normally, DOWEX resins can give a separation factor higher than 2.0 at the same temperature, while, the separation factor used in this study

is only 1.17. This low separation factor directly leads to the more adsorption columns being used in the modified configurations considered in this study.

Table 4.5 Performance comparison between modified SMBR system and Hashimoto's system at the same Q_D=0.6 ml/min

Process		Hashimoto		MC1	MC2
[1]Operating parameters					
Q_1	ml/min	3.46	3.76	4.974	4.974
Q_2	ml/min	2.716	3.304	4.23	4.23
Q_3	ml/min	2.86	3.16	5.988	5.988
Q_4	ml/min	-	-	4.374	4.374
t_s	min	7.674	7.61	12.31	12.462
Q_{R2}	ml/min	-	-	-	3.67
t_{R2}	min	-	-	-	$0.21t_s$
Column geometry					
L_S	cm	19.0	20.85	48.2	48.2
L_{R1}	cm	34.4	38.6	27.6	27.6
L_{R2}	cm	-	-	-	17.0
N_S		17	11	14	14
[2]χ		3/7/7	3/5/3	3/4/1/6	3/4/1/6
N_R		6	2	1	2
Calculated performance parameters					
X_G		48.7%	33.54%	46.0%	51.39%
Pur_F		74.84%	67.0%	73.34%	76.0%
Pr_F	g/h	0.757	0.522	0.716	0.8

1. Operating parameters for the Hashimoto's system are selected from the optimization results of Case IV in chapter 3.
2. χ refers to the number of the adsorption columns in each section.

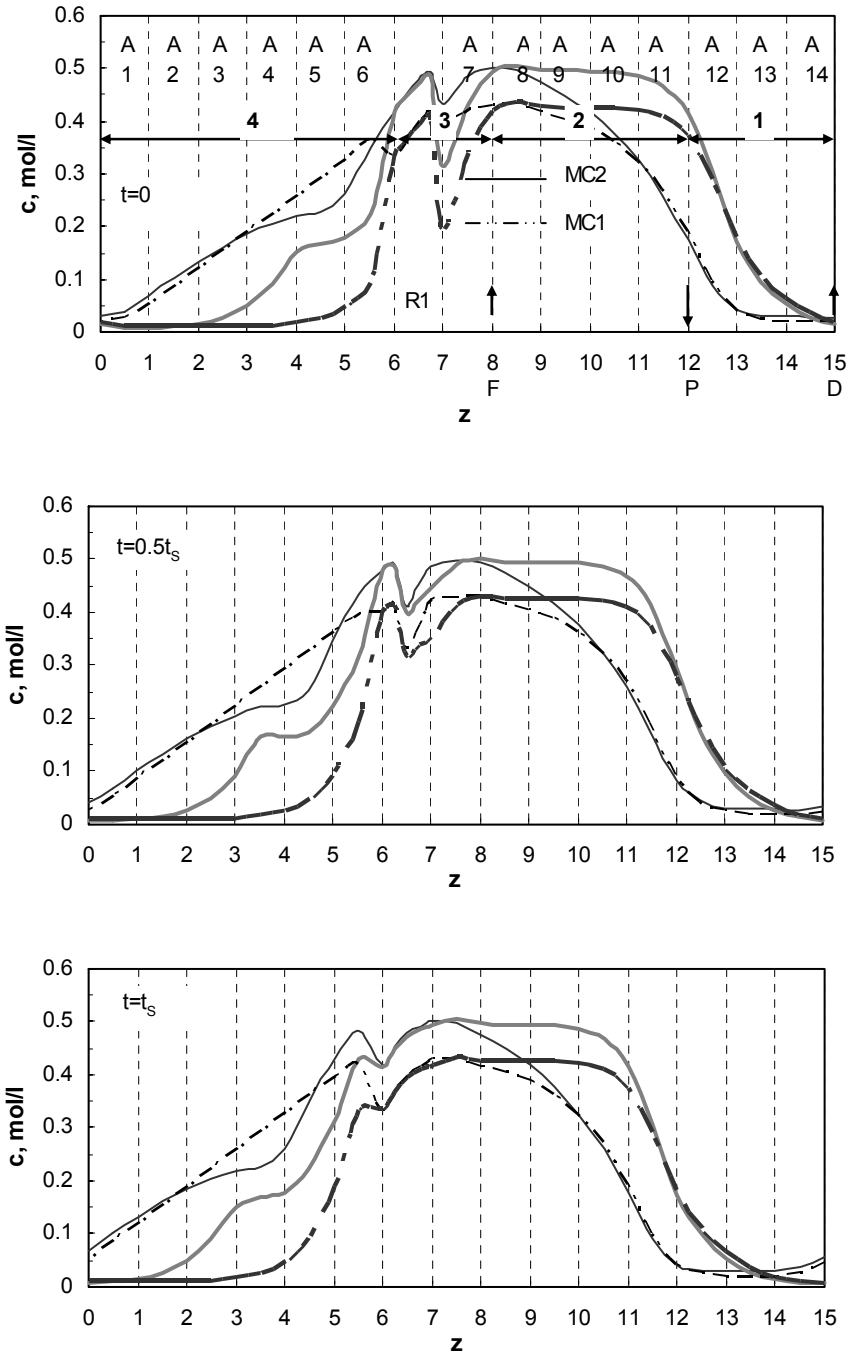

Figure 4.7 Comparison of the steady state concentration profiles for the two modified configurations (See Table 4.5 for operating conditions; thin line: c_G, thick line: c_F)

4.6 Conclusions

In this work, two modified reactive SMB configurations were introduced to produce high concentrated fructose syrup. With appropriate design of the modified systems, the performance achieved by Hashimoto's 23-column SMBR system can be realized by modified systems with just one or two reactors instead of 7 reactors. A systematic multi-objective optimization study was performed for the modified systems using an adaptation of genetic algorithm, non-dominated sorting genetic algorithm with jumping genes (NGSA-II-JG).

In modified Configuration 1 (MC1), only one reactor was used. Three processes including 17-column reactive SMB (16 adsorption columns plus 1 reactor), 15-column reactive SMB and Varicol (14 adsorption columns plus 1 reactor) were studied. Optimization results showed that relatively high liquid and solid flow rate is beneficial to system performance and incomplete regeneration of the adsorbent results in the relatively poor system performance. When less adsorption columns are used, there is a slightly decrease in the productivity and purity of fructose. However, performance of 15-column Varicol is better than that of 15-column SMBR and is almost as good as that of 17-column SMBR.

Based on the concentration profiles of MC1, one additional reactor was added at further improving system performance. One particular design for modified Configuration 2 (MC2) is that flow to the second reactor was only during the initial part of the switching period. The purpose of this design was to guarantee that the flow to the second reactor R2 contains high concentration of glucose and low concentration of fructose. Therefore, more glucose can be converted into fructose. Multi-objective optimization for MC2 showed that the design concept can further increase productivity

of fructose using less desorbent and the optimal values are even higher than that of Hashimoto's SMBR system with 6 optimum reactors.

Chapter 5 Determination of Competitive Adsorption Isotherm of Racemic Pindolol

5.1 Introduction

Chirality is a major concern in the modern pharmaceutical, chemical, and agricultural industries. This interest can be attributed largely to heightened awareness that enantiomers of a racemic drug may have different pharmacological effects in biological systems. Therefore, enantiomers of all chiral bioactive molecules have to be isolated and tested for their efficacy and safety. Based on the different stages of the development of the compounds, four major options exist for preparing the single enantiomers of chiral compounds, namely, asymmetric synthesis, enzymatic resolution, diastereomeric crystallization and direct chromatographic resolution. Thanks to the concomitant development of chiral stationary phases and efficient chromatographic techniques, chromatographic separation of the racemic compounds has been gaining increasing acceptance as a simple, rapid and applicable method for supplying pure enantiomers (Francotte et al., 1997; Francotte, 2001).

Pindolol (Figure 5.1), a type of beta blocker, is used in the treatment of hypertension. Although it is known that S-form enantiomer is the more therapeutically active component, pindolol is still marketed as racemic mixture due to the lack of efficient separation methods. However, preparative separation of racemic pindolol is of great commercial value due to the extremely high price of S-pindolol. Therefore, we will endeavor for the separation of the enantiomeric pairs of pindolol using SMB technology. In this chapter, we describe the appropriate packing for separation of pindolol and the methodology to obtain the competitive isotherm of racemic pindolol.

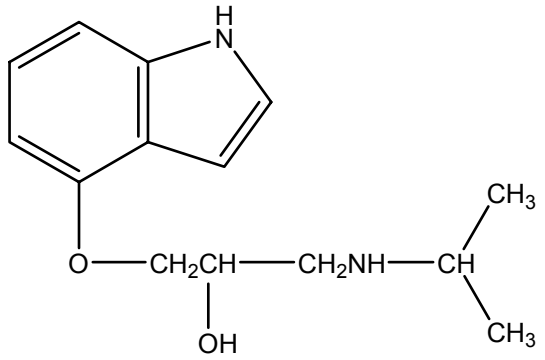

Figure 5.1 Molecular structure of pindolol

Choosing a suitable chiral stationary phase (CSP) for this chiral separation is important. Of the many available CSPs, cellulose and amylose-based phases are so far the most often used in preparative and especially SMB applications. These CSPs offer good productivities because of their high loadabilities. Although the cellulose derivatives Chiralcel OD can be used to separate racemic pindolol, however, strong adsorption of the second component on Chiralcel OD made this kind of CSP not suitable for the SMB process due to the difficulty in desorbing the strongly adsorbed species.

Protein-based CSPs, Chiral-AGP (Hermansson, 1983) is selected in this study due to its good selectivity and chemical stability. The chiral selector in the Chiral-AGP phase is alpha1-acid glycoprotein (AGP), a plasma protein composed of a single peptide chain containing 181 amino acid units and five hetero-polysaccharide units. This protein-based chiral stationary phase can tolerate high concentrations of organic solvents, high or low pH, and high temperatures. The column is operated in the reversed-phase mode and it can be used for direct resolution of enantiomers, without derivatization. Its broad applicability and the use of buffered aqueous mobile phases have made the Chiral-AGP column ideal for the separation of the different types of enantiomers (Hermansson and Grahn, 1995).

Although applications of AGP as the stationary phase for analytical purposes can be found in the published literature, this is the first attempt to apply this type of chiral stationary phase for semi-preparative enantioseparation. For preparative enantioseparation, modeling is an important prerequisite for the design and optimization of the process. Adequate simulations of a chromatographic separation progress require mainly reliable information on the adsorption equilibrium. Therefore, this study aims to acquire the competitive isotherm of racemic pindolol on chiral-AGP stationary phase. Inverse method which derives the isotherm parameters by least-square fitting model predictions to the measured elution curves is adopted in this study. Robustness and efficiency of the acquired parameters are also verified by comparing the model predictions with experimental data obtained at various operating conditions.

5.2 Theoretical

This section gives a brief review of the available methods used for acquiring the multi-component isotherm parameters and methodology used to extract the isotherm parameters from the experimental data in this work.

5.2.1 Dynamic methods in acquiring the competitive isotherm

Both static and dynamic methods can be used to determine the phase equilibrium data of the multi-component system. However, static methods are often more time consuming and less accurate than dynamic procedures. Therefore, only dynamic methods capable of measuring competitive adsorption isotherms are explained and illustrated here.

The basic principle of the dynamic methods is to inject disturbance in an equilibrated column and to analyze the column response. Based on the type of

disturbance, two most commonly used methods are distinguished for the determination of multi-component isotherm (Michel et al., 2005). Injection of a large amount of sample, with a concentration different to the existing equilibrated state, results in a breakthrough curve. Method based on this step response is called frontal analysis. The complementary case, perturbation method, involves minor disturbance to an equilibrated chromatographic system.

Frontal analysis (FA) is by far the most popular method to determine isotherms. It is operationally defined as the mode in which successive step changes in mobile phase at the column inlet are performed and the breakthrough profiles are monitored from the initial conditions until final compositions are reached. For a system with N components, (N-1) intermediate plateau concentrations and N retention times of shock fronts from each breakthrough curve have to be analyzed so that the equilibrium data can be calculated by the integral mass balance equations. The adsorption parameters can then be obtained by fitting these equilibrium data to the isotherm models by either linear or nonlinear regression. FA is considered to be the most accurate method in acquiring isotherm parameters due to the eliminated errors of kinetic effects (Zhou et al., 2003; Gritti and Guiochon, 2004). However, accurate determination of isotherm parameters requires rather large number of data points, corresponding to wide range of absolute and relative concentrations. This technique is therefore very time consuming and requires large amount of expensive pure compounds (Seidel-Morgenstern, 2004).

Perturbation method (Blümel et al., 1999; Jandera et al., 2001) determines the isotherm by measuring the retention times of small-size perturbations injected into the column equilibrated with sample solutions at different concentrations. Least-square fitting of retention times of simulated perturbation peaks to those of measured ones is used to obtain the isotherm parameters. The main advantage of perturbation method

compared to FA is that determination of the concentrations of individual compounds at the intermediate plateaus is no longer needed (Jacobson et al., 1987; Jacobson and Frenz, 1990). However, the perturbation peak method has to be performed using several mixtures of various relative compositions to obtain high accuracy, the drawback being that this approach requires pure chemical. No validation has been made of parameters determined by this method using only racemic mixtures (Lindholm et al., 2004).

A numerical method of isotherm determination, namely inverse method (IM) has been developed recently (James and Sepúlveda, 1994; Felinger et al., 2003a). This method derives the isotherm from a series of overloaded elution or breakthrough curves of the compounds. Combined with a proper column model, equilibrium isotherm is determined by tuning the values of isotherm parameters so that a minimum square deviation of the model predicted concentrations from the measured data is obtained. Contrary to FA or perturbation methods, IM is fast and needs only small amount of samples. It is now becoming popular for the determination of the competitive isotherm necessary for the preparative enantioseparation processes. Several works have demonstrated that inverse method gives rather accurate estimates of the competitive isotherm parameters under overloaded conditions. James et al. (1999) applied this method for the estimation of competitive biLangmuir and Moreau isotherms of Ketoprofen enantiomers on a chiral OJ column. Antos et al. (2000) reported the numerical determination of the isotherm of methyl deoxycholate at various mobile phase compositions in a normal phase system. Competitive isotherms of 1-phenyl-1-propanol and 1-indanol enantiomers on a cellulose tribenzoate stationary phase have recently been studied by Felinger et al. (2003a, b). Recently, Marchetti et al. (2005) applied the inverse method to derive the isotherm parameters at different

mobile phase compositions and studied the overloaded gradient elution of nociception/orphanin FQ in reversed-phase liquid chromatography. Besides, Zhang et al. (2001) also investigated the effect of the experimental error on the precision of numerically estimated isotherm parameters. Relationship between experimental error and number of experimental replicates needed to obtain isotherm parameters with a specified error was also suggested in their work.

5.2.2 Isotherm models

In multi-component adsorption systems, the amount of one compound adsorbed at equilibrium depends on the concentration of all the compounds present locally. Although several different competitive isotherm models such as Langmuir, biLangmuir, Toth and Langmuir-Freundlich are often explored to account for the equilibrium behaviors of the multi-component system, not all of them can predict the chiral separations accurately (Guiochon et al., 1994). The heterogeneous nature of the chiral stationary phase makes the commonly used homogeneous Langmuir isotherm inadequate to account for the retention mechanism of chiral separations. Toth and Langmuir-Freundlich isotherms differ from the Langmuir isotherm only by an exponent, the role of which is to take into account the heterogeneity of the distribution of sorption energies. Some research (Felinger et al., 2003a) shows that the isotherm parameters predicted by Toth model are not quite reliable when the exponent value is much lower than 1. In case of Langmuir-Freundlich isotherm, although this model provides a good empirical correlation of the binary equilibrium data for some cases, its application in elution chromatography is very difficult. The slope of the isotherm at the origin approaches infinity, which results in extremely elongated tailing.

Competitive biLangmuir isotherm seems appropriate to describe the mixed retention mechanism observed in the chiral separations (Zhou et al., 2003; Felinger et

al., 2003a, 2003b). This isotherm model assumes that surface of adsorbent is covered with two different types of sites, the nonselective sites that behave identically toward the two enantiomers and the enantioselective sites that are responsible for chiral separation. Even though non-selective sites contribute to part of the retention for both enantiomers, as implied by definition, they do not show any selectivity to either component. Therefore, both saturation capacity and equilibrium constant for the non-selective sites are identical for the enantiomeric pairs. Saturation capacity of chiral-selective sites is often the same or nearly the same for both enantiomers, while equilibrium constants are very different (Guiochon et al., 1994). BiLangmuir isotherm which account for the competitive behavior of the two enantiomers is expressed as follows:

$$q_i = \frac{q_{ns} b_{ns} c_i}{1 + b_{ns}(c_A + c_B)} + \frac{q_s b_{s,i} c_i}{1 + b_{s,A} c_A + b_{s,B} c_B} \qquad \text{(i=A or B)} \tag{5.1}$$

where, q_i is the concentration of the component adsorbed on the stationary phase, c_i is the mobile phase concentration, q_{ns} and b_{ns} are the monolayer capacity and the equilibrium constant of non-selective site, q_s and $b_{s,i}$ are the monolayer capacity and equilibrium constant of selective site. Subscripts A and B correspond to the more and less retained enantiomer, repectively.

In this study, biLangmuir isotherm has been selected to predict the equilibrium behaviors of the racemic pindolol on chiral AGP stationary phase.

5.2.3 Mathematical model for chromatographic column

Several different models, from the simplest ideal equilibrium model to the most complicated general rate model have been employed to describe the dynamic behavior of chromatographic columns in open literature (Guiochon and Lin, 2003). The ideal equilibrium model neglects the influences of axial dispersion and all mass transfer and

kinetic effects, therefore, takes less computational time but is unrealistic for most systems. While, the most complex general rate (GR) model takes into account the mass transfer kinetics with several steps, and therefore, gives more accurate solution to the preparative chromatography, but at the cost of taking longer computational time. For the best compromise between accuracy and computational time, models using only one lumped model parameter to describe band spreading of all effects have been developed (Michel et al., 2005). The equilibrium dispersive (ED) model is one of these models, which is often used. The equilibrium dispersive model assumes instantaneous equilibrium between the mobile and the stationary phases and uses a lumped apparent dispersion coefficient to account for both the axial dispersion and the finite rate of the mass-transfer kinetics. The mass balance equation of the ED model for component i in a column is expressed as following:

$$\frac{\partial c_i}{\partial t} + \varphi \cdot \frac{\partial q_i}{\partial t} + \frac{u}{\varepsilon_t} \cdot \frac{\partial c_i}{\partial z} = D_{a,i} \cdot \frac{\partial^2 c_i}{\partial z^2} \tag{5.2}$$

In this equation φ is the phase ratio related to the total column porosity ε_t, by $\varphi=(1-\varepsilon_t)/\varepsilon_t$, u is the interstitial mobile phase velocity; $D_{a,i}$ is the apparent dispersion coefficient of component i while *t* and *z* are the actual time and axial distance from the inlet of the column.

Because of high efficiency of Chiral-AGP column (plate number being higher than 800), equilibrium dispersive model was selected in this study. Integrating the isotherm model and assuming the apparent dispersion coefficients of both enantiomers being identical, mass balance equations of two-component nonlinear chromatography can be converted to the following equations.

$$(1+\varphi\frac{\partial q_A}{\partial c_A})\frac{\partial c_A}{\partial t} + \frac{u}{\varepsilon_t} \cdot \frac{\partial c_A}{\partial z} + \varphi\frac{\partial q_A}{\partial c_B} \cdot \frac{\partial c_B}{\partial t} = D_a \cdot \frac{\partial^2 c_A}{\partial z^2} \tag{5.3}$$

$$\varphi \frac{\partial q_B}{\partial c_A}\frac{\partial c_A}{\partial t} + (1+\varphi \frac{\partial q_B}{\partial c_B})\frac{\partial c_B}{\partial t} + \frac{u}{\varepsilon_t}\cdot\frac{\partial c_B}{\partial z} = D_a \cdot \frac{\partial^2 c_B}{\partial z^2} \tag{5.4}$$

Initial condition for Eqs. 5.3 & 4 is

$$c_i(0,z) = 0 \tag{5.5}$$

Boundary condition at the column inlet:

$$c_i(t,0) = c_{i,f} \qquad \text{for } 0 < t \le t_p \tag{5.6}$$

$$c_i(t,0) = 0 \qquad \text{for } t_p < t \tag{5.7}$$

Boundary condition at the column outlet:

$$\left.\frac{\partial_i c(t)}{\partial z}\right|_{z=L} = 0 \tag{5.8}$$

where, t_p is the duration of the rectangular injection; L is the column length and the subscript f indicating an inlet value. The assumption that sample is introduced into the column as a rectangular pulse of length t_p may not be valid in most practical applications. However, as the injection time is very small compared to the retention time, such a simplification still seems to be applicable (Felinger et al., 2003a).

Method of lines was used to obtain the calculated band profiles by solving Eqs.5.3 and 5.4 along with the initial and boundary conditions. In this method Finite Difference Method (FDM) is first used to discretize the PDEs in space and convert them into a set of initial value problems (IVPs) of ordinary differential equations (ODEs). The resultant ODEs of the initial value problems were then solved using the subroutine DIVPAG in IMSL for the concentration profile of each component.

5.2.4 Methodology

As already mentioned above, inverse method has been adopted in this work to

determine the competitive isotherm of enantiomer pairs of pindolol due to its inherent advantages in acquiring the competitive isotherm parameters. Based on the selected isotherm and column models, several simulations had to be performed to obtain possible ranges of the tuned parameters based on the measured retention times of the two components from the experimental band curves. An error function F(p), defined as the sum of square deviations of the predicted component concentrations from the experimental values, is then used as the objective function to derive the best-fit values of isotherm parameters:

$$F(p) = \min \sum_{j=1}^{m} [c_{j,\exp} - c_{j,\mathrm{mod}}]^2 \tag{5.9}$$

where, $c_{j,\exp}$ and $c_{j,mod}$ are the measured and model predicted concentrations of the racemic pindolol at point j of the elution curves. Optimization aimed at minimizing the error function is performed by tuning the decision variables, i.e., the value of isotherm parameters. A total of six decision variables including five isotherm parameters (q_{ns}, b_{ns}, q_s, $b_{s,A}$ and $b_{s,B}$) and one model parameter (D_a) is needed to be determined in this study. An adaptation of the state-of-the-art optimization method, non-dominated sorting genetic algorithm with jumping genes (NSGA-II-JG), was used to obtain the values of the model parameters, by minimizing the error function, F. GA is noted for its robustness and the algorithm is superior to traditional optimization algorithms in many aspects (particularly its high efficiency in finding the global optimum solution) (Bhaskar et al., 2000a, b), and has become quite popular in recent years (Zhang et al., 2002a; Wongso et al., 2005). In order to ensure that the global minimum is obtained, for each of the experimental chromatogram four optimization runs were performed with different sets of initial pool of solutions (chromosomes).

Since only concentration profiles of racemic mixture were used to derive the

isotherm parameters, a significant amount of time and experimental cost have been saved in obtaining the individual concentrations of R- and S-pindolol. Compared with other methods, inverse method requires the least number of experimental runs and therefore incurs the lowest experimental costs. However, optimization algorithm with high efficiency and accuracy is essential when applying this method.

5.3 Experimental

5.3.1 Materials

The mobile phase was a mixture of distilled deionized water and acetonitrile (90:10, v/v). Acetonitrile of HPLC grade was purchased from Fisher Scientific (Fairlawn, NJ, USA). Distilled deionized water was prepared from Micromeg System in the laboratory. The use of buffer is particularly important in separating polar compounds on reversed-phase columns, since pH can significantly alter the retention of these compounds through secondary equilibriums (Krstulović and Brown, 1982). The pH value of 7 was used for the aqueous mobile phase in this study to give a better resolution of the two components. Sodium dihydrogenphosphate (99.999%) from Aldrich (Milwaukee, WI, USA) and sodium hydroxide (97%) from Merck (Darmstadt, Germany) were employed to prepare the buffer solution. Racemic mixture of pindolol (97%) and S-pindolol (97%) were also obtained from Aldrich. Feed was prepared by dissolving the powder of racemic pindolol into the buffered mobile phase.

Chiral-AGP column (100×10 mm, 5μm) was purchased from ChromTech (Cheshire, UK). It was packed with α_1-acid glycoprotein immobilized on silica.

5.3.2 Apparatus

The chromatographic system consisted of a binary 200LC pump (Perkin-Elmer), a UV-1601PC spectrophotometer (Shimadzu) and a separate computer in which UVPC

software was installed for data analysis. 200 LC pump was connected to column to provide a rectangular pulse input with a duration of t_p. Effluent from outlet of column was connected to inlet of flow cell of the UV-1601PC photometer so that online elution curves of racemic mixture can be recorded. UV photometer was used at a wavelength of 225nm in this study. Detector was calibrated before experiments and responses from the detectors were found to be linearly proportional to concentrations.

5.3.3 Experimental procedures

All experiments were carried out at room temperature (21±0.5°C). Experiments with either small injection (pulse test) or large injection (frontal analysis) were conducted. The pulse tests aimed to obtain elution concentration profiles of racemic pindolol, which served to derive the isotherm parameters using optimization algorithm. Frontal analysis measurements were used to test the validity of isotherm parameters obtained from inverse method.

In pulse tests, before feeding the samples, column was first washed with distilled deionized water and then equilibrated with mobile phase for 1 hour. A programmable running sequence of the binary LC pump allowed the pump to first feed sample into column. After duration of the setting time (t_p), an instantaneous change of the curve in running method made mobile phase to be continuously pumped into column. Therefore, a rectangular injection pulse of width t_p was accomplished and pure mobile phase helped to elute the chemicals adsorbed on the chiral stationary phase. Online UV photometer equipped with flow cell was used to record the absorbance of R- and S-pindolol, which then can be converted into the band concentrations of the two enantimers. Three different injections of racemic mixture (20.0, 40.0, 80.0 μg) were used to determine the competitive isotherm parameters. In order to minimize experimental error, each pulse test was replicated to guarantee that experimental error

was less than 2%.

In the frontal analysis measurements, column was first pre-equilibrated with mobile phase. Sample with a certain concentration was then continuously fed into the column at predetermined flow rate. After column reached equilibrium, i.e., elution concentration was identical to feed concentration; inlet of LC pump was switched over to the mobile phase. Consequently, column was regenerated by flushing away the solutes with pure mobile phase. A series of breakthrough and desorption curves were obtained by varying feed concentrations (concentrations of racemic pindolol with 2, 4, 6, 8, 10 and 12 mg/l were utilized) in frontal analysis measurement. Sufficient long time delay between the adjacent injections of the feeds was allowed for the complete re-equilibration of the column with pure mobile phase.

5.4 Results and discussions

5.4.1 Determination of elution order

Elution order of enantiomers is important for chromatographic production process. Normally, the raffinate enantiomer can often be obtained with better economics in SMB process as it can be recovered at higher purities and concentrations (Wewers et al., 2005). In order to determine the elution order of racemic pindolol on α_1-acid glycoprotein stationary phase, elution curves for racemic pindolol, pure S-pindolol as well as mixture of racemate and S-pindolol (50:50, V/V) obtained under the same operating conditions were compared. It can be seen from the results of chromatograms shown in Figure 5.2 that S-pindolol (the desired component) eluted first, which is desirable for the SMB separation.

(a) Racemic pindolol (Q=0.9 ml/min, Wavelength= 225 nm)

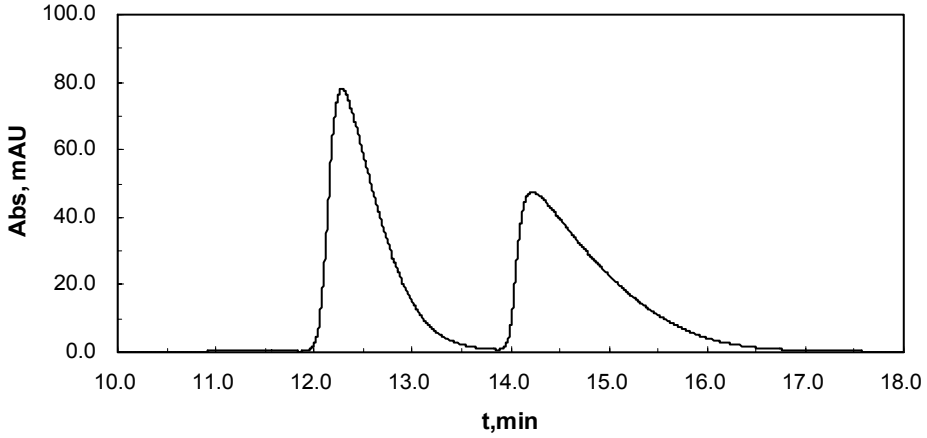

(b) Pure S-pindolol with purity of 97% (Q=0.9 ml/min, Wavelength= 225 nm)

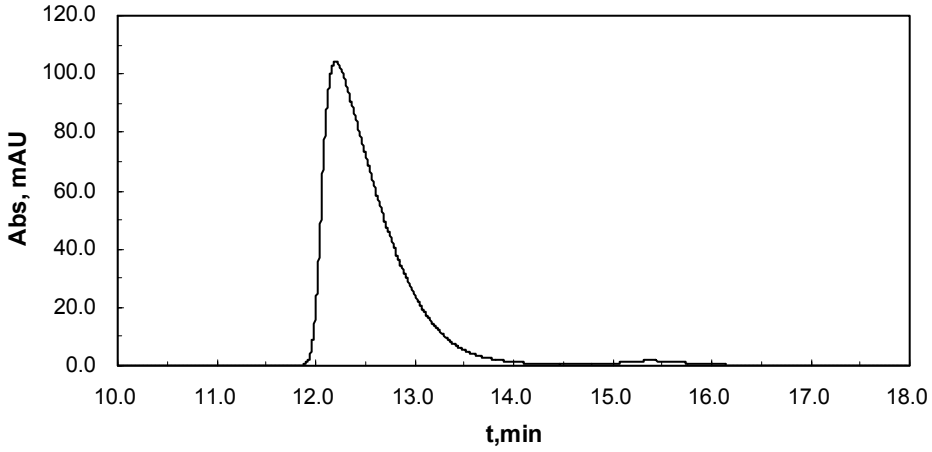

(c) Mixture of racemic and pure S-pindolol (Q=0.9 ml/min, wavelength= 225 nm)

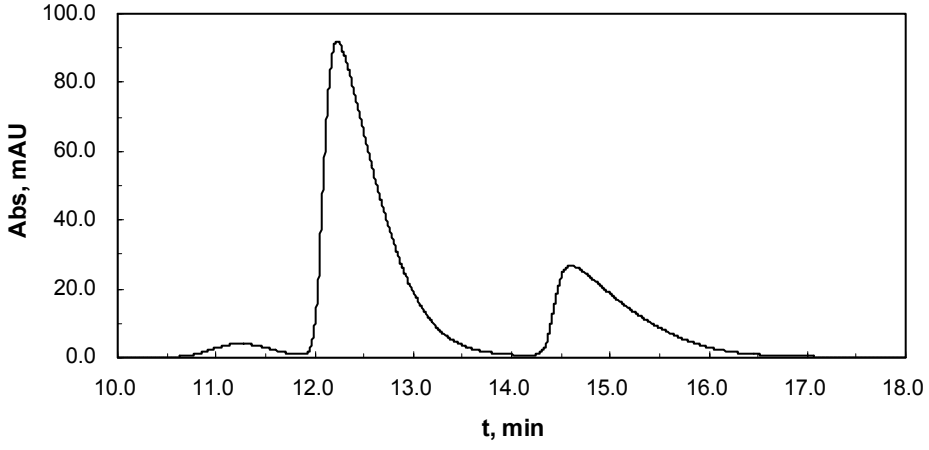

Figure 5.2 Elution order of S-pindolol

(a) Injection volume of 60µl with total feed concentration of 0.02g/l; (b) Injection volume of 60µl with feed concentration of 0.017g/l; (c) Injection volume of 60µl

5.4.2 Column parameters

Accurate measurement of void volume of a packed column is of great importance for all types of chromatography as void volume is a critical parameter for the accurate determination of isotherm parameters. In this study, total void volume (V_t) including the inter-particle and intra-particle volume was obtained from the disturbance peak method by injection of distilled deionized water. Total column porosity (ε_t = 0.714) corresponding to total void volume was calculated from $\varepsilon_t = V_t/V$. where, where V (7.854 cm^3) is the geometric volume of the column. In order to obtain the net elution volume, additional column dead volume was subtracted from all the experimental data.

Column efficiency or effective plate number (N_P) is another important parameter which influences the accuracy of isotherm parameters derived from the inverse method. As it is known the accuracy of the best-fit isotherm parameters depends largely on the calculated band profiles which are in turn decided by the column efficiency. Figure 5.3 shows the effect of plate number on the simulated band profiles together with the experimental data. It can be observed from Figure 5.3 that concentration profiles is sharper when plate number is higher (N_P=1500) and broadening of elution curves occurs (which deviates from the experimentally measured band profiles) when column efficiency (N_P=600) is lowered.

To the best of our knowledge, there is no complete research on how to determine column efficiency under nonlinear conditions and no equations are available to estimate the effective plate number under heavily loaded conditions. In this study, selection of number of plate was entirely based on the best fit of the model predicted band profiles to experimentally measured data. From our simulation results, it can be seen that the differences between the calculated band concentrations are negligibly small if number of plate is above 1200. Therefore, for the sake of simplicity, effective

plate number had been chosen as 1200 in this study.

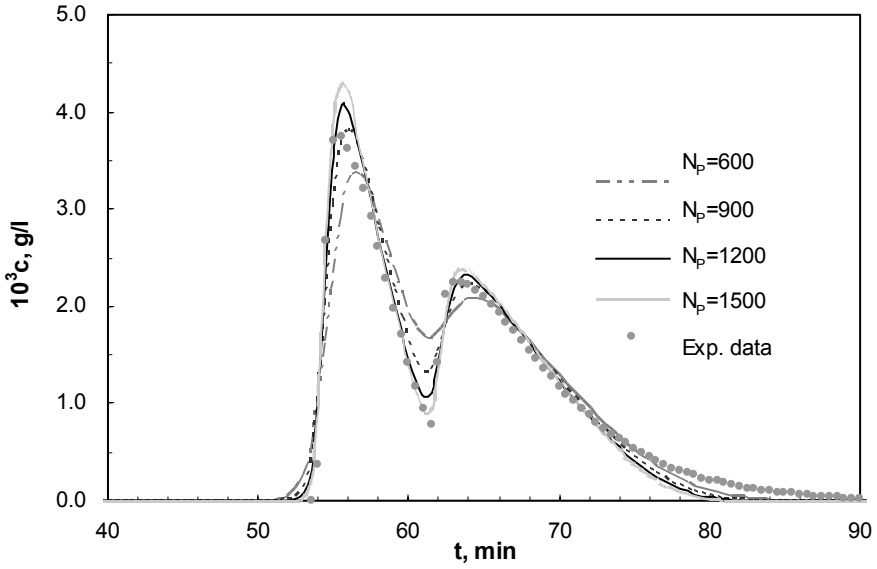

Figure 5.3 Comparison of the simulation results with different column efficiencies

Q=1.0 ml/min, t_p=1.0 min, $c_{A,f} = c_{B,f}$ =0.02 g/l, q_{ns}=1.684 g/l, b_{ns}=14.21 l/g, q_s=0.046 g/l, $b_{s,A}$=151 l/g, $b_{s,B}$=28 l/g

5.4.3 Apparent dispersion coefficient

Determination of the apparent dispersion coefficient, $D_{a,}$ is also a difficult task. D_a was also determined by fitting the model predicted band profiles to experimental data in this study. In order minimize the computational effort; the following three steps were followed. First, a wide range of D_a was used in the optimization study. It was found that for all the optimization runs D_a converged to values between $6 \times 10^{-4} \sim 1.08 \times 10^{-3}$ cm^2/min. In the second step, this narrow range of D_a ($6 \times 10^{-4} \sim 1.08 \times 10^{-3}$ cm^2/min) was used in the optimization study to obtain the best-fit value of D_a. This time D_a converged to the value around 9.67×10^{-4} cm^2/min for most of the optimization runs. Therefore, in the final stage of optimization study, D_a was fixed at 9.67×10^{-4} cm^2/min for the flow rate of 1.0 ml/min for consistency of all the results. In

fact, this final result of D_a is very close to the axial dispersion coefficient, D_L (Ruthven, 1984), which defines the contributions of eddy diffusion and molecular diffusion in the form of

$$D_L=0.7D_m+0.5u\cdot d_p, \tag{5.10}$$

Where D_m is the molecular diffusion coefficient of solute in mobile phase, u is the interstitial velocity and d_p is the particle diameter. D_m can be calculated based on diffusion coefficient in dilute solutions (Cussler, 1997) according to the following equation,

$$D_m = [D_m(x_1 = 1)]^{x_1}[D_m(x_2 = 1)]^{x_2} \tag{5.11}$$

where x_1 and x_2 are mole fraction of water and acetonitrile, x_1=0.964, x_2=0.036 in this system; $D_m(x_1=1)$ is the molecular diffusivity of pindolol in pure water while $D_m(x_2=1)$ is the molecular diffusivity of pindolol in pure acetonitrile. Since x_2 is very small, molecular diffusivity of pindolol in the mobile phase roughly approximates to that in pure water, which can be calculated from Hayduk-Laudie correlation (Braum, 1998)

$$D_m = 79.56\times10^{-4}\mu^{-1.4}V_1^{-0.589} \quad \text{cm}^2/\text{min} \tag{5.12}$$

where, μ is the water viscosity, μ=0.98×10^{-2} g/cm·s at 21ºC; V_1, the molar volume of the solute, can be estimated using Le Bas additivity constants (Braum, 1998), V_1=320 cm^3/mol. The observation of Da value close to D_L (around 6.4 × 10^{-4} cm^2/min) is consistent with that reported by Felinger et al. (2003a). This result also implies that the mass transfer between the fluid phase and stationary is very fast and the use of equilibrium dispersive model is valid.

5.4.4 Parameters of biLangmuir isotherm

Three overloaded chromatograms with different amount of injections of mixture were used in order to extract isotherm parameters and apparent dispersion coefficient.

Retention times and shape of elution curves of the two enantiomers offered some indication on the initial guesses of the isotherm parameters. Some simulations were carried out to determine possible ranges of the decision variables which were prerequisite in the optimization. Isotherm parameters were first determined from the optimization runs by fitting the simulated chromatogram to individual experimental chromatogram. Results of the isotherm parameters as well as the apparent dispersion coefficient are summarized in Table 5.1 together with the best-fit concentration profiles are plotted in Figure 5.4.

Table 5.1 Isotherm parameters obtained with biLangmuir model

Loading μg	q_{ns} g/l	b_{ns} l/g	q_s g/l	$b_{s,A}$ l/g	$b_{s,B}$ l/g	$10^4 Da$ cm^2/min
20	1.08	22.4	0.0332	238.2	48.2	9.67
40	1.48	16.59	0.0371	185.0	25.2	9.67
80	1.735	14.293	0.0453	144.8	25.08	9.67
40 & 80	1.74±0.06	14.05±0.25	0.048±0.002	149±5.0	26.4±2.0	9.67

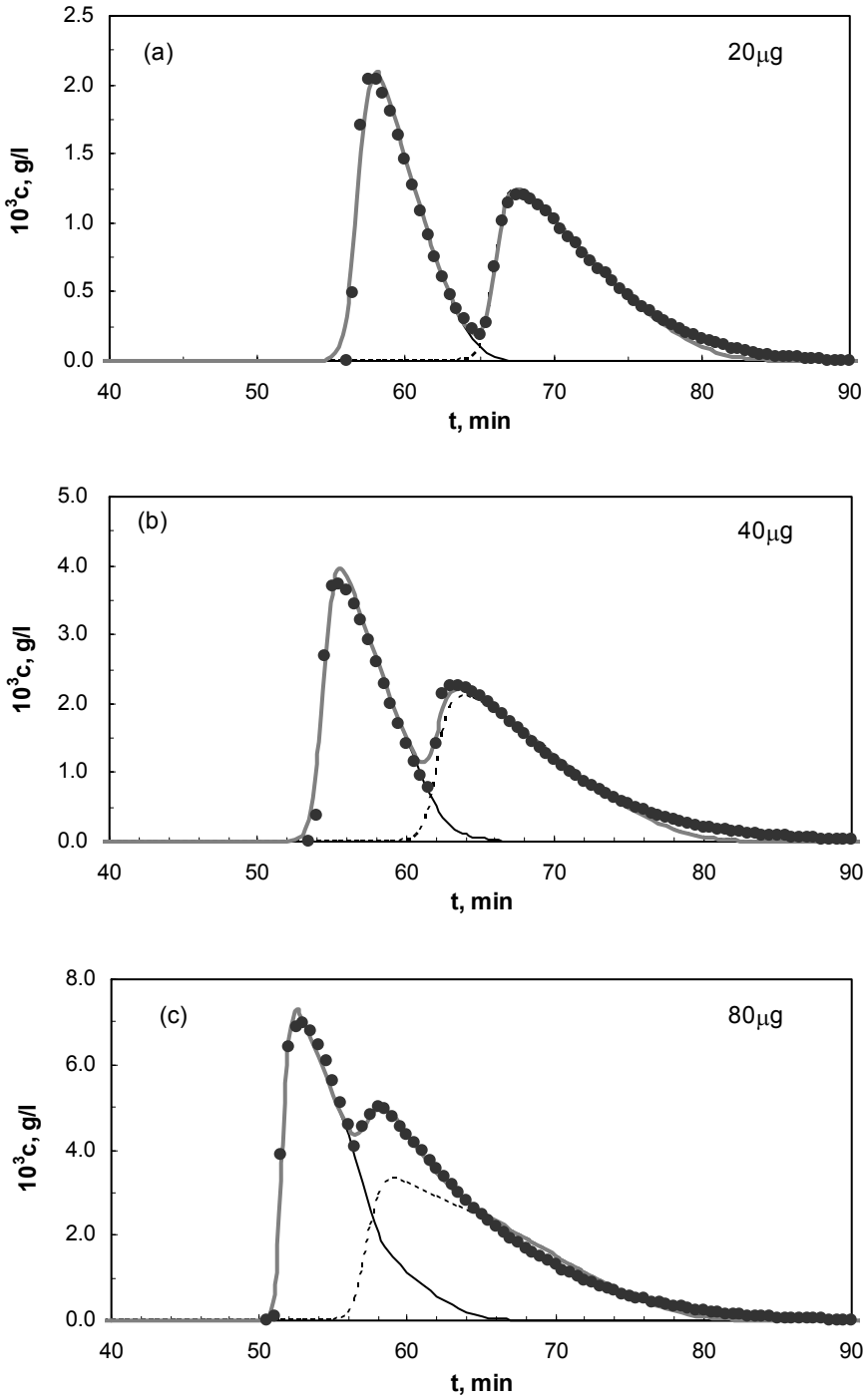

Figure 5.4 Best-fit overloaded profiles determined by the individual fit of each chromatogram

Q=1.0 ml/min, t_p=1.0 min. (a) $c_{A,f} = c_{B,f}$=0.01 g/l; (b) $c_{A,f} = c_{B,f}$ =0.02 g/l; (c) $c_{A,f} = c_{B,f}$=0.04 g/l

Results shown in Figure 5.4 indicate that the biLangmuir isotherm can account well for retention mechanism of R- and S- pindolol on the chiral AGP stationary phase. In all the three cases shown in the figure, biLangmuir isotherm predicts the concentration profiles of racemic pindolol very well. However, isotherm parameters derived from the three chromatograms converged to different values. The higher the column loading, the higher the saturation capacities for both the nonselective and selective sites are obtained, while the opposite trend is observed for the adsorption equilibrium coefficients. This observation is quite consistent with those reported in the open literature (Felinger et al., 2003a). The reason for such an observation may be ascribed to the difficulty of properly quantifying the competitive effects between the two enantiomers when column loading is too low (Seidel-Morgenstern, 2004). Classical multi-component isotherm models can be used to illustrate the competitive effects only under overloaded conditions. Therefore, the saturation capacity is under estimated if column loading is too low.

In order to acquire more reliable and uniform isotherm parameters, the strategy of tuning isotherm parameters by simultaneously fitting two chromatograms, one at the higher sample loading (80 μg) and the other at moderate loading (40 μg) was conducted. Four optimization runs were performed to obtain the global optimum solutions. As slight differences in the final results were obtained from the 4 runs, instead of assigning a specific value for each decision variable, a narrow range was acquired for each tuned parameter so that the isotherm parameters can be applied to a wide concentration range. Results for isotherm parameters derived from simultaneous fitting are also listed in Table 5.1. It can be seen that the numerical isotherm parameters obtained by fitting the two chromatograms together are very close to those derived from the largest injection alone. Figure 5.5 shows the results of fitting

biLangmuir isotherm simultaneously to the two chromatograms. The agreement between the experimental (symbol ●) and model predicted elution profiles (continuous line) is very good.

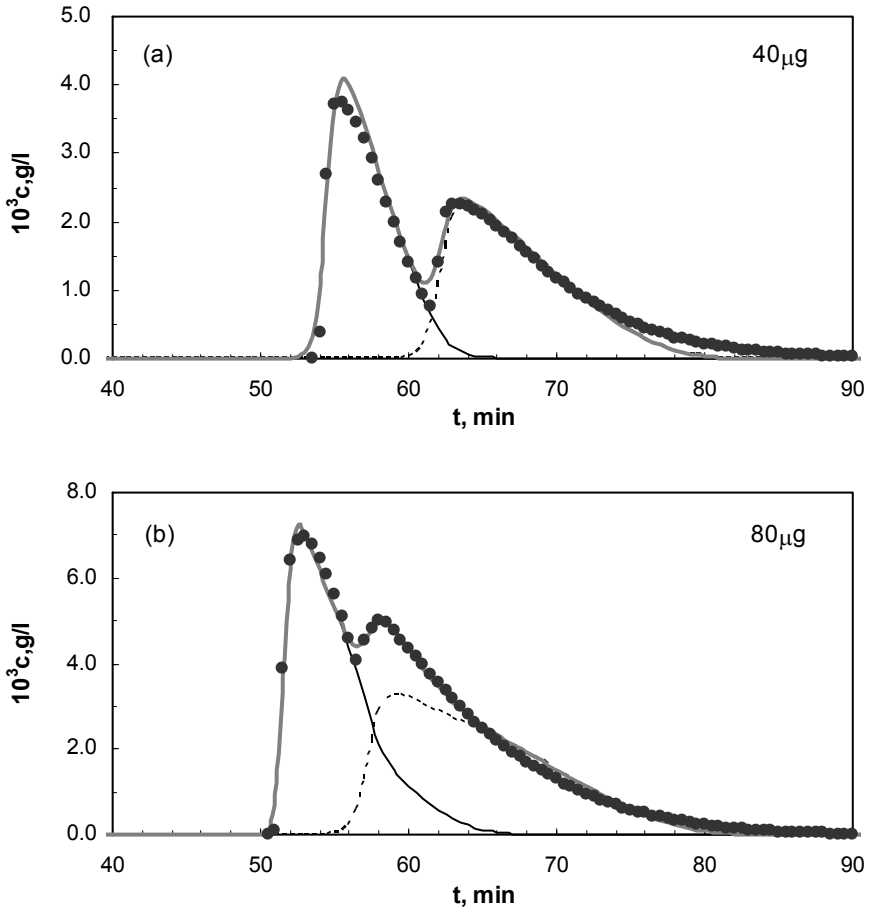

Figure 5.5 Best-fit overloaded profiles determined by simultaneous fit of two chromatograms

Q=1.0 ml/min, t_p=1.0 min. (a) $c_{A,f} = c_{B,f}$ =0.02 g/l; (b) $c_{A,f} = c_{B,f}$ =0.04 mg/l

5.4.5 Validation of isotherm parameters

Pulse tests were conducted at higher flow rates (Q = 2.0-3.0 ml/min) with different injection amounts to investigate the validity of the determined isotherm parameters. It should be mentioned that Da value under higher flow rates had been revised in the program based on the value (9.67×10^{-4} cm^2/min) at Q=1.0 ml/min. Figures 5.6 & 5.7 demonstrate comparisons between the experimental and model predicted elution profiles (using the isotherm parameters listed in the last row of Table 5.1) of pindolol at flow rate of 2.0 ml/min and 3.0 ml/min respectively. For both cases model predictions do not fit well the experimental data when the lowest injection amount is used. However, good agreements are observed at moderate and high injection amounts. These results provide evidence that competitive effects cannot be quantified accurately at lower column loading and chromatograms recorded for lower injection amounts appear to be less valuable for the isotherm estimation when inverse method is applied.

The accuracy of the derived isotherm parameters (listed in the last row of Table 5.1) was also validated by using them to simulate the breakthrough and desorption curves, which were compared with experimental ones of frontal analysis. Figure 5.8a–d shows the experimental data (represented by symbol ●) and corresponding simulated breakthrough and desorption curves (thick continuous line) of racemic mixture at various step inputs. Results indicate that the isotherm parameters obtained from the inverse method can make accurate predictions of the breakthrough and desorption curves with the feed concentrations varying between 4 and 10 mg/l. Injection amounts of pindolol increased greatly in frontal analysis because of volume overload and the highest injection amount was up to 850 μg, which is 10 times higher than that used in pulse test. Good agreement between the calculated and the

experimental breakthrough and desorption curves achieved in frontal analysis (see Fig. 5.8a–d) indicates that the derived parameters are able to cover a broad range of the isotherm.

Verification of the parameters by both the pulse test and frontal analysis indicates that isotherm parameters obtained from the inverse method are quite robust and can be used over a wide range of concentration. However, small discrepancies between the measured and calculated concentration profiles still can be observed in Figures 5.4-5.7. The possible reasons for such small discrepancy may stem from three aspects. The first possible reason is the deviation of input profiles of sample in the pulse test from ideal rectangular pulse injection assumed in the mathematical model used for the simulation. Therefore, inaccuracy of boundary conditions in the mathematical model may lead to some discrepancies in simulation results. The second possible reason may be errors in the measured concentrations. As already mentioned, all the experimentally measured concentrations were transferred from online absorbance data. Both drift of the baseline and noise of the signals will bring about small errors in the experimental data recorded. Last but not the least, the selected biLangmuir model may also lead to some theoretical errors in predicting elution or breakthrough curves. Because of the highly complex structure of the selector, chromatographic mechanism involved in the chiral discrimination has not yet been clarified for Chiral-AGP stationary phase. More complicated isotherms, such as triLangmuir isotherm or even some semi-empirical correlation, may describe the adsorption equilibrium on Chiral-AGP better.

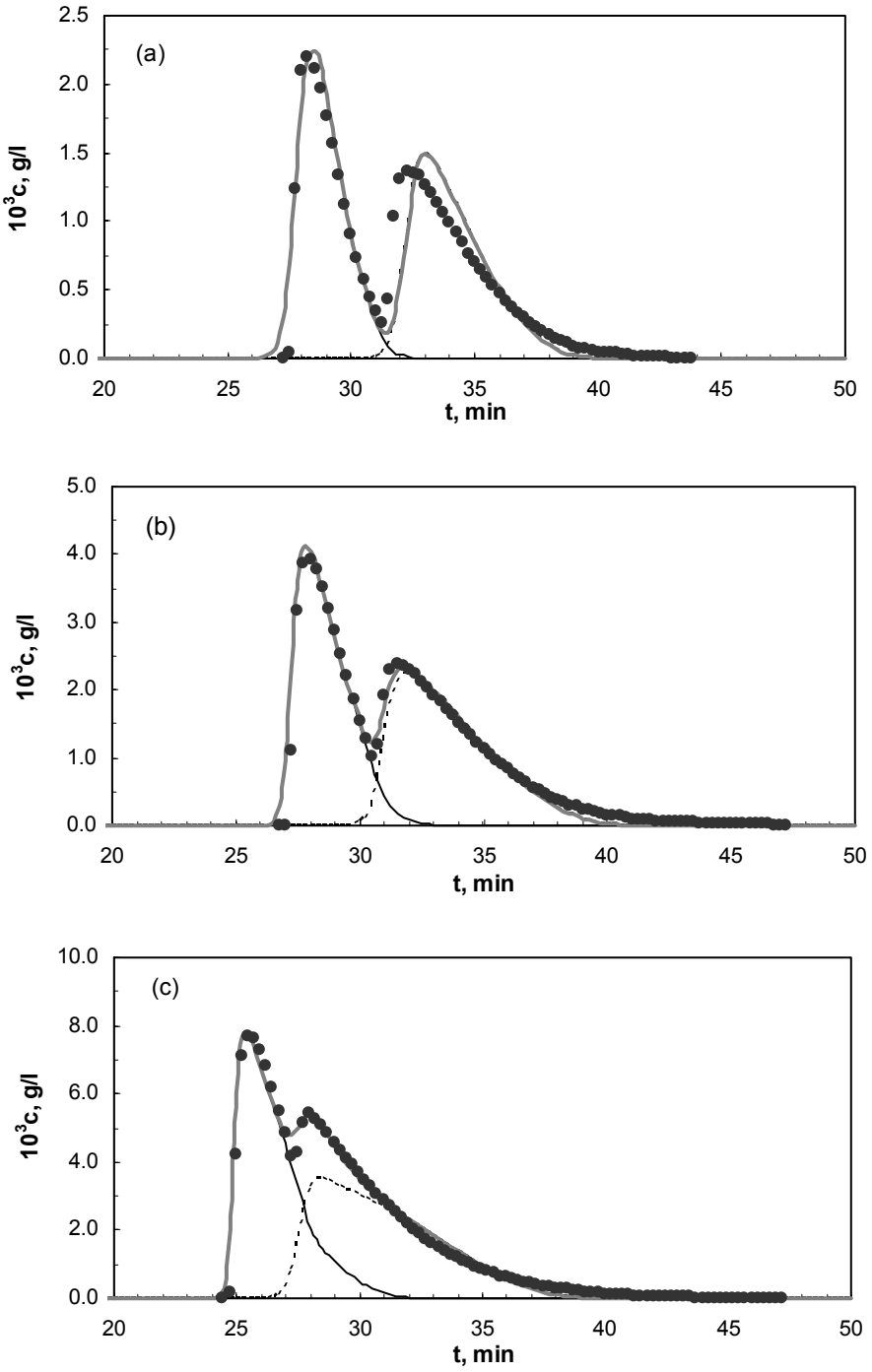

Figure 5.6 Comparison of the simulated and experimental band profiles for pindolol at *Q*=2.0 ml/min

Q=2.0 ml/min, t_p=0.5 min. (a) $c_{A,f} = c_{B,f}$ =0.01 g/l; (b) $c_{A,f} = c_{B,f}$ =0.02 g/l; (c) $c_{A,f} = c_{B,f}$ =0.04 g/l

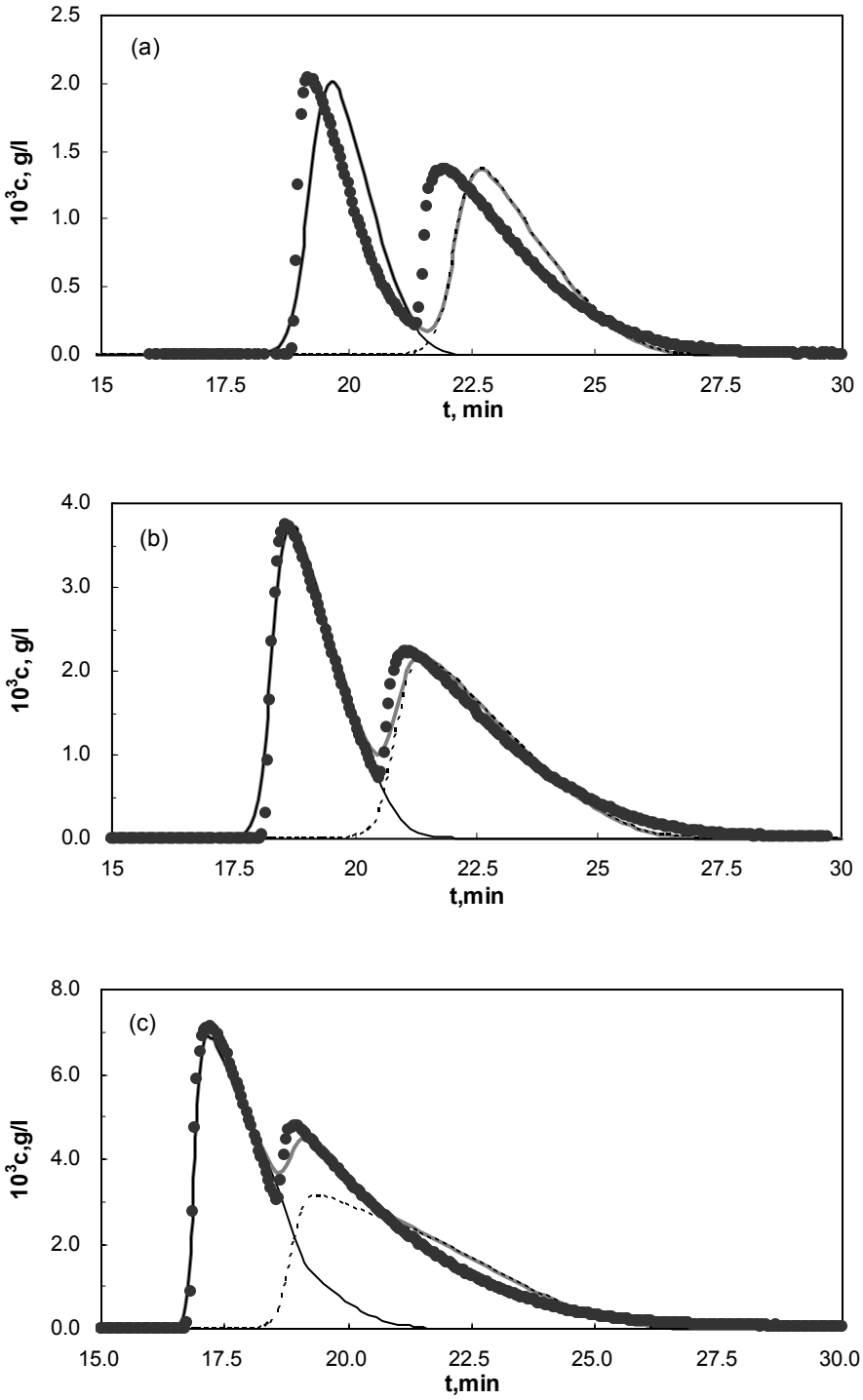

Figure 5.7 Comparison of the simulated and experimental band profiles for pindolol at *Q*=3.0 ml/min

Q=3.0 ml/min, t_p=0.3 min. (a) $c_{A,f} = c_{B,f}$ =0.01 g/l; (b) $c_{A,f\ f} = c_{B,f}$ =0.02 g/l; (c) $c_{A,f} = c_{B,f}$ =0.04 g/l

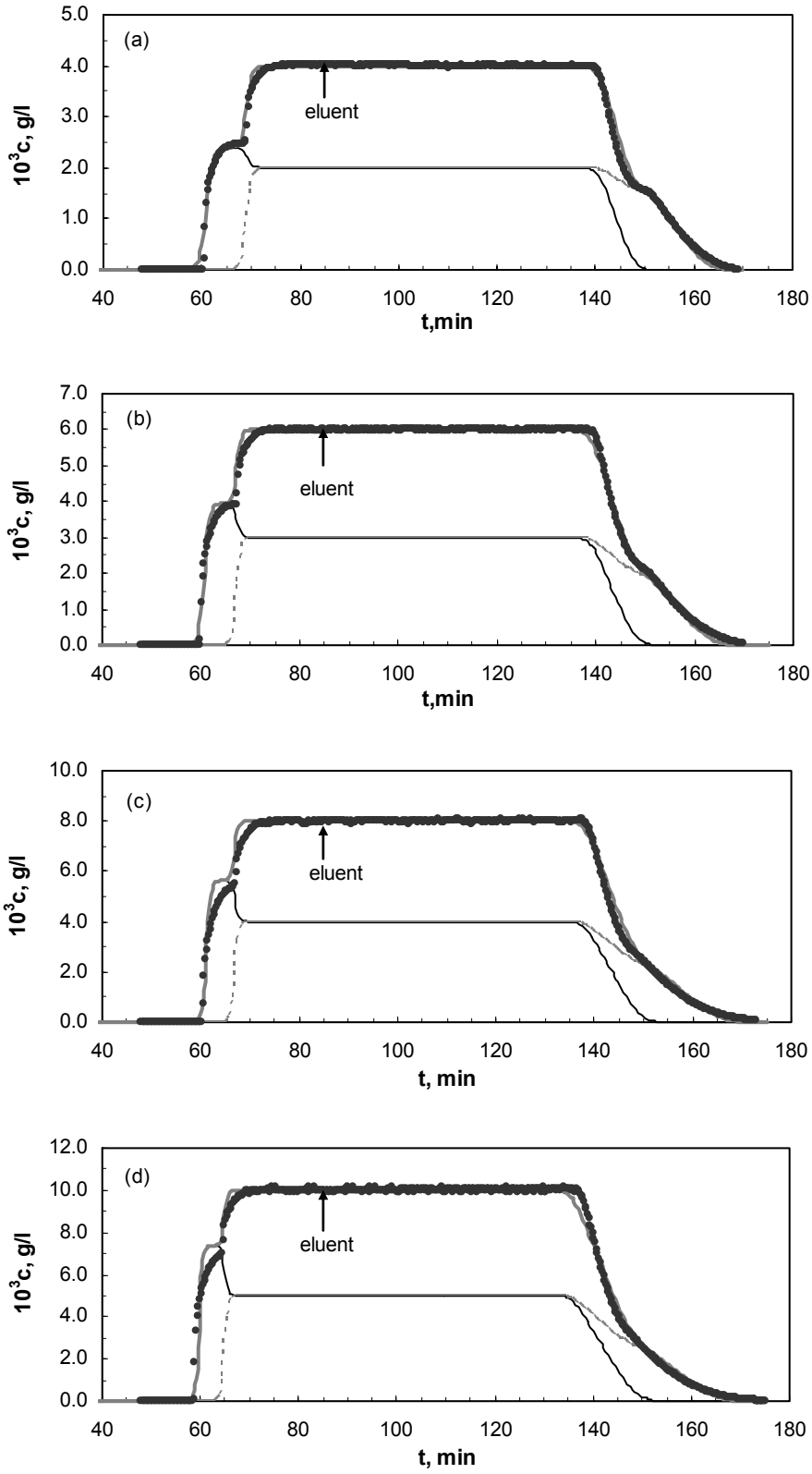

Figure 5.8 Comparison of the simulated and experimental breakthrough and desorption curves for racemic pindolol

5.4.6 Effect of column degradation on thermodynamics

Observations of column degradation for the silica-based reversed-phase high-performance liquid chromatography have been reported in the open literature (Glajch et al., 1987; Kirland et al., 1995; Schulte and Strube, 2001). Although the pH value not higher than 7.0 for the aqueous mobile phase had been strictly fulfilled during all the experimental work in this study, change in the elution characteristics of pindolol on the stationary phase (shown in Figure 5.9) still occurred after a period of repeated use of the column.

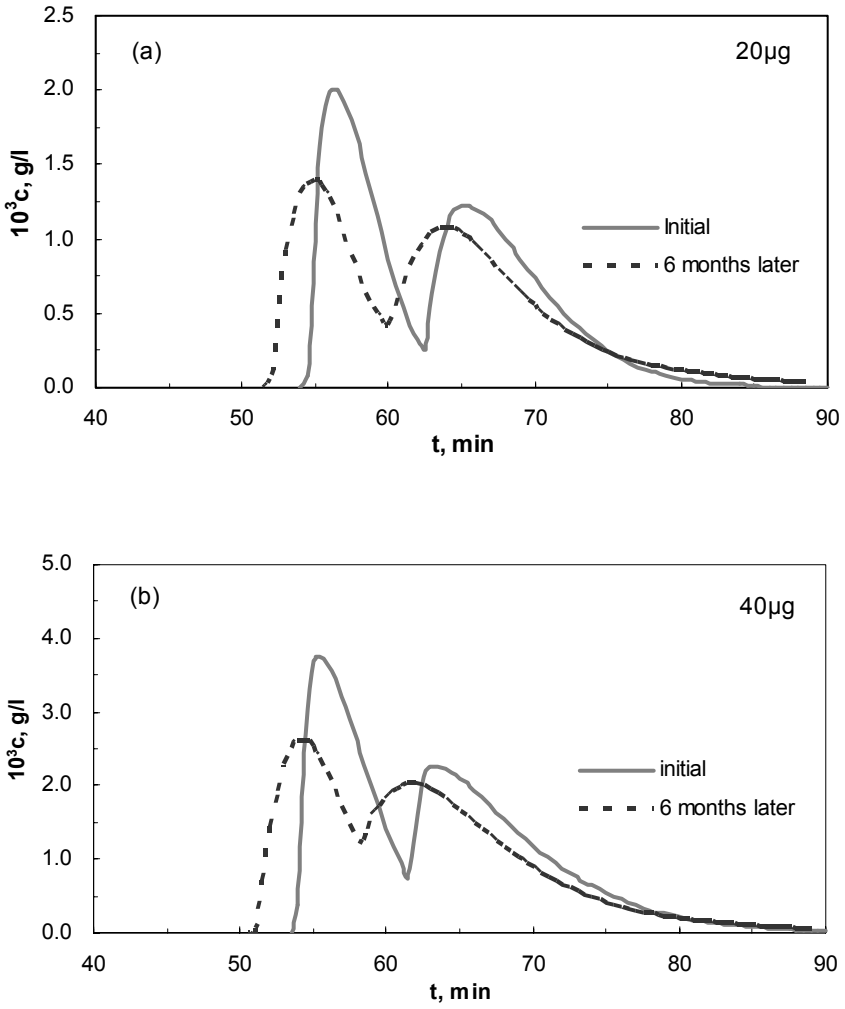

Figure 5.9 Change in the elution characteristics of pindolol on Chiral-AGP

Q=1.0 ml/min, t_p=1.0 min. (a) $c_{A,f} = c_{B,f}$=0.01 g/l; (b) $c_{A,f} = c_{B,f}$ =0.02 g/l;

Decreases of retention times for both components and loss of efficiency can be observed from Figure 5.9 due to part of the sorption sites permanently occupied by strong retention compounds (Schulte and Strube, 2001). Such considerable retention time decay arising from column degradation or fouling will definitely affect the thermodynamics of pindolol. In addition, protein-based CSPs have generally much smaller loadabilities because fewer large molecules (e.g., proteins) can be immobilized on silica, resulting in a lower density of the enantioselective sites, as compared to smaller selectors. Therefore, the effect of column degradation on the variation of the isotherm parameters should be considered in this case.

Since both solute and solvent may have complicated sorption mechanism on Chiral-AGP (Thompson et al., 2001; Gyimesi-Forrás et al., 2003), elution curves from the "used" column as well as some SMB experimental data were employed to correct isotherm parameters derived from the "fresh" column. The final isotherm parameters are listed in Table 5.2. Compared with the results listed in the last row of Table 5.1, capacity of the nonselective sites has decreased about 7%, while capacities of the selective sites have decreased 4.9% and 0.2% for the more and less retained components respectively. Decrease in capacity of the nonselective sites is more significant. These results coincide with those reported by Götmar et al. (2002). Although a loss of sorption sites takes place in Chiral-AGP columns after a period of usage, the apparent separation factor of the two components does not change significantly, this can be seen from Figure 5.9. Therefore, isotherm parameters given in Table 5.2 are used in the modeling of the SMB process, which will be discussed thoroughly in the next chapter.

Table 5.2 Isotherm parameters after correction

q_{ns} g/l	b_{ns} l/g	q_s g/l	$b_{s,A}$ l/g	$b_{s,B}$ l/g	$10^3 Da$ cm^2/min
1.32	16.85	0.042	155.0	30.6	1.16

5.5 Conclusions

Inverse method has been used in this study to determine the biLangmuir isotherm of pindolol enantiomers on α_1-acid glycoprotein chiral stationary phase using an adaptation of genetic algorithm, non-dominated sorting genetic algorithm with jumping genes (NSGA-Ⅱ-JG), as the optimization method. By fitting the chromatograms at moderate and high sample loads (40 and 80 μg) simultaneously, the isotherm parameters were determined. Good agreement was observed between model predicted and experimental elution concentrations. In order to determine how robust the derived isotherm parameters are, some sensitivity studies were performed by varying flow rates and feed concentrations. In addition, the validity of isotherm parameters was also tested by comparing experimental and simulated breakthrough curves for various step inputs. Results from both the pulse tests and the frontal analysis indicate that isotherm parameters derived from the inverse method are reliable and can be used for a wide range of concentrations.

Not surprisingly, column degradation took place after six months of repeated use of columns. Decrease in retention time and loss of efficiency were observed due to part of the sorption sites permanently occupied by strong retention compounds or impurities. In order to obtain the more robust isotherm parameters which can be used in the modeling of SMB process, isotherm parameters obtained from the fresh column were corrected from experimental data of both single-column as well as SMB operations. Results indicate decrease in capacity for the non-selective sites is more

significant, while the apparent separation factor does not change obviously.

In this study only single chromatogram of the racemic mixtures was applied to derive isotherm parameters, which saves considerable time and experimental cost in obtaining individual concentrations of R- and S- pindolol. Due to the less number of experiments need to be conducted and thereby lower experimental cost involved, inverse method becomes more and more attractive in obtaining the competitive adsorption isotherm parameters.

Chapter 6 Enantioseparation of Racemic Pindolol by SMB and Varicol

6.1 Introduction

Simulated moving bed (SMB) chromatography, as mentioned earlier, is a practical implementation of the continuous counter-current chromatographic process, which overcomes the limitations of batch chromatography and provides significant benefits in terms of productivity and solvent consumption due to the increased exchange capabilities between the two phases. Because of its high separation power, SMB chromatography has been implemented successfully as a separation technique in the petrochemical and food industries in a multi-ton scale. During the last decade, with the event of stable stationary phases for chromatographic enantioseparations, SMB has been successfully downscaled to the pharmaceutical industry to prepare enantiomeric-pure pharmaceuticals in small scale as well as up to 100 ton scale. However, the advantages of SMB processes are achieved by a higher complexity with respect to layout and operation, which makes the empirical design not applicable (Schulte et al., 2005). Therefore, modeling and simulation is necessary for process design and optimization.

Following chapter 5, enantioseparation of racemic pindolol using SMB and Varicol processes will be presented in this chapter. Results from the last chapter indicated that pindolol shows nonlinear characteristic even under low concentrations. Design and operation of SMB and Varicol for such a nonlinear system with axial dispersion still remains a big challenge in the application of SMB technology. Few theories so far provide a direct guidance in how to choose the proper operating parameters for such a complex design problem. Trial and error approach based on numerical simulations seems to be the

only possible choice. The purpose of the current study is to develop a short-cut design strategy so that computational work for such a trial and error process can be reduced without a considerable loss of accuracy in the obtained operating parameters which give the desired separation.

In the first part of this study, a shortcut method for selecting the operating conditions is presented based on the mathematical model and experimentally determined adsorption isotherm. Several SMB and Varicol experiments were then carried out to validate the model predictions under a relative wide range of operating parameters. Factors influencing SMB performance are discussed subsequently.

6.2 Modeling and Design

Successful design and operation of a SMB process depends on the proper selection of the switching time and the flow rates in each section. Designed for high productivity separations, SMB units usually operate at high feed concentrations leading to non-linear competitive adsorption behaviors. Therefore, modeling and simulation tools are of crucial importance in determination of the operating parameters.

6.2.1 Mathematical model for SMB and Varicol

Several different models can be applied to simulate the counter-current moving bed chromatography. The equilibrium dispersive (ED) model was adopted in this study as this model is the best compromise between accuracy and computation time. Instantaneous equilibrium between the mobile and the stationary phases is assumed because of the high efficiency of the Chiral-AGP column (Np > 800). Axial dispersion for the fluid phase is incorporated and a lumped apparent dispersion coefficient is used to account for both the

axial dispersion and the finite rate of the mass-transfer kinetics within the column. Transient mass balance equations for component i in the j^{th} column during the N^{th} switching period are as follows.

$$\frac{\partial c_{ij}^{N}}{\partial t}+\frac{1-\varepsilon_t}{\varepsilon_t}\cdot\frac{\partial q_{ij}^{N}}{\partial t}+\frac{u}{\varepsilon_t}\cdot\frac{\partial c_{ij}^{N}}{\partial z}=D_{a,ij}\cdot\frac{\partial^2 c_{ij}^{N}}{\partial z^2} \qquad (\text{i=A,B}) \tag{6.1}$$

Adsorption on chiral stationary phases is known to be well described by biLangmuir isotherm given by

$$q_{ij}^{N}=\frac{q_{ns}b_{ns}c_{ij}^{N}}{1+b_{ns}(c_{Aj}^{N}+c_{Bj}^{N})}+\frac{q_{s}b_{s,i}c_{ij}^{N}}{1+b_{s,A}c_{Aj}^{N}+b_{s,B}c_{Bj}^{N}} \tag{6.2}$$

The initial conditions for the system are

When $N=0$; $c_{ij}^{0}=0$ (6.3)

When $N\geq 1$

$$c_{ij}^{N}=c_{i,j+1}^{N-1} \quad \text{for} \quad j=1\sim(N_T\text{-}1)$$

$$c_{ij}^{N}=c_{i1}^{N-1} \quad \text{for} \quad j=N_T \tag{6.4}$$

The boundary conditions for the system are:

Eluent inlet point:

$$c_{i,1}^{N}\,|_{z=0}=\frac{Q_4}{Q_1}c_{i,N_T}^{N-1}\big|_{z=L} \tag{6.5}$$

Extract withdrawal point:

$$c_{i,N_1+1}^{N}\,|_{z=0}=c_{i,N_1}^{N}\,|_{z=L} \tag{6.6}$$

Feed point:

$$c_{i,N_1+N_2+1}^{N}\,|_{z=0}=\frac{Q_2}{Q_3}c_{i,N_1+N_2}^{N}\big|_{z=L}+\frac{Q_f}{Q_3}c_{i,f} \tag{6.7}$$

Raffinate withdrawal point:

$$c^{N}_{i,N_1+N_2+N_3+1}\,|_{z=0} = c^{N}_{i,N_1+N_2+N_3}\,|_{z=L} \tag{6.8}$$

The SMB performance can be characterized by purities and recoveries of the two components collected at the raffinate and extract streams respectively. They are defined as

$$Pur_{Ra} = \int_0^{t_S} \frac{c_{B,Ra}}{c_{A,Ra}+c_{B,Ra}}dt \tag{6.9}$$

$$Pur_{Ex} = \int_0^{t_S} \frac{c_{A,Ex}}{c_{A,Ex}+c_{B,Ex}}dt \tag{6.10}$$

$$\mathrm{Re}c_A = \frac{\int_0^{t_S}(Q_1-Q_2)c_{A,Ex}dt}{Q_f c_{A,f} t_S} \tag{6.11}$$

$$\mathrm{Re}c_B = \frac{\int_0^{t_S}(Q_3-Q_4)c_{B,Ra}dt}{Q_f c_{B,f} t_S} \tag{6.12}$$

Equations 6.1 and 6.2, together with initial and boundary conditions (Eqs. 6.3-6.8) were solved numerically using the method of lines. Parameters used in the calculation are derived from the single column experimental data presented in Chapter 5. Column volume is V=7.854 cm^3 and the overall void fraction (ε_t) is 0.714. For the isotherm parameters, q_{ns}=1.32 g/l, b_{ns}=16.85 l/g, q_s=0.042 g/l, $b_{s,A}$=155.0 l/g and $b_{s,B}$=30.6 l/g. Here A denotes the more retained enantiomer R-pindolol and B the less retained S-pindolol. The same value of the apparent dispersion coefficient Da_i is used for the two enantiomers, which is 1.16×10^{-3} cm^2/min at the flow rate of 1.0 ml/min. The apparent axial dispersion coefficient in each section of the SMB unit is corrected with the real flow rate in that section based on the value obtained from the single column experiments. Periodic steady states have been achieved for all the simulations confirmed by the overall and single-component mass

balance.

6.2.2 Design strategy

Important design parameters for a SMB process are the net mass flow rate ratios $m_{ø}$, defined as the ratio between the net fluid mass flow rate and the adsorbed phase mass flow rate in each section of the unit in the form of

$$m_{\phi} = \frac{Q_{\phi} t_S - V\varepsilon_t - V_{\phi}^{D}}{V(1-\varepsilon_t)} \tag{6.13}$$

where, Q_{Φ} is the fluid flow rate in section Φ, V_{ϕ}^{D} is extra-column dead volume in section Φ, V is the column volume and ε_t is the total column porosity. In the frame work of equilibrium theory the optimal conditions for SMB are obtained by calculating the region of complete separation on the (m_2, m_3) plane. This design approach was proposed as "Triangle theory" (Storti et al., 1993; Mazzotti et al., 1997; Migliorini et al., 1998). Triangle Theory has been proven efficient in the design and optimization of SMB for linear system under ideal conditions. However, for nonlinear system in the presence of dispersive effects, a large number of numerical simulations are required to find the triangular region that guarantees the desired purity and yield for a given feed composition. One aim of this study is to present a shortcut method using less number of simulation runs to find the approximate separation region on the (m_2, m_3) plane.

As feed concentration and purity requirement have a considerable effect on the final separation region (Silva et al., 2004), feed concentration of 0.01 g/l for each component, purity criteria of 99.0% for raffinate and 90.0% for extract were used for all configurations considered in this part. The reasons for selection of asymmetric purity criteria for the two enantiomers are (a) S-pindolol collected at the raffinate port is the more desired

component and (b) strong adsorptions of both components on the Chriral-AGP stationary phase makes it difficult in achieving high purity of the extract at higher column load.

Prior to the introduction of how to determine the complete separation regions on the (m_2, m_3) plane, flow rate ratios in sections 1 and 4 (m_1 and m_4) had to be quantified to guarantee the complete regeneration of the adsorbent and the desorbent in sections 1 and 4 respectively. In particular, flow-rate-ratio parameter, m_1, has to be large than a critical value while m_4 has to be smaller than a specific value. Once both such conditions are satisfied, results obtained for the (m_2, m_3) plane should not be affected by any improper operation of sections 1 and 4. However, unlike the design of ideal systems where constraints of m_1 and m_4 are found to be explicit, constraints of m_1 and m_4 in this design problem cannot be explicitly calculated due to the mathematical and isotherm models used. Recently, a simplified approach based on analyses of the propagations of shock fronts and desorption fronts in the relative sections of SMB unit (Susanto et al., 2005) was reported to approximate the constraints of m values for Langmuir-type isotherms. Pais and coworkers (Pais et al., 1998b) applied the same method to their studies and the same were also adopted in this study:

$$m_1 > \left.\frac{\partial q_A}{\partial c_A}\right|_{c_A=c_B=0} = 28.75 \tag{6.14}$$

$$m_4 < \left.\frac{q_B}{c_B}\right|_{c_A=0, c_B=c_{B,f}} = 20.0 \tag{6.15}$$

As flow rate in section 1 (Q_1) is the highest in a SMB unit, choice of Q_1 is usually restricted to the constraints of the maximum permissible pressure drop of the system and limitations of the pump performance. Though the optimum of chromatographic

separations with preparative purpose is often achieved at the highest flow rate possible (Kaspereit et al., 2002), 3.05 ml/min was selected for Q_1 in this design by considering the system pressure drop. Therefore, the switching time can be estimated by Q_1 and m_1 value which satisfies the constraint.

$$t_S = \frac{V[m_1(1-\varepsilon_t)+\varepsilon_t]+V_1^D}{Q_1} \tag{6.16}$$

Since the extra-column dead volume in each section of a SMB unit changes slightly due to the port switching, an accurate estimate of the extra-column dead volume in each section is difficult. In this study, the extra-column dead volume was estimated to be 0.64 ml per column and the time through the extra-column dead volume was negligible small compared with the retention time of pindolol through the AGP column. Therefore, in the following calculation, effect of the extra-column dead volume on the choice of $m_{ø}$ values was neglected (V_{ϕ}^D was omitted in the calculation of m_{ϕ} value). Parameters of Q_1=3.05ml/min (i.e., m_1=31.45), Q_4=1.6 ml/min (i.e., m_4=15.31) and switching time t_s=25.0 min were selected and held constant in all the simulation calculations.

Subsequently, we will focus on how to get the complete separation area on (m_2, m_3) plane using the shortcut method. By fixing the solid velocity ($u_S = L/t_S$), the strategy we adopted here is to find possible range of flow rates in section 2 and 3 (Q_2 and Q_3) which result in purities above 99.0% and 90.0% for raffinate and extract streams respectively. Separation region on (m_2, m_3) plane is then obtained by converting the flow rates into flow rate ratios through Eq. 6.13. Sine the relationship between Q_2 and Q_3 can be expressed as $Q_2 = Q_3 - Q_F$, only Q_3 needs to be determined for each simulation for a specific feed flow rate. Starting from the lower feed flow rate, e.g. Q_F = 0.002 ml/min, the highest and lowest

Q_2 and Q_3 which meet the purity requirement can be found from the simulation calculations. Therefore, a pair of points *a*1 and *b*1 representing the respective maximum and minimum combinations of m_2 and m_3 value were located on the (m_2, m_3) plane (see Figure 6.1). By increasing the feed flow rate, a series of points *a*2, *b*2, *a*3, *b*3 etc. were fixed on the (m_2, m_3) plane. Two line segments *aw* and *bw* were obtained by connecting all the points titled with a and b respectively (see Figure 6.1). The area enclosed within line segments *aw*, *bw* and the diagonal is the complete separation region for the given feed composition. The vertex *w* of the separation region represents the optimal operating conditions in terms of minimum solvent consumption and maximum productivity. Therefore, all pairs of m_2 and m_3 within the separation area leading to purity values in extract and raffinate higher than the given pair of values were identified in Figure 6.1a for SMB unit with configuration of 1/1/2/1. Same strategy was applied to obtain the separation region shown in Figure 6.1b for configuration of 1/2/1/1. This design method shows great flexibility, once the feasible flow rates of Q_1 and Q_4, which fulfill the requirement of complete regeneration of the adsorbent and desorbent in sections 1 and 4, are determined, the choice of t_s does not affect the final separation region. The selection of the number of pairs of m_2 and m_3 used in determining the final separation region is also flexible, but certainly the more number of pairs one uses, the more accurate the complete separation region.

6.2.3 Choice of operating conditions

It is easier to decide the operating conditions based on the chosen m_ϕ values once the complete separation region for a given feed composition is obtained. Either Q_1 or t_S can be determined beforehand while other parameters are then calculated from Eq. 6.13.

Operating parameters derived from any combination of m_2 and m_3 within the separation region will assure the desired separation. In this study, operating parameters determined from the above method for different feed compositions and feed flow rates were adopted in five-column SMB and Varicol experimental operations to verify the model predictions. The operating parameters and the corresponding m_ϕ values were listed in Table 6.1.

(a)

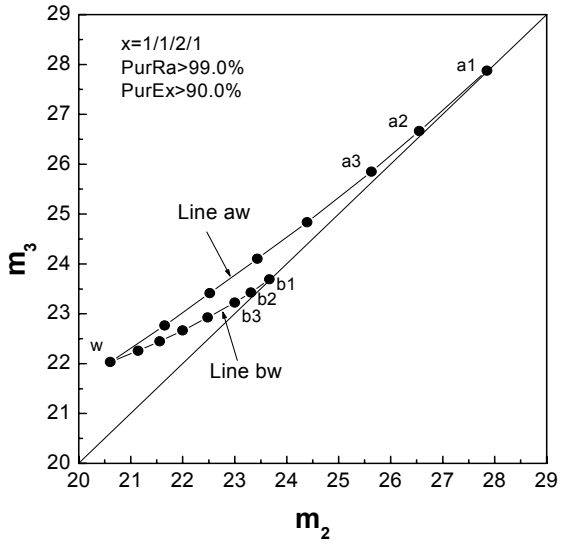

(b)

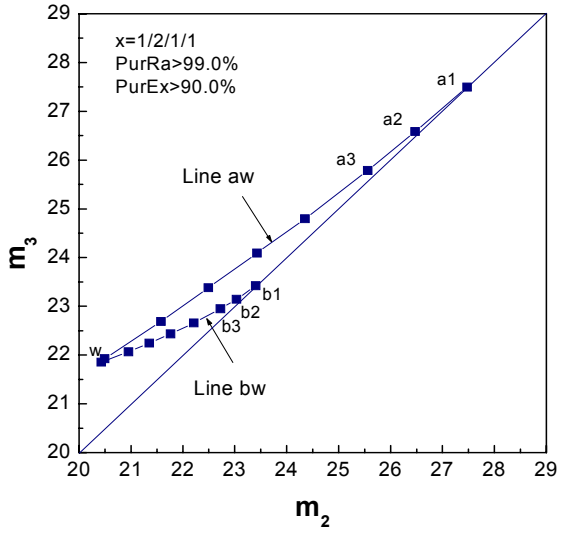

Figure 6.1 Complete separation region on the (m_2, m_3) plane

Table 6.1 Operating parameters for enantioseparation of racemic pindolol

Run	1	2	3	4	5
Process	SMB				Varicol
Zone flow rates (ml/min)					
Q_1	2.55	3.05	3.05	3.05	3.05
Q_2	1.9	2.15	2.15	2.15	2.15
Q_3	2.0	2.3	2.3	2.3	2.3
Q_4	1.37	1.6	1.6	1.56	1.6
t_s, min	27.9	23.5	23.5	22.7	22.67
Flow rate ratios					
m_1	29.18	29.41	29.41	28.33	28.29
m_2	21.1	20.0	20.0	19.23	19.2
m_3	22.34	21.57	21.57	20.75	20.72
m_4	14.52	14.24	14.24	13.27	13.65
Other parameters					
χ	1/2/1/1	1/1/2/1	1//2/1/1	1/1/2/1	1/2/1/1-2/1/1/1
Q_f, ml/min	0.1	0.15	0.15	0.15	0.15
$c_{T,f}$, g/l	0.02	0.02	0.02	0.025	0.025

*χ represents the column configuration. The 1/2/1/1 column configuration means that number of columns in sections 1 to 4 are 1, 2, 1 and 1 respectively.

Table 6.2 Comparison of the calculated and experimental results of SMB and Varicol

	Run 1	Run 2	Run 3	Run 4	Run 5
Cal. Pur_{Ra}	99.84%	99.92%	99.88%	99.2%	99.69%
Exp. Pur_{Ra}	*98.44%*	*98.61%*	*97.39%*	*98.28%*	*99.155%*
Cal. Pur_{Ex}	95.36%	85.93%	87.16%	81.41%	82.18%
Exp. Pur_{Ex}	*96.23%*	*88.9%*	*92.86%*	*83.65%*	*84.83*
Cal. Rec_B	97.65%	83.5%	86.45%	78.78%	80.464%
Exp. Rec_B	*97.22%*	*85.64%*	*91.9%*	*83.0%*	*84.52%*
Cal. Rec_A	99.84%	100%	100%	99.81%	100%
Exp. Rec_A	*99.2%*	*100%*	*97.07%*	*100%*	*100%*

6.3 Materials and methods

6.3.1 Materials

Mixture of distilled deionized water (DDW) obtained from Micromeg System and HPLC grade acetonitrile form Fisher (90:10, v/v) was used as the mobile phase. Phosphate buffer at pH 7 were prepared from 99.99% sodium dihydrogenphosphate (Aldrich) and 1M sodium hydroxide (Merck) solution. Racemic mixture of pindolol with purity of 97% was also purchased from Aldrich. Feed was prepared by dissolving the powder of racemic pindolol into the buffered mobile phase.

6.3.2 Apparatus

6.3.2.1 SMB laboratory set-up

The laboratory SMB unit shown schematically in Figure 6.2 consists of five semi-preparative Chiral-AGP columns (10cm×1cm, 5μm) and is installed in a temperature controlled room for isothermal operations. Since the outlet stream of section 4 is not directly recycled to section 1 but introduced to the desorbent tank instead, five flows (feed, eluent, rafiinate, extract and recycled eluent) have to be dealt with in the unit. Accurate control of these five flow rates is of great importance in achieving the successful operation of SMB separation. In this study, two HPLC pumps (a PU-1580 pump (Jasco) and an ISO-1000 digital pump (ChromTech)) are used to supply constant feed and eluent flow rates. Flow rates of raffinate and extract are controlled by two Quantim Coriolis mass flow controllers QMAC and QBBC2L (Brooks Instruments) respectively. The overall mass balance in the unit is used to determine the flow rate of the recycled eluent. Port switching is accomplished by five (12+1)-port multi-position valves (Vici-Valco EMTCSD12UW), which are connected to each of the five columns. In order to avoid the cross-contamination,

five check valves are inserted on the pipelines connecting the adjacent two columns. In addition, an online vacuum degasser DU2010 (Uniflows) was used to remove the bubbles in feed and eluent continuously before they were pumped into the system. A stationary sampling port located at the outlet of the first column (shown in Figure 6.2) permits to obtain the column concentration profile.

6.3.2.2 Analytical apparatus

The assay of samples was carried out on a HP 1,100 Series (Agilent Technology), equipped with a VWV detector at a wavelength of 225nm using an analytical Chiral-AGP (Chrom Tech) column (10cm ×0.46cm, 5μm). Mixture of DDW and acetonitrile (90:10, v/v) was also used as the mobile phase, with a flow rate of 0.9 ml/min at a column temperature of 23°C.

6.3.3 SMB experiments

Four SMB and one Varicol operations have been conducted for the separation of racemic pindolol. All the experiments were performed at a room temperature of 22±0.3°C. Before each SMB experiment, the entire unit was first washed with DDW and then flushed with the mobile phase at the setting value for at least 4 hours. After flow rates of the eluent, raffinate, extract and recycled eluent stream become constant, feed was pumped into the system continuously. Flow rates of the five streams were checked periodically during the experiment to ensure the accuracy. Shift of the inlet and outlet ports after a preset interval (switching period) in the direction of mobile phase flow was accomplished by the five multi-position valves actuated by the control system. Samples were collected from raffinate port and extract port over an entire switching period between two complete cycles (here 1 complete cycle means five switches of the ports) and the average

concentrations were analyzed by HPLC 1100 Series. Dynamic behavior of each SMB experiment was then obtained and compared with the model predictions. After the system ran over 20 cycles (100 switches), the system reached the periodic steady state. Steady state concentration profiles were then obtained by analyzing the samples collected from the sampling port at the same time (t = 0.8 t_S) for the continuous five switching steps during a whole cycle. After SMB experiments, all columns were regenerated simultaneously with the mobile phase. Mixture of DDW and 2-propanol (90:10, V/V) was then fed into the column for storage.

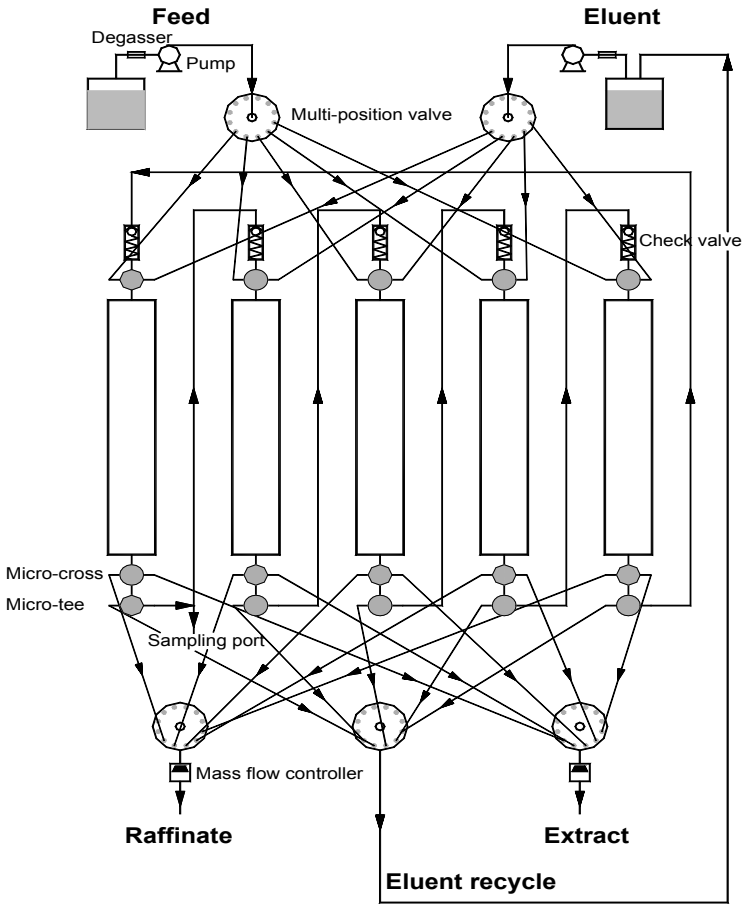

Figure 6.2 Schematic diagram of the laboratory SMB set-up

6.4 Results and discussions

6.4.1 Comparison of simulation results with experimental runs

Periodic steady state purities and recoveries of the raffinate and extract obtained from Runs 1-5 are compared with those of simulations and are given in Table 6.2. Results indicated that purities and recoveries obtained in all the five runs are in good agreement with the simulation results. All the experimental raffinate purities are a little lower than those of simulations, while, extract purities are all slightly higher. Although improvement of productivity of S-pindolol could be achieved either by increasing the feed flow rate or feed concentration, the cost will be the drop of raffinate recovery. Effect of throughput can be observed from the results of Run1 and Run3. When feed flow rate increased from 0.1 ml/min to 0.15 ml/min, recovery of the S-pindolol (Rec_B) decreased from 97.22% to 91.9%. Similar situation was also found from the results of Run2 and Run4 when total feed concentration increased from 0.02 g/l to 0.025 g/l with feed flow rates keeping at 0.15ml/min for both runs.

A more detailed comparison between the simulations and experiment can be made from the dynamic behaviors of the system and the column concentration profiles at 80% of the switching time during the final cycle as illustrated in Figure 6.3-6.7. Let us first look at the results from Run 1 shown in Figure 6.3. The experimental raffinate purity is on average 1.2% lower than that of simulations for all the cycles. Conversely, extract purity is about 2.4% higher than that of simulation. One possible reason for such deviations may come from the errors of the analytical data. Since both purities of raffinate and extract are extremely higher, only small integration errors of the analytical data from the HPLC 1100 series would cause some deviation. Another reason could be the isotherm parameters used in the simulations. Since deviations of the purity for all the five runs are quite consistent, it

is not difficult to infer that simulation did not give us the exact predictions due to the small errors in isotherm parameters. Recovery of raffinate obtained from experiment shows extremely good agreement with that of model predictions as shown in Figure 6.3b; while, recovery of extract is slightly lower than the simulation result. This observation complies with the results of raffinate purity. Relatively lower raffinate purity obtained from the experiment implies small amount of R-pindolol was lost in the raffinate. Therefore, recovery of R-pindolol at extract was lower than that of model prediction. Comparison of the steady state concentration profiles at 80% of the switching time was also illustrated in Figure 6.3c. It can be seen that movement of the two components in this SMB unit was well predicted by the simulations except for small deviations of the concentration of the more retained R-pindolol. This discrepancy may be due to the fact that the sample could not collected precisely at 80% of the switching time.

Comparisons of the dynamic behaviors and column concentration profiles at 80% of the switching time for Runs 2 to 5 are also presented in Figure 6.4 to 6.7. Close agreement between the simulation and experimental data was also achieved for these four runs. However, the cyclic fluctuation poses a problem for raffinate and extract samples as the purities and recoveries fluctuated for different cycles. During the operation, constant flow rates of the feed, raffinate and extract were obtained with the help of Jasco PU1580 pump and mass flow controllers. Nevertheless, the eluent flow rate (i.e. Q_1 in this open mode SMB) fluctuated synchronously with the change of the system pressure drop arising from the port switching. Therefore, internal flow rates in other sections fluctuated with eluent flow rate accordingly, which results in the undesirable variations of purities and recoveries of raffinate and extract.

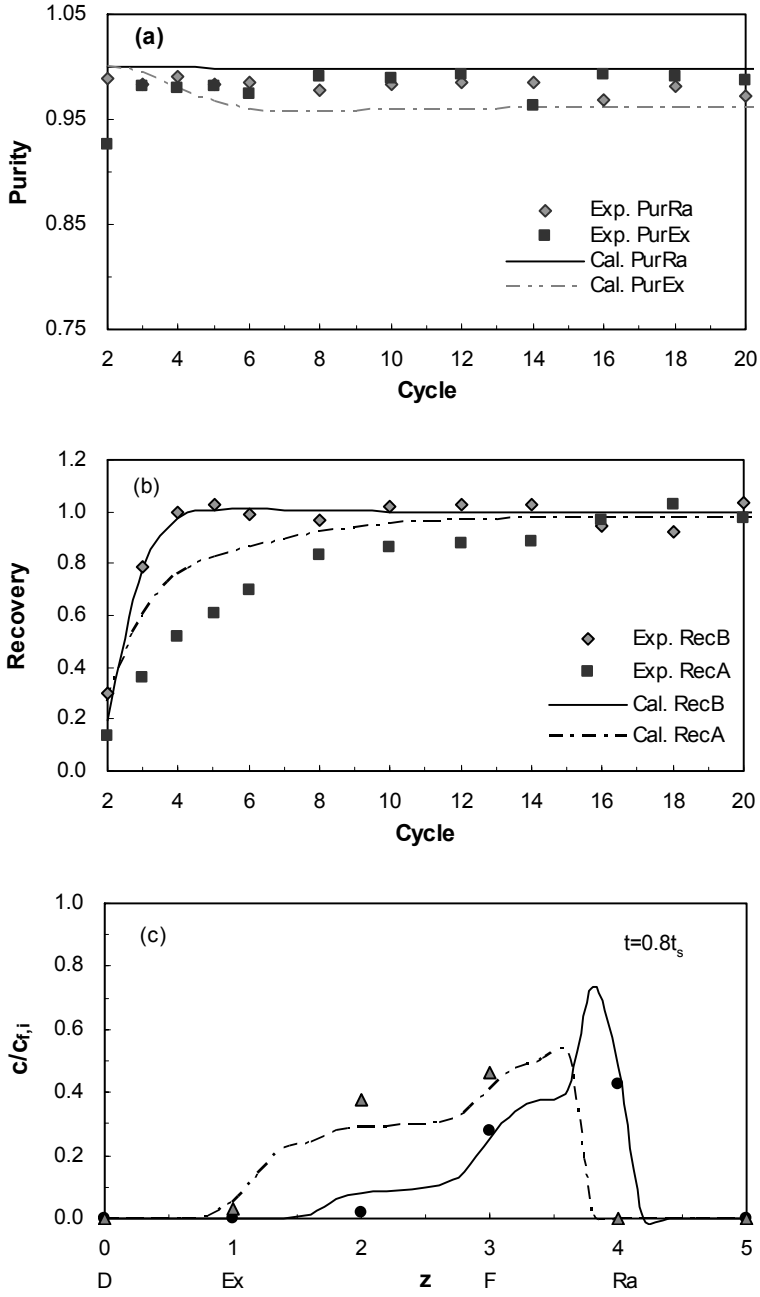

Figure 6.3 Experimental data and simulation results of Run 1

(a) History of the raffinate and extract purities; (b) History of the raffinate and extract recoveries; (c) Steady state concentration profiles at 80% of the switching time

($c_{A,f} = c_{B,f}$ =0.01 g/l)

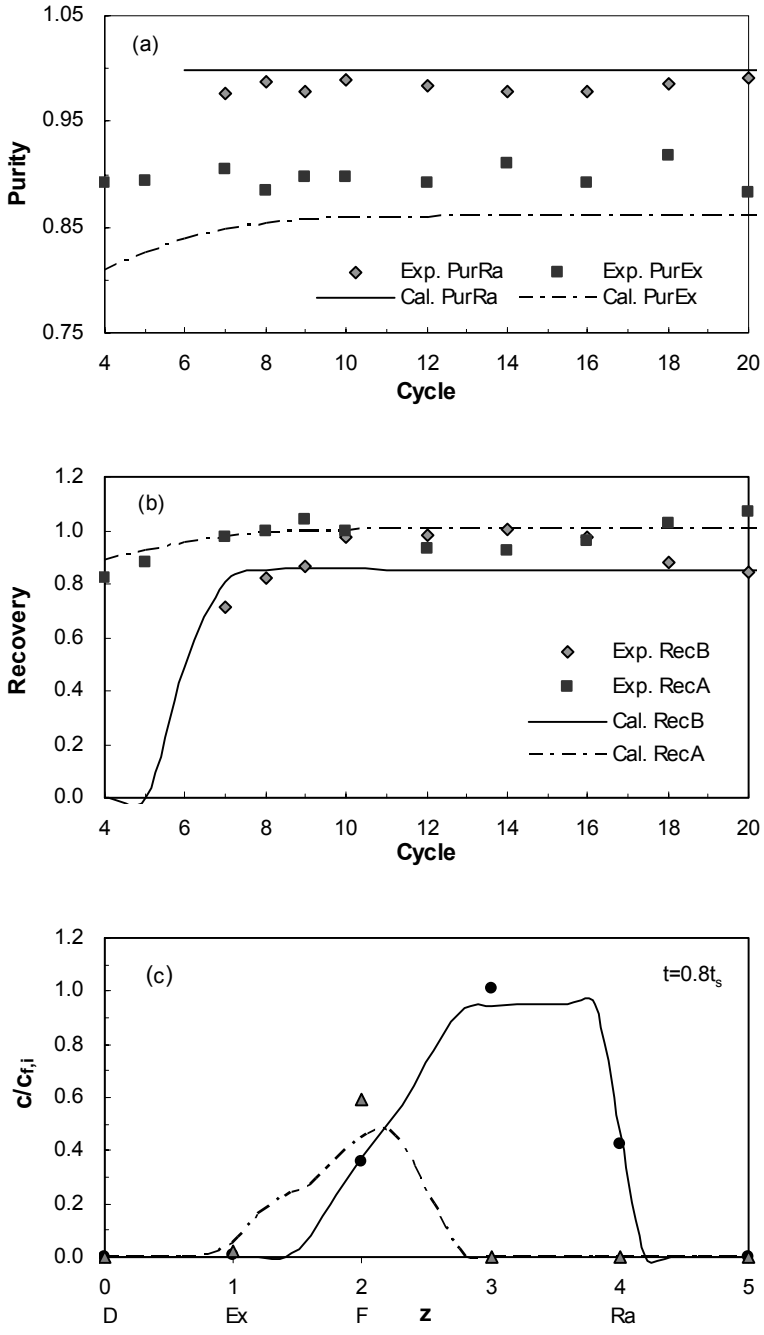

Figure 6.4 Experimental data and simulation results of Run 2

(a) History of the raffinate and extract purities; (b) History of the raffinate and extract recoveries; (c) Steady state concentration profiles at 80% of the switching time

($c_{A,f}=c_{B,f}$=0.01 g/l)

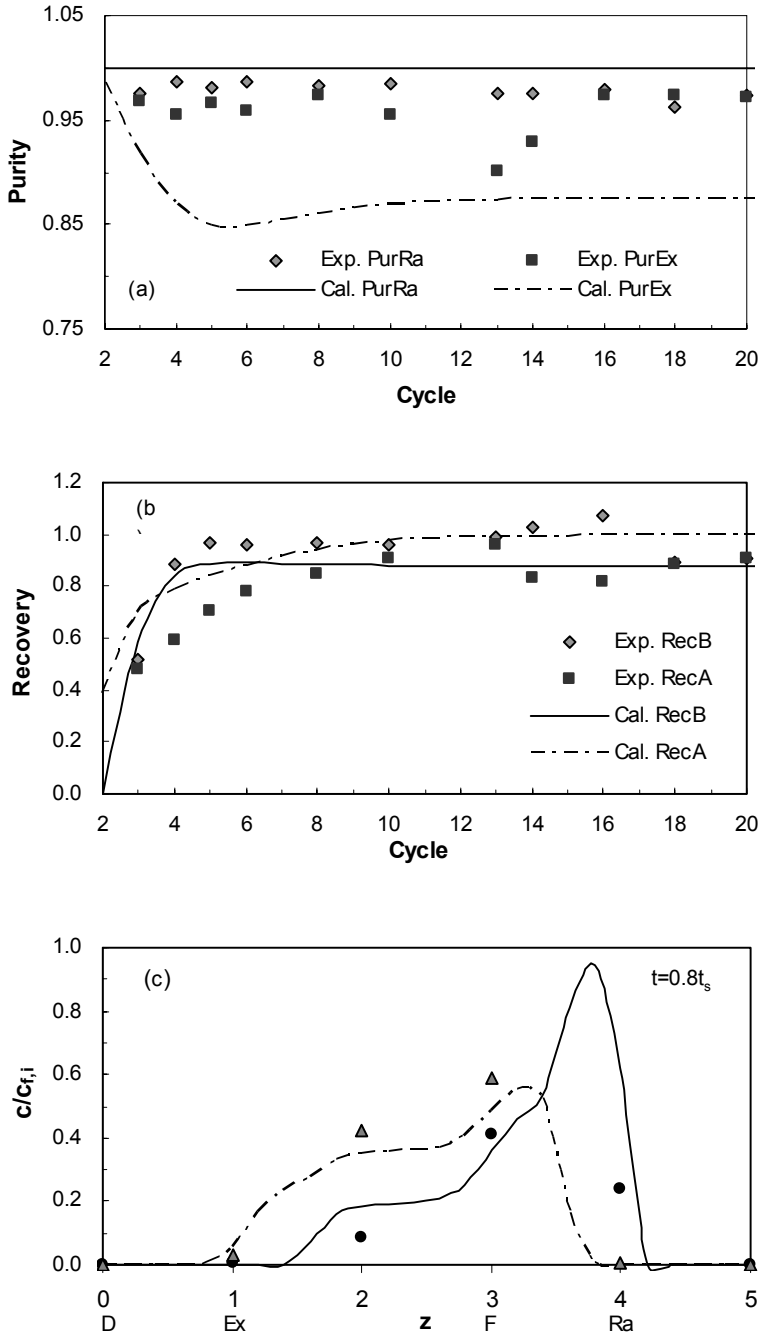

Figure 6.5 Experimental data and simulation results of Run 3

(a) History of the raffinate and extract purities; (b) History of the raffinate and extract recoveries;

(c) Steady state concentration profiles at 80% of the switching time

($c_{A,f} = c_{B,f}$ =0.0125 g/l)

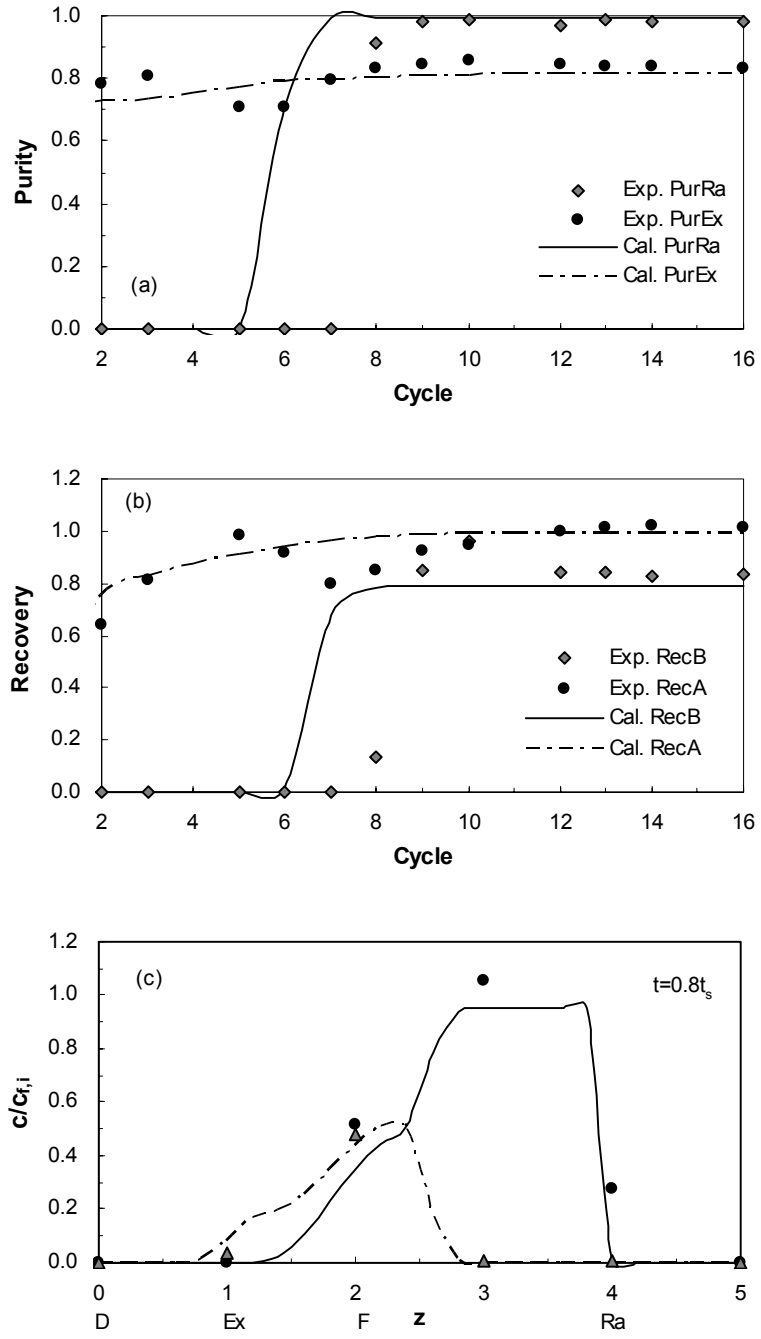

Figure 6.6 Experimental data and simulation results of Run 4

(a) History of the raffinate and extract purities; (b) History of the raffinate and extract recoveries; (c) Steady state concentration profiles at 80% of the switching time

($c_{A,f} = c_{B,f}$ =0.0125 g/l)

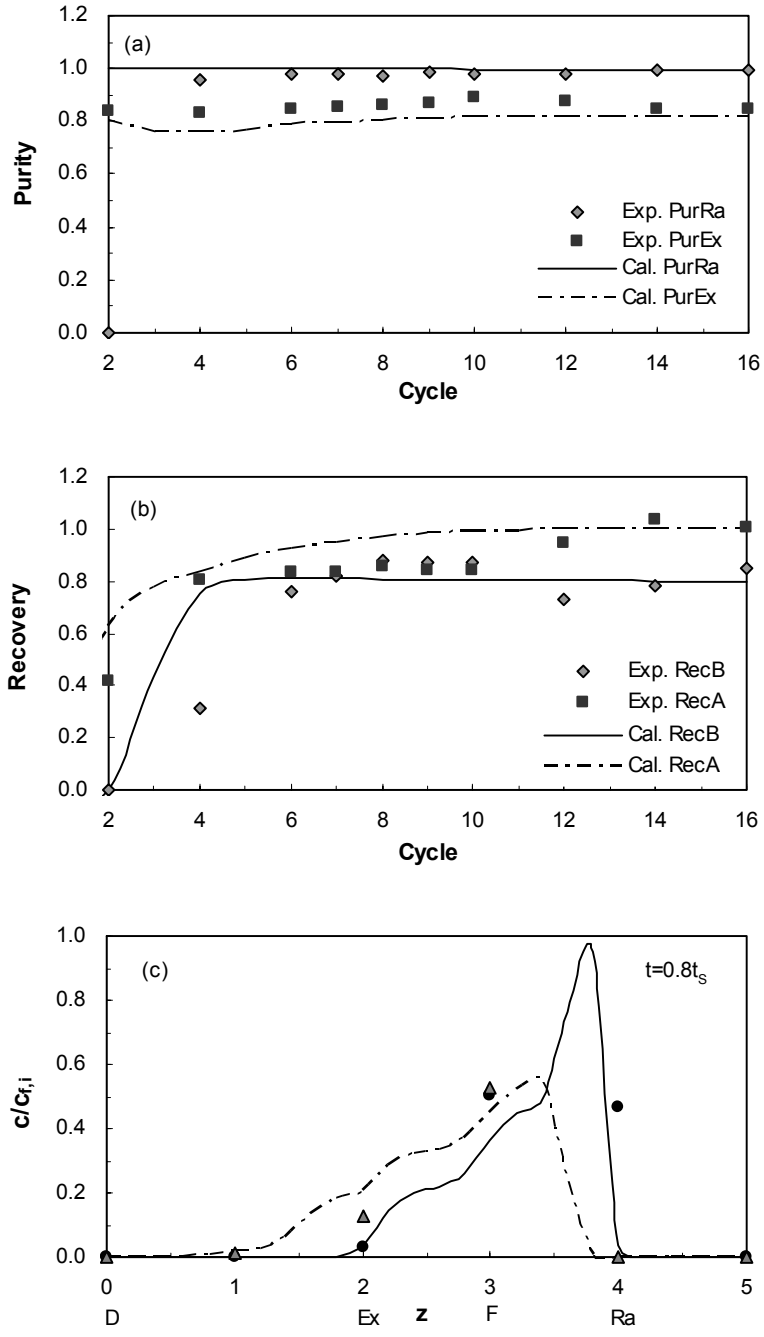

Figure 6.7 Experimental data and simulation results of Run 5

(a) History of the raffinate and extract purities; (b) History of the raffinate and extract recoveries; (c) Steady state concentration profiles at 80% of the switching time

($c_{A,f} = c_{B,f}$ =0.0125 g/l)

6.4.2 Effect of column configuration

Distribution of the number of columns in each section, i.e. column configuration will determine the pseudo solid-phase velocity in that section. Thus, it will undoubtedly affect the SMB performance. Since all the operating parameters of Run 2 and Run 3 were the same except for the column configuration. Results of the Run 2 and Run 3 would help us to understand the effect of column configuration on this SMB separation more clearly. Simulation results indicate that column configuration with 1/2/1/1 of Run 3 was superior to 1/1/2/1 of Run 2 in achieving a relatively higher raffinate recovery without a compromise of the raffinate purity. However, experimental results reveal that raffinate purity of Run 3 is 1.22% lower than that of Run 2. The achievement of this experimental result manifests that χ=1/2/1/1 is favorable to obtaining the relatively higher extract purity, while χ=1/1/2/1 tends to give higher raffinate purity.

The reason for the above observation may be easily understood by the comparison of steady state concentration profiles of Run 2 and Run 3 shown in Figure 6.8. Both Run 2 and Run 3 were operated at the region with only pure raffinate due to the higher throughput used and limitation of fluid flow rates. Lower fluid and solid velocity were required to obtain high raffinate purity. As a result, extract port was polluted by S-pindolol in both runs because of the severe tailing of the disperse front of S-pindolol. Extract purity of Run 2 is even lower due to the higher concentration of S-pindolol in the extract at the beginning of the switching (t=0). As only one column was used in section 2 for Run 2, extract outlet will switch at the beginning of each switching interval to the previous feed inlet, leading to a decrease of extract purity. The use of the second column in section 2 (Run 3) avoids this problem and increases the extract purity by desorbing more amount of

S-pindolol in section 2. However, the use of two columns in section 2 will decrease the length of section 3 with the restricted number of total columns ($N_T = 5$). Therefore, small deviations of the internal flow rates during the experiment would cause the decrease of raffinate purity in Run 3.

Results of Run 4 and Run 5 once again proved that Varicol, a modification of the classical SMB operation has advantages in achieving better system performance by introducing more flexibility in column configuration. Both raffinate purity and extract purity obtained from Varicol were higher than those from the traditional SMB. An increase of raffinate recovery was also obtained in Varicol due to the increase of extract purity. Column configuration used in Run 5 was 1/2/1/1 during the first half of the switching period and then changed to 2/1/1/1 by merely moving the extract port one column ahead along the direction of the fluid flow at half of the switching period. Therefore, configuration of Run 5 became 1.5/1.5/1/1 during the global switching period. Better performance achieved in Run 5 demonstrates that one more column in section 2 and section 1 is beneficial to balancing the purity requirements of both raffinate and extract at higher throughput. As mentioned above, the use of 2 columns in section 2 was helpful in achieving higher extract purity. The requirement of 2 columns in section 1 during the second half switching would favor the maintenance of high raffinate purity by desorbing more R-pindolol in section 1. This result emphasizes the importance of solid regeneration in this process.

It should be pointed out that Varicol operation allows an unlimited number of configurations. In Run 5 we only limited our study by using 4 sub-intervals in a global switching time and the operating parameters were selected only based on those of Run 4

for comparison. A systematic optimization of Varicol process should be implemented in order to achieve further enhancement.

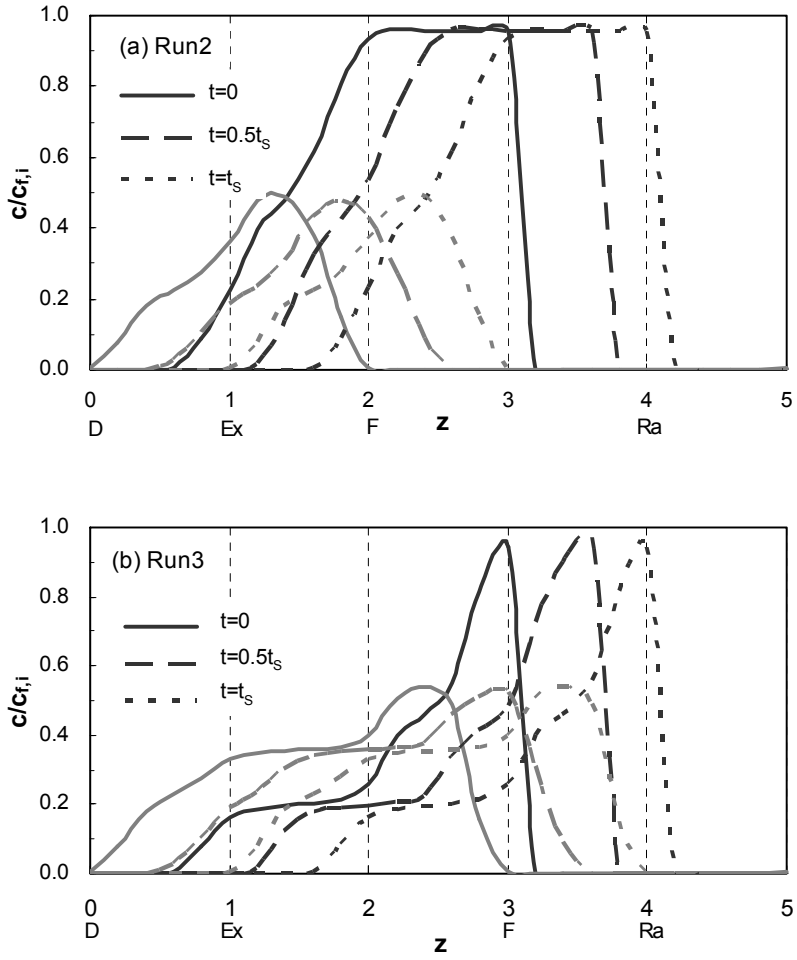

Figure 6.8 Steady state concentration profiles of Runs 2 and 3
(Q_i=0.15 ml/min, $c_{A,f} = c_{B,f}$ =0.01g/l)

6.4.3 Effect of isotherm parameters

Quite a few studies investigated the effect of nonlinear adsorptions on SMB performance (Mazzotti et al., 1997; Migliorini et al., 1998); relatively little is published on the influence of the individual isotherm parameters on SMB performance. It is well known that successful design and operation of SMB and Varicol largely depends on the accurate estimation of isotherm parameters. However, measurement error and limitation of the methods make it rather difficult to obtain the accurate isotherm parameters for the multi-component system. In particular, decrease of the saturation capacities was often observed on chiral stationary phases after a period of repeated use due to part of the sorption sites permanently occupied by strong retention compounds (Schulte and Strube, 2001). Therefore, it is important to be aware of the effects of variations in isotherm parameters on SMB performance.

Similar to the case of linear system where the retention factor of each component is proportional to its distribution coefficient, the retention factor for nonlinear system is also highly related to the slope of the isotherm at infinite dilution (i.e. $\left.\frac{\partial q_A}{\partial c_A}\right|_{c_A=c_B=0}$ and $\left.\frac{\partial q_B}{\partial c_B}\right|_{c_A=c_B=0}$ for component A and B). Therefore, in the following discussion, $\left.\frac{\partial q_A}{\partial c_A}\right|_{c_A=c_B=0}$ and $\left.\frac{\partial q_B}{\partial c_B}\right|_{c_A=c_B=0}$ will be kept constant to see how the variation of saturation capacity and equilibrium constant affect SMB performance without a significant change in the apparent separation factor, i.e., the ratio of the retention factors of the two components. Since biLangmuir isotherm was applied in this study, influences of isotherm parameters of the two sorption sites were investigated by the following manner. Firstly, saturation

capacity (q_{ns}) and equilibrium constant (b_{ns}) for the nonselective site were changed systematically while parameters of the selective site were remained at their reference values to observe the effect of the nonselective site parameters. Then, the effect of the selective site parameters were studied by holding the values of q_{ns} and b_{ns} constant while changing the values of q_s, $b_{s,A}$ and $b_{s,B}$. Finally, the combined effects of the two sites were investigated by changing the isotherm parameters of the two sites simultaneously.

Essential design parameters as well as purities and recoveries obtained at various isotherm parameters are summarized in Table 6.3. Isotherm parameters of Run A listed in the first line of Table 6.3 were used as reference values. The same constraint of raffinate purity was adopted as previous in the simulation (Pur_{Ra}>99.0%) for a reasonable comparison. Results from Table 6.3 demonstrate that decreases of either q_{ns} or q_s value caused a decrease in the raffinate recovery and the change of the selective site parameters had a more remarkable influence on SMB performance. From the comparison of Run C and Run F with Run A, it is observed that raffinate recovery decreases from 87.37% in Run C to 86.45% in Run A when q_{ns} value decreased 10% from 1.45g/l to 1.32g/l while raffinate recovery decreases from 89.15% to 86.45% when q_s value changed 10% from 0.046g/l in Run F to 0.042g/l in Run A. Another outcome of the thermodynamic change is the shift of the switching time in SMB. Results in table 3 indicated that t_s need to be decreased slightly when either of the two saturation capacities decreases.

The reason for the above results is that the total amount of the racemic compound adsorbed onto the stationary phase decreased when the saturation capacities of sorption sites decreased despite the separation factor being held constant. Compared with nonselective site, the same amplitude variation of the saturation capacity of the selective

site will result in a more significant change in the quantity of solutes adsorbed due to the higher equilibrium constants of the selective site (both $b_{s,A}$ and $b_{s,B}$ are higher than b_{ns}). Since saturation capacity is only a property of the solid lattice and the adsorbed species, chiral stationary phase giving higher saturation capacity for the solutes is always desirable for enantioseparation.

Table 6.3 Effect of isotherm parameters on SMB performance

(The flow rates used for Run A-J are the same with those of Run 3 in Table 6.1)

Run	Isotherm parameters					t_s, min	Purity		Recovery	
	q_{ns}, g/l	b_{ns},l/g	q_s, g/l	$b_{s,A}$, l/g	$b_{s,B}$, l/g		Pur_{Ex}	Pur_{Ra}	Rec_A	Rec_B
A*	1.32	16.85	0.042	155.0	30.6	23.5	87.16%	99.88%	100%	86.45%
B	1.58	14.08				23.84	87.99%	99.89%	100%	87.74%
C	1.45	15.34	0.042	155.0	30.6	23.69	87.66%	99.84%	100%	87.37%
D	1.19	18.69				23.3	86.73%	99.8%	100%	86.93%
E			0.05	130.2	25.7	23.85	90.54%	99.85%	100%	91.1%
F	1.32	16.85	0.046	141.5	27.94	23.69	89.0%	99.85%	100%	89.15%
G			0.038	171.3	33.82	23.31	85.17%	99.8%	100%	83.77%
H	1.58	14.08	0.05	130.2	25.7	24.18	91.4	99.85%	100%	92.12%
I	1.45	15.34	0.046	141.5	27.94	23.86	89.4%	99.9%	100%	89.58%
J	1.19	18.69	0.038	171.3	33.82	23.11	84.78%	99.66%	100%	83.28%

* The isotherm parameters in Run A were adopted in this study and used as reference values. Constraint for raffinate purity is Pur_{Ra}>99.0%, column configuration is 1/2/1/1.

6.5 Conclusions

Separation of racemic pindolol on the Chiral-AGP stationary phase using four-section SMB and Varicol was investigated in this work. Equilibrium dispersive model combined with biLangmuir isotherm was applied to describe the dynamic behavior of the SMB and Varicol. In order to reduce the course of trial-and-errors for the design of this nonlinear system in the presence of dispersion effects, a shortcut design strategy based on triangle theory was presented. Four SMB and one Varicol operations were carried out at various operating conditions to verify the model predictions. Good agreement between experimental data and simulation results were obtained for all the five runs. This achievement indicated that the simulation results could give extremely good predictions of both SMB and Varicol process and confirmed that the mathematical model and the isotherm parameters used in the simulations were quite reliable and robust.

Effect of column configuration on system performance was studied by comparing the results from experiments. For SMB operation, column configuration with 1/2/1/1 is favorable in achieving higher purity of both raffinate and extract. Varicol operation with configuration of 1.5/1.5/1/1 showed its advantage of obtaining better performance over SMB process. Results indicate that regeneration of the solids has great importance in achieving the desired separation for this system. Intense adsorption of both components on the chiral stationary makes the complete desorption rather difficult, and therefore, more columns should be used in the sections 1 and 2.

Effect of variation of isotherm parameters on SMB performance was also studied. Influences of isotherm parameters of the two sorption sites for biLangmuir isotherm were investigated individually. Results demonstrate that the decrease of saturation capacity of

either site will cause a decrease in the raffinate recovery. And the variation of the selective site has a more remarkable influence on SMB performance. Chiral stationary phase supplying higher saturation capacity for the solutes is always desirable for enantioseparation.

Chapter 7 Multi-objective Optimization of SMB and Varicol for Enantioseparation of Racemic Pindolol

7.1 Introduction

The necessity for systematic optimization of SMB process arises from the requirement of either maximizing product yield (or product quality), or minimizing the cost of separation. Numerous parameters and complex dynamic behavior make pure empirical design and optimization of SMB process infeasible (Susanto et al., 2005). Optimization based on accurate mathematical models becomes essential. Modeling, simulation and experimental study of SMB and Varicol processes for the separation of racemic pindolol have already been studied in Chapter 6. Achievement of good agreement between experimental data and the simulated results proved that mathematical model and isotherm parameters are quite reliable and robust to describe the dynamic behavior of SMB and Varicol processes. However, operating parameters selected for experimental investigations were only based on the design strategy, in which some of the parameters were fixed and the effect of these parameters on system performance have not been discussed thoroughly. Besides, it is generally accepted that factors influencing the economy of a given separation process are multiple and often in conflict with each other (Zhang et al., 2002a, b, 2003, Yu et al., 2003b, Wongso et al., 2004). A typical example of such conflict effects is that maximizing productivity by increasing the feed flow rate will leads to the decrease of product purity. Therefore, rigorous multi-objective optimization of SMB and Varicol processes is proposed in this chapter for the separation of racemic pindolol.

Various formulations aimed at improving productivity and purity of the desired

component or reducing the separation cost were applied to both SMB and Varicol processes in this work. Firstly, simultaneous maximization of raffinate and extract purities was carried out for a given capacity with different feed concentrations to evaluate the effect of feed concentration on Pareto solutions and system performance. This was followed by maximizing recovery of S-pindolol while minimizing desorbent flow rate. Pareto solutions for the existing set-up were then verified with several experimental runs. Finally, optimization at design stage was carried out to maximize recovery of S-pindolol using minimum amount of fresh solvent.

Systemic multi-objective optimization of SMB and Varicol processes for this nonlinear system in the presence of dispersive effects was quite difficult since large amount of computation was required. Particularly, both continuous and discrete decision variables are needed to be optimized in SMB and Varicol processes. This makes the traditional optimization algorithms inapplicable. Thanks to the development of the elitist Non-dominated Sorting Genetic Algorithm (NSGA-II), multi-criteria optimization of such complicated problems becomes possible. Robustness and efficiency of NSGA-II indicated that it is probably the unique choice for this kind of complex optimization problems.

7.2 Mathematical model

The experimentally verified mathematical model describing the dynamic behavior of SMB and Varicol was presented in detail in Chapter 6 and is not included here for brevity. Since periodic switching is imposed on the system, SMB columns always work under transient conditions. However, a periodic steady state is eventually reached after certain numbers of switching. For both SMB and Varicol, cyclic steady state was attained after 40 switching cycles (200 switches for a 5-column system). All the

simulations and optimizations in this work were performed on the Compaq GS320 alphaserver in Supercomputing & Visualization Unit at the National University of Singapore.

Purity, recovery and productivity are the most often used objective functions to evaluate the efficiency and quality of chromatographic separations. As only two components are separated in this study and the less retained S-pindolol is the desired component, purities of raffinate and extract streams (Pur_{Ra} and Pur_{Ex}) as well as recovery of S-pinsolol (Rec_B) defined in Chapter 6 are used as objective functions.

7.3 Multi-objective optimization

Two distinct types of problems may be considered in the multi-objective optimization of SMB and Varicol systems. One is the performance enhancement of an existing set-up by determining the optimal operating parameters. The other is optimization at design stage by including some of the design parameters in decision variables for a more competitive new plant. In this work, a few double-objective optimization studies have been performed. Cases 1 and 2 dealt with optimization for the existing set-up, while Case 3 was performed for design purpose.

7.3.1 Case 1. Simultaneous maximization of raffinate and extract purity

High product purity is an important requirement in the drug manufacture, simultaneous maximization of purities in the extract (Pur_{Ex}) and in the raffinate (Pur_{Ra}) stream for a given productivity was, therefore, selected as two objective functions in this case. Optimizations of both SMB and Varicol processes were employed for the existing laboratory set-up. Two optimization problems were investigated to study the effect of feed concentration on the two objectives by fixing the production capacity, i.e., the product of feed concentration and feed flow rate.

7.3.1.1 Case 1a. Optimization with lower feed concentration

The first optimization problem was carried out using relative lower feed concentration ($c_{T,f}$ = 0.02 g/l) and higher feed flow rate (Q_f=0.15 ml/min). To compare the results with those obtained in the last chapter, length (L) and total number of column (N_T), recycling flow rate (Q_4), feed flow rate (Q_f) and feed concentration ($c_{T,f}$) were fixed. Four decision variables, i.e., extract (Q_{Ex}) and desorbent flow rates (Q_D), switching time (t_s) and column configuration (χ) are used in this optimization study. Because Q_4 has already been fixed at 2.0ml/min, the highest bound for Q_D was set to 1.5 ml/min to meet the constraints of the highest flow rate in the system ($Q_1 \leq$ 3.5 ml/min), under which the pump can work properly. Bounds for t_s should lie between the breakthrough times of the two components and were estimated by some preliminary sensitivity analyses of the mathematical model. For a 5-column system (N_T=5), 4 possible column configurations as reported in the first part of Table 7.1 can be used. In SMB, only one column configuration is applied during the entire switching period. However, column configuration for Varicol is very flexible due to many choices of the subintervals. In order to somehow restrict this variety, only 4-subinterval process has been considered for Varicol in this study, assuming that in each subinterval the unit can choose any of the configurations designed for SMB unit. Optimization formulation and bounds of decision variables are summarized in Table 7.2 (Case 1a).

Figure 7.1 shows Pareto optimal solutions and the corresponding operating variables for this problem. Purities for raffinate and extract streams above 90% were obtained for both SMB and Varicol operations. It can be seen that points on lines ABC and EFGH do constitute Pareto sets, i.e., as purity of raffinate increases (desirable), the purity of extract decreases (undesirable). One cannot improve purity of one stream

without sacrificing purity of the other stream. Optimal solutions of Q_D for both systems almost reach the highest bound. However, optimal solutions for Q_{Ex} and t_s vary with different requirements of raffinate purity. The higher the raffinate purity, the higher the Q_{Ex} and t_s are obtained. Selection of higher t_s and Q_{Ex} is quite reasonable since relatively lower solid and fluid migration velocities resulted from higher t_s and Q_{Ex} help to maintain higher raffinate purity. Despite that optimal solutions for Q_{Ex} and t_s are scattered, optimal flow rate ratios in the four sections (m_ϕ) shown in Figure 7.2a are quite close for both SMB and Varicol processes, especially for the m_2 and m_3 values.

Table 7.1 Possible column configurations for N_T=5 and N_T=6

N_T=5			
χ	column configuration	χ	column configuration
A	2/1/1/1	C	1/1/2/1
B	1/2/1/1	D	1/1/1/2
N_T=6			
E	1/1/1/3	J	1/3/1/1
F	1/1/2/2	K	2/1/1/2
G	1/1/3/1	L	2/1/2/1
H	1/2/1/2	M	2/2/1/1
I	1/2/2/1	N	3/1/1/1

Optimal column configurations of SMB and Varicol processes are listed in Table 7.3. As shown in Figure 7.1 and Table 7.3, for 5-column SMB system, χ=B (1/2/1/1) is the best configuration when high purity of extract is desired while χ=C (1/1/2/1) is the best configuration when high purity of raffinate is desired. As for 5-column Varicol, column configuration varies with the increase of raffinate purity from χ=B-B-B-A to

χ=B-B-A-A and χ=C-C-B-A, which corresponds to 1.25/1.75/1/1, 1.5/1.5/1/1 and 1.25/1.25/1.5/1 respectively. Optimal column configurations obtained for both SMB and varicol demonstrate the importance of complete desorption for the two components in this separation system. More reasonable distribution of the solids benefiting from the more flexible Varicol process helps to obtain better performance in terms of the two objectives.

Table 7.2 Description of optimization formulations for enantioseparation of racemic pindolol

<table>
<tr><th colspan="2">Case</th><th>Obj. functions</th><th>Constraints</th><th>*Decision variables</th><th>Fixed variables</th></tr>
<tr><td rowspan="2">I
(Existing set-up)
SMB & Varicol</td><td>1a</td><td rowspan="2">Max Pur_{Ra}
Max Pur_{Ex}</td><td rowspan="2">Pur_{Ra}≥90%
Pur_{Ex}≥90%
Q_1<3.5 ml/min</td><td rowspan="2">18.0≤ t_s ≤24.0 min
1.0≤Q_D≤1.5 ml/min
0.7≤Q_{Ex}≤1.1 ml/min
χ</td><td>$c_{T,f}$ =0.02 g/l
Q_f=0.15 ml/min
Q_4=2.0 ml/min
d=1.0 cm
L=10.0 cm
N_T = 5</td></tr>
<tr><td>1b</td><td>$c_{T,f}$ =30 mg/l
Q_f=0.1 ml/min
Others are same as problem 1a</td></tr>
<tr><td colspan="2">II
(Existing set-up)
SMB & Varicol</td><td rowspan="2">Max Rec_B
Min Q_D</td><td>Pur_{Ra}≥97.15±d%
(d=0.1%)
Pur_{Ex}≥90%
Q_1<3.5 ml/min</td><td>18.0≤t_s≤24.0 min
1.0≤Q_D≤1.5 ml/min
0.7≤Q_{Ex}≤1.0 ml/min
χ</td><td>Same as problem1a</td></tr>
<tr><td colspan="2">III
(Design stage)
SMB & Varicol</td><td>Pur_{Ra}≥99%
Pur_{Ex}≥95%
Q_1<4.0 ml/min</td><td>13.0≤ t_s≤30.0 min
1.0≤Q_D≤1.5 ml/min
0.7≤Q_{Ex}≤1.0ml/min
8.0≤L≤15.0 cm
χ</td><td>$c_{T,f}$ =0.03 g/l
Q_f=0.1 ml/min
Q_4=2.5 ml/min
d=1.0 cm
N_T = 5/6</td></tr>
</table>

* The bounds of the decision variables were restricted to even narrow ranges in some optimization runs to achieve smooth distribution for the decision variable plots.

Compared with the experimental data obtained in Run 2 and Run 3 in Chapter 6, improvement of product purity in raffinate and extract streams has been achieved for both SMB and Varicol processes by applying multi-objective optimization. Let us first look at the optimization results for SMB process. Compared with the experimental results of Run 2, extract purity can be improved from 88.8% to 92.59% while raffinate purity keeping the same around 98.6%. Although optimization result shows only small improvement (about 0.1%) in product purity compared to those obtained in Run 3, an improvement approximate to 2.45% in recovery of S-pindolol is achieved. Such performance improvements are more notable in Varicol process. Extract purity is improved 4.01% and 1.25% respectively corresponding to those of Run 2 and Run 3, while, recovery of S-pindolol increases 3.1% and 8.62% respectively.

Probably, three main factors contribute to the above performance enhancement. The first is the increase of internal flow rates due to the relatively higher Q_4. Higher internal flow rates result in higher wave velocities for both the adsorption shock front and the dispersed desorption front, which helps to increase extract purity for this separation. High desorbent flow rate (Q_D) is the second cause for performance enhancement. Optimal solutions of Q_D, which almost approach the highest permission value as shown in Figure 7.1 help to increase the raffinate purity by desorbing more amount of R-pindolol in section 1. In addition, column configuration plays a very important role in gaining improved performance. Optimal column configurations obtained for SMB and Varicol once again proved that complete desorption of the two components is of great importance in achieving higher product purity.

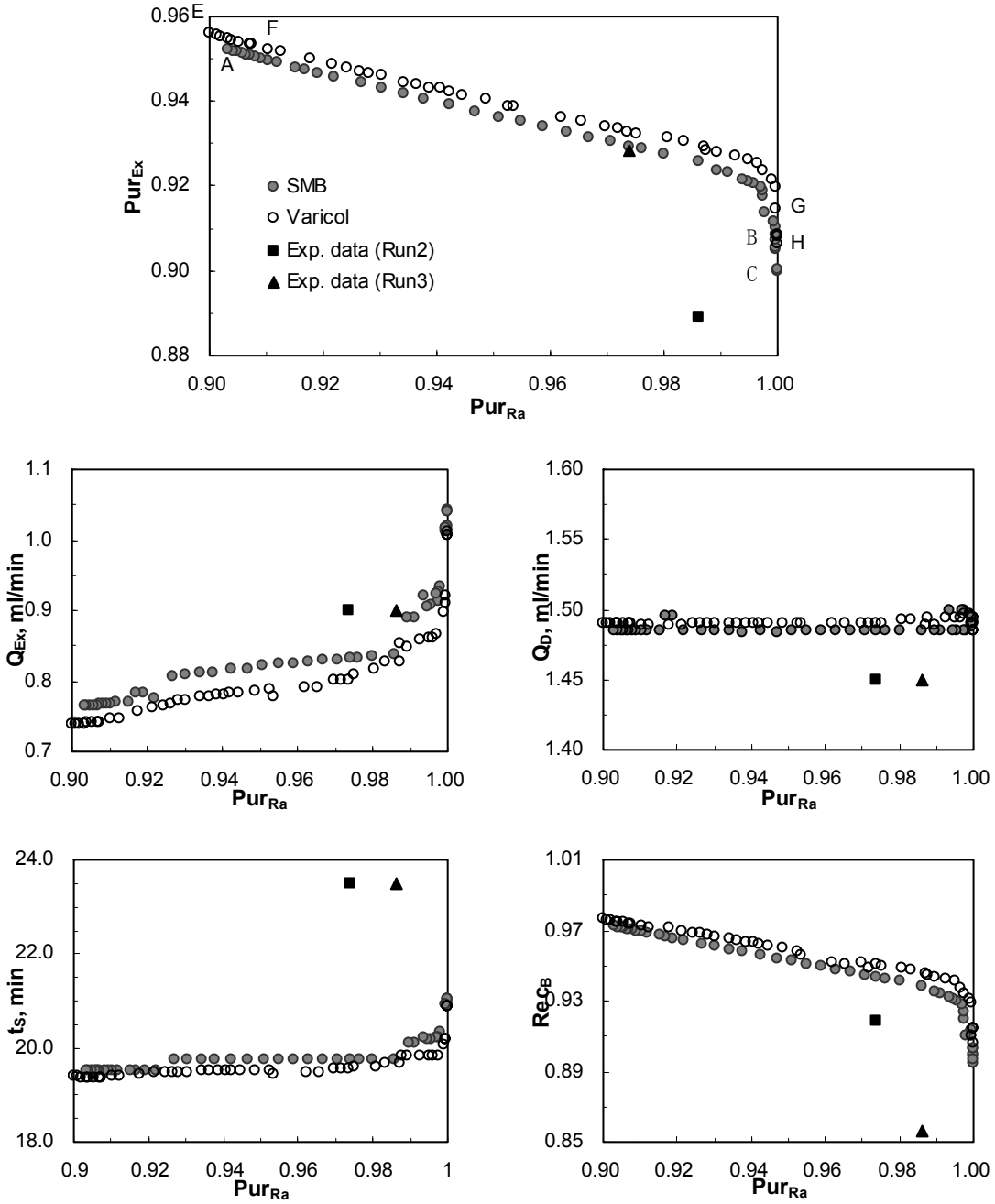

Figure 7.1 Pareto optimal solutions and the corresponding decision variables (Case 1a) for SMB and Varicol ($c_{T,f}$ =0.02 g/l, Q_f=0.15 ml/min)

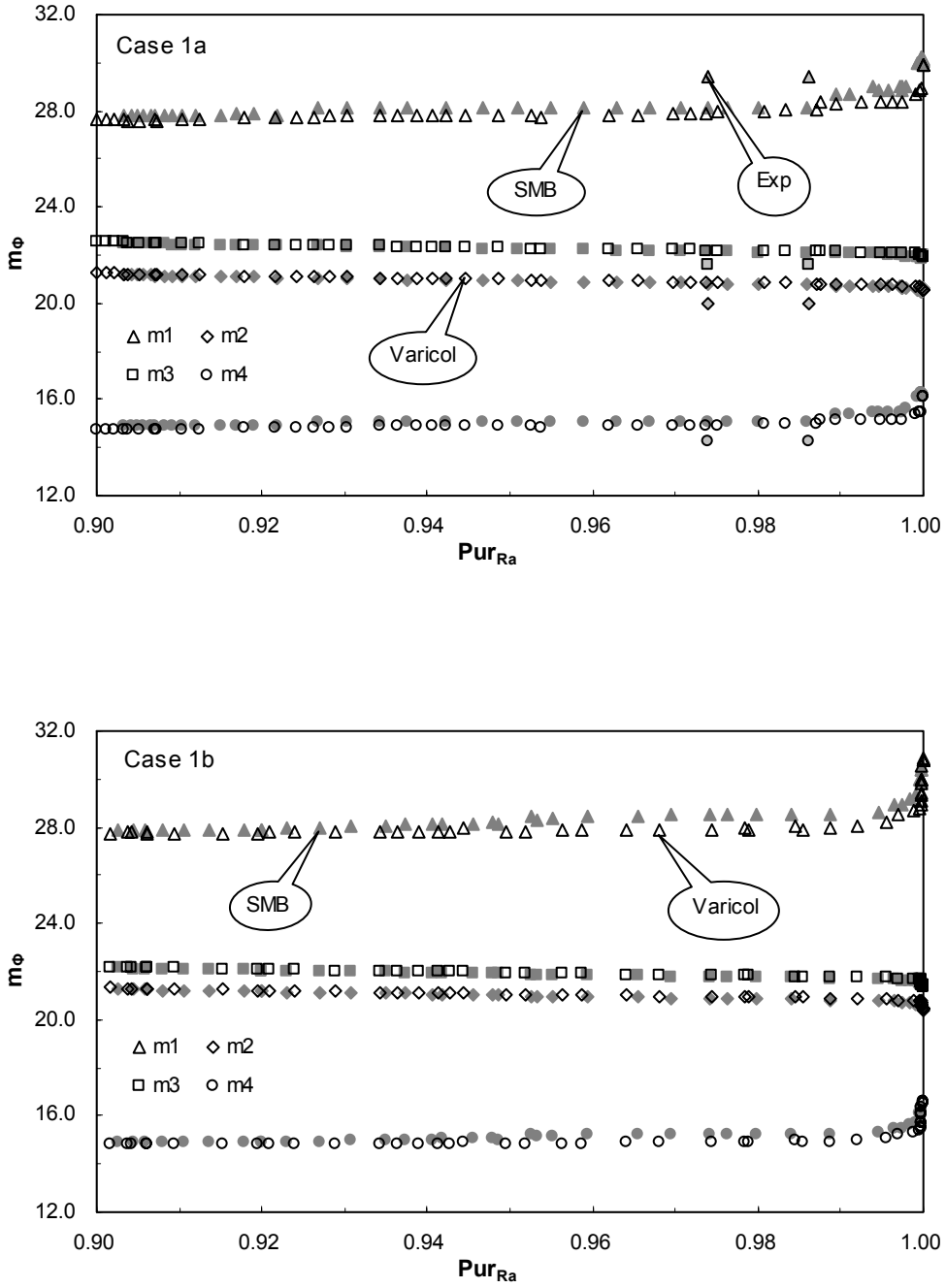

Figure 7.2 Optimal flow rate ratios corresponding to points on Pareto sets obtained in Case 1a & 1b

7.3.1.2 Case 1b. Optimization with higher feed concentration

Except for a different feed concentration ($c_{f,T}$ =0.03 g/l), optimization formulation of this problem (Case 1b) is the same as that of Case 1a. Q_f was set to 0.1 ml/min due to the increase of feed concentration for the same productivity. From the optimization results of Case 1b shown in Figure 7.3, it is observed that similar trend for the optimum raffinate and extract purities as those of Case 1a is obtained. This time Q_D also converges to the highest permissible value, which demonstrates that higher desorbent flow rates do favor the achievement of higher purities both in raffinate and in extract by removing the strongly adsorbed R-pindolol from solids to extract. Compared with the results obtained in Case 1a, optimal solutions for Q_{Ex} and t_s are slightly higher at higher raffinate purity. This may be due to the slight decrease of internal flow rate in section 3 (Q_3) caused by the lower feed flow rate (Q_3=Q_4+Q_f, Q_4 is fixed at 2.0 ml/min). Slightly higher Q_{Ex} is used to decrease Q_2 consistently with Q_3 while slightly higher t_s is expected to balance the decreased fluid velocities in sections 2 and 3. Optimal flow rate ratios in the four sections are also presented in Figure 2b and the corresponding optimal column configurations for SMB and Varicol processes are listed in Table 7.3.

Although Varicol still shows its advantage in obtaining higher raffinate and extract purities over SMB from Figure 7.3, improvement obtained from Varicol in Case 1b is less significant than that of Case 1a. From the aforementioned analysis it is known that internal flow rates in the middle two sections decrease slightly due to a relatively lower feed flow rate used in Case 1b, while flow rates in sections 1 and 4 are almost the same as those in Case 1a. In such a case, complete desorbtion of S-pindolol in section 2 is of crucial importance in Case 1b due to the decrease of Q_2. Rather good

system performance can be achieved by SMB with configuration B (2 columns in section 2). Nevertheless, Varicol with configuration of χ=B-B-B-A and χ=B-B-A-A, still outperforms SMB in achieving either higher raffinate purity or higher extract purity in Case 1b.

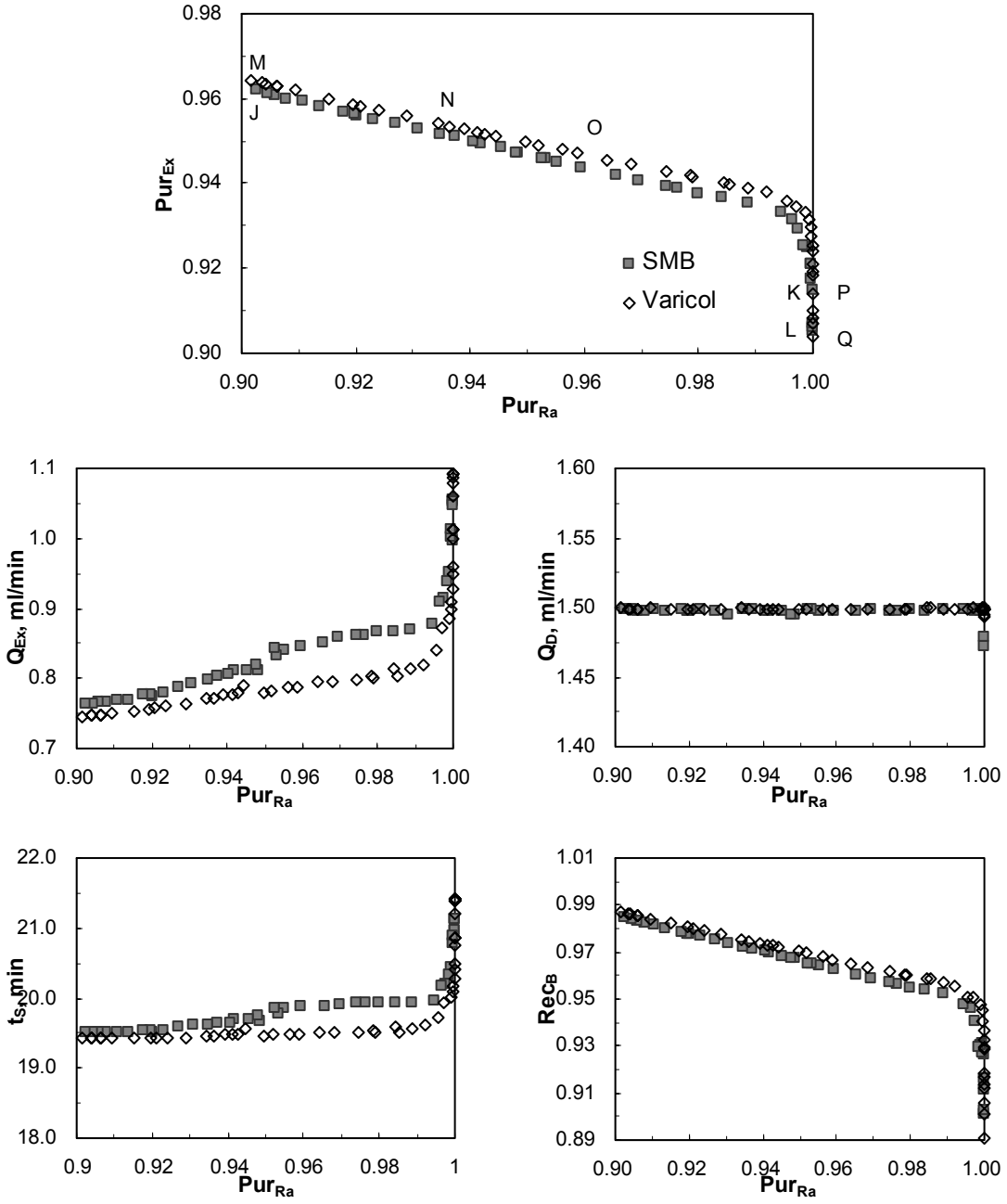

Figure 7.3 Pareto optimal solutions and the corresponding decision variables (Case 1b) for SMB and Varicol ($c_{T,f}$ =0.03 g/l, Q_{I}=0.1 ml/min)

7.3.1.3 Effect of feed concentration

Comparison of Pareto solutions of Case 1a & 1b in terms of Pur_{Ra} and Pur_{Ex} is illustrated in Figure 7.4. Results demonstrate that combination of higher feed concentration and lower feed flow rate is superior to that of lower feed concentration and higher feed flow rate in achieving higher product purity without consuming more amount of desorbent. This observation is also proved by SMB enantioseparations of EMD 53986 (Charton and Nicoud, 1995). Reason for such an improvement may be better comprehended from the comparison of concentration profiles (Figure 7.5) of two SMB simulations carried out at optimal operating conditions corresponding to Points 1 & 2 on the Perato sets of Cases 1a and 1b shown in Figure 7.4.

From Figure 7.5, it is observed that concentrations of the two components in case of Point 2 are slightly higher than those of Point 1 in section 3 because of the lower raffinate flow rate. On the contrary, concentration of the less retained S-pindolol in case of Point 2 is slightly lower than that of Point 1 due to the relatively higher extract flow rate. Therefore, extract purity in case of Point 2 increases slightly. In the meantime, the relative lower internal flow rates (Point 2 Case 1b) make the migration velocities of concentration waves slower in section 3. Therefore, high purity of raffinate is still obtained in the case of Point 2. Another interesting phenomenon observed from Figure 7.5 is that concentration waves in case of Point 1 seem to be more spread during the first half of the switching period. This also results in the lower purity in the extract and raffinate streams.

Based on the above analyses, we conclude that low injection concentrations should be avoided. In chromatographic separation, high injection concentration and low injection volume is recommended. However, even if achievable, very high concentration leads to a very low feed flow-rate, which might be difficult to control.

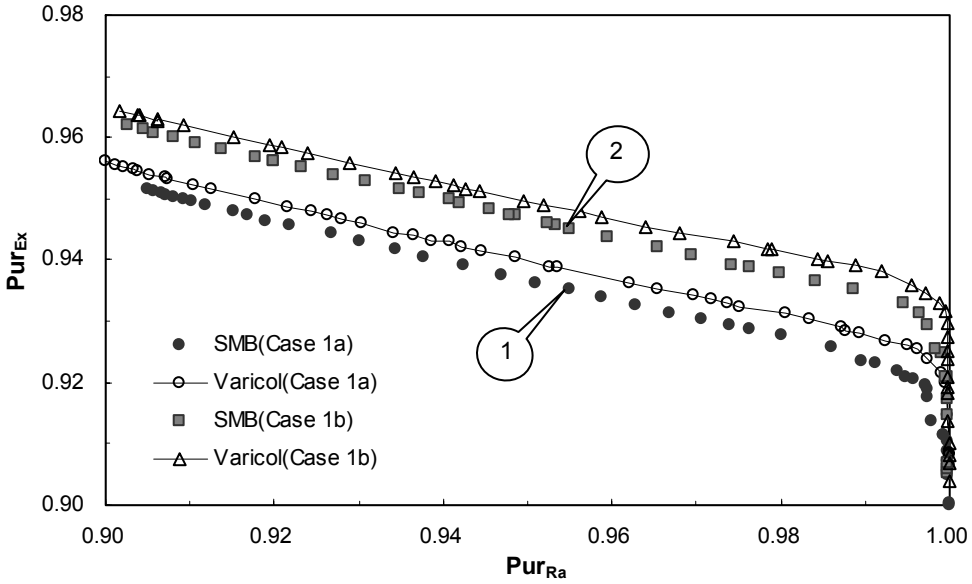

Figure 7.4 Effect of feed concentrations on system performance

Table 7.3 Optimum column configurations (χ) for Cases 1-3

Case		Figure	Pareto line	χ
1a	5-column SMB	7.1	AB	B
			BC	C
	5-column Varicol		EF	B-B-B-A
			FG	B-B-A-A
			GH	C-C-B-A
1b	5-column SMB	7.3	JK	B
			KL	A
	5-column Varicol		MN	B-B-A-A
			NO	B-B-B-A
			OP	B-B-A-A
			PQ	C-C-B-A
2	5-column SMB	7.6		B
	5-columnVaricol			B-B-A-A
3	5-column SMB	7.8		B
	5-column Varicol			B-B-A-A
	6-column SMB			M

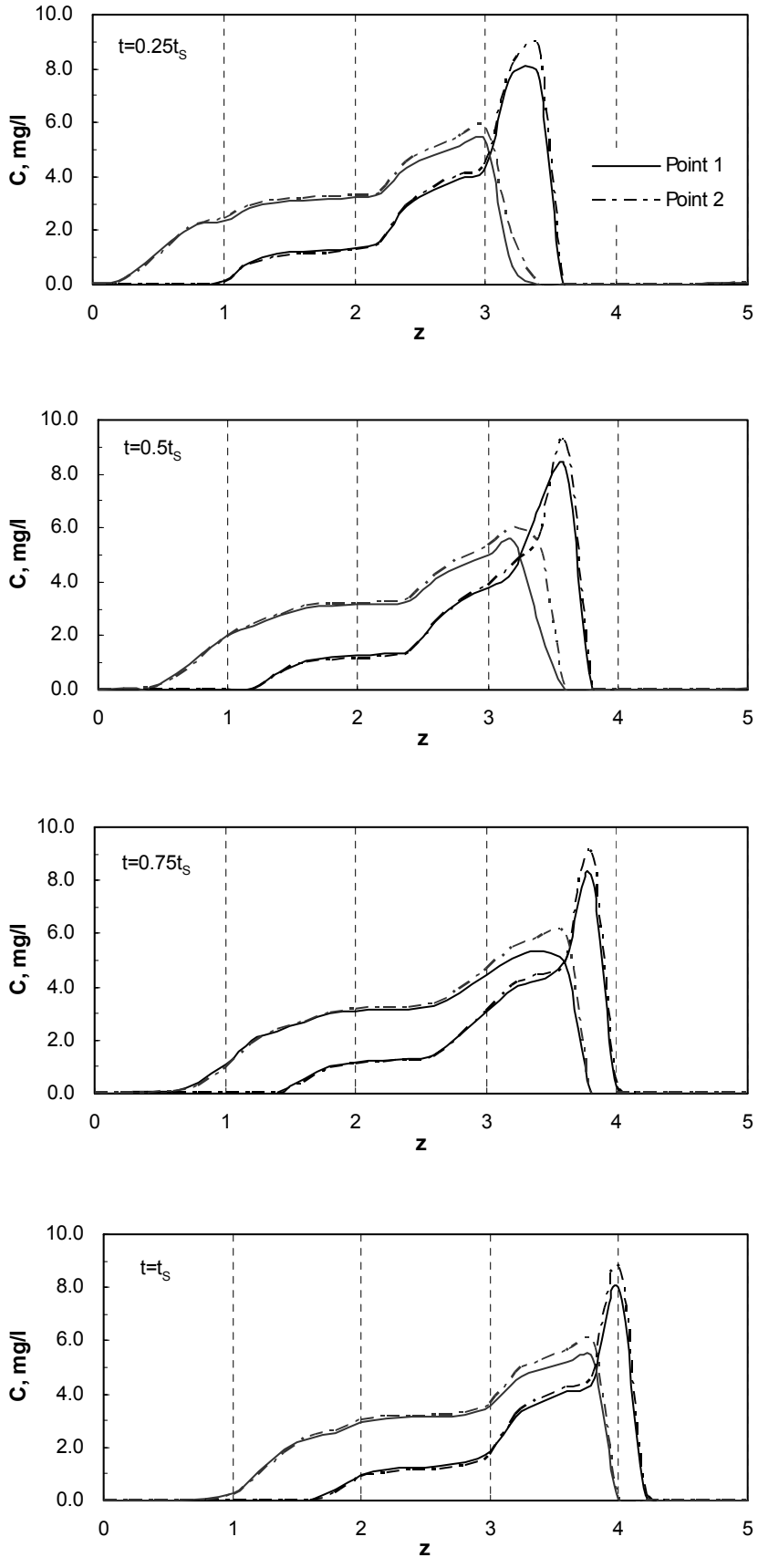

Figure 7.5 Comparison of the concentration profiles for points 1 & 2 in Figure 7.4

7.3.2 Case 2. Maximization of recovery of S-pindolol and minimization of desorbent flow rate

Perhaps one of the most serious problems associated with chromatographic process is that though they are efficient in separation, the resultant product streams are quite dilute due to the high desorbent requirements. Even if desorbent is cheap it is desirable to get concentrated product streams since dilute systems result in higher operational cost in the subsequent downstream separation processes. Reducing desorbent consumption can therefore help in improving the economics of the overall process. Hence, the goal of the second case is to improve recovery of S-pindolol while reducing desorbent consumption.

Fixed parameters and the decision variables in Case 2 are the same as those chosen in Case 1a. However, the constraint of raffinate purity is different. Purity requirement for raffinate is set to 97.1% plus or minus 0.1% in this case due to the fact that purity of the commercial optical-pure S-pindolol in the market is 97.0%. The purpose of this case is to improve recovery of S-pindolol without sacrificing its purity too much by using the least possible amount of desorbent. Mathematical description for this case is given in Table 7.2.

Plots for solutions of the two objectives and the associated decision variables are illustrated in Figure 7.6 for desired purity requirements of extract and raffinate streams. The corresponding optimal column configurations are shown in Table 7.3. Each point on the Pareto sets represents the maximum possible of recovery of S-pindolol at each specific eluent flow rate. Pareto solutions obtained here provide decision makers more flexibility in selecting the desired operating conditions (called the preferred solution), which is unobtainable if conventional single-objective optimization was applied.

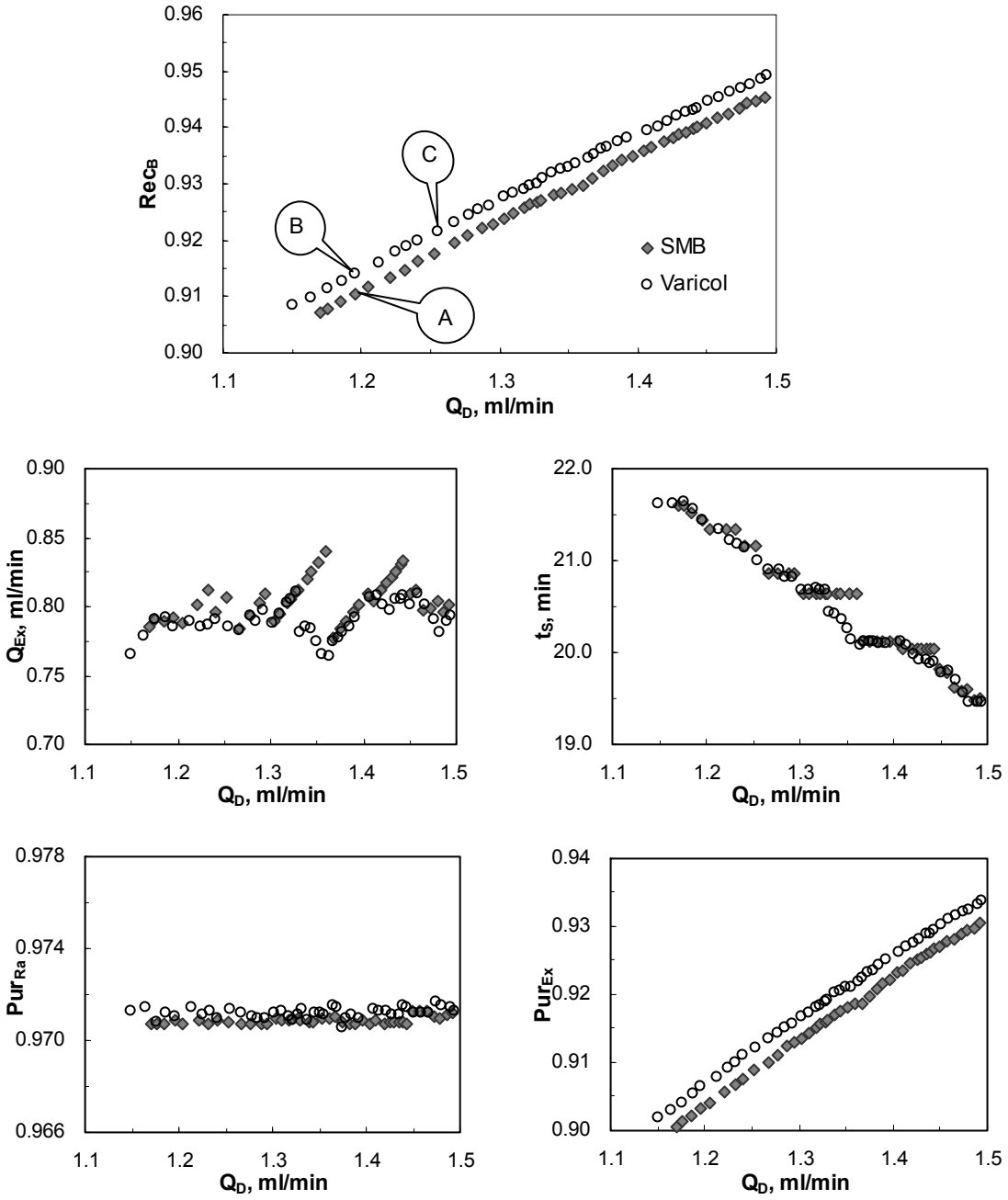

Figure 7.6 Pareto optimal solutions and the corresponding decision variables (Case 2) for SMB and Varicol ($c_{T,f}$ =0.02 g/l, Q_f=0.15 ml/min)

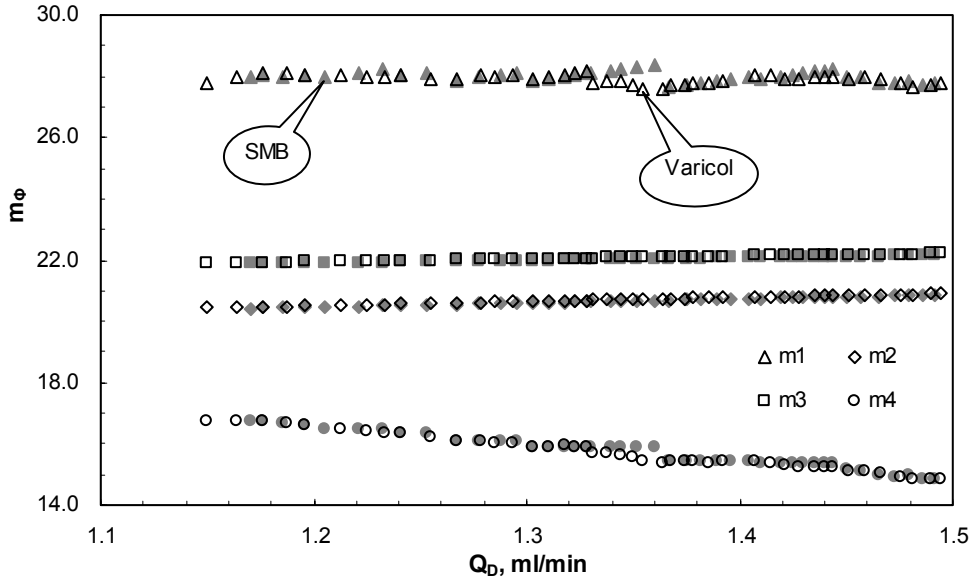

Figure 7.7 Optimal flow rate ratios corresponding to points on Pareto sets for 5-column SMB and Varicol in Case 2

A close scrutiny of Figure 7.6 reveals that covery of S-pindolol is increased proportionally to the increase of Q_D for both SMB and Varicol processes. An approximate linear relationship between Rec_B and Q_D was observed. The maximum recovery of S-pindolol is about 94.5% and 95.0% for SMB and Varicol process with its purity higher than 97.0%. Optimal solutions for Q_{Ex} converged to the range of 0.76-0.84 ml/min and did not show regular variations with Q_D. However, optimal solutions for t_s converged to different values at different Q_D and t_s decreased with the increase of Q_D. This is because slightly higher solid velocity is needed by decreasing t_s to balance the increased fluid velocity when Q_D increases. In analogy to Case 1, optimal m_2 and m_3 values at various Q_D shown in Figure 7.7 are quite close notwithstanding the dispersed solutions of Q_{Ex} and t_s.

Results form Figure 7.6 also indicate that under fixed purity requirement and maximum system pressure drop, Varicol can achieve higher recovery of S-pindolol

than an equivalent SMB with the same desorbent consumption; or Varicol consumes less amount of desorbent for the same recovery of S-pindolol. This implies that Varicol process can save some of the operating cost for fixed desired target purity. Improvement in recovery of S-pindolol or the decrease of eluent flow rate is almost identical throughout the entire range of Q_D.

Results of optimal column configuration also merit attention. Unlike the various optimal column configurations obtained in case 1, uniform optimum column configuration was obtained irrespective of different Q_D and Rec_B for both SMB and Varicol processes. Optimum configuration was B for SMB, whereas optimum configuration was B-B-A-A for a 4-subinterval Varicol process. This result suggested that when higher purity of S-pindolol is required, configuration with 2 columns in section 2 is favorable in obtaining high recovery of S-pindolol for SMB process, while χ=1.5/1/5/1/1 is the best choice for Varicol process.

Three experimental operations were carried out at optimal operating conditions corresponding to the points in the Pareto sets shown in Figure 7.6 to verify the optimization results obtained in Case 2. One common feature of the operating parameters for the three points is the relatively lower Q_D. The reason for selecting the relative lower Q_D is the limitation of pump performance. It is quite difficult for ISO-1000 pump to provide constant flow rate for Q_1 (Q_1=Q_4+Q_D) if higher Q_D is used in this open mode SMB operation. Thus, more robust operating parameters had to be chosen for the experiments to verify the optimization results. Table 7.4 compares experimental results with those of numerical optimizations.

It was found that experimental results deviate from model predictions for all the three runs. Although purities of raffinate are slightly higher than model predictions,

extract purity and recovery of S-pindolol obtained from experiments are much lower than the calculated optimal solutions. The major cause for such deviations comes from the severe fluctuation of recycling flow rate (Q_4), which could not be avoided during experimental operation. It was observed that Q_4 of 2.0 ml/min was hardly achieved during the operation because of the extremely high pressure drop within the system. Q_4 fluctuated from 1.88 ml/min to 1.97 ml/min with the change of system pressure arising from the port switching. Therefore, all the internal flow rates fluctuated and decreased with Q_4, which resulted in the decrease of extract purity and recovery of S-pindolol. Actually, all experimental data matched the simulation results if 1.95 ml/min was used for Q_4 instead of 2.0 ml/min in the simulation program. This result demonstrates that the mathematical model is reliable.

Table 7.4 Comparison of optimal predictions with experimental results

Run	A	B	C
Process	SMB	Varicol	
Calculated zone flow rates, ml/min			
Q_1	3.2	3.2	3.26
Q_2	2.403	2.414	2.47
Q_3	2.553	2.564	2.62
Q_4	2.0	2.0	2.0
t_s min	21.45	21.4	21.0
χ	1/2/1/1	1/2/1/1-2/1/1/1	1/2/1/1-2/1/1/1
Optimal solutions			
Pur_{Ex}	90.2%	90.58%	91.19%
Pur_{Ra}	97.1%	97.2%	97.18%
Rec_B	91.0%	91.56%	92.3%
Experimental Results			
Pur_{Ex}	83.54%	83.46%	84.0%
Pur_{Ra}	97.48%	98.0%	98.13%
Rec_B	81.3%	81.45%	83.3%

Other operating conditions: Q_F=0.15 ml/min, $c_{T,f}$ =0.02 g/L

The above experimental results clearly state the great importance of flow rate control and pump performance in SMB and Varicol operation. In addition, experimental deviation from the optimal solutions caused by the smallest disturbance in flow rates confirms the lack of robustness of the optimal operating points (Pedeferri et al., 1999). Operating conditions for SMB and Varicol processes should be selected as a compromise between separation performance and robustness.

7.3.3 Case 3. Maximization of recovery of S-pindolol and minimization of desorbent flow rate at design stage

So far we have accomplished two optimization cases for the existing laboratory SMB set-up. Undoubtedly, design parameters also have a significant influence on process performance in terms of various objective functions (Zhang et al., 2002a, b, Yu et al., 2003b, Susanto et al., 2005). In the third case, the focus will be on the optimization of column geometry (such as L and N_T). Optimization in this case was formulated to simultaneously maximize recovery of S-pindolol and minimize the desorbent flow rate with the constraints of raffinate and extract purities higher than 99.0% and 95.0% respectively.

Unlike the former cases, the highest bound of Q_1 in this case was relaxed to 4.0 ml/min, the recommended highest flow rate by manufacturer under which the column can be used, without consideration of the pump performance. Since one of our objectives is to minimize desorbent flow rate, the highest bound for Q_D keeps the same as that of previous cases. Recycling flow rate (Q_4) was, therefore, increased to 2.5 ml/min in this case. 15.0 cm was selected as the highest bound for column length based on the highest pressure drop which pump could endure nominally. In addition, 6-column SMB was optimized in this case to study the effect of number of columns on SMB performance. Complete optimization formulation is shown in Table 7.2. Possible

column configuration for 5- and 6-column systems can be found in Table 7.1.

Performances of 5-column SMB and Varicol as well as 6-column SMB is assessed under the same conditions and results are illustrated in Figure 7.8. Optimum configurations for the three systems were listed in Table 7.3. Results from Figure 7.8 clearly show that 6-column SMB offers more room for improvements as indicated by the magnitude of Pareto set, followed by 5-column Varicol and 5-column SMB. Although 5-column Varicol outperforms 5-column SMB in acquiring high recovery of S-pindolol, the maximum attainable recovery of S-pindolol at the same Q_D in 5-column Varicol is less than that obtained in 6-column SMB. Performance enhancement achieved in 6-column SMB due to the increase of one column outweighs the improvements attainable due to the increase in flexibility in a 5-column four-subinterval Varicol system.

Column length (L) converged to different values for the three different systems. The highest value of column length was obtained for 5-column SMB, followed by 5-column Varicol and 6-column SMB. To meet the strict constraints of purity requirements in the raffinate and extract streams, column length around 14.7 cm is required for 5-column SMB, while 12.9 cm and 10.6 cm are needed for 5-column Varicol and 6-column SMB respectively to meet the same constraints. Different sets of t_s were therefore obtained for the three systems to match optimal column lengths. Besides, highest optimal Q_{Ex} is also observed for 5-columnn SMB while the corresponding value for 6-column SMB is the lowest. Despite the various Q_{Ex} and t_s obtained, flow rate ratios at different Q_D for the three systems are almost identical as shown in Figure 7.9.

The highest recovery of S-pindolol with raffinate purity higher than 99.0%

acquired in Case 1b (Point D for 5-column SMB and Point E for 5-column Varicol) was also plotted in Figure 7.8 for comparison. It can be seen that recovery of S-pindolol for 5-clolumn SMB increased from 94.7% to 98.6% and recovery of S-pindolol for 5-clolumn Varicol increased from 95.5% to 99.0% by incorporating the column length as decision variable. However, both the increase of L and Q_4 contribute to such performance improvement. It is known that either production capacity or product quality can be enhanced by increasing the column length. For this separation system, large number of simulations indicates that performance enhancement is not so significant by merely increasing column length, particularly when higher Q_D is used. Actually, considerable improvement of either raffinate purity or recovery of S-pindolol is attributed to the increase of recycling flow rate (Q_4). This observation coincided with the results reported by Nicoud et al., (1993), who used SMB process to separate 1a,2,7,7a-tetrahydro-3-Methoxynaphth-[2,3b] oxirene on cellulose triacetate. Therefore, if possible, increasing recycling flow rate seems to be more economic in achieving high recovery of S-pindolol in this system.

Another important observation is the effect of the total number of columns. Results from Figure 7.8 demonstrate that better performance can be achieved by increasing the total number of column (N_T) while having a reduced length (L). Compared with 5-column SMB and Varicol, 6-column SMB with shorter column length can improve recovery of S-pindolol about 1% and 0.4% respectively for the same raffinate purity. This is possible because more columns would provide an additional flexibility for the operation. Column configuration of 2/2/1/1 for the 6-column SMB provides the possibility of complete regeneration of solids, which helps to obtain both high recovery and high purity of S-pindolol.

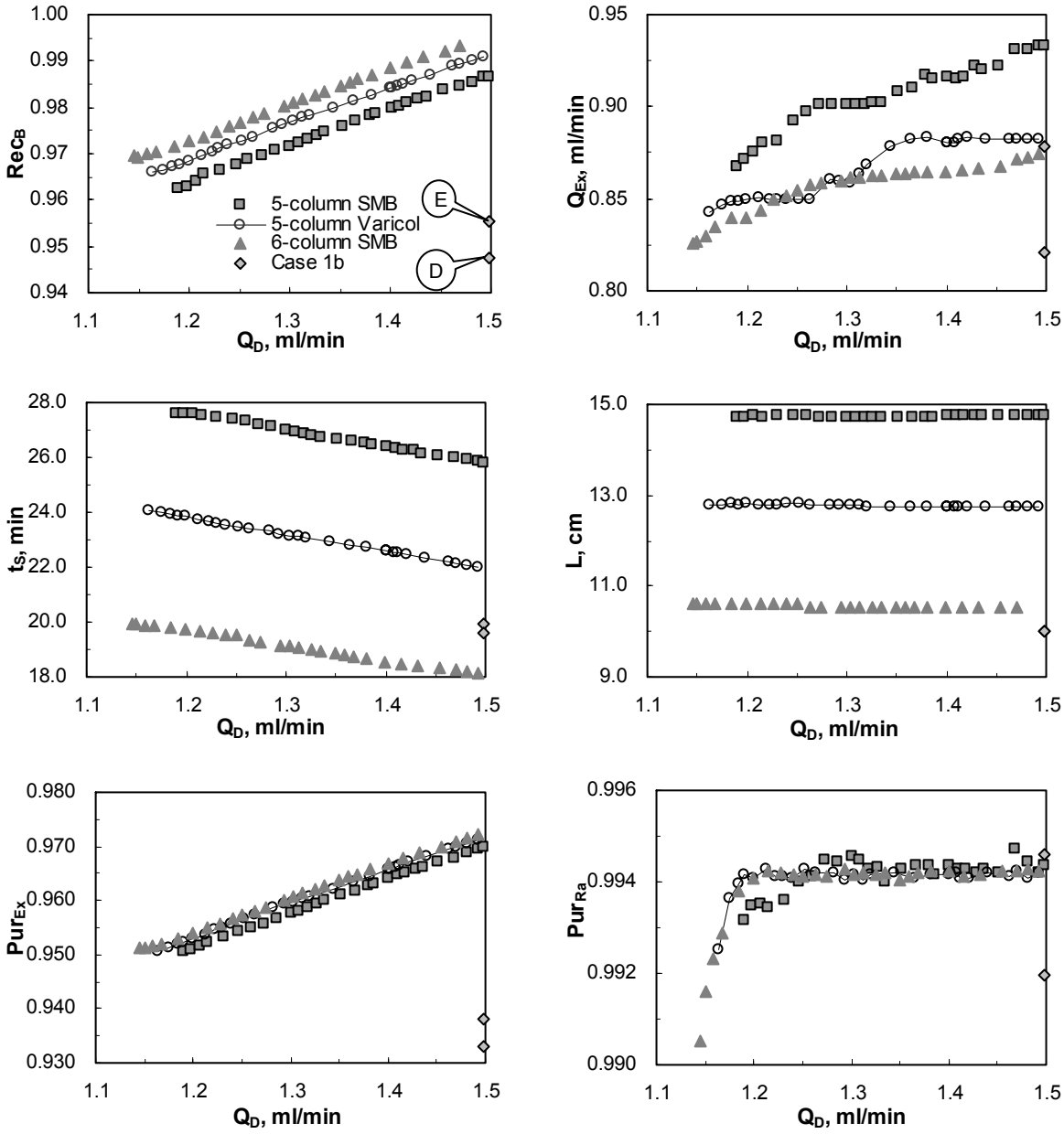

Figure 7.8 Pareto optimal solutions and the corresponding decision variables (Case 3) for SMB and Varicol ($c_{T,f}$ =0.03 g/l, Q_f=0.1 ml/min)

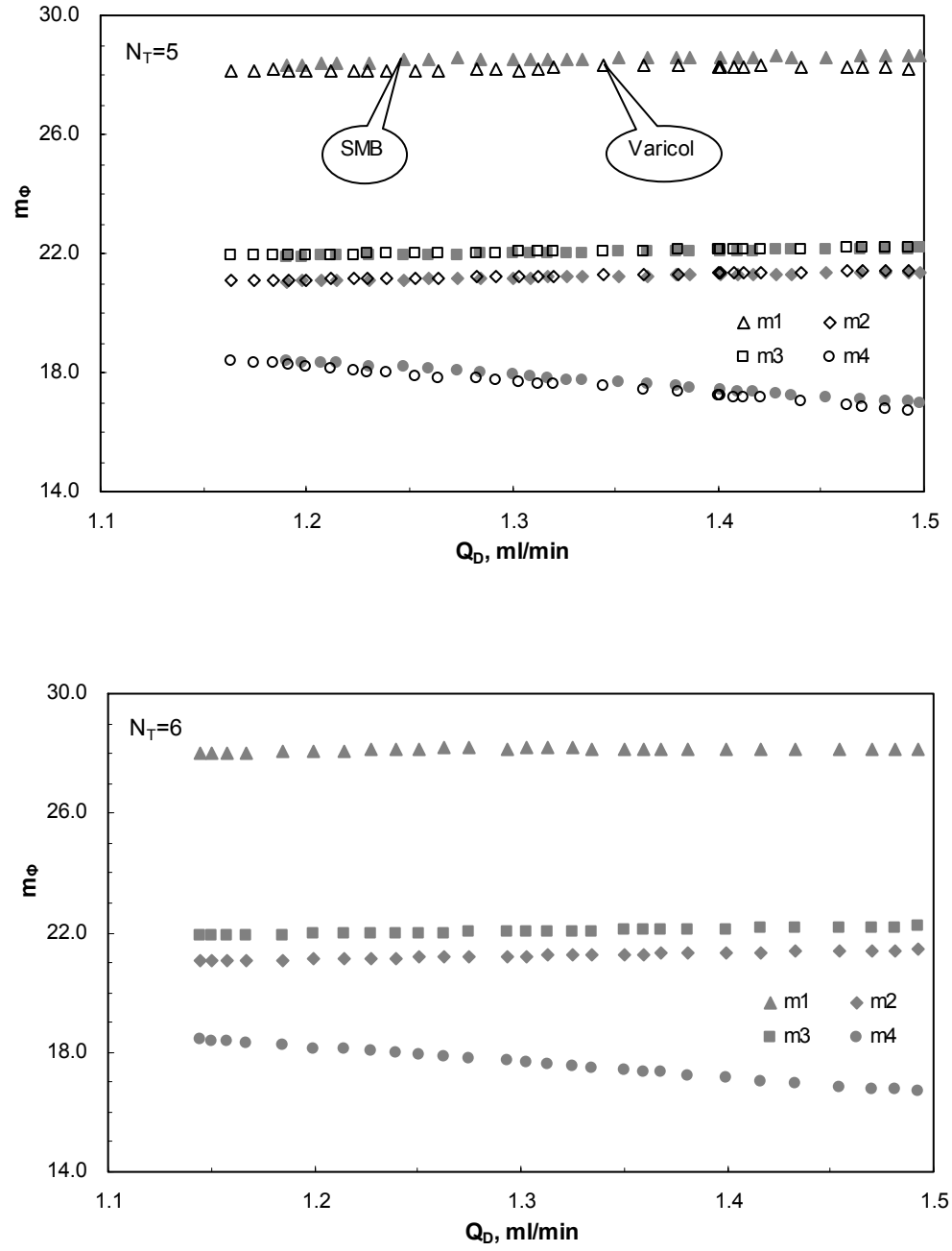

Figure 7.9 Optimal flow rate ratios corresponding to the points on Pareto sets in Case 3

7.4 Validity of the design strategy presented in Chapter 6

In order to verify the short-cut design strategy presented in the last chapter, calculated optimal flow rate ratios obtained from the rigorous optimization in Case 1a, which lead to raffinate purity higher than 99.0% and extract purity higher than 90.0%, are compared with those obtained from Chapter 6. From Figure 7.10 it can be seen that all the optimal combinations of m_2 and m_3 obtained in Case 1a for both 5-column SMB and Varicol process fall completely into the separation region acquired from short-cut design strategy presented in Chapter 6. In addition, optimal calculated m_1 and m_4 values for all the three optimization cases fully meet the corresponding constraints used in the design strategy. These results demonstrated that short-cut design strategy presented in Chapter 6 is reliable and robust in obtaining the complete separation region.

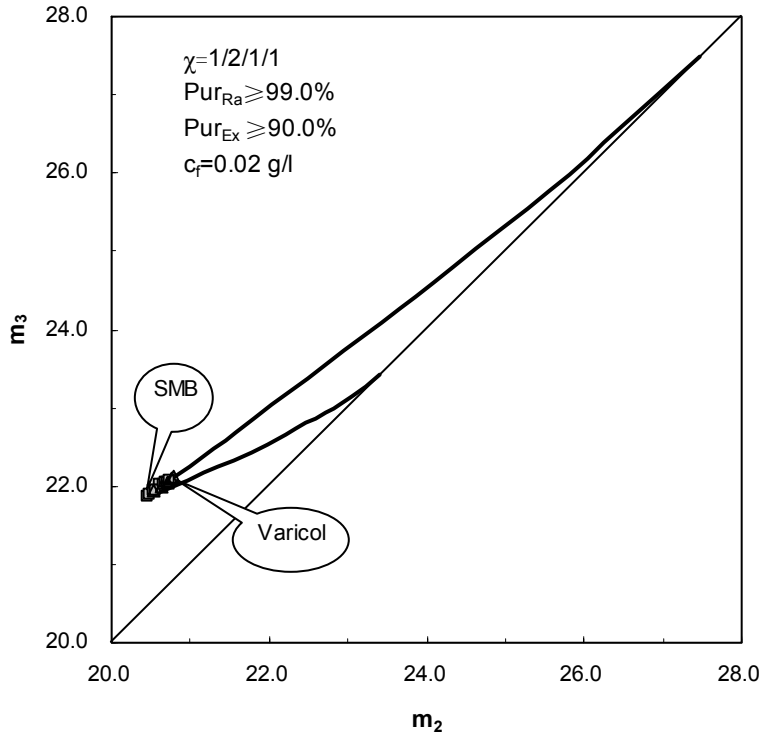

Figure 7.10 Comparison of optimal flow rate ratios obtained in Case 1a with those from the design strategy

7.5 Conclusions

Systematic multi-objective optimization study of SMB and Varicol process for enantioseparation of racemic pindolol were performed in this chapter using NSGA-II-JG. Simultaneous maximization of raffinate and extract purities were firstly performed for a given capacity with different feed concentrations to evaluate the effect of feed concentration on Pareto solutions and system performance. Results indicated that combination of higher feed concentration and lower feed flow rate is superior to that of lower feed concentration and higher feed flow rate in achieving higher product purity without consuming more amount of desorbent. Relatively lower Q_2 and Q_3 are favorable to achieve higher purities both in the raffinate and in the extract when lower feed flow rate and higher feed concentrations are applied.

Optimizations aimed at maximizing recovery of S-pindolol and minimizing desorbent flow rate were carried out both for the existing laboratory set-up as well as for design purpose. An approximate linear increase of recovery of S-pindolol was observed with the increase of eluent flow rate. Although purity and recovery of S-pindolol do increase by increasing column length, such improvements are less considerable compared with those arising from the increase of recycling flow rate. Therefore, if possible, increasing recycling flow rate seems to be more economic in achieving high recovery of S-pindolol in this system. However, experimental results aimed at verifying the optimization calculations demonstrated that higher recycling flow rate was difficult to achieve due to the extremely high pressure drop in this system. Operating conditions for SMB and Varicol processes should be selected as a compromise between separation performance and robustness.

Total number of columns also has an important influence on separation performance. Results indicate that better performance can be achieved by increasing

the number of columns. Besides, all optimization results proved that Varicol outperforms SMB in either achieving higher purity or recovery of S-pindolol using the same desorbent consumption or consuming less amount of desorbent for the same purity and recovery requirements.

Chapter 8 Conclusions and Recommendations

8.1 Conclusions

This dissertation presents comprehensive studies on the optimal design and operation of non-reactive and reactive SMB systems for enantioseparation of a racemic drug and an enzymatic catalytic reaction. NSGA-II with jumping genes, a new adaptation of genetic algorithm was used as the optimization algorithm. In the first two chapters, Hashimoto's hybrid SMBR system and its modifications were presented and optimized for production of high concentrated fructose syrup (HFS55) by isomerization of glucose. Productivity of fructose has been greatly improved by applying the systematic multi-objective optimization without consuming more amount of desorbent. In the later chapters, a comprehensive study of performances of SMB and Varicol for enantioseparation of racemic pindolol was carried out. Based on a short-cut design strategy for this nonlinear system with the presence of dispersion effect, complete separation of the two enantiomers was achieved on a laboratory SMB set-up. Results from the subsequent rigorous optimization study further proved the validity of this design strategy.

8.1.1 Optimization of hybrid SMBR systems for production of high concentrated fructose syrup

Simulation and multi-objective optimization study for the isomerization of glucose to fructose in Hashimoto's hybrid simulated moving bed reactor (SMBR) was firstly performed to predict the optimal operating conditions for such an important industrial reaction and separation process. After the dynamic SMBR model was verified by comparing the model predictions with the published experimental results,

systematic multi-objective optimization was conducted to maximize the net productivity of fructose using the minimum desorbent consumption. By optimizing the operation of 23-column SMBR system with different feed compositions, feed stream containing 100% glucose offered the highest productivity while purity of fructose was the lowest (still higher than 55%). On the contrary, system with 50% glucose and 50% fructose as feed gave the lowest productivity. It was found that productivity of fructose could be further improved by incorporating column lengths into decision variables. In addition, total number of columns also showed considerable influence on the system performance, the more columns used, the higher productivity of fructose could be obtained.

Hashimoto's SMBR system with variable feed flow rate was also optimized in this study to see the advantages of this operation mode. Although slightly improvement of productivity and purity of fructose were achieved, results indicated that manipulation based on changing the wave velocity did not yield much benefit in this SMBR system. Efforts should be made to increase the conversion of glucose within reactors.

From the optimization study of Hashimoto's 3-zone SMBR system, it could be seen that conversion of glucose in each reactor was quite low due to the insufficient separation of glucose and fructose at the inlet of each reactor when feed is a 50/50 blend of glucose and fructose. To overcome the disadvantages of Hashimoto' systems, two different configurations of modified system with four sections were developed.

In modified Configuration 1 (MC1), only one reactor was used. Unlike the conventional 4-zone SMB, raffinate stream in MC1 was fed to the reactor, where glucose was converted into fructose by enzyme isomerase and the outlet stream from the reactor was recycled back with the fresh feed. Three processes including

17-column reactive SMB (16 adsorption columns plus 1 reactor), 15-column reactive SMB and Varicol (14 adsorption columns plus 1 reactor) were studied. Results showed that relatively high liquid and solid flow rate was beneficial to system performance and incomplete regeneration of the adsorbent resulted in the relatively poor system performance. When less adsorption columns were used, there was a slightly decrease in the productivity and purity of fructose. Results demonstrated that productivity of fructose for MC1 consisting 17 columns could rival the value obtained by Hashimoto's system consisting of 7 reactors was optimized. Performance of 15-column Varicol is better than that of 15-column SMBR and is almost as good as that of 17-column SMBR.

Based on the concentration profiles of MC1, one additional reactor was added between the first and the third adsorption columns in section 4 to further improve productivity of fructose. One particular design for modified Configuration 2 (MC2) is that flow to the second reactor was only during the initial part of the switching period. The purpose of this design was to guarantee that the flow to the second reactor contains high concentration of glucose and low concentration of fructose. Therefore, more glucose can be converted into fructose. Multi-objective optimization for MC2 showed that the design concept could further increase productivity of fructose using less desorbent and the optimal productivity of fructose for MC2 (14 adsorption columns and 2 reactors) were even higher than that achieved by Hashimoto's SMBR system (17 adsorption columns and 6 reactors).

Remarkable performance of MC1 and MC2 manifested that with appropriate optimal design, performance achieved by Hashimoto's 23-column SMBR system could be realized by modified systems with just one or two reactors. Hence, total length of reactor is reduced remarkably and the efficiency of reactor has been improved greatly.

8.1.2 Design and optimization of SMB and Varicol for enantioseparation of racemic pindolol

Modeling, design and operation of SMB and Varicol process for enantioseparation of racemic pindolol were accomplished in this work. To achieve complete separation of the two enantiomers using SMB technology, reliable information of adsorption equilibrium is an important prerequisite for the design and optimization. Therefore, study aimed at acquiring the competitive isotherm of racemic pindolol on α1-acid glycoprotein stationary phase was firstly carried out. Inverse method was adopted in this study to determine the biLangmuir isotherm parameters of pindolol enantiomers by a least-square fitting of the model simulations to experimental elution curves of racemic pindolol. By fitting the chromatograms at the moderate and high sample loads (40 and 80 μg) simultaneously, isotherm parameters were extracted. Good agreement was observed between the model predicted and experimental elution concentrations. Robustness of isotherm parameters was verified by comparing the calculated and experimental elution and breakthrough curves for both the pulse tests and frontal analysis at various operating conditions. Although inverse method shows the advantage of taking the lowest experimental cost in acquiring the competitive isotherm, this method is confined to the use of single and binary system and requires an optimization algorithm with high efficiency.

As pindolol shows nonlinear characteristic even under low concentrations, few theories so far can give a direct guidance in how to choose the proper operating parameters of SMB and Varicol process for such a nonlinear system with the presence of axial dispersion. Trial and error approach based on numerical simulations seems to be the only possible choice. In order to reduce the course of trial-and-error, a shortcut design strategy based on triangle theory was presented to obtain the complete

separation region. Four SMB runs and one Varicol operation were carried out using the laboratory SMB set-up at various operating conditions to verify the model predictions. Good agreement between the experimental data and simulations results was obtained for all the five runs. Such achievement indicated that selected mathematical model could give extremely good predictions of both SMB and Varicol process and confirmed that design strategy was quite reliable and robust in obtaining the suitable operating parameters.

Effect of column configuration on system performance was studied by comparing the experimental results of different configurations. For SMB operation, column configuration with 1/2/1/1 was favorable to achieving higher purities in both raffinate and extract. Varicol operation with configuration of 1.5/1.5/1/1 showed its advantage of achieving better performance over SMB process. These results indicated that regeneration of the solids has great importance in achieving the desired separation for this system. Intense adsorption of the compounds on the chiral stationary makes the complete desorption of them rather difficult, and therefore, more columns should be used in the sections 1 and 2.

Influences of the derived isotherm parameters on SMB performance were also studied. It was found that decrease of saturation capacity of either site (non-selective and selective sites for biLangmuir isotherm) will cause a decrease in the raffinate recovery. And variation of the selective site parameters has a more remarkable influence on SMB performance. This result suggests that chiral stationary phase with higher saturation capacity is always desirable for enantioseparation.

Subsequently, systematic multi-objective optimization study of SMB and Varicol processes for enantioseparation of racemic pindolol were carried out. The first multi-objective optimization problem aimed at simultaneous maximization of the

raffinate and extract purities with different feed concentrations to evaluate the effect of feed concentration on Pareto solutions and system performance. Results showed that combination of higher feed concentration and lower feed flow rate was superior to that of lower feed concentration and higher feed flow rate in achieving higher product purity. Relatively lower flow rate in sections 2 and 3 are beneficial to achieving higher purities both in the raffinate and in the extract when lower feed flow rate and higher feed concentrations are applied.

Optimizations aimed at maximizing recovery of S-pindolol and minimizing the desorbent flow rate were carried out both for the existing laboratory set-up as well as at design stage. An approximate linear increase of recovery of S-pindolol was observed with the increase of eluent flow rate. Although purity and recovery of S-pindolol do increase by increasing column length, such improvements are less considerable compared with those arising from the increase of recycling flow rate. If possible, increasing recycling flow rate seems to be more economic in achieving high recovery of S-pindolol in this system. However, experimental study aimed at verifying the optimization results demonstrated that higher recycling flow rate was difficult to achieve in this system due to the extremely high pressure drop within the system. Operating conditions for SMB and Varicol processes should be selected as a compromise between separation performance and robustness.

The number of columns also had an important influence on separation performance. It was found that better performance could be achieved by increasing the total number of columns while having a reduced column length. Besides, all the optimization results confirmed that Varicol outperforms SMB in either achieving higher purity or recovery of S-pindolol using the same desorbent consumption or consuming less amount of desorbent for the same purity and recovery requirements.

By comparison of the calculated optimal flow rate ratios obtained from the rigorous optimization with those obtained from short-cut design strategy, it was observed that all the optimal combinations of m_2 and m_3 obtained from systematic optimization fall completely into the separation region acquired from the short-cut design strategy. Short-cut design strategy used in this study has been proved to be efficient and reliable for the design of SMB and Varicol process dealing with nonlinear isotherm under non-ideal conditions.

It should be emphasized that methods used in both projects of this PhD study are generic and could be applied to other systems. In addition, systematic optimization of the two systems could provide much useful information for the optimal design and operation of other SMB processes. With the results from this study large-scale SMB/SMBR process can be designed using the scale-up formulas.

8.2 Recommended future works

In this study, two modified configurations of Hashimoto's SMBR system was optimized without the experimental verification due to the limitation of time. Experimental investigation of the modified system for isomerization of glucose using the recent developed DOWEX MONOSPHERE 99 Ca resin could be conducted in the future to examine feasibility of the design concept presented in this work.

As for the enantioseparation of racemic pindolol, both SMB and Varicol processes show high sensitivities to disturbances and tendency to instability when operating condition is close to the economic optimum. Development and implementation of a suitable control framework is necessary to exploit the full economic potential of the process. On-line optimization and control of the process naturally becomes the next task.

Results from both the experimental study and optimization calculation pronounced the importance of desorption for the two enantiomers. Therefore, solvent gradient operation mode can be attempted in this process to either increase the production capacity or product quality.

In this investigation, NSGA-II-JG is used to obtain the Pareto optimal solutions. NSGA-II-JG is adequate for solving the multi-objective problems formulated in this study. However, its robustness is potentially affected when complexity of the problem increases, e.g., increase in the number of objective functions or decision variables. Hence, modification of this algorithm or work for a more robust multi-objective optimization algorithm is still required.

References

Abel, S., M. Mazzotti and M. Morbidelli. Solvent Gradient Operation of Simulated Moving beds I. Linear Isotherm, J. Chromatogr. A, *944*, pp. 23-39. 2002.

Abel, S., M. Mazzotti and M. Morbidelli. Solvent Gradient Operation of Simulated Moving beds - 2. Langmuir Isotherms, J. Chromatogr. A, *1026*, pp. 47-55. 2004.

Adam, P., R.-M. Nicoud, M. Bailly and O. Ludemann-Hombouger. Process and Device for Separation with Variable Length, US patent, 6 136 198. 1998.

Akintoye, A., G. Ganetsos and P.E. Barker. Preparative Scale Chromatographic Systems as Combined Biochemical Reactor-Separators. In Advances in Separation Processes, I. Chem. E. Symp. Ser., *118*, 21-28. 1990.

Akintoye, A., G. Ganetsos and P.E. Barker. The Inversion of Sucrose in a Semi-Continuous Countercurrent Chromatographic Bioreactor-Separator, Trans. I. Chem. E., *69C*, pp.35-44. 1991.

Ando, M., M. Tanimura and M. Tamura. Method of Chromatographic Separation, US Patent 4 970 002. 1990.

Antos, D., W. Piatkowski and K. Kaczmarski. Determination of Mobile Phase Effect on Single-Component Adsorption Isotherm by Use of Numerical Estimation, J. Chromatogr. A, *874*, pp. 1-12. 2000.

Azevedo, D.C.S. and A.E. Rodrigues. Bi-linear Driving Force Approximation in the Modeling of Simulated Moving Bed Using Bidisperse Adsorbent, Ind. Eng. Chem. Res., *38*, pp. 3519-3529. 1999.

Azevedo, D.C.S. and A.E. Rodrigues. Design of a Simulated Moving Bed in the Presence of Mass-Transfer Resistances, AIChE J., *45*, pp. 956-966. 1999.

Azevedo, D.C.S. and A.E. Rodrigues. Fructose-Glucose Separation in a SMB Pilot Unit; Modeling, Simulation, Design and Operation, AIChE J., *47*, pp. 2042-2051. 2001.

Barker, P.E., I. Zafar and R.M. Alsop. Production of Dextran and Fructose in a Chromatographic Reactor-Separator. In Separation for Biotechnology, ed by M.S. Verral and M.J. Hudson, pp. 127-155. London: Ellis-Horwood. 1987.

Barker, P.E. and G. Ganetsos. Chemical and Biochemical Separations Using Preparative and Large-scale Batch and Continuous Chromatography, Separ. Purif. Methods, *17*, pp. 1-65. 1988.

Barker, P.E., G. Ganetsos, J. Ajongwen and A. Akintoye. Bioreaction-separation on Continuous Chromatographic systems, BioChem. Eng. J. *50*, pp. B23-B28. 1992.

Bhaskar, V., S.K. Gupta and A.K. Ray. Applications of Multiobjective Optimization in Chemical Engineering, Rev. Chem. Eng., *16*, pp.1-54. 2000a.

Bhaskar, V., S.K. Gupta and A.K. Ray. Multiobjective Optimization of an Industrial Wiped-Film Pet Reactor, AIChE J., *46*, pp. 1046-1058. 2000b.

Bhaskar, V., S.K. Gupta and A.K. Ray. Multiobjective Optimization of an Industrial Wiped Film Poly (Ethylene Terephthalate) Reactor: Some Further Insights, Comput. Chem. Eng., *25*, pp. 391-407. 2001.

Biressi, G., O. Ludemann-Homburger, M. Mazzotti, R.-M. Nicoud and M. Morbidelli. Design and Optimization of a Simulated Moving Bed Unit: Role of Deviation from Equilibrium Theory, J. Chromatogr. A, *976*, pp. 3-15. 2000.

Blümel, C., Blümel, P. Hugo and A. Seidel-Morgenstern. Quantification of Single Solute and Competitive Adsorption Isotherms Using a Closed-Loop Perturbation Method, J. Chromatogr. A, *865*, pp. 51-71. 1999.

Braum, E.J. Chemical Property Estimation: Theory and Application. pp. 253-258, New York: Lewis Publishers. 1998.

Broughton, D.B. and C.G. Gerhold. Continuous Sorption Process Employing Fixed Bed of Sorbent and Moving Inlets and Outlets, US Patent 2 985 589. 1961.

Broughton, D.B. Molex: Case History of a process, Chem. Eng. Prog., *64*, pp. 60-65. 1968.

Broughton, D.B., R.W. Neuzil, J.M. Pharis and C.S. Breasley. The Parex Process for Recovering P-xylene, Chem. Eng. Prog., *66*, pp. 70-75. 1970.

Broughton, D.B. Productive-Scale Adsorptive Separations of Liquid-Mixtures by Simulated Moving-Bed Technology, Separ. Sci. Technol., *19*, 723-736. 1984.

Buckley, M. and G. Norton. Experiences with a new Molasses separation Plant at Mallow, Int. Sugar J., *93*, pp. 204-209. 1991.

Camacho-Rubio, F., E. Jurado-Alameda, P. Gonzalez-Tello and G. Luzon-Gonzalez. Kinetic Study of Fructose-Glucose Isomerization in a Recirculation Reactor, Can. J. Chem. Eng., *73*, 935-939. 1995.

Cauley, F.G. Y. Xie and N.H.-L. Wang. Optimization of SMB Systems with Linear Adsorption Isotherms by Standing Wave Annealing Technique, Ind. Eng. Chem. Res., *43*, pp. 7588-7599. 2004.

Cavoy, E., M.-F. Deltent, S. Lehoucq and D. Miggiano. Laboratory-Developed Simulated Moving Bed For Chiral Drug Separations. Design of the System and Separation of Tramadol enantiomers, J. Chromatogr. A, *769*, pp. 49-57. 1997.

Chankvetadze, B. Enantioseparation of Chiral Drugs and Current Status of Electromigration Techniques in This Field, J. Sep. Sci., *24*, pp. 691-705. 2004

Charton, F. and R.-M. Nicoud. Complete Design of a Simulated Moving-Bed, J. Chromatogr A., *702*, pp. 97-112. 1995.

Chiang, A.S.T. Continuous Chromatographic Process Based on SMB Technology, AIChE J., *44*, pp. 1930-1932. 1998.

Ching C.B. and D.M. Ruthven. Experimental Study of a Simulated Counter-Current Adsorption System-IV. Non-Isothermal Operation, Chem. Eng. Sci., *41*, pp. 3063-3071. 1986.

Ching, C.B., B.G. Lim, E.J.D. Lee and S.C. Ng. Preparative Resolution of Praziquantel Enantiomers by Simulated Countercurrent Chromatography, J. Chromatogr., *634*, pp. 215-219. 1993.

Clavier, J.Y., R.M. Nicoud and M. Perrut. A New Efficient Fractionation Process: The Simulated Moving Bed with Supercritical Eluent. In High Pressure Chemical Engineering: Proc. of the 3rd International Symposium on High Pressure Chemical Engineering, October 1996, Zurich, Switzerland, pp. 429-434.

Cussler, E.L. Diffusion: Mass Transfer in Fluid Systems. pp. 116-120, New York: Cambridge University Press. 1997.

Deb, K. Multi-Objective Optimization using Evolutionary Algorithm. pp. 13-249 UK: Wiley, Chichester. 2001.

Deb, K., A. Pratap, S. Agarwal and T. Meyarivan. A Fast and Elitist Multi-Objective Genetic Algorithm: NSGA-II. IEEE Transactions on Evolutionary Computation, *6*, pp. 182-197. 2002.

Denet, F., W. Hauck, R.M. Nicoud, O. Di Giovanni, M. Mazzotti, J.N. Jaubert and M. Morbidelli. Enantioseparation through Supercritical Fluid Simulated Moving Bed (SF-SMB) Chromatography. Ind. Eng. Chem. Res., *40*, pp. 4603-4609. 2001.

Di Giovanni, O., M. Mazzotti, M. Morbidelli, F. Denet, W. Hauck and R.M. Nicoud. Superficial Fluid Simulated Moving Bed Chromatography. II. Langmuir Isotherm, J. Chromatogr. A, *919*, pp. 1-12. 2001.

Dünnebier, G. and K.U. Klatt. Optimal Operation of Simulated Moving Bed Chromatographic Processes, Comput. Chem. Eng., *23*, pp. S195-S198. 1999.

Dünnebier, G., J. Fricke and K.U. Klatt. Optimal Design and Operation of Simulated Moving Bed Chromatographic Reactors, Ind. Eng. Chem. Res., *39*, pp. 2290-2304. 2000.

Felinger, A., A. Cavazzini and G. Guiochon. Numerical Determination of the Competitive isotherm of Enantiomers, J. Chromatogr. A, *986*, pp. 207-225. 2003a.

Felinger, A, D. Zhou and G. Guiochon. Determination of the Single Component and Competitive Adsorption Isotherms of the 1-Indanol Enantiomers by the Inverse Method, J. Chromatogr. A, *1005*, pp. 35-49. 2003b.

Francotte, E. and P. Richert. Applications of Simulated Moving-Bed Chromatography to the Separation of the Enantiomers of Chiral Drugs, J. Chromatogr. A, *769*, pp. 101-107. 1997.

Francotte, E., P. Richert, M. Mazzotti and M. Morbidelli. Simulated Moving Bed Chromatographic Resolution of a Chiral Antitussive, J. Chromatogr. A, *796*, pp. 239-248. 1998.

Francotte, E. Enantioselective Chromatography as a Powerful Alternative for the Preparation of Drug Enantiomers, J. Chromatogr. A, *906*, pp. 379-397. 2001.

Fricke, J., M. Meurer and H. Schnidt-Traub. Design and Layout of Simulated-Moving Bed Chromatographic Reactors, Chem. Eng. Technol., *22*, pp. 835-839, 1999a.

Fricke, J., M. Meurer, J. Dreisörner and H. Schnidt-Traub. Effect of Process Parameters on the Performance of a Simulated Moving Bed Chromatographic Reactor, Chem. Eng. Sci., *54*, pp. 1487-1492. 1999b.

Giordano, R.L.C., R.C. Giodano and C.L. Cooney. A Study on Intra-particle Diffusion Effects in Enzymatic Reactions: Glucose-Fructose Isomerization, Bioprocess Eng., *23*, 159-166. 2000.

Glajch, J.L., J.J. Kirkland and J. Köhler. Effect of Column Degradation on the Reversed-Phase High-Performance Liquid Chromatographic Separation of Peptides and Proteins, J. Chromatogr., *384*, pp. 81-90. 1987.

Goicoechea, A., D.R. Hansen and L. Duckstein. Multiobjective Decision Analysis with Engineering and Business Applications. pp. 30-75, New York: Wiley. 1982.

Götmar, G., N.R. Albareda and T. Fornstedt. Investigation of the Heterogeneous Adsorption Behavior of Selected Enantiomers on Immobilized α_1-Acid Glycoprotein, Anal. Chem., *74*, pp. 2950-2959. 2002.

Gritti, F. and G. Guiochon. Accuracy and Precision of Adsorption Isotherm Parameters Measured by Dynamic Methds, J. Chromatogr. A, *1043*, pp.159-170. 2004.

Guest, D.M. Evaluation of Simulated Moving Bed Chromatography for Pharmaceutical Process Development, J. Chromatogr. A, *760*, pp. 159-162. 1997.

Guiochon, G., D.G. Shirazi and A.M. Katti. Fundamentals of Preparative and Nonlinear Chromatography. pp. 35-75, Boston: Academic Press. 1994.

Guiochon, G. and B. Lin. Modeling for Preparative Chromatography. pp. 246-320, Amsterdam: Academic Press. 2003.

Gyimesi-Forrás, K., G. Szász, Z. Dudvári-Bárány and A. Gergely. New Data on the Sorption Properties of α_1-Acid Glycoprotein Chiral Stationary Phase, Chirality, *11*, pp. 212-217. 2003.

Hashimoto, K., S. Adachi, H. Noujima and Y. Ueda. A New Process Combining Adsorption and Enzyme Reaction for producing Higher Fructose Syrup, Biotechnol. Bioeng., *25*, pp. 2371-2392. 1983a.

Hashimoto, K., S. Adachi, H. Noujima and H. Maruyama. Models for the Separation of Glucose/Fructose Mixture Using a Simulated Moving-Bed Adsorber, J. Chem. Eng. Jpn., *16*, pp. 400-406. 1983b.

Hashimoto, K., S. Adachi and Y. Shirai. Development of New Bioreactors of a Simulated Moving-Bed Type. In Preparative and Production Scale Chromatography, ed by G. Ganestos and P. E. Barker, pp. 395-420. New York: Marcel Dekker. 1993.

Hermansson, J. Direct Liquid Chromatographic Resolution of Racemic Drugs Using α_1-Acid Glycoprotein as the Chiral Stationary Phase, J. Chromatogr., *269*, pp. 71-80.1983.

Hermansson, J. and A. Grahn. Optimization of the Separation of Enantiomers of Basic Drugs: Retention Mechanisms and Dynamic Modification of the Chiral Bonding Properties on an α_1-Acid Glycoprotein Column, J. Chromatogr. A, *694*, pp. 57-69. 1995.

Holland, J.H. Adaptation in Natural and Artificial Systems; An Introductory Analysis with Applications to Biology, Control and Artificial Intelligence, pp. 1-183, Ann Arbor: University of Michigan Press. 1975.

Hongisto, H.J. Chromatographic Separation of Sugar Solutions, the Finnsugar Molasses Desugarization Process I, Int. Sugar J., *79*, pp. 100-104. 1977a.

Hongisto, H.J. Chromatographic Separation of Sugar Solutions, the Finnsugar Molasses Desugarization Process II, Int. Sugar J., *79*, pp. 131-134. 1977b.

Hotier, G., G. Terneuil, J.M. Toussaint and D. Lonchamp. Continuous Process and Apparatus for Chromatographic Separation of a Mixture of at Least Three Components into Three Purified Effluents by Means of Two Solvents, European Patent 1990-402334, 1990.

Imamoglu, S. Simulated Moving Bed Chromatography (SMB) for Application in Bioseparation. In series of Advances in Biochemical Engineering Biotechnology 76: Modern Advances in Chromatography, ed by R. Freitag, pp. 211-231. New York: Springer. 2002.

Jacobson, J.M., J. Frenz and Cs. Horváth. Measurement of Competitive Adsorption Isotherms by Frontal Chromatography, Ing. Eng. Chem. Res., *26*, pp. 43-50. 1987.

Jacobson, J.M., and J. Frenz. Determination of Competitive Adsorption isotherms for Modeling Large-Scale Separations in Liquid Chromatography, J. Chromatogr., *499*, pp. 5-20. 1990.

James F. and M. Sepúlveda. Parameter Identification for a Model of Chromatographic Column, Inverse Probl., *10*, pp. 1299-1314. 1994.

James, F., M. Sepúlveda, F. Charton, I. Quiñones and G. Guiochon. Determination of Binary Competitive Equilibrium Isotherms from the Individual Chromatographic Band Profiles, Chem. Eng. Sci., *54*, pp. 1677-1696. 1999.

Jandera, P., S. Bunčeková, K. Mihlbachler, G. Guiochon, V. Bačkovská and J. Planeta. Fitting Adsorption Isotherms to the Distribution Data determined using Packed Micro-columns for High-Performance Liquid Chromatography, J. Chromatogr. A, *925*, pp, 19-29. 2001.

Karlsson, S., F. Pettersson and T. Westerlund. A MILP-Method for Optimizing a

Preparative Simulated Moving Bed Chromatographic Separation Process, Comput. Chem. Eng., *23*, pp. S487-S490. 1999.

Kasat, R., D. Kunzru, D.N. Saraf and S.K. Gupta. Multiobjective Optimization of Industrial FCC Units Using Elitist Non-dominated Sorting Genetic Algorithm, Ind. Eng. Chem. Res., *41*, pp. 4765-4776. 2002.

Kaspereit, M., P. Jandera, M. Škavrada and A. Seidel-Morgenstern. Impact of Adsorption Isotherm Parameters on the Performance of Enantioseparation Using Simulated Moving Bed Chromatography, J. Chromatogr. A, *944*, pp. 249-262. 2002.

Kawase, M., T.B. Suzuki, K. Inoue, K. Yoshimoto and K. Hashimoto. Increased Esterification Conversion by Application of the Simulated Moving Bed Reactor, Chem. Eng. Sci., *51*, pp. 2971-2876. 1996.

Kawase, M., A. Pilgrim, T. Araki and K. Hashimoto. Lactosucrose Production Using a Simulated Moving Bed Reacotr, Chem. Eng. Sci., *56*, pp. 453-458. 2001.

Kirland, J.J., M.A. van Straten and H.A. Claessens. High pH Mobile Phase Effects on Silica-Based Reversed-Phase High-Performance Liquid Chromatographic Columns, J. Chromatogr. A, *691*, pp. 3-19. 1995.

Kloppenburg, E. and E.D. Gilles. A New Concept for Operating Simulated Moving-Bed Process, Chem. Eng. Technol., *22*, pp. 813-817. 1999.

Krstulović, A.M. and P. R. Brown. Reversed-Phase High-Performance Liquid Chromatography: Theory, Practice and Biomedical applications. pp. 20-89, New York: John Wiley & Sons. 1982.

Kurup, A. S., K. Hidajat and A.K. Ray. Optimal Design and Operation of SMB Bioreactor for Sucrose Inversion, Chem. Eng. J., *108*, pp. 19-33. 2005a.

Kurup, A.S., K. Hidajat and A.K. Ray. Optimal Operation of an Industrial-Scale Parex Process for the Recovery of p-Xylene from a Mixture of C-8 Aromatics, Ind. Eng. Chem. Res., *44*, pp. 5703-5714. 2005b.

Kurup, A.S., K. Hidajat and A.K. Ray. Optimal Operation of a Pseudo-SMB Process

for Ternary Separation under Non-Ideal Conditions, Sep. Purif. Technol., *51*, pp. 387-403. 2006.

Küsters, E., G. Gerber and F. Antia. Enantioseparation of a Chiral Epoxide by Simulated Moving Bed Processes, AIChE J., *42*, pp. 154-160. 1995.

Lefevre, L.J., Separation of Fructose from Glucose Using Cation Exchange resin Salts, US Patent 3 004 905. 1962.

Lehoucq, S., D. Verhève, A.V. Wouwer and E. Cavoy. SMB Enantioseparation: Process Development, Modeling and Operating Conditions, AIChE J., *46*, pp. 247-256. 2000.

Lindholm, J., P. Forssén and T. Fornstedt. Validation of the Accuracy of the Perturbation Peak Method for Determination of Multicomponent Adsorption Isotherm Parameters in LC, Anal. Chem., *76*, pp. 5472-5478. 2004.

Lode, F., M. Houmard, C. Migliorini, M. Mazzotti and M. Morbidelli. Continuous Reactive Chromatography, Chem. Eng. Sci., *56*, pp. 269-291. 2001.

Ludemann-Hombourger O., R.-M. Nicoud and M. Bailly. The "Varicol" Process: A New Multicolumn Continuous Chromatographic Process, Separ. Sci. Technol., *35*, pp. 1829-1862. 2000.

Ludemann- Hombourger O., G. Pigorini, R.-M. Nicoud, D.S. Ross and G. Terfloth. Application of the Varicol Process to the Separation of the Isomers of the SB-553261 Racemate, J. Chromatogr. A, *947*, pp.59-68. 2002.

Ma, Z. and N.-H.L. Wang. Standing Wave Analysis of SMB Chromatography: Linear Systems, AIChE J., *43*, pp. 2488-2508. 1997.

Magee, E.M. Course of Reaction in a Chromatographic Column, Ind. Eng. Chem. Fund., *2*, pp. 32-36. 1963.

Mallmann, T., B.D. Burris, Z. Ma and N.-H.L. Wang. Standing Wave Design of Nonlinear SMB Systems for Fructose Purification, AIChE J. *44*, pp. 2628-2646. 1998.

Marchetti, N., F. Dondi, A. Felinger, R. Guerrini, S. Salvadori and A. Cavazzini.

Modeling of Overloaded Gradient Elution of Nociceptin/Orphanin FQ in Reversed-Phase Liquid Chromatography, J. Chromatogr. A, *1079*, pp. 162-172. 2005.

Masuda, T., T. Sonobe, F. Matsuda and M. Horie. Process for Fractional Separation of Multi-Component Fluid Mixture, US Patent 5 198 120. 1993.

Mata, V.G. and A.E. Rodrigues. Separation of Ternary Mixtures by Pseudo-Simulated Moving Bed Chromatography, J. Chromatogr. A, *939*, pp. 23-40. 2001.

Mazzotti, M., G. Storti and M. Morbidelli. Robust Design of Countercurrent Adsorption Separation Process: 2. Multicomponent Systems, AIChE J., *40*, pp. 1825-1842. 1994.

Mazzotti, M., G. Storti and M. Morbidelli. Robust Design of Countercurrent Adsorption Separation Process: 3. Nonstoichiometric Systems, AIChE J., *42*, pp. 2784-2796. 1996a.

Mazzotti, M., R. Baciocchi, G. Storti and M. Morbidelli. Vapor-phase SMB Adsorptive Separation of Linear/Nonlinear Paraffins, Ind. Eng. Chem. Res., *35*, pp. 2313-2321. 1996b.

Mazzotti, M., G. Storti and M. Morbidelli. Optimal Operation of Simulated Moving Bed Units for Nonlinear Chromatographic Separations, J. Chromatogr. A, *769*, pp. 3-24. 1997.

Meurer, M., U. Altenhoner, J. Strube, A. Untiedt and H. Schmidt-Traub. Dynamic Simulation of a Simulated-Moving-bed Chromatographic Reactor for the Inversion of sucrose, Starch/Starke, *48*, pp. 452-457. 1996.

Michel, M., A. Epping, A. Jupke. Modeling and Determination of Model Parameters. In Preparative Chromatography of Fine Chemicals and Pharmaceutical Agents, ed by H. Schmidt-Traub, pp. 247-291. Weinheim: Wiley-VCH. 2005.

Migliorini, C., M. Mazzotti and M. Morbidelli. Continuous Chromatographic Separation through Simulated Moving Beds under Linear and Nonlinear Conditions, J. Chromatogr. A, *827*, pp. 161-173. 1998.

Migliorini, C., A. Gentilini, M. Mazzotti and M. Morbidelli. Design of Simulated Moving Bed Units under Nonideal Conditions, Ind. Eng. Chem. Res., *38*, pp. 2400-2410, 1999a.

Migliorini, C., M. Fillinger, M. Mazzotti and M. Morbidelli. Analysis of Simulated Moving-Bed Reactors, Chem. Eng. Sci., *54*, pp. 2475-2480, 1999b.

Migliorini, C., M. Wendlinger, M. Mazzotti and M. Morbidelli. Temperature Gradient Operation of a Simulated Moving Bed Unit, Ind. Eng. Chem. Res., *40*, pp. 2606-2617. 2001.

Migliorini, C., M. Mazzotti, G. Zenoni and M. Morbidelli. Shortcut Experimental Method for Designing Chiral SMB Separations, AIChE J., *48*, pp. 69-77. 2002.

Mihlbachler, K., A. Seidel-Morgenstern and G. Guiochon. Detailed Study of Tröger's Base Separation by SMB process. AIChE J., *50*, 611-624. 2004.

Miller, L., C. Grill, T. Yan, O. Dapremont, E. Huthmann and M. Juza. Batch and Simulated Moving Bed Chromatographic Resolution of a Pharmaceutical Racemate, J. Chromatogr. A, *1006*, 267-280. 2003.

Minceva, M., and A.E. Rodrigues, Modeling and Simulation of a Simulated moving Bed for the Separation of p-Xylene, Ind. Eng. Chem. Res., *41*, pp. 3454-3461. 2002.

Minceva, M., and A.E. Rodrigues. Two-Level Optimization of an Existing SMB for p-Xylene Separation, Comput. Chem. Eng., *29*, pp. 2215-2228. 2005.

Mun, S., Y. Xie, J.H. Kim and N.-H.L. Wang. Optimal Design of a Size-Exclusion Tandem Simulated Moving Bed for Insulin Purification, Ind. Eng. Chem. Res., *42*, 1977-1993. 2003.

Nagamatsu, S., K. Murazumi and S. Makino. Chiral Separation of a Pharmaceutical Intermediate by a Simulated Moving Bed Process. J. Chromatogr. A, *832*, pp. 55-65. 1999.

Navarro, A., H. Caruel and L. Rigal. Continuous Chromatographic Separation Process:

Simulated Moving Bed Allowing Simultaneous Withdrawal of Three Fractions, J. Chromatogr. A, *770*, pp. 39-50. 1997.

Negawa, M. and F. Shoji. Optical resolution by simulated moving-bed adsorption technology, J. Chromatogr., *590*, pp. 113-117. 1992.

Nicolaos, A., L. Muhr, P. Gotteland, R.-M. Nicoud and M. Bailly. Application of Equilibrium Theory to Ternary Moving Bed Configurations (Four + Four, Five + Four, Eight and Nine zones) I. Linear Case, J. Chromatogr. A, *908*, pp. 71-86. 2001a.

Nicolaos, A., L. Muhr, P. Gotteland, R.-M. Nicoud and M. Bailly. Application of the Equilibrium Theory to Ternary Moving Bed Configurations (4 + 4, 5 + 5, 8 and 9 zones) II. Langmuir Case, J. Chromatogr. A, *908*, pp. 87-109. 2001b.

Nicoud, R.M., G. Fuchs, P. Adam, M. Bailly, E. Küsters, F.D. Antia, R. Reuille and E. Schmid. Preparative Scale Enantioseparation of a Chiral Epoxide: Comparison of Liquid Chromatography and Simulated Moving Bed Adsorption Technology, Chirality, *5*, pp. 267-271. 1993.

Pais, L.S., J.M. Loureiro and A.E. Rodrigues. Modeling, Simulation and Operation of a Simulated Moving Bed for Continuous Chromatographic Separation of 1,1'-bi-2-Naphthol Enantiomers, J. Chromatogr. A*, 769*, pp. 25-35. 1997.

Pais, L.S., J.M. Loureiro, and A.E. Rodrigues. Separation of enantiomers of a chiral epoxide by simulated moving bed chromatography. J. Chromatogr. A*, 827*, pp. 215-233. 1998a.

Pais, L.S., J.M. Loureiro and A.E. Rodrigues. Modeling Strategies for Enantiomers Separation by Simulated Moving Bed Chromatography, AIChE J., *44*, pp. 561-569. 1998b.

Pais, L.S., J.M. Loureiro and A.E. Rodrigues. Chiral separation by SMB chromatography, Sep. Purif. Technol., *20*, pp. 67-77. 2000.

Pedeferri, M., G. Zenoni, M. Mazzotti and M. Morbidelli. Experimental Analysis of a Chiral Separation through Simulated Moving Bed Chromatography, Chem. Eng. Sci., *54*, pp. 3735-3748. 1999.

Peper, S., M. Lübbert, M. Johannsen and G. Brunner. Separation of Ibuprofen Enantiomers by Supercritical Fluid Simulated Moving bed Chromatography, Sep. Sci. Technol., *37*, pp. 2545-2566. 2002.

Pilgrim A., M. Kawase, F. Matsuda and K. Miura. Modeling of the Simulated Moving-Bed Reactor for the Enzyme-Catalyzed Production of Lactosucrose, Chem. Eng. Sci., *61*, pp. 353-362. 2006.

Proll, T., and E. Kusters. Optimization Strategy for Simulated Moving Bed Systems, J. Chromatogr. A, *800*, pp. 135-150. 1998.

Rajesh, J.K., S.K. Gupta, G.P. Rangaiah and A.K. Ray. Multi-Objective Optimization of Industrial Hydrogen Plants, Chem. Eng. Sci., *56*, pp. 999-1010. 2001.

Ray, A.K. The Simulated Countercurrent Moving Bed Chromatographic Reactor: A Novel Reactor-Separator. Ph.D. Dissertation, University of Minnesota. 1992.

Ray, A.K., R.W. Carr and R. Aris. The Simulated Countercurrent Moving-Bed Chromatographic Reactor- A Novel Reactor and Separator, Chem. Eng. Sci., *49*, pp. 469-480. 1994.

Ray, A.K. and R.W. Carr. Experimental-Study of a Laboratory-Scale Simulated Countercurrent Moving-Bed Chromatographic Reactor, Chem. Eng. Sci., *50*, pp. 2195-2202. 1995a.

Ray, A.K. and R.W. Carr. Numerical Simulation of a Simulated Countercurrent Moving Bed Chromatographic Reactor, Chem. Eng. Sci., *50*, pp. 3033-3041. 1995b.

Rodrigues, A.E. and L.S. Pais. Design of SMB Chiral Separation Using the Concept of Separation Volume, Separ. Sci. Technol., *39*, pp. 245-270. 2004.

Roginskii, S.Z., M.I. Yanovskii and G.A. Gaziev. Chemical Reaction Under Chromatographic Conditions, Dokl. Akad. Nauk SSSR (Engl. Transl.), *140*, pp. 771-776. 1961.

Rosset, A.J. de, R.W. Neuzil and D.J. Korous. Liquid Column Chromatography as a

Predictive Tool for Continuous Countercurrent Adsorptive Separations, Ind. Eng. Chem. Proc. Des. Dev., *15*, pp. 261-266. 1976.

Ruthven, D.M. Principles of Adsorption and Adsorption Process. pp. 207-213. New York: Wiley. 1984.

Ruthven, D.M. and C.B. Ching. Counter-Current and Simulated Counter-Current Adsorption Separation Processes, Chem. Eng. Sci., *44*, pp. 1011-1038. 1989.

Sayama, K., T. Kamada, S. Oikawa and T. Masuda. Production of Raffinose: A New Byproduct of the Beet Sugar Industry, Zucherind., *117*, pp. 893-899. 1992.

Schulte, M., R. Ditz, R.M. Devant, J.N. Kinkel and F. Charton. Comparison of the Specific Productivity of Different Chiral Stationary Phases Used for Simulated Moving-Bed Chromatography, J. Chromatogr. A, *769*, pp. 93-100. 1997.

Schulte, M. and J. Strube. Preparative Enantioseparation by Simulated Moving Bed Chromatography, J. Chromatogr. A, *906*, pp. 399-416. 2001.

Schulte, M., K. Kekenborg and W. Wewers. Process Concepts. In Preparative Chromatography of Fine Chemicals and Pharmaceutical Agents, ed by H. Schmidt-Traub, pp. 193- 204. Weinheim: Wiley-VCH. 2005.

Seidel-Morgenstern, A. Experimental Determination of Single Solute and Competitive Adsorption isotherms, J. Chromatogr. A, *1037*, pp. 255-272. 2004.

Seko, M., H. Takeuchi and T. Inada. Scale-up for Chromatographic Separation of p-Xylene and Ethyl Bezene, Ind. Eng. Chem. Prod. Res. Dev., *21*, pp. 656-661. 1982.

Shieh, M.T. and P.E. Barker. Saccharification of Modified Starch to Maltose in a Semi-Continuous Counter-Current Chromatographic Reactor-Separator (SCCR-S), J. Chem. Tech. Biotechnol., *63*, pp. 125-134. 1995.

Silva, E.A.B, A.A.U. de Souza, S.G.U. de Souza and A.E. Rodrigues. Analysis of the High-Fructose Syrup Production Using Reactive SMB Technology, Chem. Eng. J., *118*, pp.167-181. 2006.

Silva, V. M.T., M. Minceva and A.E. Rodrigues. Novel Analytical Solution for a Simulated Moving Bed in the Presence of Mass-Transfer Resistance, Ind. Eng. Chem. Res., *43*, pp. 4494-4502. 2004.

Silva, V. M.T. M. and A.E. Rodrigues. Noval Process for Diethylacetal Syhthesis, AIChE J., *51*, pp. 2752-2768, 2005.

Srinivas, N. and K. Deb. Multiobjective Function Optimization using Non-dominated Sorting Genetic Algorithm, Evolutionary Computing, *2*, pp. 221-248. 1995.

Storti, G., M. Masi, R. Paludetto, M. Morbidelli and S. Carra. Adsorption Separation Processes: Countercurrent and Simulated Countercurrent Operations, Comput. Chem. Eng., *12*, pp. 475-482. 1988.

Storti, G., M. Masi, S. Carra and M. Morbidelli. Optimal Design of Multi-Component Countercurrent Adsorption Separation Processes Involving Nonlinear Equilibria, Chem. Eng. Sci., *44*, pp. 1329-1345. 1989.

Storti, G., M. Mazzotti, M. Morbidelli and S. Carra. Robust Design of Binary Countercurrent Adsorption Separation Processes, AIChE J., *39*, pp. 471-492. 1993.

Storti, G., R. Baciocchi, M. Mazzotti and M. Morbidelli. Design of Optimal Operating Conditions of Simulated Moving Bed Adsorptive Separation Units, Ind. Eng. Chem. Res. *34*, pp. 288-301. 1995

Strube, J., U. Altenhöner, M. Meurer, H. Schmidt-Traub and M. Schulte. Dynamic Simulation of Simulated Moving-Bed Chromatographic Processes for the Optimization of Chiral Separations, J. Chromatogr. A, *769*, pp. 81-92. 1997.

Strube, J., A. Jupke, A. Epping, H. Schmidt-Traub, M. Schulte and R. Devant. Design, Optimization and operation of SMB Chromatography in the production of Enantiomerically Pure Pharmaceuticals, Chirality, *11*, pp. 440-450. 1999.

Subramani, H.J., K. Hidajat and A.K. Ray. Optimization of Reactive SMB and Varicol Systems, Comput. Chem. Eng., *27*, pp. 1883-1901. 2003.

Susanto, A., K. Wekenborg, A. Epping and A. Jupke. Model Based Design and

Optimization. In Preparative Chromatography of Fine Chemicals and Pharmaceutical Agents, ed by H. Schmidt-Traub, pp. 314-366. Weinheim: Wiley-VCH. 2005.

Thompson, R., V. Drasad, N. Grinberg, D. Ellison and J. Wyvratt. Mechanistic Aspects of the Stereospecific Interactions of Immobilized Alpha(1)-Acid Glycoprotein, J. Liq. Chromatogr. R. T., *24*, 813-825. 2001.

Tonkovich, A.L., R.W. Carr and R. Aris. Enhanced C_2 Yields from Methane Oxidative Coupling by Means of a Separative Chemical Reactor, Science, *262*, pp. 221-223. 1993.

Toumi, A., F. Hanisch and S. Engell. Optimal Operation of Continuous Chromatographic Processes: Mathematical Optimization of the Varicol Process, Ind. Eng. Chem. Res., *41*, pp. 4328-4337. 2002.

Toumi, A., S. Engell, O. Ludemann-Hombourger, R.M. Nicoud and M. Bailly. Optimization of Simulated Moving Bed and Varicol Processes. J. Chromatogr. A, *1006*, pp. 15-31. 2003.

Toumi, A and S. Engell. Optimization-Based Control of a Reactive Simulated Moving Bed Process for Glucose Isomerization, Chem. Eng. Sci., *59*, pp. 3777-3792. 2004.

Vos, H.J., D.J. Groon, J.J.M. Pottors and K. Ch. A.M. Luyben. Countercurrent Multistage Fluidized Bed Reactor for Immobilized Biocatalysis: I. Modeling and Simulation, Biotechnol. Bioeng. *36*, pp. 367-376. 1990.

Wang, X. and C.B. Ching. Chiral Separation of Beta-Blocker Drug (Nadolol) by Five-Zone Simulated Moving Bed Chromatography, Chem. Eng. Sci., 60, pp. 1337-1347. 2005.

Wewers, W., J. Dingenen, M. Schulte and J. Kinkel. Selection of Chromatographic Systems. In Preparative Chromatography of Fine Chemicals and Pharmaceutical Agents, ed by H. Schmidt- Traub, pp. 107- 170. Weinheim: Wiley-VCH. 2005.

Wongso, F., K. Hidajat and A.K. Ray. Optimal Operating Mode for Enantioseparation of SB-553261 Racemate Based on Simulated Moving Bed Technology, Biotechnol. Bioeng., *87*, pp. 704-722. 2004.

Wongso, F., K. Hidajat and A.K. Ray. Improved Performance for Continuous Separation of 1-1'-Bi-2-Naphnol Racemate Based on Simulated Moving Bed Technology, Sep. Purif. Technol., *46*, pp. 168-191. 2005.

Wooley, R., Z. Ma and N.-H.L. Wang. A Nine-Zone Simulated Moving Bed for the Recovery of Glucose and Xylose from Biomass Dydrolyzate, Ind. Eng. Chem. Res., *37*, pp. 3699-3709. 1998.

Wu, D.-J., Y. Xie, Z. Ma and N.-H.L. Wang. Design of Simulated Moving-Bed Chromatography for Amino Acid Separations, Ind. Eng. Chem. Res., *37*, pp.4023-4035. 1998.

Wu, D.-J., Z. Ma and N.-H.L. Wang. Optimization of Throughput and Desorbent Consumption in Simulated Moving-Bed Chromatography for Paclitaxel Purification, J. Chromotogr. A., *855*, pp.71-89. 1999.

Xie, Y., S. Mun, J.H. Kim and N.-H.L. Wang. Standing Wave Design and Experimental Validation of a Tandem Simulated Moving Bed Process for Insulin Purification, Biotechnol. Progr., *18*, pp. 1332-1344. 2002.

Xie, Y., C.A. Farrenburg, C.Y. Chin, S. Mun and N.-H.L. Wang. Design of SMB for a Nonlinear Amino Acid System with Mass-Transfer Effects, AIChE J., *49*, pp. 2850-2862. 2003.

Yu, W., K. Hidajat and A.K. Ray. Modeling, Simulation and Experimental Study of a Simulated Moving Bed Reactor for the Synthesis of Methyl Acetate Ester, Ind. Eng. Chem. Res., *42*, pp. 6743-6754. 2003a.

Yu, W., K. Hidajat and A.K. Ray. Application of Multiobjective Optimization in the Design and operation of Reactive SMB and its Experimental Verification, Ind. Eng. Chem. Res., *42*, pp.6823-6831. 2003b.

Zang, Y. and P.C. Wankat. SMB Operation Strategy – Partial Feed, Ind. Eng. Chem. Res., *41*, pp. 2504-2511. 2002.

Zenoni, G., M. Pedeferri, M. Mazzotti and M. Morbidelli. On-Line Monitoring of

Enantiomer Concentration in Chiral Simulated Moving Bed Chromatography, J. Chromatogr. A, *888*, pp. 73-83. 2000.

Zhang, L., J. Selker, A. Qu and A. Velayudhan. Numerical Estimation of Multicomponent Adsorption Isotherms in Preparative Chromatography: Implications of Experimental Error, J. Chromatogr. A, *924*, pp. 13-29. 2001.

Zhang, Z., K. Hidajat, A.K. Ray and M. Morbidelli. Multiobjective Optimization of SMB and Varicol Process for Chiral Separation, AIChE J., 48, pp. 2800-2816. 2002a.

Zhang, Z., K. Hidajat and A.K. Ray. Multiobjective Optimization of Simulated Countercurrent Moving Bed Chromatographic Reactor (SCMCR) for MTBE Synthesis, Ind. Eng. Chem. Res., *41*, pp. 3213-3232. 2002b.

Zhang, Z., M. Mazzotti and M. Morbidelli. PowerFeed Operation of Simulated Moving Bed Units: Changing Flow-Rates during the Switching Interval, J. Chromatogr. A, *1006*, pp. 87-99. 2003.

Zhang, Z., M. Morbidelli and M. Mazzotti. Experimental Assessment of PowerFeed Chromatography, AIChE J., *50*, pp. 625-632. 2004.

Zhong, G. and G. Guiochon. Analytical Solution for the Linear Ideal Model of Simulated Moving Bed Chromatography, Chem. Eng. Sci., *51*, pp. 4307-4319. 1996.

Zhou, D., K. Kaczmarski and G. Guiochon. Comparison of the Binary Equilibrium Isotherms of the 1-Indanol Enantiomers on Three High-Performance Liquid Chromatography Columns of Different Sizes, J. Chromatogr. A, *1015*, pp. 73-87. 2003.